Addis Ababa University

College of Natural Sciences

Department of Chemistry

Ph.D. Dissertation On:

Chemical Studies of the Resin of *Commiphora erlangeriana*

and

Some Plants in Yayu Nature Reserve

By: Mesfin Getachew (ID: GSR/1258/05)

Advisor: Ermias Dagne (Prof)

Co-Advisor: Yang Ye (Prof)

April, 2018

CHEMICAL STUDIES OF THE RESIN OF *COMMIPHORA ERLANGERIANA* AND SOME PLANTS IN YAYU NATURE RESERVE

PH.D. DISSERTATION

BY: MESFIN GETACHEW

ADVISOR: PROFESSOR ERMIAS DAGNE

CO-ADVISOR: PROFESSOR YE YANG

ADDIS ABABA UNIVERSITY

COLLEGE OF NATURAL AND COMPUTATIONAL SCIENCES

DEPARTMENT OF CHEMISTRY (ORGANIC STREAM)

APRIL, 2018

ADDIS ABABA, ETHIOPIA

Approval Sheet

Addis Ababa University
College of Natural and Computational Sciences
School of Graduate Studies
Department of Chemistry

This is to certify that the thesis prepared by **Mesfin Getachew**, entitled: **Chemical Studies of the Resin of *Commiphora erlangeriana* and Some Plants in Yayu Nature Reserve**, submitted in partial fulfillment of the requirement of the degree of Doctor of Philosophy in Chemistry (Organic stream) complies with the regulation of the University and meets the accepted standards with respect to originality and quality.

Approved by the examining committee:

Name	**Signature**	**Date**
External examiner		
_____	_____	_____
Internal examiner		
_____	_____	_____
Internal examiner		
_____	_____	_____
Advisor		
_____	_____	_____
Chairman of the Department		
_____	_____	_____

DECLARATION OF THE CANDIDATE

I, hereby, declare that this thesis submitted for the degree of Doctor of Philosophy (Ph.D.) in Chemistry (Organic stream) at Addis Ababa University, College of Natural and Computational sciences, Addis Ababa, Ethiopia, is my own original work and has not been submitted previously to any institution or higher education. All sources of materials used in this work have been accordingly acknowledged.

Abstract

The resinous and gummy materials that ooze out from the bark of species in the genus *Commiphora* are important substances in indigenous medicines of many countries of eastern Africa, Arabia, India, and China. The most well-known member of this genus that occurs in Ethiopia, Kenya, and Somalia is *C. myrrha (*Syn: *C. molmol)*, which yields a culturally and medicinally significant gum-resin known in the trade as myrrh. The main topic of this dissertation is the study of the chemistry of the resin of species known as *C. erlangeriana.* This resin was a topic of a previous dissertation from our research group (Dekebo A., 1999) and the paper (Dekebo A., *et al*, J. Nat. Prod., 2002) which described the isolation and characterization of four unique podophyllotoxin- and polgamatin-types compounds named as Erlangerins A to D (structures shown in **Group I** below). We report here results of further chemical work on this resin which yielded 30 additional lignans: 15 podophyllotoxin- and polygamatin-types (**Group II**), 10 dibenzylbutyrolactone-type (**Group III**) and 5 other types (**Group IV**).

The results are significant because podophyllotoxin and the related aryltetralin lignans and their precursors are well known antineoplastic and antiviral agents. We believe that some of the compounds reported here for the first time may also serve as starting compounds for the semi-synthesis of the commercially available anticancer drugs, e.g., etoposide (**127**), teniposide (**128**), and etopophos (**129**).

Group-I

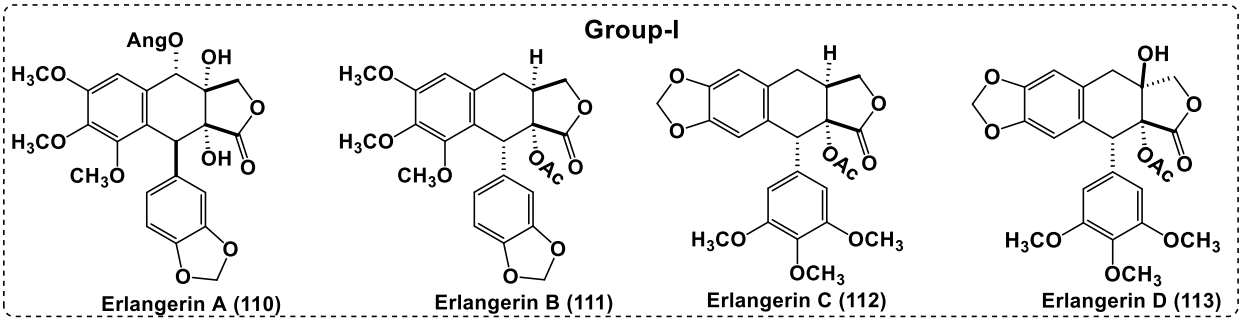

Group-II

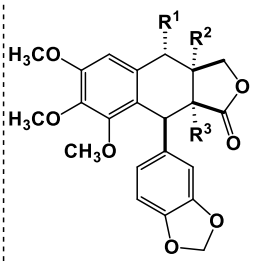

	R^1	R^2	R^3
Erlangerin E (139*)	Angelate	OH	Angelate
Erlangerin F (140*)	Angelate	Angelate	OH
Erlangerin G (141*)	Tiglate	OH	OH
Erlangerin H (142*)	H	OH	OH
Erlangerin I (148*)	H	H	OH
Erlangerin J (149*)	2-Methylbutanoate	H	Acetae
Erlangerin K (150*)	Angelate	H	Acetae
Erlangerin L (151*)	OH	H	Acetae

Angelate = (Ang)

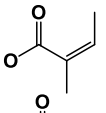

Tiglate = (Trig)

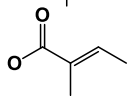

2-Methyl-butanoate =

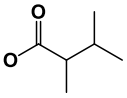

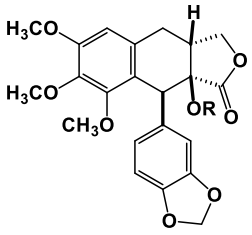

Erlangerin M (146*) R= Ac
Erlangerin N (147*) R= H

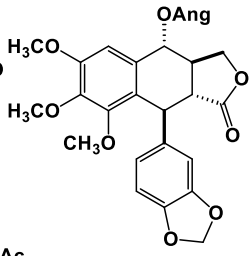

Erlangerin O (153*)

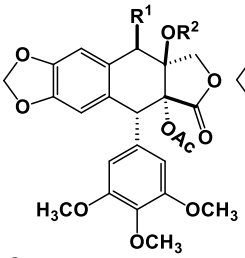

Erlangerin P (143*) R^1= Acetae, R^2= H
Erlangerin Q (144*) R^1= H, R^2= Acetate

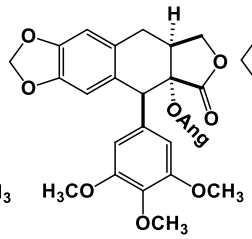

Erlangerin R (145*)

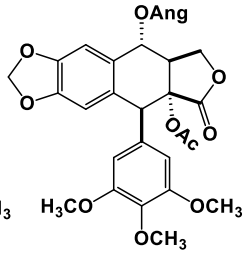

Erlangerin S (152*)

Group-III

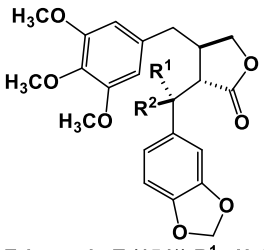

Erlangerin T (154*) R^1= H, R^2= OH
Erlangerin U (155*) R^1= OH, R^2= H
Erlangerin V (156*) R^1= OAc, R^2= H
Erlangerin W (157*) R^1= H, R^2= OAng
Erlangerin X (158*) R^1= OAng, R^2= H

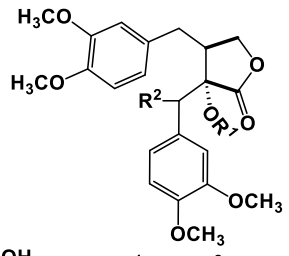

159 R^1= Ac, R^2= H
Erlangerin Y (160*) R^1= Ang, R^2= H
Erlangerin Z (162*) R^1= Ac, R^2= OAc

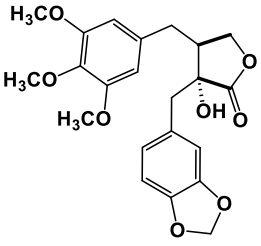

Erlangerin Z1 (161*)

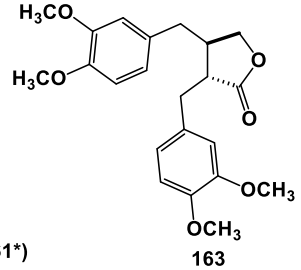

163

Group-IV

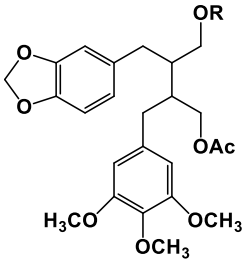

Erlangerin Z2 (164*) R= Ang
Erlangerin Z3 (165*) R= 2-Methylbutanoyl

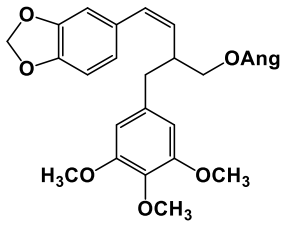

Erlangerin Z4 (166*)

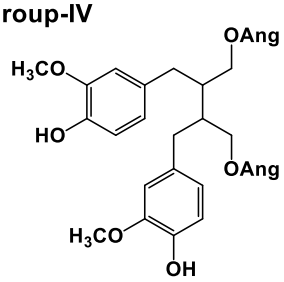

Erlangerin Z5 (168*)

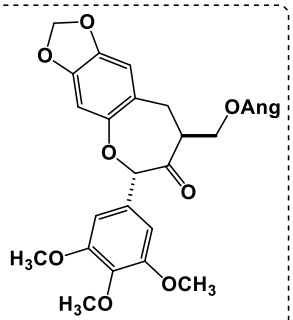

Erlangerin Z6 (169*)

Acknowledgments

I express my deep gratitude to my advisor, Professor Ermias Dagne for the support at every brick wall that I encountered since my MSc. Mostly I would like to offer gratitude to him for allowing me to benefit from his wide knowledge in the field of Natural product chemistry.

I also thankful to my advisor Professor Ye Yang (SIMM) for encouragement and guidance during the course of this research work. I also acknowledge him for hosting me as a senior visiting student and for all the support he offered and giving so generously of his time and expertise.

I would like to express my deepest gratitude to Professor Wendimagegn Mammo for his special feedback on this dissertation and also for his genuine comments on different courses and seminars. I would also like to express my appreciation to Dr. Tatekegn Gebreyesus for sharing of his wide knowledge in the field of natural products and biosynthesis. Dr. Estifanos Ele should also be acknowledged for his scientific feedback during seminars and other related activities. I am also indebted to Dr. Ahmed Mustefa, head of the department, the technical and administrative staff of the department of chemistry, AAU.

I would like to thank all students and technical staffs of Professor Ye Yang group. I am especially grateful to Dr. Chunping Tang, Professor Sheng Yao and Mr. Chang-Qiang Ke.

I would like to acknowledge my family: my wife, Selamawit Abune, has been extremely supportive of me throughout this entire process and has made countless sacrifices to help me get to this point; my children, Estifanos Mesfin and Lidya Mesfin, for the love you showed; my mother, father, father-in-law, mother-in-law, brothers and sisters deserve special thanks for their continued support and encouragement.

I am also indebted to the Chinese Academy of Sciences (CAS) and Shanghai Institute of Materia Medica (SIMM) for hosting me for six months, Addis Ababa Science and Technology University (AASTU) for sponsorship and Addis Ababa University for hosting.

Contents

Table of Figures

List of Tables

List of Abbreviations and Acronyms

Abbs	Acronyms	Abbs	Acronyms
2D NMR	2-Dimensional NMR	IR	Infrared Spectroscopy
Abbs	Abbreviations	*J*	Coupling Constant
Ac	Acetone	JASCO	
bs	broad singlet	LCMS	Liquid Chromatography Mass Spectrometry
Calcd.	Calculated	LD_{50}	Lethal Dose, 50%
CC	Column Chromatography	LH-20	
$CDCl_3$	Deuterochloroform	m/z	mass-to-charge ratio
$CHCl_3$	Chloroform	max	Maximum
COSY	COrrelation SpectroscopY	MeOH	Methanol
COX	Cyclooxygenase	MIC	Minimal Inhibitory Concentration
d	doublet	multi.	multiplet
dd	doublet of doublets	NADH	Nicotinamide adenine dinucleotide
ddd	doublet of doublet of doublets	NADPH	Nicotinamide adenine dinucleotide phosphate

DEPT-135	Distortionless Enhancement by Polarization Transfer 135	NMR	Nuclear Magnetic Resonance
DNA	Deoxyribonucleic acid	NO	Nitric oxide
dq	doublet of quartets	NOESY	Nuclear Overhauser Effect SpectroscopY
EA	Ethyl acetate	ODS	
ECD	Electronic Circular Dichroism	OMT	O-Methyl Transferase
EIMS	Electron Ionization Mass Spectroscopy	ORTEP	Oak Ridge Thermal-Ellipsoid Plot Program
EIMS	Electron Ionization Mass Spectroscopy	PDA	Photodiode Array
ELSD		PE	Petrol
EtOAc	Ethyl acetate	PLR	Pinoresinol-Lariciresinol Reductase
EtOH	Ethanol	ppm	*parts-per-million*
Fig.	Figure	PTLC	Preparative Thin-layer Chromatography
Fr	Fraction	*qd*	quartet of doublets
HMBC	Heteronuclear Multiple Bond Correlation	ROESY	Rotating frame Overhause Effect *SpectroscopY*
HMQC	Heteronuclear Multiple Quantum Coherence	SIRD	Secoisolariciresinol Dehydrogenase
HPLC	High-Performance Liquid Chromatography	*t*	triplet
HREIMS	High-Resolution Electron Ionization Mass Spectrometry	*td*	triplet of doublets
Hz	Hertz	TLC	Thin Layer Chromatography
IC_{50}	Inhibitory Concentration	UV	Ultraviolet and Visible Spectroscopy
IKK	Inhibitor of NF-kB kinase		

Part 1: Chemical Studies of the Resin of *Commiphora erlangeriana*

1.1 Literature Review of the Chemistry of the Genus *Commiphora*

Plant resins are frequently called gums commercially. However, there is in principle clear distinction between resins and gums [1, 2]. Resins are solid or semisolid organic substances exuded by plants or insects feeding on plants. Resins are insoluble in water but soluble in alcohol or ether [3]. Plant resins are formed in specialized structures called ducts, located either inside or on the surface of plant parts. The initially liquid resin exudes out from the bark and hardens on exposure to air. Chemically, resins are mixtures of volatile and nonvolatile terpenoids or phenolics [1, 2, 4].

On the other hand, gums are formed by a process called gummosis and are dried exuded sap from trees and shrubs, slowly forming an amorphous brittle mass [5]. Gums are complex chains of polysaccharides derived from monosaccharide moieties such as galactose, arabinose, and rhamnose, and hence, are neither terpenoids nor phenolics in origin. A typical example of a natural gum is gum Arabic, which is readily soluble in water. However, some plants members of the genera *Commiphora* and *Mangifera* (mango) produce natural products that are on the one hand like gums because they dissolve partly in water and also are like resins due to their partial solubility in lipophilic solvents such as petroleum ether [1, 2, 4]. These intermediate substances are known as gum-resins.

Ethiopia has extensive dry woodland forests in the Horn of Africa, largely made up of resin- and gum-producing species such as *Acacia, Boswellia,* and *Commiphora.* It is one of the world's leading producers of incense, notably frankincense (product of *Boswellia* spp.) and myrrh and myrrh-like gum-resin products (from *Commiphora* spp.). The estimated annual production potential of commercial gums and resins is over 300,000 tons. However, information obtained from Ethiopian Revenue and Customs Authority (ERCA) [6] shows that only less than 1% of this potential has been exploited. In 2016, for example, the total export of natural resins, gums, and gum-resins from Ethiopia was 2,224 tons valued at Birr 190 million (US $ 6.8 million) [7-9]. However, the global demand for these natural products is likely to increase [9, 10].

1.1.1 The Family Burseraceae

Burseraceae is a member of the order *Sapindales*, which includes other familiar families such as *Sapindaceae*, *Hippocastanaceae*, *Aceraceae*, *Meliaceae*, *Rutaceae*, and *Anacardiaceae*. It is closely related to the last family, with which it shares certain characteristics such as pinnately compound leaves, peeling bark, and resinous sap. *Burseraceae* is of modest size, with about 600 species of flowering plants in about 17 genera. The family includes both trees and shrubs, which are native to tropical regions of Africa, Asia, and the Americas [11, 12].

Plants in *Burseraceae* family are further divided into three subfamilies: *Bursereae, Canarieae,* and *Protieae*. The subfamily *Bursereae* consists of the well-known resin producing genera *Bursera, Boswellia,* and *Commiphora.* Some taxonomists have included the species of *Bursera* in *Commiphora* whereas others have considered *Bursera* closer to *Boswellia*. Through molecular studies, however, some taxonomists supported the view that *Bursera* is monophyletic and more closely related to *Commiphora* than *Boswellia* [11, 12].

1.1.2 Botanical Aspects of the Genus *Commiphora*

The genus *Commiphora* consists of 150 species. They are primarily distributed in the warm and dry areas of the tropics; from southern Africa, eastward through tropical east Africa and the Horn of Africa. They are also found in the Arabian Peninsula and dry areas of Iran, Pakistan, and India. The name *Commiphora* is derived from two Greek words, *kommi*, meaning gum, and *phoreus*, meaning carrying, referring to the gummy resins produced by most species. The bark of most *Commiphora* species is papery and peels off into papery flakes, revealing a green bark underneath [7, 12].

The diversity of *Commiphora* species in Eastern Africa is the highest in the world. About fifty-two species of *Commiphora* are known to exist in Ethiopia and fourteen of the species are endemic. Some of the *Commiphora species* found in Ethiopia are listed in Table 1. However, very few are used to collect resin (Table 1). The chief *Commiphora* resin of high

economic importance is myrrh. It is largely produced by *C. myrrha*, *(*Synonym: *C. molmol)* [7].

Table 1: List of Commiphora species available in flora of Ethiopia

C. africana (♦)	*C. cyclophylla* (♦)	*C. longipedicellata*	*C. samharensis*
C. alaticaulis	*C. ellenbeckii* (♦)	*C. mildbraedii*	*C. schimperi* (♦)
C. albiflora	*C. erlangeriana* (♦)	*C. monoica* (♦)	*C. serrulata* (♦)
C. ancistrophora	*C. gileadensis*	*C. myrrha* (♦)	*C. sphaerocarpa*
C. boiviniana	*C. gowlello*	*C. erosa*	*C. sphaerophylla*
C. boranensis (♦)	*C. guidotti* (♦)	*C. erythraea* (♦)	*C. staphyleifolia*
C. bruceae	*C. habessinica* (♦)	*C. obovata*	*C. tenuis*
C. campestris	*C. hildebrandtii* (♦)	*C. ogadensis*	*C. terebinthina*
C. ciliata	*C. hodai* (♦)	*C. pedunculata*	*C. truncata* (♦)
C. confusa (♦)	*C. horrida*	*C. quadricincta*	*C. tubuk* (♦)
C. coronillifolia	*C. incisa* (♦)	*C. rostrata*	*C. unilobata*
C. corrugata (♦)	*C. kua* (♦)		

(♦) Resin producing species

1.1.2.1 Traditional Uses

The most frequently employed and investigated *Commiphora* species are *C. myrrha, C. opobalsamum,* and *C. mukul*. The resin of these plants exhibits diverse medicinal values such as wound, pain, fracture, mouth ulcer, inflammatory disease, stomach disorders and microbial infection.

C. myrrha was valued as much as gold and is mentioned numerous times in the Old Testament. It was presented as one of the three gifts to Christ by the Magi. It was also mentioned as a principal ingredient in the holy anointing oil.

Myrrh is one of the oldest medicines in the world. It has been mentioned in Egyptian medical texts since 2,800 B.C [13]. In traditional Egyptian medicine, myrrh is an excellent remedy for mouth and throat problems, for skin problems, atherosclerosis, hemorrhoid, high cholesterol, immune-depression and hyperglycemia [14]. It is also commonly used in Arab medicine for the treatments of some inflammatory conditions, bronchial complaints, tumors of the spleen, liver, stomach, and breast [15].

In the Ayurvedic medical system, myrrh is used to treat mouth ulcers, gingivitis (gum inflammation), pharyngitis (inflammation of the pharynx), respiratory catarrh (inflammation of a mucous membrane), to treat rheumatoid arthritis, heart ailments, neurological disorders, skin infections, and obesity. It is also used as an astringent topical application to ulcers and as a gargle for spongy gums. Myrrh tincture is also used to treat many disorders associated with the female reproductive cycle, particularly dysmenorrhea and amenorrhea, and to help relieve some of the uncomfortable symptoms of menopause [15].

The use of myrrh, called *Mo Yao* in Chinese, was also recorded in China in A.D. 600 during the Tang Dynasty. Myrrh is still in use in traditional Chinese medicine to treat impact injury, incised wounds, chest pains, bone pain, leprosy, cancers, hemorrhoids, for stimulating blood circulation and treating painful swellings, menstrual pain due to blood stagnation. It is used in the preparation of various topical plaster-adhesives and lotions, including ‘‘*Die-Da Yao-Jing*’’ (Traumatic Injury Medicinal Extract) [13, 15, 16].

In Ethiopia and Somalia, myrrh is used for the treatments of allergies, snake and insect bites, colds, coughs, diarrhea, headaches, syphilis, stomach complaints, back complaints, disinfection, and to correct female disorders during menopause [15].

The medicinal value of *C. mukul* resin, known as *Guggul*, in Ayurvedic medical system dates from thousands of years ago [17]. Guggul-gum resin has been prescribed as anti-obesity, anti-inflammatory, antibacterial, and anticoagulant. It also benefits the heart, liver, kidney, thyroid, and skin [18].

The bark of *C. kerstingii* is used in Nigeria to treat fever, cancer, diarrhea, measles, asthma, rheumatism and venereal diseases and sometimes used as an antidote to arrow poison [19]. In Jordan *C. berryi* is used for the treatment of inflammation, pain, and relieving stomach aches, cold and fever [14].

The traditional use of *Commiphora* species for the treatment of different ailments is also common in Africa. For example, In Eastern Africa, *C. kua* is used against snakebite, gonorrhea, and stomach disorders. In Somalia, *C. guidottii* is used for stomach complains,

wound, and diarrhea. In Ethiopia, *C. erythraea* is used for skin infection and ailments caused by ticks. *C. schimperi* (in Kenya) and *C. habessinica* (in Uganda) are used for malaria and eye pain, respectively. In Nigeria, *C. africana* is used for expelling tapeworms and wound. *C. holtziana*, in Eastern Africa, is used to kill and repel tick pest populations on camel and cattle [14].

1.1.2.2 Pharmacological Aspects

A clinical study performed on the resin of *C. mukul* indicated a significant improvement of osteoarthritis [20]. Triterpenoids, steroids, and lignans isolated from this resin have been also tested for their NO production and COX inhibitory activities and the tested compounds significantly prevented the production of NO and COX with different IC_{50} [21, 22]. The volatile oil and the petroleum ether extract of *C. myrrha*, *(*Synonym: *C. molmol)* resin showed inhibitory activity against carrageenan-induced inflammation and cotton pellet granuloma cells [23, 24]. The stem bark extract of *C. pyracanthoides* also exhibited a strong anti-inflammatory activity with IC_{50} of 27.86 mg/mL [25].

Oral administration of EtOH extracts of *C. myrrha*, *(*Synonym: *C. molmol)* resin and *C. caudata* leaves inhibited inflammation of paw edema-induced by formalin in rats [26, 27]. The hexane extract of *C. erythraea* resin was evaluated for anti-inflammatory activity against croton oil-induced mice ear edema assay and exhibited strong anti-edematous effect [28].

Mice pretreated with 10% suspension of grounded *C. myrrha* resin increased the licking latency in a hot plate test (52°C metal plate). The active fraction was separated by different chromatographic techniques and resulted in the isolation of furano-sesquiterpenes. This analgesic activity could explain the use of myrrh as a painkiller in ancient times [29]. An alkaloid fraction of *C. africana* assayed against several pathogenic microorganisms using the agar diffusion method, exhibited antimicrobial activities against all the test microorganisms [30]. Investigation of the anthelmintic activity of aqueous extract of *C. africana* against earthworm demonstrated a concentration-dependent activity at tested concentrations of 10-80 mg/ml [31]. The dihydroflavonol glucoside

phellamurin, isolated from a CH_2Cl_2-MeOH extract of *C. africana*, was identified as the active principle responsible for the DNA cleavage [32].

Evaluation of the cytoprotective activity of EtOH extracts of *C. caudata* bark and resin against EtOH-induced and aspirin-induced gastric lesions in rats resulted in significant reduction of the formation of gastric lesions [33, 34]. The non-polar portion of *C. erythraea* resin exhibited strong larvicidal and repellent activity against the lone star tick, the American dog tick, and adult deer tick [35]. The hexane extract of the resin of *C. holtziana* tested for its activity against the cattle tick, *Boophilus microplus*, exhibited a repellent effect lasting up to 5 h [36]. The aqueous extract of the resin of *C. incisa* significantly inhibited both the maximal edema response and the total edema response during 6 h of carrageenan-induced rat paw edema [37].

Pretreatment with EtOH extract of *C. opobalsamum* resin prevented the prolongation of the barbiturate sleeping time and replenished the non-protein sulfhydryl of the liver associated with carbon tetrachloride-induced liver damage in mice [38]. The bark extract of *C. berryi* [39] and resin extract of *C. myrrha*, *(*Synonym: *C. molmol)* [40] were also reported to exhibit hepatoprotective activity. Methanolic extract of *C. parvifolia* exhibited a strong activity against Gram-positive bacteria including multi-resistant *Staphylococcus* strains [41].

T-cadinol isolated from *C. guidottii* resin displayed smooth muscle relaxing effect on the isolated guinea pig ileum and an inhibition of cholera toxin-induced intestinal hypersecretion in mice [42].

Direct cell growth inhibitory activity of compounds isolated from *C. erlangeriana* resin have confirmed the toxicity of this resin to humans and animals [43]. Acute toxicity studies of *C. erlangeriana* resin extract and erlangerin D conducted on Swiss albino mice demonstrated LD_{50} of 410 for the extract and 140 mg/kg body weight for the compound [44]. Compounds isolated from both polar and non-polar fractions of *C. myrrha* exhibited strong cytotoxic activity against human gynecologic cancer cells [16]. The resinous material obtained from *C. myrrha*, *(*Synonym: *C. molmol)* exhibited a very strong

molluscicidal effect on *Biomphalaria arabica* snails at low concentration (40 ppm) after 48 hours exposure [45].

C. erlangeriana resin was a topic of previous work in our research group. From this resin four aryltetralin lignans (erlangerin A-D) were isolated in large quantities [46]. And this dissertation is a continuation of the chemical works of this resin, the following sections will give a brief introduction about aryltetralin and dibenzylbutyrolactone lignans.

1.1.3 Review of Aryltetralin and Dibenzylbutyrolactone Lignans

Lignans are naturally occurring phenolic compounds consisting of two phenylpropanoids (C_6-C_3) units linked at the central β-carbon (Fig.1) [47]. They are widely distributed in a large number of plant species and are also found in the urine of humans and other mammals [48].

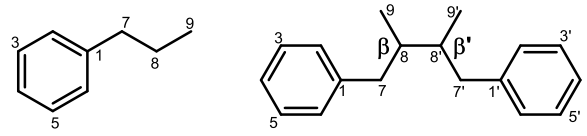

Phenylpropanoid unit **Lignan structure**

Figure 1: Phenylpropanoid unit and Lignan structure.

Lignan receives much attention in the field of natural product chemistry ever since the discovery of podophyllotoxin (**1**). Plants with high lignan contents have been extensively used in traditional Chinese, Japanese and the Eastern world folk medicine. Many lignans are known for their biological activities. The activities include reverse transcriptase inhibition, anti-HIV activity, immunomodulatory activity, effects on cardiovascular system, anti-leishmaniosis, effects on high-density lipoproteins, antifungal, anti-rheumatic, anti-psoriasis, and anti-malaria [48, 49].

1.1.3.1 Classification of Lignans

Most of the naturally available lignans are oxidized at C-9 and C-9’ and on the basis of oxygen incorporation into the skeleton and the cyclization patterns, a large number of lignans with different structural types can be formed. In general, lignans are classified into

eight groups. Fig. 2 displayed the main classes of lignans, as well as their subgroups [47, 50].

Furan, furofuran, dibenzylbutane, dibenzylbutyrolactol and dibenzylbutyrolactone lignans are simple lignans since they have a single carbon-carbon bond through the β-β' positions of the phenylpropane unit. Arylnaphtalene, aryltetralin, and dibenzocycooctadiene are cyclolignans. In addition to the above β-β'-linkage, cyclolignans have another carbon-carbon bond, giving rise rings of different size [51].

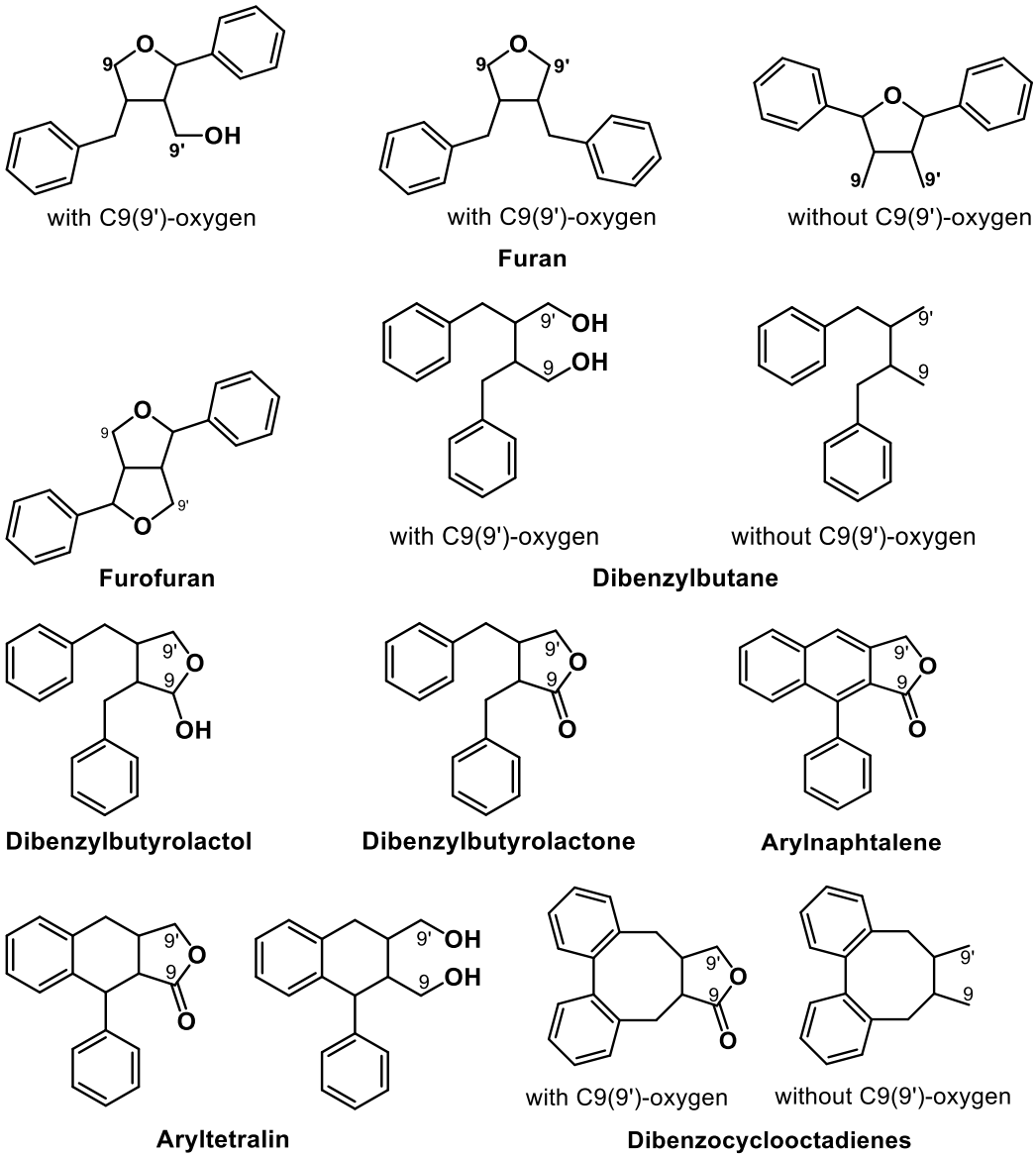

Figure 2: Main classes of lignans.

1.1.3.2 Lignan Numbering

On studying the literature concerning podophyllotoxin and related aryltetralin lignans, at least two different numbering systems have been found. These are shown in Fig.3. The first system is based on the biogenesis of lignans, where the two phenylpropane residues are numbered from 1 to 9 and 1´ to 9´. The second numbering system is based on the systematic nomenclature of the IUPAC; it considers naphthalene as the basic system giving priority, for the start of numbering, to the carbon supporting the trimethoxyphenyl group or related groups [48, 51]. The latter numbering system is followed throughout this work.

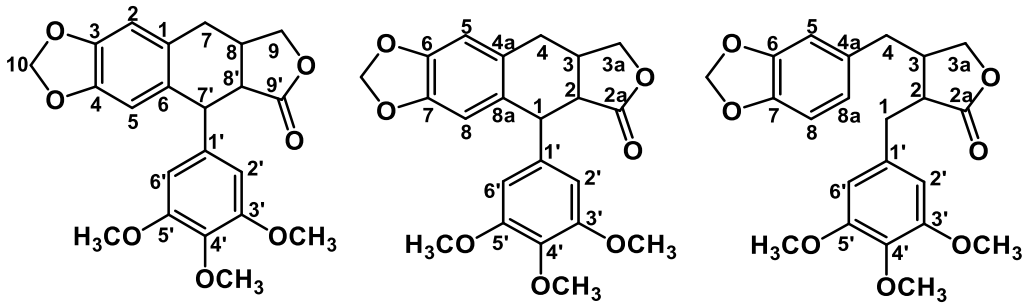

Figure 3: Numbering systems according to A) biogenesis, B and C) systematic.

1.1.3.3 Aryltetralin Lignans

Podophyllotoxin (**1**) and many closely related aryltetralin lignans are known to have important antineoplastic and antiviral properties. They have been extensively studied over the last two centuries [52-54]. Podophyllotoxin was first isolated from *Podophyllum peltatum* and *P. hexandrum* in the 1880s but its correct structure was only reported in the 1950s [55, 56].

Podophyllum is the name given for a drug obtained from the dried roots and rhizomes of these two species of *Podophyllum* [57]. It was included in the US Pharmacopoeia in 1820 and the use of this resin was prescribed for the treatment of venereal warts, attributing this action to podophyllotoxin [55].

The supply of podophyllotoxin mainly depends on the roots and rhizomes of *P. hexandrum* and *P. peltatum*, which contain 4% and 0.2%, respectively [58]. These two

species are not the only natural sources of podophyllotoxin. It has been reported from other plants such as *Sinopodophyllum emodi* [59], *Linum flavum* [60] and *Hernandia Sonora* [61].

Major Reported Grouping of Aryltetralin Lignans are the Following:

1. **Podophyllotoxins**: *epi*-podophyllotoxin (**2**) from *P. peltatum* and *P. emodi* [62]; 4-deoxypodophyllotoxin (**3**) from *P. hexandrum* [59, 61, 63, 64] and *S. emodi* [59]; 3'-demethylpodophyllotoxin (**4**) from *Linum species* [65]; 4'-demethylpodophyllotoxin (**5**) from *Dysosma versipellis* [66]; hernandin (**6**), podophyllotoxin acetate (**7**), 5-methoxypodophyllotoxin (**8**), 5-methoxypodophyllotoxin acetate (**9**) from *H. sonora* and *L. flavum* [60, 61]; 5'-desmethoxy-β-peltatin A methyl ether (**10**) from *B. fagaroides* [67]; α-peltatin (**11**), β-peltatin (**12**) from *L. flavum* [60, 68]; 5-methoxypodophyllotoxin (**13**) from *J. sabina* [69]; 4-acetyl-4'-demethylpodophyllotoxin (**14**) from *S. emodi* [59]; 4-butyrylpodophyllotoxin (**15**) from *B. microphylla* [70], 6,7-demethylenedeoxypodophyllotoxin (**19**) from *H. ovigera* [71]; 3',4'-demethylenedeoxy-podophyllotoxin (**20**) and 3',4'-demethylenedeoxy-4-demethylpodophyllotoxin (**21**) from *S. emodi* [59].
2. **Isopodophyllotoxins**: isopodophyllotoxin (**16**) from *P. peltatum* and *P. emodi* [62]; *epi*-isopodophyllotoxin (**17**) from *P. peltatum* and *P. emodi* [62]; 4'-demethyl-deoxyisopodophyllotoxin (**18**) from *S. emodi* [59] and *P. hexandrum* [71].
3. **Picropodophyllotoxins**: picropodophyllotoxin (**22**) from *H. sonora* [61]; 7'-acetyl-picropodophyllotoxin (**23**) from *H. ovigera* [71] and *Bursera fagaroides* [67]; β-peltatin B methylether (**24**), 5-methoxyepipicropodophyllotoxin (**25**), 5-methoxyepipicro-podophyllotoxin acetate (**26**), 5-methoxypicropodophyllotoxin (**27**), 5-methoxypicro-podophyllotoxin acetate (**28**) form *J. sabina* [69].
4. **Aryltetralin lignans containing two methylenedioxy groups**: cleistantoxin (**29**), cleisindoside A (**30**), cleisindoside C (**31**), cleisindoside D (**32**) and cleisindoside E (**33**) from *Cleistanthus indochinensis* [72]; austrobailignan 9 (**34**) and austrobailignan 1 (**35**) from *Austrobaileya scandens* [73].
5. **Other glycoside aryltetralin lignans**: Sinolignan A (**36**), 4-demethylepi-podophyllotoxin-7'-O-β-D-glucopyranoside (**37**), 4-demethylpodophyllotoxin-7'-O-β-

D-glucopyranoside (**38**), podophyllotoxin-7'-O-β-D-glucopyranoside (**39**) and 4-demethyldeoxypodophyllotoxin-4-O-β-D-glucopyranoside (**40**) from *S. emodi* [59, 63, 64]; β-peltatin 5-O-glucoside (**41**) and α-peltatin 5-O-glucoside (**42**) from *P. versipelle* [74].

6. **Podophyllones**: isopicropodophyllone (**43**) from *S. emodi* [59]; 4'-demethylisopicro-podophyllone (**44**) from *P. versipelle* [74]. And polgamatin (**45**) *Polygala polygama* [75].

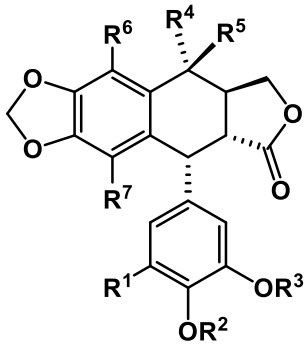

	R^1	R^2	R^3	R^4	R^5	R^6	R^7
1:	OCH_3	CH_3	CH_3	OH	H	H	H
2:	OCH_3	CH_3	CH_3	H	OH	H	H
3:	OCH_3	CH_3	CH_3	H	H	H	H
4:	OCH_3	CH_3	H	OH	H	H	H
5:	OCH_3	H	CH_3	H	OH	H	H
6:	OCH_3	CH_3	CH_3	H	H	H	OCH_3
7:	OCH_3	CH_3	CH_3	OAc	H	H	H
8:	OCH_3	CH_3	CH_3	OH	H	H	OCH_3
9:	OCH_3	CH_3	CH_3	OAc	H	H	OCH_3
10:	OCH_3	CH_3	CH_3	OH	H	H	H
11:	OCH_3	H	CH_3	H	H	OH	H
12:	OCH_3	CH_3	CH_3	H	H	OH	H
13:	OCH_3	CH_3	CH_3	OH	H	OCH_3	H
14:	OCH_3	H	CH_3	OAc	H	H	H
15:	OCH_3	H	CH_3	Butyrate	H	H	H

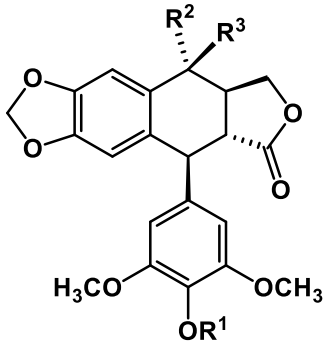

	R^1	R^2	R^3
16	CH_3	OH	H
17	CH_3	H	OH
18	H	H	H

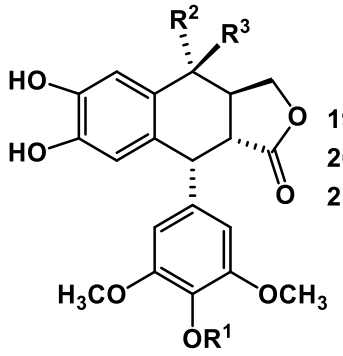

	R^1	R^2	R^3
19	CH_3	H	H
20	CH_3	OH	H
21	H	OH	H

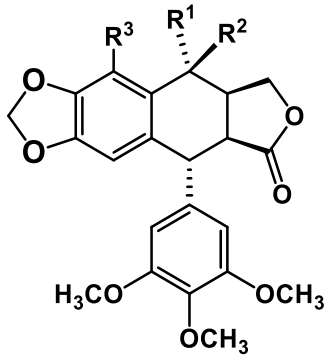

	R^1	R^2	R^3
22	OH	H	H
23	OAc	H	H
24	H	H	OCH_3
25	OH	H	OCH_3
26	H	OAc	OCH_3
27	OH	H	OCH_3
28	OAc	H	OCH_3

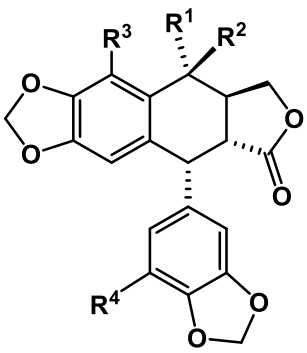

	R^1	R^2	R^3	R^4
29	OH	H	OCH_3	H
30	H	O–β–D-Glc	H	H
31	H	O–β–D-Glc-^{6}-Glc	H	H
32	O–β–D-Glc	H	OCH_3	H
33	O–β–D-Glc-^{6}-Ac	H	OCH_3	H
34	H	H	OCH_3	OCH_3
35	H	H	H	OCH_3

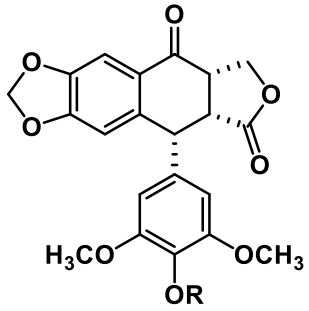

43 R = CH_3
44 R = H

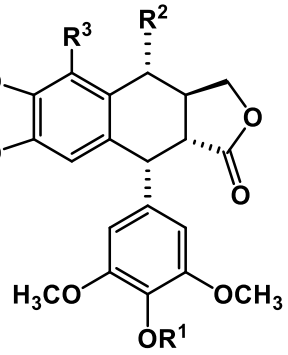

	R^1	R^2	R^3
36	CH_3	O–β–D-Glc-^{6}-Ac	H
37	H	β–O–β–D-Glc	H
38	H	α–O–β–D-Glc	H
39	CH_3	α–O–β–D-Glc	H
40	O–β–D-Glc	H	H
41	CH_3	H	O–β–D-Glc
42	H	H	O–β–D-Glc

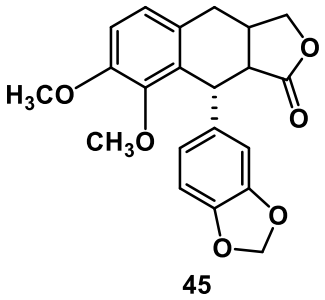

45

1.1.3.4 Dibenzylbutyrolactone Lignans

Dibenzylbutyrolactone lignans like aryltetralin lignans represent a unique group of plant secondary metabolites with increasing significance in medicine. Over 85 natural dibenzylbutyrolactone lignans are known to date [76] and exhibited a vast number of biological activities [46, 77]. Some of these lignans including their sources are listed in Table 2.

Table 2: Reported dibenzylbutyrolactone lignans in different articles

Compounds	**Plant Source**	**Ref**
arctiin (**46**), arctigenin (**47**), matairesinol (**48**) and demethyl-traxillagenin (**49**)	*Forsythia species, W. sikokiana, B. fructus, S. medusa* and *A. lappa*	[78-82]
wikstromol (**50**)	*W. sikokiana*	[79]
cubebininolide (**51**), 3',4',5',6,7-pentamethoxydibenzylbutyro-lactone (**52**), 4',7-dihydroxy-3',5',6-trimethoxydibenzylbutyro-lactone (**53**), 4'-hydroxy-3',6,7,8-tetramethoxydibenzylbutyro-lactone (**54**) and 3',4',6,7,8-pentamethoxydibenzylbutyrolactone (**55**)	*P. cubeba*	[83]
6-demethyl-5'-hydroxymatairesinol (**56**) and 6-demethyl-5'-methoxymatairesinol (**57**)	*M. pomiferus*	[84]
traxillagenin (**58**) and traxillaside (**59**)	*T. nucifera*	[85]

2,3',4'-trihydroxy-6,7-dimethoxybenzylbutyrolactone (**60**), 2,3'-dihydrox-6,7-dimethoxy-4'-O-β-D-glucopyranosyldibenzylbutyrolactone (**61**), 2,3',4',6,7-pentahydroxydibenzylbutyrolactone (**62**), 2,3',7-trihydroxy-6-methoxy-4'-O-β-D-glucopyranosyldibenzylbutyrolactone (**63**) and 2,3'-dihydroxy-6,7-dimethoxy-4'-O-β-D-glucopyranosyldibenzylbutyrolactone (**64**)	*P. rugosus*	[86]
trachelogenin (**65**)	*I. cairica*	[87]
enterolactone (**66**)	Mammal	[71]
4-hydroxyararctigenin (**67**)	Safflower seeds	[71]
(-)-traxillagenin (**68**) and (-)-7-demethyltraxillagenin (**69**)	*T. nucifera*	[88]
nortrachelogenin (**70**)	Knotwood extracts (Tree species)	[89]
(2R,3R)-matairesinol-4'-O-β-D-xylopyranosyl-(1→2)-O-β-D-glucopyranoside (**71**)	*Symplocos caudate*	[90]
4-hydroxynortrachelogenin (**72**) and allohydroxymatairesinol (**73**)	*T. cuspidate*	[91]
4,7-dihydroxy-3',6-dimethoxy-4'-O-β-D-glucopyranosyldibenzylbutyrolactone (**74**)	*A. fructus*	[92]
yatein (**75**) and 8-methoxyyatein (**76**)	*L. yateensis* and *M. pomiferus*	[84, 93]
kusunokinin (**77**)	*W. sikokiana*	[79]
3',4'-methylenedioxy-5',6,7,8-tetramethoxy-4'-O-β-D-glucopyranosyldibenzylbutyrolactone (**78**) and (-)-cubebinone (**79**)	*P. cubeba*	[83]
(-)-hinokinine (**80**)	*V. sebifera*	[94, 95]
(-)-methylpluviatolide (**81**)	*Z. naranjillo*	[95]
2-hydroxy-3',4',6,7-dimethylenedioxydibenzylbutyrolactone (**82**)	*I. cairica*	[87]
8-methoxyyatein (**83**)	*M. pomiferus*	[84]
(-)-pluviatolide (**84**) and (-)-haplomyrfolin (**85**)	*Chamaecyparis obtuse*	[96]
bursehernin (**86**), podorhizol (**87**) and podorhizol-1-O-β-D-glucopyranoside (**88**)	*H. ovigera* and S. *emodi*	[63, 97]
podorhizol acetate (**89**)	*J. sabina*	[69]
epi-podorhizol (**90**)	*H. verticillata*	[98]
4-hydroxymatairesinol (**91**)	*P. abies*	[99]
dimethylmatairesinol (**92**)	*C. camphora*	[100]
styraxlignolide C (**93**), styraxlignolide D (**94**) and styraxlignolide E (**95**)	*S. japonica*	[101]
wasabisides A (**96**), wasabisides B (**97**) and wasabisides C (**98**)	*W. japonica* and *Patrinina villosa*	[102, 103]
dextrobursehernin (**99**) and heliobuphthalmin lactone (**100**)	*P. urinaria*	[104]
(2S,3S)-3',4',6,7-dimethylenedioxy-5',8-dimethoxydibenzylbutyrolactone(**101**), (2S,3S)-4'-hydroxy-6,7-methylenedioxy-3',8-dimethoxydibenzylbutyrolactone(**102**) and (2S,3S)-4'-hydroxy-6,7-methylenedioxy-3',5',8-trimethoxydibenzylbutyrolactone(**103**)	*Peperomia duclouxii*	[105]
(2R,3S)-2-acetoxy-6,7-methylenedioxy-3',4'-dimethoxydibenzylbutyrolactone (**104**)	*Bupleurum acutifolium*	[106]
cis-dibenzylbutyrolactone (**105**)	*P. santalinus*	[71]
(2R,3S)-3',4'-methylenedioxy-6.7-dimethoxydibenzylbutyrolactone (**106**)	*Virola sebifera*	[94]
savinin (**107**)	*P. santalinus*	[107]

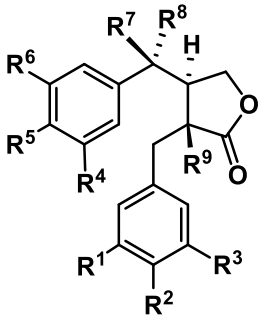

	R^1	R^2	R^3	R^4	R^5	R^6	R^7	R^8	R^9
46	H	O-D-Glc	OCH_3	H	OCH_3	OCH_3	H	H	H
47	H	H	OCH_3	H	OCH_3	OCH_3	H	H	H
48	H	H	OCH_3	H	OH	OCH_3	H	H	H
49	H	H	OCH_3	OCH_3	OH	OCH_3	H	H	H
50	H	H	OCH_3	H	OH	OCH_3	H	H	H
51	OCH_3	OCH_3	OCH_3	OCH_3	OCH_3	OCH_3	H	H	H
52	OCH_3	OCH_3	OCH_3	H	OCH_3	OCH_3	H	H	H
53	OCH_3	OH	OCH_3	H	OH	OCH_3	H	H	H
54	OCH_3	OH	H	OCH_3	OCH_3	OCH_3	H	H	H
55	OCH_3	OCH_3	H	OCH_3	OCH_3	OCH_3	H	H	H
56	OCH_3	OH	OCH_3	H	OH	OH	H	H	H
57	OCH_3	OCH_3	OCH_3	H	OH	OH	H	H	H
58	H	OH	OCH_3	OCH_3	OCH_3	OCH_3	H	H	H
59	H	O-D-Glc	OCH_3	OCH_3	OCH_3	OCH_3	H	H	H
60	H	OH	OH	H	OCH_3	OCH_3	H	H	OH
61	H	O-D-Glc	OH	H	OCH_3	OCH_3	H	H	OH
62	H	OH	OH	H	OH	OCH_3	H	H	OH
63	H	O-D-Glc	OH	H	OH	OCH_3	H	H	OH
64	H	O-D-Gal	OH	H	OCH_3	OCH_3	H	H	OH
65	H	OCH_3	OCH_3	H	OH	OCH_3	H	H	OH
66	H	H	OH	H	H	OH	H	H	H
67	H	OH	OCH_3	H	OCH_3	OCH_3	OH	H	H
68	H	OH	OCH_3	OCH_3	OCH_3	OCH_3	H	H	H
69	H	OH	OCH_3	OCH_3	OH	OCH_3	H	H	H
70	H	OH	OCH_3	H	OH	OCH_3	H	H	OH
71	H	O-D-Glc-^{6}-Glc	OCH_3	H	OH	OCH_3	H	H	H
72	H	OH	OCH_3	H	OH	OCH_3	OH	H	OH
73	H	OH	OCH_3	H	OH	OCH_3	H	OH	OH
74	H	O-D-Glc	OCH_3	H	OH	OCH_3	H	H	OH

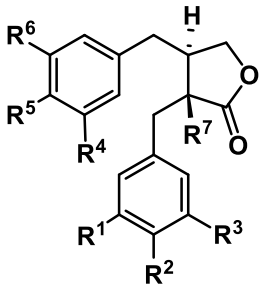

	R^1	R^2	R^3	R^4	R^5	R^6	R^7
75	OCH_3	OCH_3	OCH_3	H	O-CH_2-O		H
76	OCH_3	OCH_3	OCH_3	CH_3	O-CH_2-O		H
77	H	O-CH_2-O		H	OCH_3	OCH_3	H
78	OCH_3	O-CH_2-O		OCH_3	OCH_3	OCH_3	H
79	H	O-CH_2-O		OCH_3	OCH_3	OCH_3	H
80	H	O-CH_2-O		H	O-CH_2-O		H
81	H	OCH_3	OCH_3	H	O-CH_2-O		H
82	H	O-CH_2-O		H	O-CH_2-O		OH
83	OCH_3	OCH_3	OCH_3	OCH_3	O-CH_2-O		H
84	H	OH	OCH_3	H	O-CH_2-O		H
85	H	O-CH_2-O		H	OH	OCH_3	H

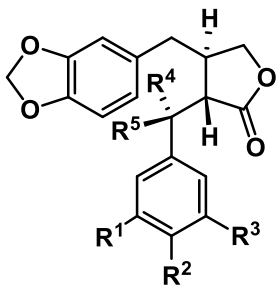

	R^1	R^2	R^3	R^4	R^5
86	H	OCH_3	OCH_3	H	H
87	OCH_3	OCH_3	OCH_3	H	OH
88	OCH_3	OCH_3	OCH_3	H	O-β-D-Glc
89	OCH_3	OCH_3	OCH_3	H	OAc
90	OCH_3	OCH_3	OCH_3	OH	H

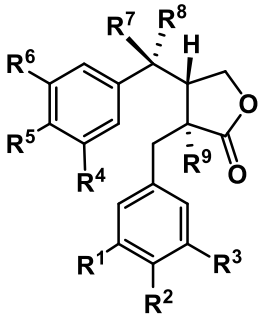

	R^1	R^2	R^3	R^4	R^5	R^6	R^7	R^8	R^9
91	H	OH	OCH_3	H	OH	OCH_3	OH	H	H
92	H	OCH_3	OCH_3	H	OCH_3	OCH_3	H	H	H
93	H	O-D-Glc	OCH_3	H	OCH_3	OH	H	H	H
94	H	O-D-Glc	OCH_3	H	OH	OH	H	H	H
95	H	OH	OCH_3	H	O-D-Glc	OCH_3	H	H	H
96	H	OH	OCH_3	H	OH	OCH_3	H	O-D-Glc	H
97	H	OH	OCH_3	H	O-D-Glc	OCH_3	H	OH	H
98	H	OH	OCH_3	OCH_3	O-D-Glc	OCH_3	H	OH	H
99	H	OCH_3	OCH_3	H	$O-CH_2-O$		H	H	H
100	H	$O-CH_2-O$		H	$O-CH_2-O$		H	H	H
101	OCH_3	$O-CH_2-O$		OCH_3	$O-CH_2-O$		H	H	H
102	H	OH	OCH_3	H	$O-CH_2-O$		H	H	H
103	OCH_3	OH	OCH_3	H	$O-CH_2-O$		H	H	H

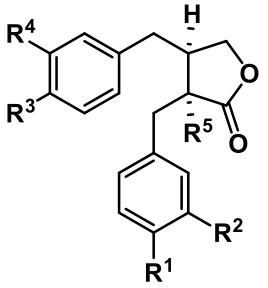

	R^1	R^2	R^3	R^4	R^5
104	OCH_3	OCH_3	OCH_3	OCH_3	OAc
105	$O-CH_2-O$		OCH_3	OCH_3	H

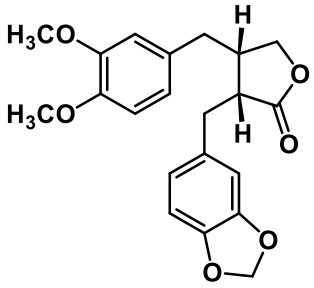

106

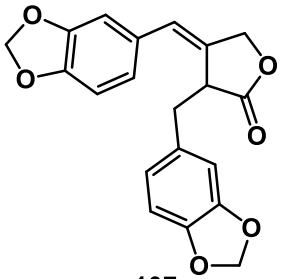

107

1.1.3.5 Lignans Reported from *Commiphora* Species

Only six lignans so far reported from *Commiphora* species, four are reported from our research group *i.e.* erlangerins A-D (**110**-**113**) from *C. erlangeriana* [109]. The two others are polygamain (**108**) and picropolygamain (**109**) from *C. incisa* and *C. kua* [108]. Erlangerins C and D have a podophyllotoxin-type skeleton, closely follow the activity profile of podophyllotoxin [43].

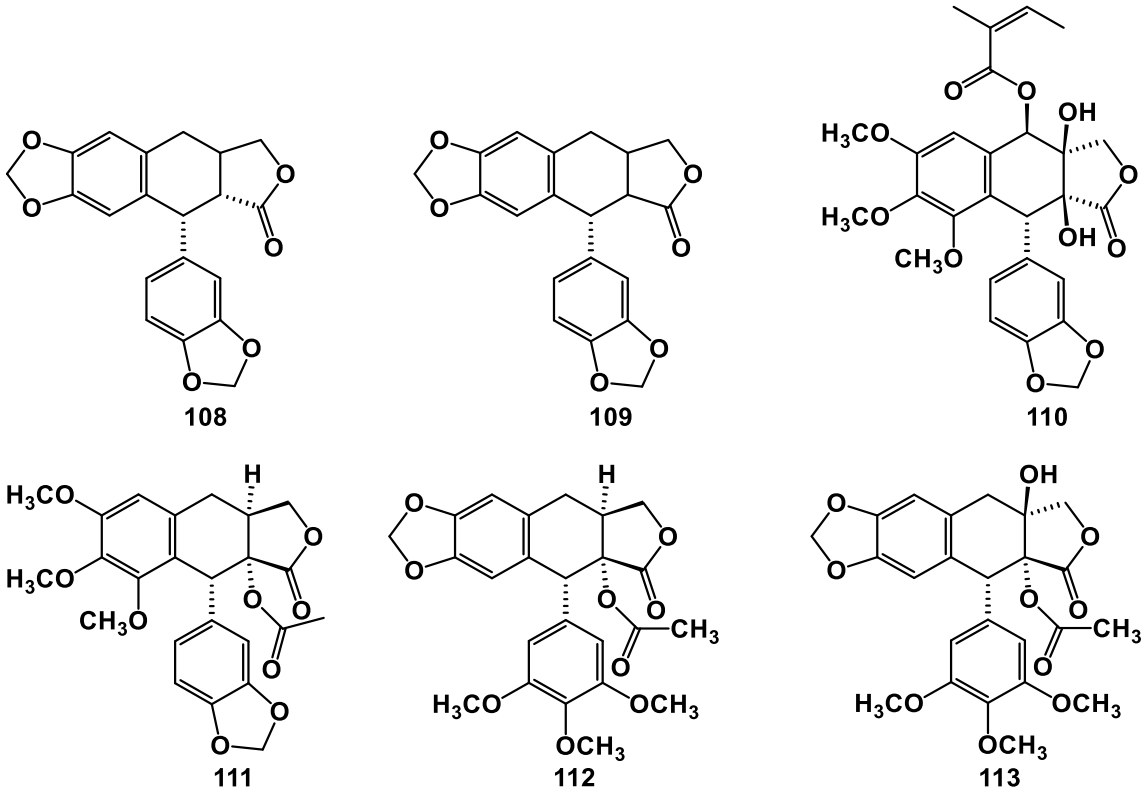

1.1.3.6 Biosynthesis of Aryltetralin and Dibenzylbutyrolactone Lignans

The limited availability and high demands for the source plants of podophyllotoxin and its derivatives have led to the exploration of alternative sources for these compounds. Hence, several studies have been carried out in different species of *Forsythia, Linun,* and *Podophyllum* to elucidate the biogenetic pathways of podophyllotoxins and their precursor dibenzylbutyrolactone lignans [110-115].

The methoxy groups other than 6 and 3'-methoxys are introduced into phenylpropanoid monomers (coniferyl alcohol), by lignan-OMT-catalyzed post-coupling methylation of the corresponding hydroxyl group [111]. The enzymes that catalyze each step and the precursor molecules involved in the biosynthesis of aryltetralin and dibenzylbutyrolactone lignans are depicted in Fig. 4.

In the initial step, coniferyl alcohol (**115**) is biosynthesized from phenylalanine by the action of phenylpropanoid enzymes. The first precursor, pinoresinol (**116**), is synthesized by the stereospecific coupling of two units of achiral *E*-coniferyl alcohol in the presence

of a dirigent protein (DIR). A pinoresinol-lariciresinol reductase (PLR) converts **116** to secoisolariciresinol (**118**) via lariciresinol (**117**) in an enantiospecific manner, and subsequently, secoisolariciresinol dehydrogenase (SIRD) changes **118** to matairesinol (**119**). In the next step, the methylenedioxy group is introduced to **119** with the help of the enzyme CYP719A23 to form pluviatolide (**120**). Then, the 4'-hydroxyl group on **120** is methylated to give 5'-desmethoxyyatein (**121**) by O-methyltransferase (OMT). The hydroxylating enzyme CYP71CU1 changes **121** to desmethylyatein (**122**), then the second OMT converts **122** to the most common dibenzylbutyrolactone lignan yatein (**123**).

The ring closing step, conversion of dibenzylbutyrolactone lignan **123** to aryltetralin lignan (**124**), is performed by incubating the enzyme 2-ODD with **123** as the substrate. The final step of (–)-podophyllotoxin biosynthesis involves hydroxylation of (-)-Deoxy-podophyllotoxin (**124**). (–)-4'-Desmethylepipodophyllotoxin (**126**), the direct precursor to etoposide, could be obtained biosynthetically from **124** by demethylation of the 4'-methoxy group and then hydroxylation of the C-4 position using the enzyme CYP71BE54 and CYP82D61, respectively [116].

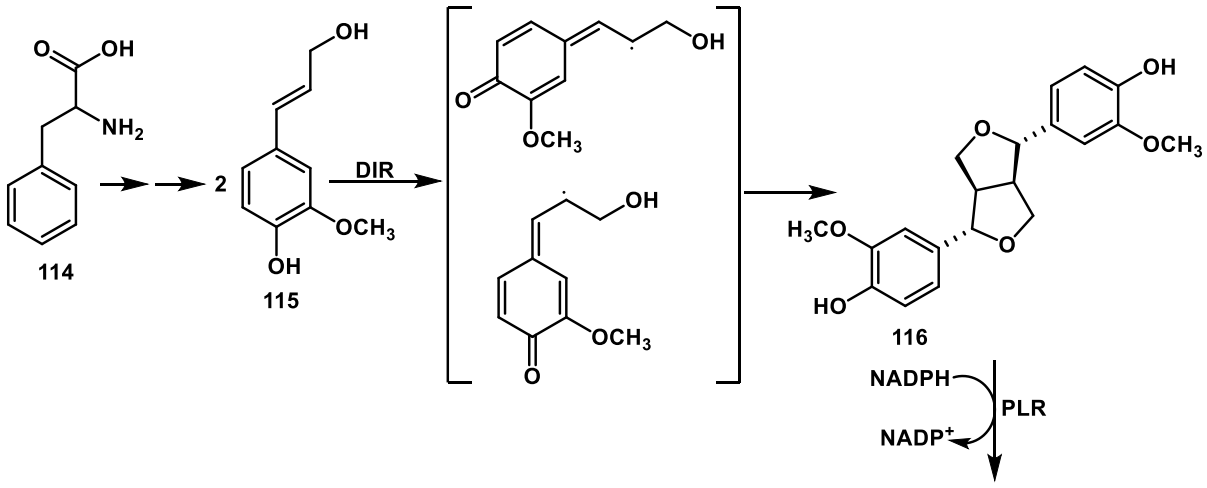

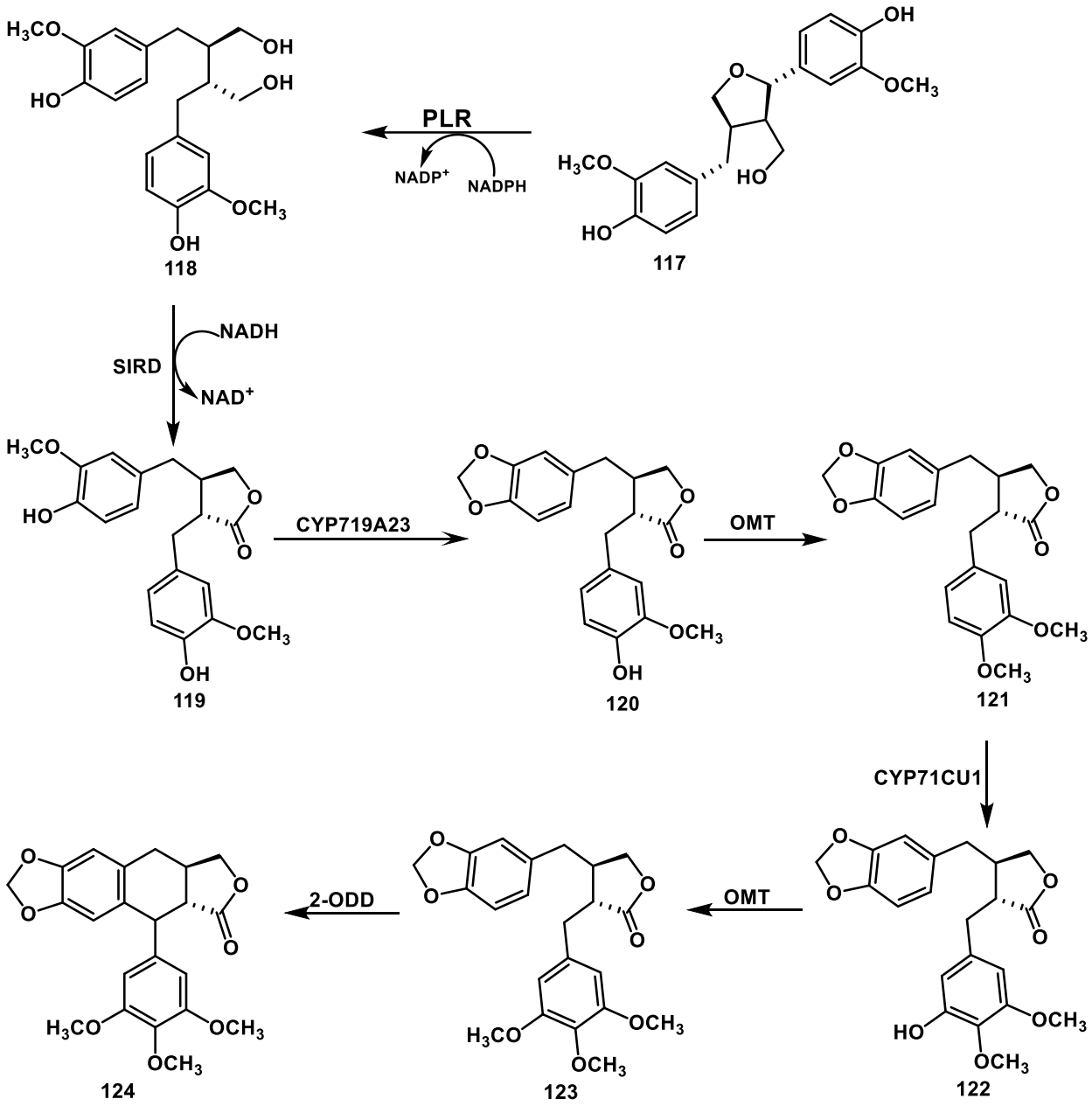
PLR
NADP+
NADPH
118
117
SIRD
NADH
NAD+
CYP719A23
OMT
119
120
121
CYP71CU1
2-ODD
OMT
124
123
122

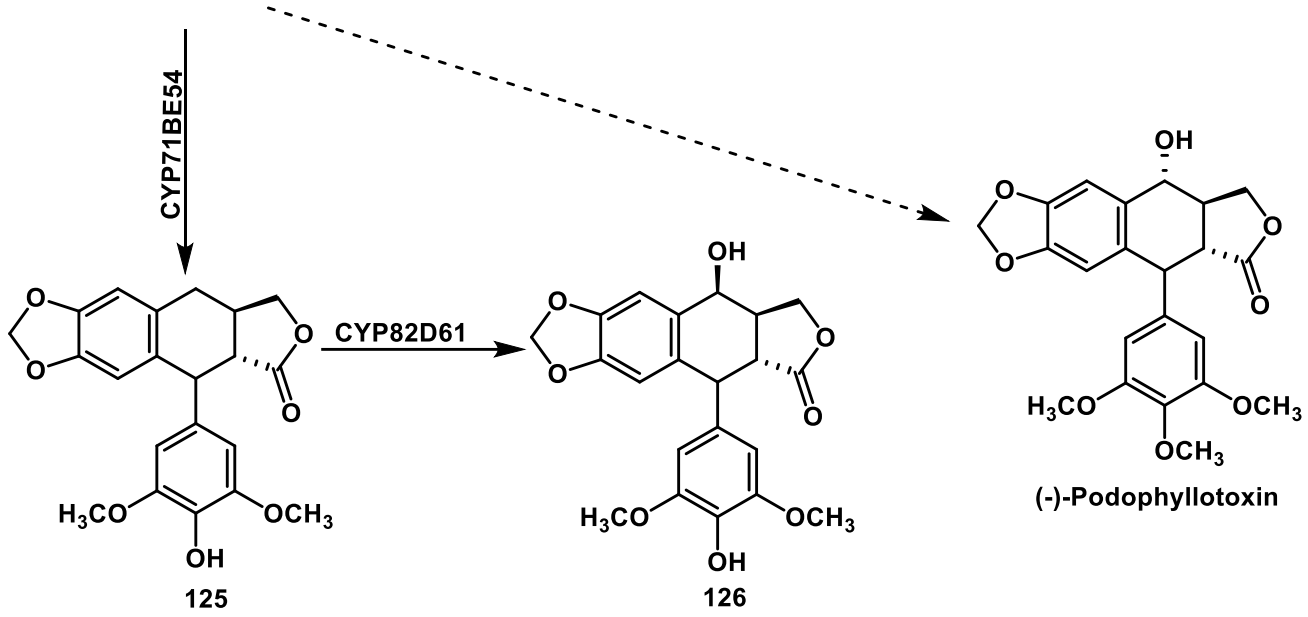

Figure 4: Biosynthesis of aryltetralin and dibenzylbutyrolactone lignan.

1.1.3.7 Anticancer Drugs of Podophyllotoxin Derivatives

The aryltetralin lignan, podophyllotoxin, and its natural derivatives have become one of the most attractive subjects due to their broad spectrum of pharmacological activities. They are used as the starting compounds for the semi-synthesis of commercially available anticancer drugs such as etoposide (**127**), teniposide (**128**) and etopophos (**129**) Figure 5 [117, 118].

Etoposide (Trade names: Toposar and VePesid) is marketed for testicular cancer, small cell lung cancer, Hodgkin's disease, leukemia, ovarian cancer, brain tumors etc., and in combination trials. Teniposide (Trade name: Vumon) is used for childhood acute lymphocytic leukemia (ALL), Hodgkin's lymphoma, certain brain tumors, and other types of cancer etc., and in combination trials. Etoposide Phosphate (Trade name: Etopophos) is marketed for testicular cancer, lung cancer, lymphoma leukemia, ovarian cancer and in combination trials [51, 119, 120].

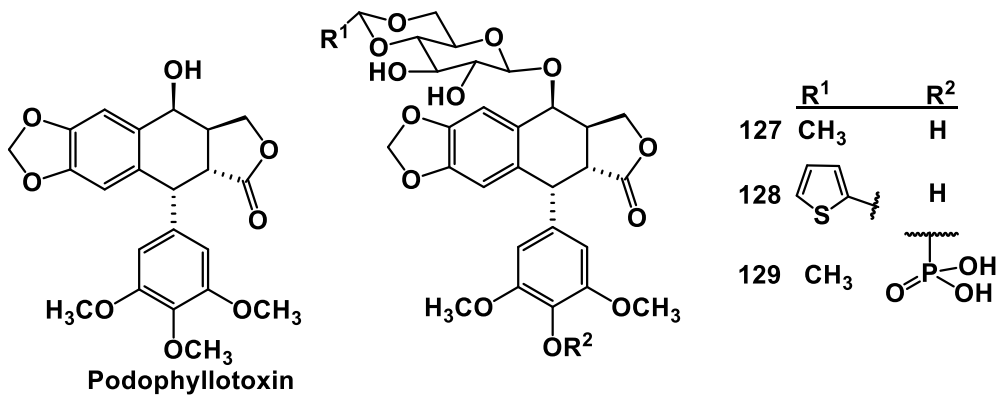

Figure 5: Structure of podophyllotoxin derivatives in clinical use.

In spite of the fact that the above three drugs are clinically valuable anticancer agents, several adverse effects and drug resistance have been associated with the use of these drugs. Based on these, a great number of potential drug candidates were semi-synthesized. Figure 6 shows the structures of new anticancer candidates developed from podophyllotoxin chemical skeleton. All of these compounds entered the different clinical trial stages [51, 62, 118, 119, 121]

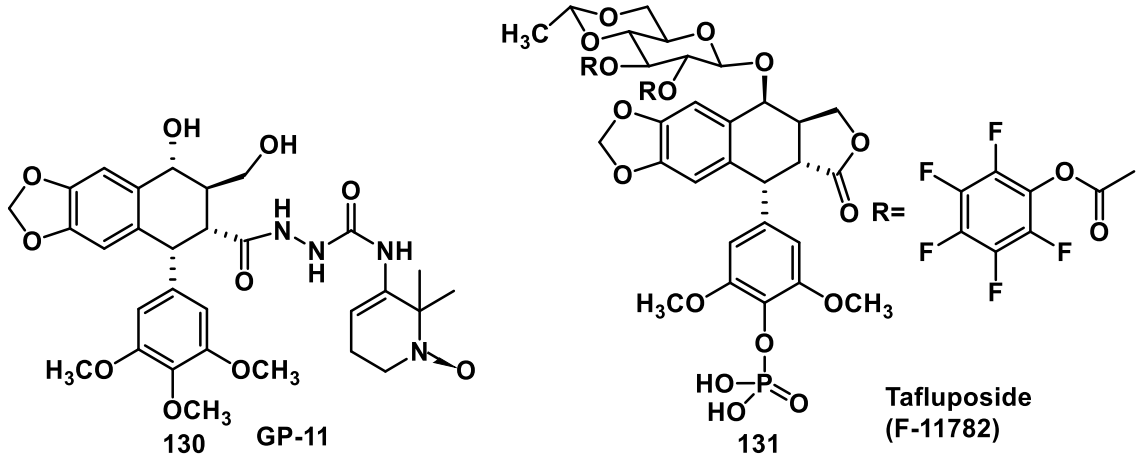

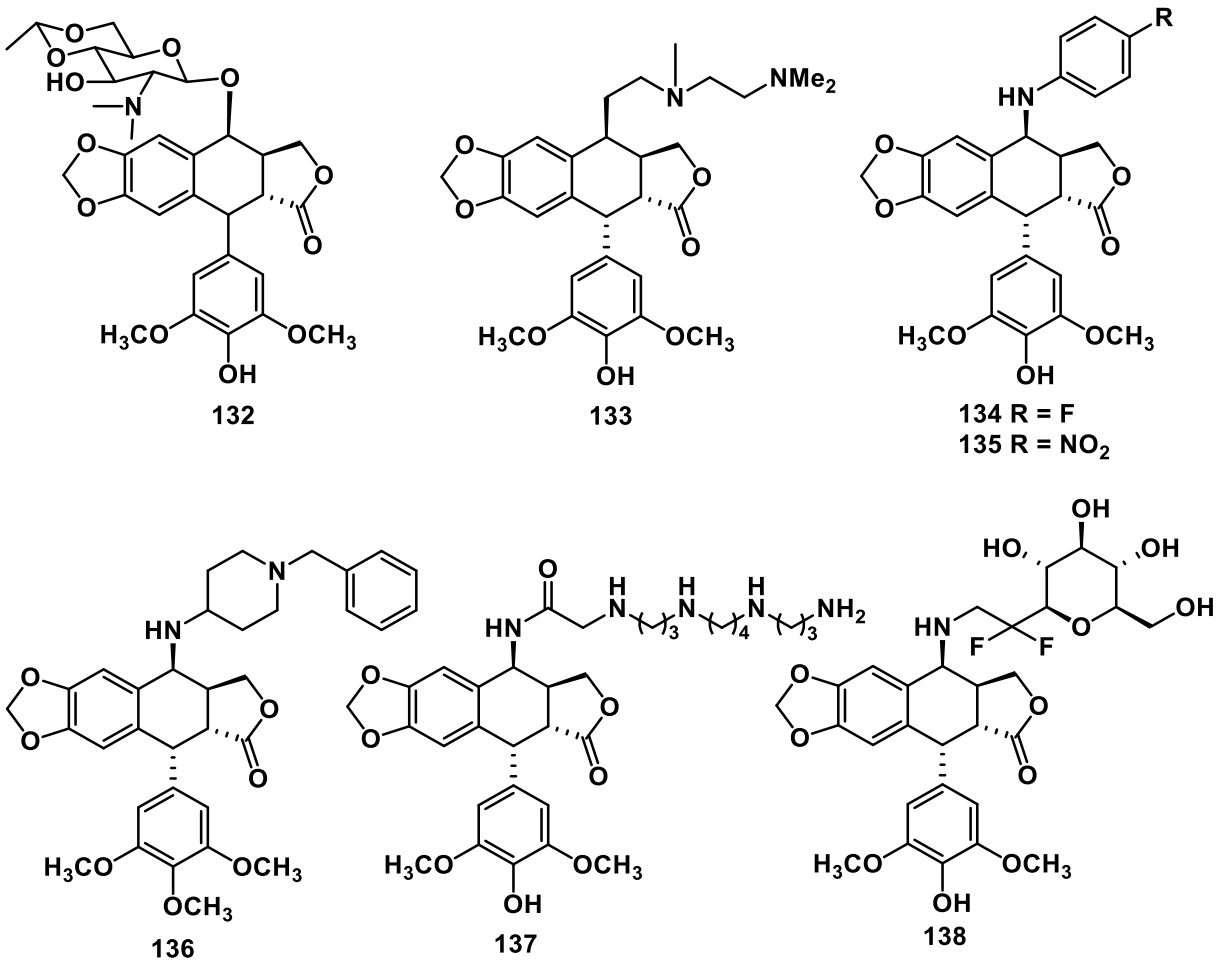

Figure 6: podophyllotoxin derivatives currently in clinical trials

1.1.3.8 The Mode of Action of Podophyllotoxin and Its Derivatives

Podophyllotoxin inhibits the formation of microtubules. *In vitro,* it binds to tubulin dimers giving podophyllotoxin-tubulin complexes. This binding stops the further formation of the microtubules at one end but does not stop the disassembly at the other end leading to the degradation of the microtubules. Cells treated with podophyllotoxin are arrested in the metaphase of the mitosis [51].

The clinically applied podophyllotoxin-derivatives etoposide, teniposide, and etopophos have a completely different mode of action. These compounds are topoisomerase II inhibitors. Topoisomerase II is an enzyme that cleaves double-stranded DNA and seals it again after unwinding. It is crucial in the processes of DNA replication and repair. For its function, topoisomerase II binds covalently to the broken DNA. Podophyllotoxin-

derivative drugs stabilize the DNA-topoisomerase II complex in such a way that resealing of the DNA strands becomes impossible. Cells that are duplicating their DNA for the mitosis are very sensitive to this mechanism. The overall effect of these anticancer drugs is the arrest of the cells in late S or early G2 phase of the cell cycle [122].

1.1.4 The Aim of This Study

The resin of *C. erlangeriana*, locally known as *Dunkel*, is used by the local people as an arrow poison to kill a wild animal like a hyena. As mentioned above, previous chemical investigation in this plant resin revealed that the resin possesses four novel aryltetralin type lignans. Two of these lignans namely erlangerin C and erlangerin D were exhibited cytotoxic activity comparable with the known podophyllotoxin.

Therefore, the main objective of this dissertation was to isolate and characterize more aryltetralin (podophyllotoxin and polygamatin-types) and other forms of lignans from the resin of *C. erlangeriana* collected from Ethiopia.

1.2 Results and Discussion

In this work, we report 28 new and 6 known compounds from the resin of *C. erlangeriana*. The 34 compounds can be classified into 19 aryltetralins (podophyllotoxin- and polygamatin-types), 10 dibenzylbutyrolactone-type and 5 other type. The four known lignans, namely erlangerins A-D were reported previously as novel compounds by our research group from the same resin [109]. The new compounds have been named as erlangerins E to Z and Z1 to Z7. We describe the characterization of all the isolated compounds in this work.

1.2.1 Characterization of Compounds

Characterization of 139 (Erlangerin E)

Compound **139** was obtained as a white crystal with mp 164-166 ^{0}C. It has an optical rotation of $[\alpha]_D^{20}$ +86.0 (*c* 0.10, MeOH). The molecular formula $C_{32}H_{34}O_{12}$, was determined from the $[M + Na]^+$ peak at m/z 633.1949 in the ESIHRMS spectrum. The UV spectrum showed absorption maxima (λ_{max}) at 207 and 284 nm and the IR spectral data indicated the presence of OH (3471 cm^{-1}), aromatic ring (1603, 1504 and 1457 cm^{-1}), lactone carbonyl (1786 cm^{-1}), ester carbonyl (1716 cm^{-1}), C-O group (1034 cm^{-1}), methylenedioxy (928 cm^{-1}) and 1,2,3-trisubstituted aromatic ring (848 cm^{-1}) [123].

The ^{1}H NMR spectrum of **139** (Table 3) revealed the presence of four aromatic protons at δ_H 6.71 (2H, m), 6.67 (d, *J*=8.1 Hz, H-6) and 6.93 (s, H-5), together with two olefinic protons, represented by the proton signals at δ_H 6.15 (1H, q, *J*=7.2 Hz) and 6.24 (q, *J*=6.7 Hz). The presence of three aromatic methoxy groups and a methylenedioxy group was indicated by signals at δ_H 3.69, 3.84 and 3.90 and δ_H 5.93 (dd, *J* = 8.9, 1.5 Hz), respectively. The aliphatic proton signals at δ_H 4.47 (d, *J* = 10.9 Hz) and 4.00 (d, *J* = 10.9 Hz) were due to oxymethylene protons. The two methine proton signals at δ_H 5.15 (s) and 5.96 (s) were assignable to benzylic protons of H-1 and H-4. The spectrum also contained three methyl proton signals for four methyl groups at δ_H 2.07 (m), 1.80 (d, *J* = 7.3 Hz) and 1.73 (s).

The ^{13}C NMR spectrum (Table 3) showed 32 signals for 32 carbons. The two aromatic ring carbons were represented twelve signals between δ_C 121.0 – 153.3. The methylenedioxy and oxymethylene carbons were represented by signals at δ_C 101.3 and 80.1, respectively. The carbon signals at δ_C 44.2 and 71.8 were assignable to the two benzylic carbons (C-1 and C-4). The oxygenated quaternary signals appeared at δ_C 85.5 and 79.6 were due to lactone ring junction carbons of C-2 and C-3, respectively. The three methoxy carbons were represented by three signals at δ_C 61.6, 61.0 and 56.0. The carboxylate signals at δ_C 171.8, 169.0 and 167.3 were due to a lactone and two angeloyl carbonyl carbons, respectively. The remaining four methyl signals together with four olefinic carbon signals at 142.7, 140.6, 126.8, and 126.4 were assigned to the angeloyl groups.

Detailed analysis of ^1H-^1H COSY and HMBC spectra (Figure 7) revealed the presence of two angelate groups. One of the angelate groups contained the olefinic proton (δ_H 6.24) and the two overlapped methyls (δ_H 2.07) and the second angelate group contained the olefinic proton (δ_H 6.15) together with the two methyls (δ_H 1.80 and 1.73).

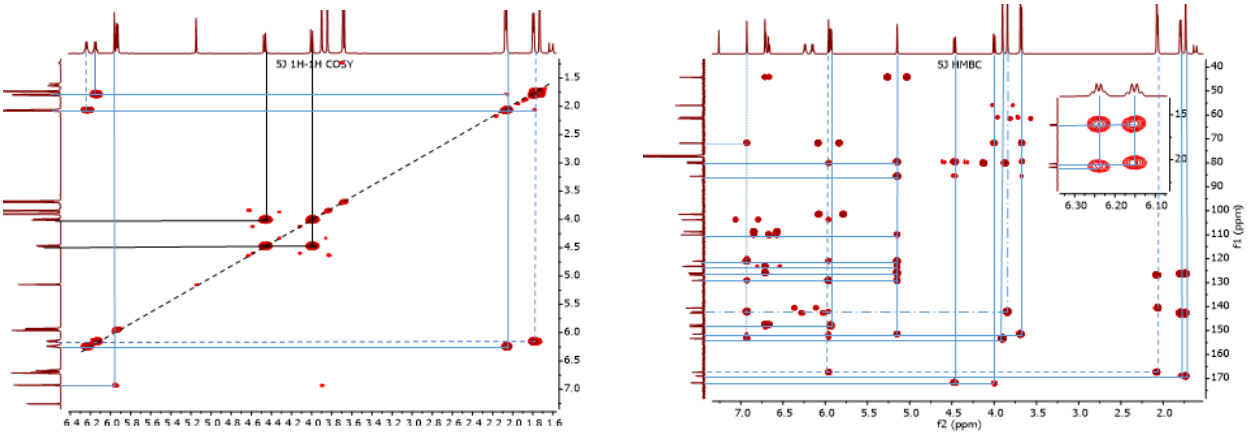

Figure 7: ^1H-^1H COSY and HMBC spectra of **139.**

The HMBC spectrum showed cross-peaks from H-1 (δ_H 5.15) to δ_C 151.5 (C-8), 110.0 (C-2') and 123.2 (C-6'), supporting the linkage of C-1 to both aromatic rings (ring-A and ring D). HMBC cross-peaks between H-5 (δ_H 6.93) and C-4 (δ_C 71.8) and between H-4 (δ_H 5.96) and C-8a (δ_C 121.0) confirmed the C-4a and C-4 connection (Figure 8). And the presence of the lactone ring was confirmed by cross-peaks between the oxymethylene

protons at δ_H 4.47 and 4.00 (H_2-3a) and the ester carbonyl carbon C-2a (δ_C 171.8). The three-bond correlations between the methylenedioxy protons at δ_H 5.94 and C-3' (δ_C 147.6) and C-4' (δ_C 148.3) indicated the position of the methylenedioxy group at C-3' and C-4' of the D-ring.

The position of the angelate moiety containing the carbonyl at δ_C 167.3 was obtained from HMBC correlation between H-4 (δ_H 5.96) and the carbonyl carbon (δ_C 167.3). HMBC correlation between the OH proton (δ_H 3.67) and C-3 directed the hydroxyl group to the C-3 position. Therefore, the second angelate moiety, containing the carbonyl carbon at δ_C 169.0, was assigned to C-2, which was the only possible position for this group. Finally, the positions of the methoxy groups at C-6, C-7, and C-8 were assigned from the HMBC cross-peaks formed between the methoxy signals at δ_H 3.90, 3.84 and 3.69 to the carbon signals C-6, C-7, and C-8, respectively. Therefore, the above spectral data indicated that **139** had a substituted polygamatin skeleton.

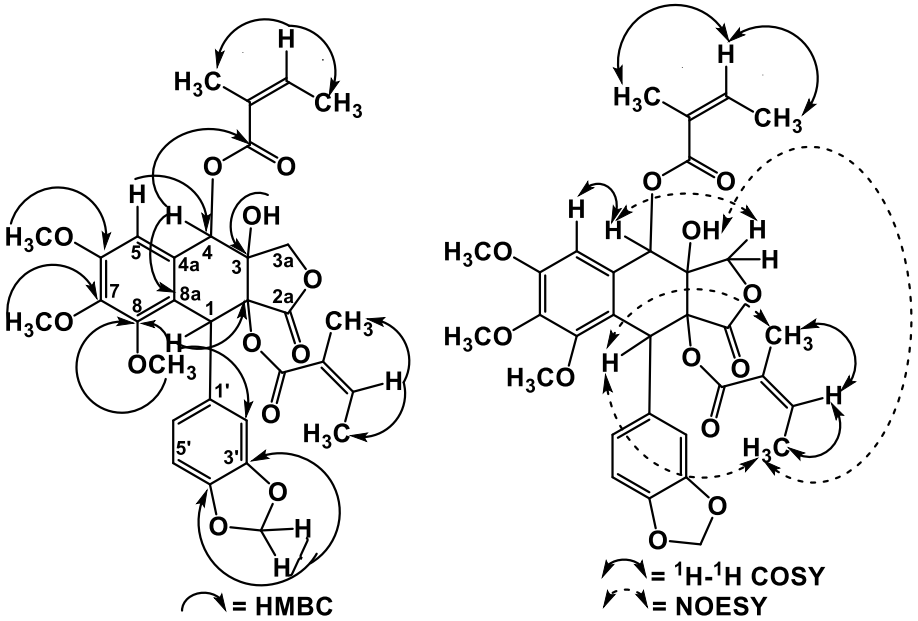

Figure 8: Selected HMBC, ^{1}H-^{1}H COSY and NOESY correlations of compound **139.**

The presence of two angelate groups was also supported by the observation in the mass spectrum fragment ions at m/z 510 (Fig. 9) derived from the loss of one-unit of angelic acid and m/z 410 due to the loss of the second unit of angelic acid. Peaks at m/z 100, 83 and 55 also supported the presence of angelate side chains. The fragment ion peak

situated at m/z 135 confirmed benzylic cleavage of the molecular ion to yield a methylenedioxy benzyl ion.

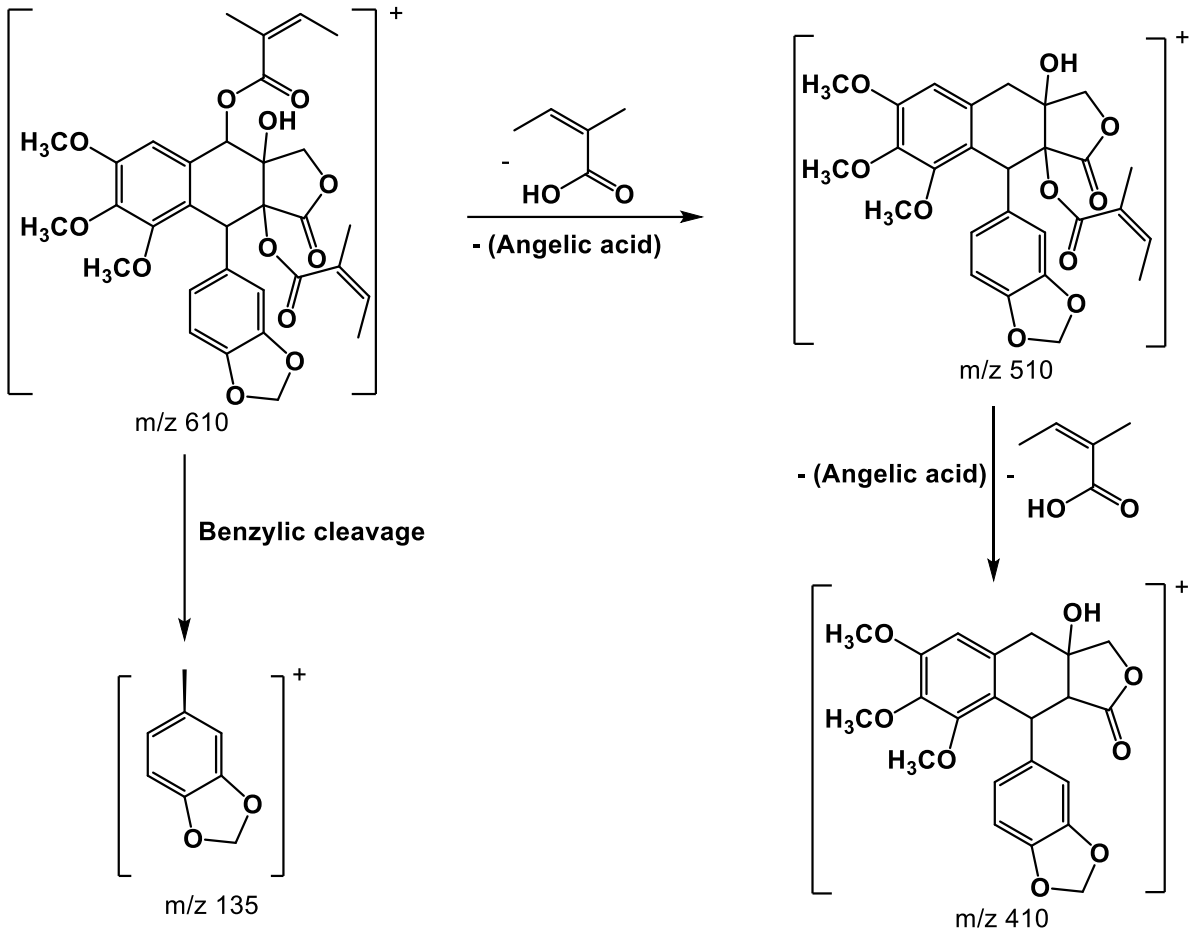

Figure 9: Mass fragmentation pathway for compound **139.**

The relative configuration of **139** was deduced from NOESY experiment in which interactions of H-1 and two methyl protons of the bottom angelate; OH proton and methyl protons of the bottom angeloyl; and H-4 and oxymethylene protons were noted. The absolute configuration (1S) was established by examination of the ECD spectrum of **139** (Fig. 10), which gave a negative Cotton effect at 296 nm (Δε -3.07). The sign of the first couplet is determined by the configuration of the aryl substituent at C-1, negative for 1S and positive for 1R [124]. Thus, C-1 was assigned an S configuration. On the basis of the relative configurations determined above, the configurations of the chiral centers C-2, C-3, and C-4 were assigned to be R, S, and S, respectively.

Analysis of the X-ray diffraction data (Fig. 10) further confirmed the absolute configuration of the compound at C-1, C-2, C-3, and C-4. It also revealed the Z-configurations for the double bonds of the two angelate moieties. Therefore, the novel compound **139** was characterized as (1S,2R,3S,4S)-3-hydroxy-2,4-diangeloyl-6-methoxypolygamatin, to which the trivial name erlangerin E has been given.

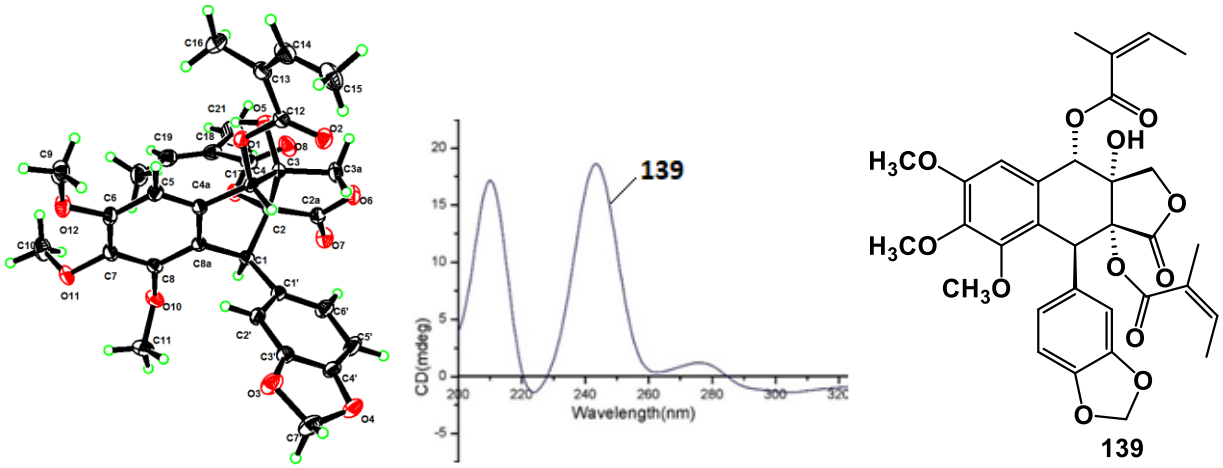

Figure 10: Perspective ORTEP drawing (left), ECD spectrum (middle) and chemical structure (right) of compound **139.**

Characterization of 140 (Erlangerin F)

Compound **140** was obtained as a white powder with an optical rotation of $[\alpha]_D^{20}$ +92.5 (*c* 0.10, MeOH). The compound exhibited the same molecular formula as **139** ($C_{32}H_{34}O_{12}$).

Analysis of the NMR data (Table 3) of **140** indicated that it is structurally quite similar to **139**, with the main difference being that the signals for the carbon atoms in **140** [80.6 (C-2), 86.4 (C-3), 75.6 (C-3a)] were shifted compared to those of **139** [δ_C 85.5 (C-2), 79.6 (C-3), 80.1 (C-3a)], suggesting that the hydroxyl and the angeloyl group (with carbonyl δ_C 167.6) have exchanged their positions. The HMBC correlation (Fig. 11 and Fig. 12) between the hydroxyl proton (δ_H 3.44) and C-1, C-2 and C-2a confirmed the location of the hydroxyl group to be at C-2. Therefore, the angelate group with a carbonyl resonance at δ_C 167.6 appears at the C-3 position. Analysis of the ^{1}H-^{1}H COSY, HSQC, and HMBC data verified the planar structure of **140**.

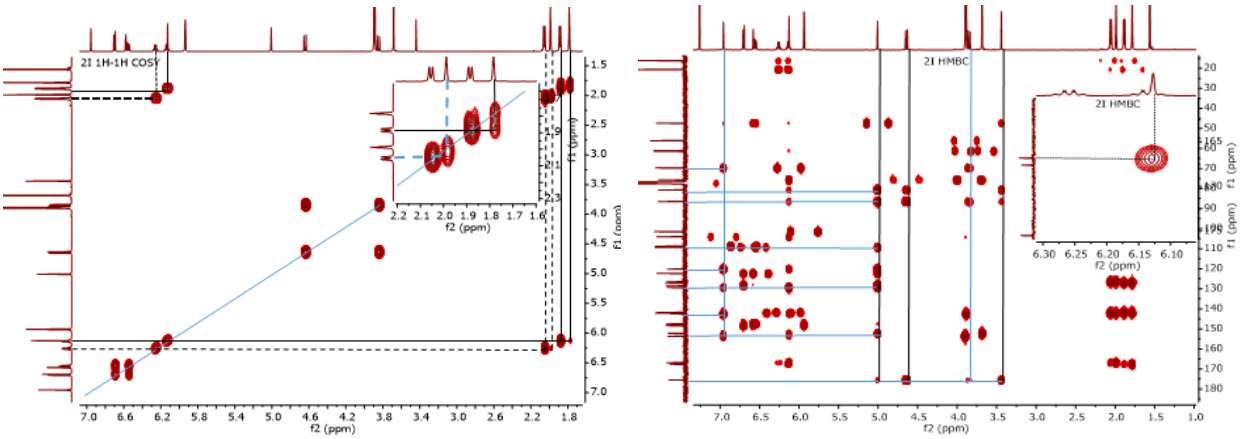

Figure 11: ^{1}H-^{1}H COSY (left) and HMBC spectra (right) of compound **140.**

The relative configuration of **140** was deduced from its ROESY spectrum (Fig. 12) and its absolute configuration was determined to be 1S,2R,3S,4S by comparing the ECD spectrum with that of **139** (Fig. 13). Thus, the structure of **140** was elucidated as (1S,2R,3S,4S)-2-hydroxy-3,4-diangeloyl-6-methoxypolygamatin and designated as erlangerin F.

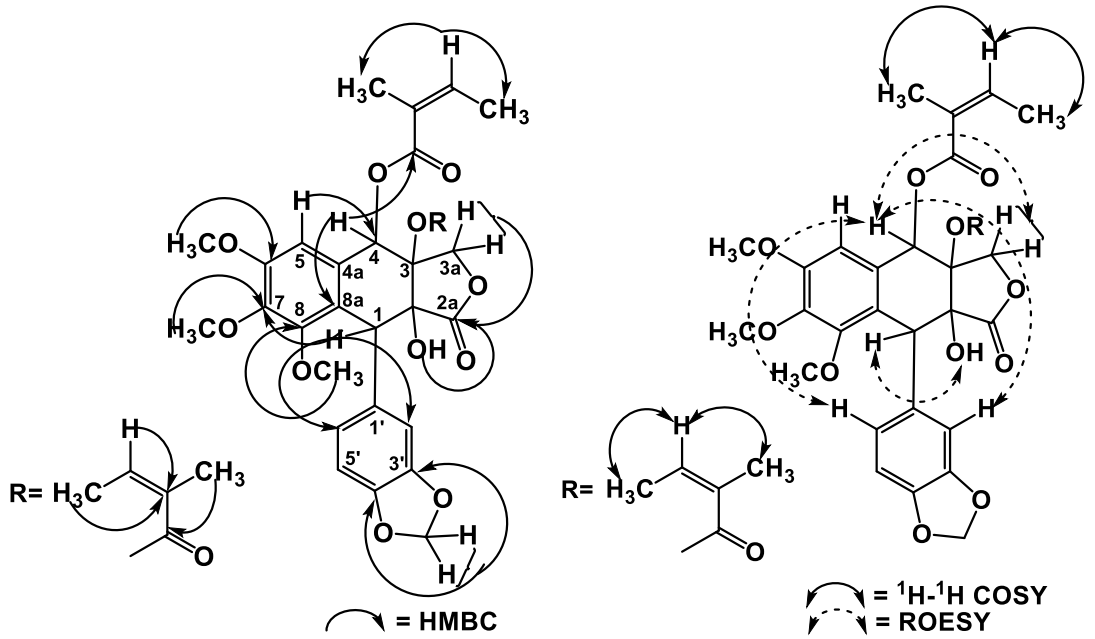

Figure 12: Selected HMBC (left), ^{1}H-^{1}H COSY and ROESY correlations (right) of compound **140.**

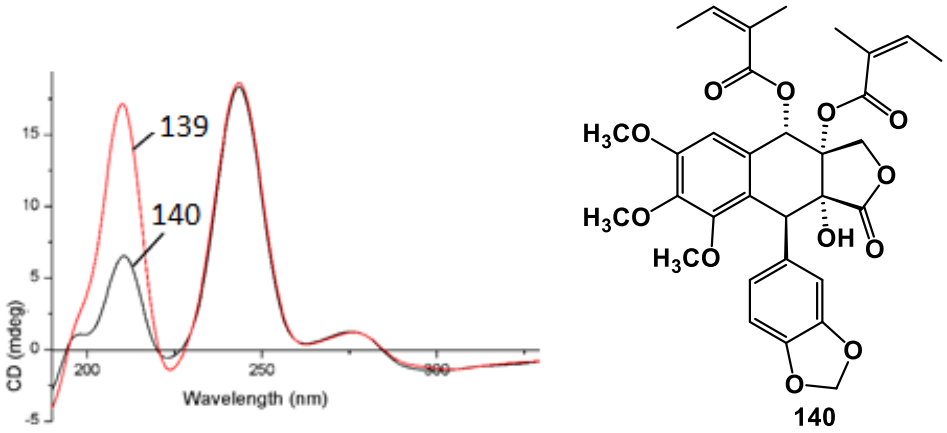

Figure 13: Overlapped ECD spectra of compounds **140** and **139** (left) and structure of compound **140** (right).

Characterization of 141 (Erlangerin G)

Compound **141** was obtained as a white amorphous powder, with an optical rotation of $[\alpha]_D^{20}$ +57.0 (*c* 0.10, MeOH). Its UV spectrum, measured in MeOH, displayed absorption bands at 206 and 286 nm. The IR spectrum exhibited characteristics absorption bands of hydroxyl group (3453 cm^{-1}), lactonic carbonyl (1783 cm^{-1}), ester carbonyl (1714 cm^{-1}), aromatic group (1600 and 1492 cm^{-1}), C-O (1039s cm^{-1}), methylenedioxy group (928 cm^{-1}) and 1,2,3-trisubstituted aromatic ring (850 cm^{-1}). The molecular formula $C_{27}H_{28}O_{11}$ derived from the HREIMS of **141** was found to be the same as that reported for **110.**

Inspection of 1D (Table 3) and 2D NMR data indicated that **141** is structurally quite similar to **110.** The major difference between their structures was that the olefinic proton resonance in **110** which appeared at δ_H 6.24 shifted to the downfield region in **141** to δ_H 7.07 suggesting that the angeloyl group (Z-configuration) changed to the tigloyl group (E-configuration). Moreover, the methyl group in **110** geminal to the carboxylate group (C''-5) appears at δ_C 20.6 and that geminal to the vinyl proton (C''-4) at δ_C 16.0. The ^{13}C NMR chemical shift values of the methyl groups found in these two compounds were consistent with those reported for angelate and tiglate ester, respectively [125].

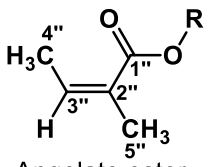

Angelate ester

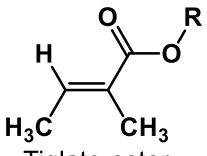

Tiglate ester

The position of the tigloyl group was deduced from the correlation between H-4 (δ_H 5.76) and the carboxylate (δ_c 167.8). The position of the OH group (δ_H 3.18) was assigned to the C-3 from its ^{1}H-^{1}H COSY correlation (Fig.14) with one of the methylene protons at δ_H 3.57. The relative stereochemistry of compound **141** was deduced from its NOESY spectrum (Fig. 14), by comparing its 1D NMR data with that of **110**, and by comparing the ECD spectrum with that of **110** and **139**. Thus, compound **141** was characterized as the E-isomer of erlangerin A and designated as erlangerin G. The absolute configuration 1S,2R,3S,4S was deduced by comparing its ECD spectrum with that of **139** (Fig. 15).

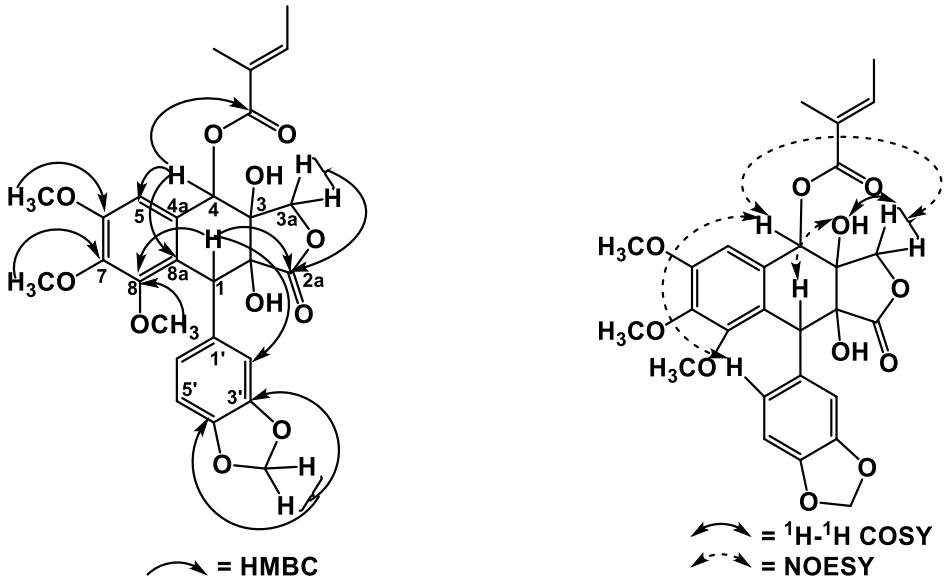

Figure 14: Selected HMBC (left), ^{1}H-^{1}H COSY and NOESY correlations (left) of compound **141.**

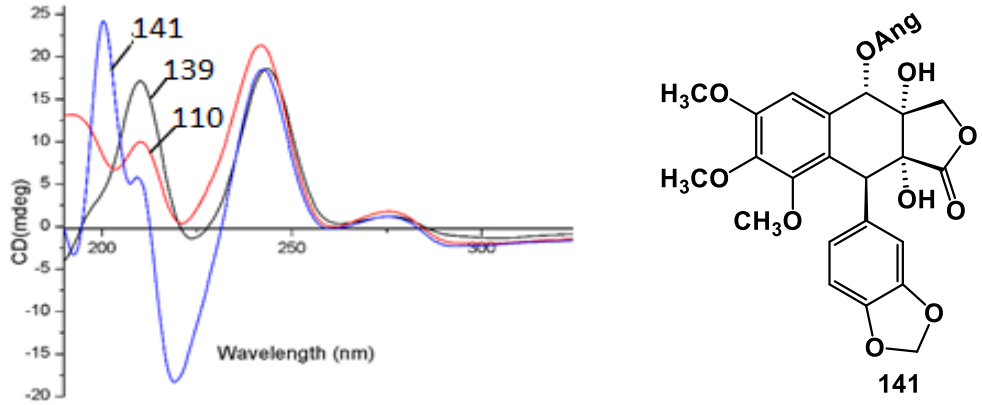

Figure 15: Overlapped ECD spectra of compounds **141**, **139** and **110** (left) and chemical structure (right) of compound **141.**

Characterization of 142 (Erlangerin H)

Compound **142** had a molecular formula $C_{22}H_{22}O_9$, as derived from the ([M + Na]$^+$ peak at m/z 453.1167 in its ESIHRMS spectrum. It has an optical rotation of $[\alpha]_D^{20}$ +207.0 (*c* 0.10, MeOH). The IR spectrum indicated the presence of OH (3451 cm^{-1}), lactone (1776 cm^{-1}) and aromatic (1603 and 1500 cm^{-1}) functionalities.

The ^{1}H NMR spectrum (Table 3) of **142** had the same characteristics peaks as **110** except that the C-4 was occupied by methylene protons (δ_H 3.17, 3.02, each d, *J* = 17.5 Hz). Detailed analysis of HMBC correlations of **142** (Fig. 16) revealed the exact locations of the three methoxy and methylenedioxy groups. The HMBC correlation also suggested that the lactone junction carbons, C-2 and C-3, were oxygenated. From the spectral data analysis, the planar structure of **142** was established as a polygamatin-type skeleton with hydroxyl substituted at C-2 and C-3 positions. The absolute configuration was deduced by comparing its ECD spectrum with that of **110** (Fig.16). Thus, compound **142** was characterized as (1S,2R,3R)-2,3-dihydroxy-6-methoxy-polygamatin, to which the trivial name erlangerin H has been given.

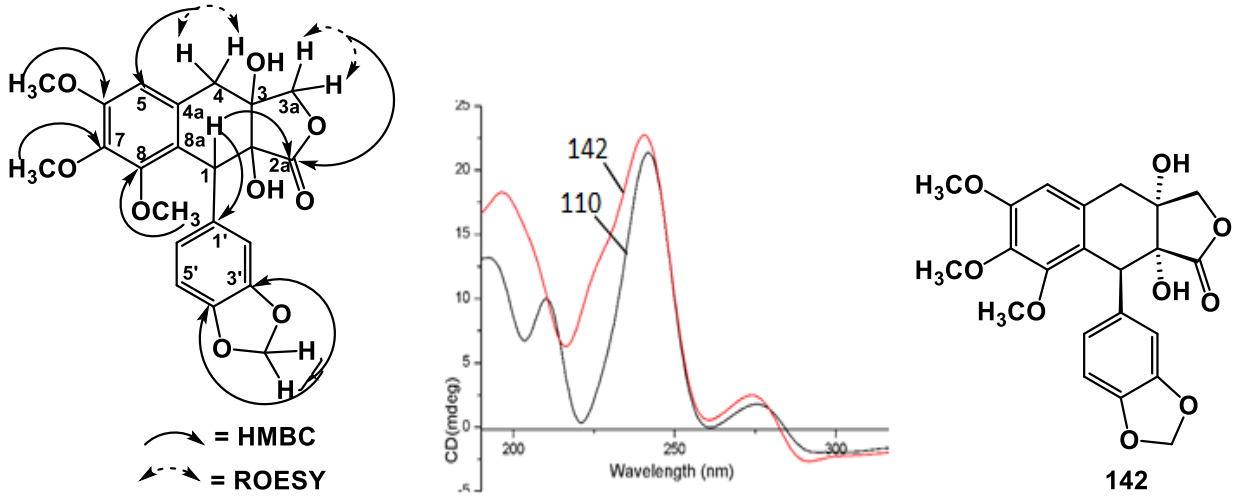

Figure 16: Selected HMBC, and ROESY correlations (left), overlapped ECD spectra of compounds **142** and **110** (middle) and structure (right) of compound **142.**

*Table 3: ^{1}H [ppm, mult., (J in Hz)] and ^{13}C NMR spectroscopic data of compounds **139**, **140**, **141** and **142** in $CDCl_3$*

Position	139		140		141		142	
	δ_C	δ_H	δ_C	δ_H	δ_C	δ_H	δ_C	δ_H
1	44.2	5.15, s	47.3	5.00, s	46.0	4.94, s	46.9	4.87, s
2	85.5	-	80.6	-	77.1	-	80.0	-
2a	171.8	-	175.5	-	177.4	-	180.1	-
3	79.6	-	86.4	-	79.7	-	76.0	-
3a	80.1	4.47, d (10.9) 4.00, d (10.9)	75.6	4.64, d (11.8) 3.85, d (11.8)	78.3	4.33, d (10.7) 3.57, d (10.7)	77.5	4.23, d (9.8); 3.40, d (9.8)
4	71.8	5.96, s	69.7	6.13, s	70.0	5.76, d (1.2)	38.4	3.17, d (17.4); 3.02, d (17.4)
4a	129.1	-	129.3	-	129.0	-	120.8	-
5	103.8	6.93, s	104.0	6.95, s	104.8	6.95, s	107.6	6.59, s
6	153.3	-	153.6	-	153.4	-	153.3	-
7	142.1	-	142.4	-	142.5	-	141.4	-
8	151.5	-	152.2	-	152.0	-	152.3	-
8a	121.0	-	120.1	-	121.1	-	129.6	-
1’	126.0	-	128.2	-	128.4	-	129.5	-
2’	110.0	6.71, overlap	109.2	6.58, d (2.0)	108.9	6.52, d (2.0)	109.1	6.49, s
3’	147.6	-	147.5	-	147.6	-	148.1	-
4’	148.3	-	148.3	-	148.4	-	147.4	-
5’	108.7	6.71, overlap	108.7	6.70, d (8.1)	108.8	6.69, d (8.0)	108.5	6.67, d (8.6)
6’	123.2	6.67, d (8.1)	122.3	6.55, dd (8.1, 2.0)	122.1	6.50, dd (8.0, 2.0)	122.1	6.50, d (8.6)
OCH_2O	101.5	5.93, dd (8.9, 1.5)	101.4	5.94, m	101.5	5.93, s	101.4	5.92, m
6-OCH_3	56.0	3.90, s	56.1	3.90, s	56.1	3.91, s	56.2	3.89, s
7-OCH_3	61.0	3.84, s	61.0	3.88, s	61.0	3.88, s	61.3	3.61, s
8-OCH_3	61.6	3.69, s	61.3	3.68, s	61.4	3.66, s	61.0	3.85, s
Angeloyl (upper)	167.3	-	166.8	-	167.8	-	-	-
	126.8	-	126.5	-	128.0	-	-	-
	140.6	6.24, q (6.7)	141.8	6.26, qd (7.3, 1.6)	139.4	7.07, qd (7.2, 1.5)	-	-
	16.1	2.07, d (6.7)	16.2	2.05, dd (7.3, 1.6)	14.8	1.87, dd (7.2, 1.5)	-	-
	20.8	2.07, s	20.6	1.99, p (1.6)	12.3	1.96, t (1.4)	-	-
Angeloyl (upper)	169.0	-	167.6	-	-	-	-	-
	126.4	-	126.9	-	-	-	-	-
	142.7	6.15, q (7.3)	142.0	6.14, qd (7.3, 1.6)	-	-	-	-
	16.2	1.80, d (7.3)	16.2	1.88, dd (7.3, 1.6)	-	-	-	-
	20.4	1.73, s	20.6	1.78, p (1.6)	-	-	-	-
OH	-	-	-	-	-	3.18, s	-	-
OH	-	-	-	-	-	3.50, s	-	-

Characterization of 143 (Erlangerin P)

Compound **143** was obtained as white crystals, with an optical rotation of $[\alpha]_D^{20}$ +88.0 (***c*** 0.10, MeOH). The molecular formula $C_{26}H_{26}O_{12}$ was determined from the $[M + NH_4]^+$ peak at m/z 548.1776 in the ESIHRMS spectrum. The UV spectrum showed absorption maxima (λ_{max}) at 203 and 292 nm and the IR spectral data indicated the presence of OH (3432 cm^{-1}), lactone carbonyl (1800 cm^{-1}), ester carbonyl (1740 and 1736 cm^{-1}), aromatic ring (1590 and 1511 cm^{-1}), C-O (1035 cm^{-1}), methylenedioxy group (933 cm^{-1}) and 1,2,3-trisubstituted aromatic ring (860 cm^{-1}).

The ^1H NMR spectrum (Table 4) displayed two singlets in the aromatic region at δ_H 7.12 and 5.97 assigned to two aromatic protons at C-2' and C-6'. The other two signals appearing as singlets at δ_H 6.73 and 6.41 were attributed to the two remaining aromatic protons at C-5 and C-8, respectively. The three methoxy groups were represented by three singlets which appeared at δ_H 3.89, 3.83 and 3.65 and the methylenedioxy group at δ_H 5.93 and 5.97. The ^{13}C NMR spectrum (Table 4) displayed 25 carbon signals which represent 26 carbons. The signal for C-3’ and C-5’ are overlapped and represented by a single signal at δ_C 152.7.

From the HMBC spectra, it was possible to establish the basic structure of **143**. Therefore, long-range $^1H–^{13}C$ correlations (Fig. 18) were observed between the methylenedioxy protons and the oxygenated carbons at δ_C 147.9 (C-7), and 147.4 (C-6); between the methoxy protons δ_H 3.65, 3.83 and 3.89 and the respective quaternary carbons at δ_C 152.7 (C-3’), 137.9 (C-4’) and 152.7 (C-5’). Another set of HMBC correlations were observed between δ_H 6.72 (H-4) and δ_C 74.3 (C-3a), 106.2 (C-5), and 110.2 (C-8). The benzylic methine proton at δ_H 4.68 (H-1) showed correlations with δ_C 80.2 (C-2), 107.4 (C-6’) and 112.0 (C-2’). All of the above spectroscopic data indicated that **143** had a podophyllotoxin-skeleton.

The NMR spectral data also confirmed the presence of two acetate groups whose carbonyl resonances appeared at δ_C 171.4 and 166.9. The position of the acetate group with a carbonyl resonance at δ_C 171.4 was determined from its correlation with the proton signal at δ_H 6.27 (H-4). However, it was impossible to deduce whether the second acetate

group was attached to the C-2 or C-3 position based on the above data. The uncertainty about the position of these two substituents was resolved by single crystal X-ray diffraction experiment (Fig. 19). The relative configuration was deduced from the ROESY spectrum (Fig. 18). The R configuration of C-1 was determined from the positive cotton effect at 289 nm in the ECD spectrum (Fig. 19). The R-configuration was also assigned to the other three chiral centers on the basis of the X-ray data analysis. Compound **143** was thus identified as (1R,2R,3R,4R)-2,4-diacetoxy-3-hydroxyisopodophyllotoxin, to which the trivial name erlangerin P has been given.

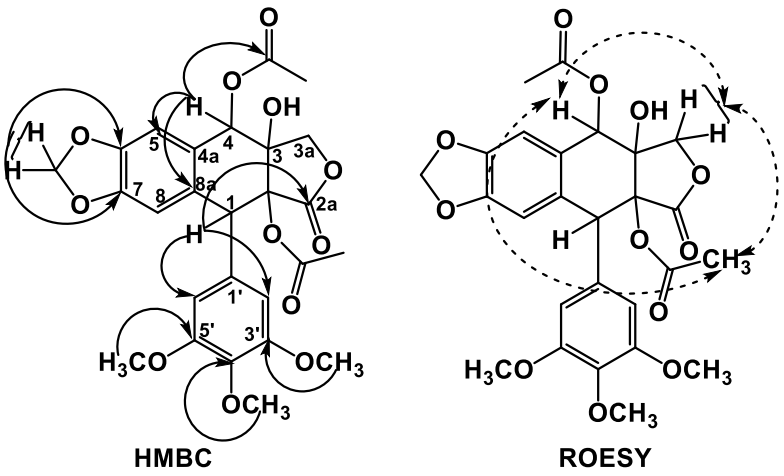

Figure 17: Selected HMBC (left) and ROESY correlations (right) of compound **143.**

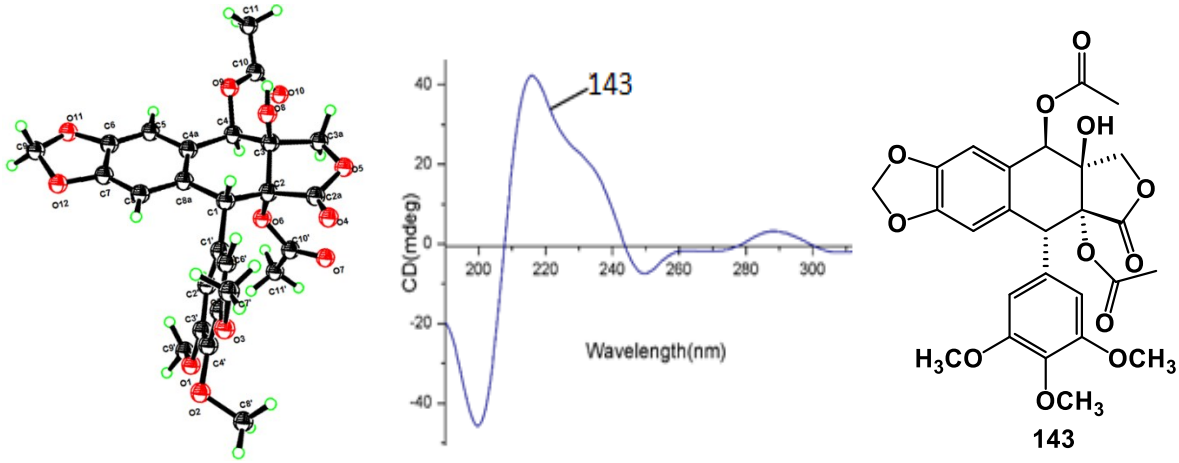

Figure 18: Perspective ORTEP drawing (left), ECD spectrum (middle) and structure (right) of compound **143.**

Characterization of 144 (Erlangerin Q)

Compound **144** was isolated as a white powder, with an optical rotation of $[\alpha]_D^{20}$ +38.0 (*c* 0.10, MeOH). The molecular formula $C_{26}H_{26}O_{11}$ was deduced from the $[M + NH_4]^+$ peak at m/z 532.1826 in its ESIHRMS spectrum. The UV spectrum showed absorption maxima (λ_{max}) at 292 and 207 nm and IR spectrum of compound **144** suggested the presence of lactone (1800 cm^{-1}), ester (1749 cm^{-1}), aromatic (1588, 1501 cm^{-1}), methylenedioxy group (933 cm^{-1}), and 1,2,3-trisubstituted aromatic ring (851 cm^{-1}).

The ^1H and ^{13}C NMR spectroscopic data (Table 4) revealed that compound **144** possessed a podophyllotoxin-type skeleton as in **143**. The absence of a hydroxyl group at the C-4 position in ring C of **144** produced a substantial upfield chemical shift in the H-4 proton resonances (δ_H 3.70, 3.35 each d, *J* = 16.9 Hz) relative to their position in the spectrum of **143** (δ_H 6.27). The position of the acetate groups was determined from weak HMBC correlations (Fig. 20 and 21) of their methyl protons with the respective carbons of the lactone ring. The relative configuration of **144** was deduced from its ROESY spectrum (Fig. 20).

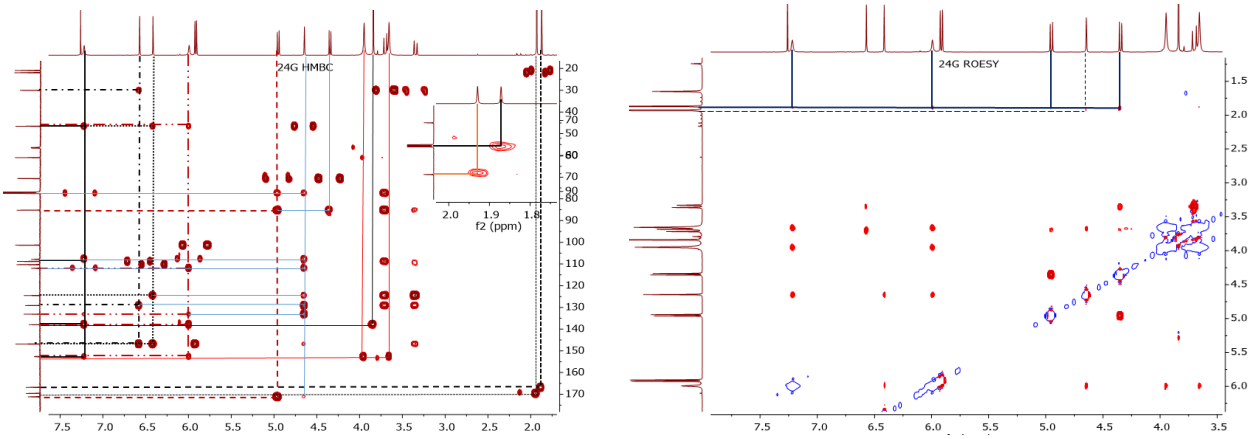

Figure 19: HMBC (left) and ROESY spectra (right) of compound **144.**

The absolute configurations at C-1, C-2, and C-3 were determined by single crystal X-ray diffraction experiment (Fig. 21). Therefore, compound **144** was established as (1R,2R,3S)-2,3-diacetoxyisodeoxypodophyllotoxin and designated as erlangerin Q.

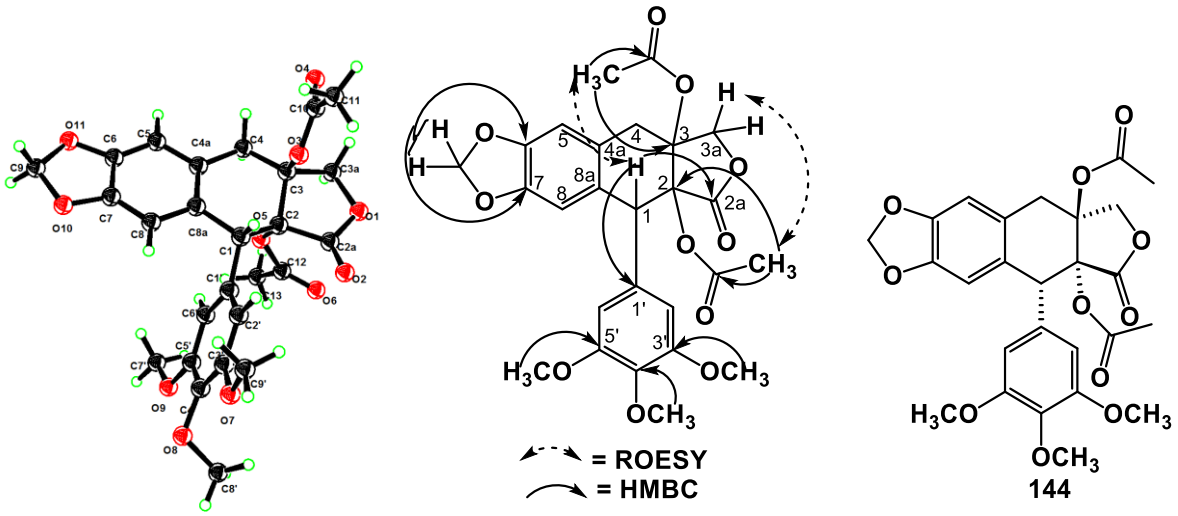

Figure 20: Perspective ORTEP drawing (left), Selected HMBC and ROESY (middle), and chemical structure (right) of compound **144.**

Characterization of 145 (Erlangerin R)

Compound **145** was obtained as a white powder, with an optical rotation of $[\alpha]_D^{20}$ +132.7 (*c* 0.10, MeOH). Its molecular $C_{27}H_{28}O_9$ was determined from the $[M + Na]^+$ peak at m/z 519.1637 in the ESIMS spectrum. Its UV spectrum showed absorption maxima (λ_{max}) at 292 and 207 nm. The IR spectrum of compound **145** confirmed that it contained absorption bands for lactone group (1770 cm^{-1}), an ester group (1716 cm^{-1}) and aromatic ring (1648 and 1585 cm^{-1}).

Its ^{13}C NMR spectrum (Table 4) displayed the occurrences of 23 signals which represent 27 carbon atoms. The overlapped signals include δ_C 56.3 (OCH_3 at C-3' and OCH_3 at C-5'), δ_C 108.1 (C-2' and C-6'), δ_C 147.4 (C-6 and C-7) and δ_C 152.8 (C-3' and C-5').

The ^1H NMR spectrum (Table 4) showed signals due to one unsymmetrical 1,2,4,5-tetra-substituted aromatic ring (δ_H 6.72 and 6.64, each singlet), one symmetrical 1,3,4,5-tetrasubstituted aromatic ring (δ_H 6.53, s, 2H), an oxymethylene (δ_H 4.84 (t, J = 8.8 Hz) and 3.91 (dd, J = 8.8, 4.5 Hz)), one aliphatic methine (δ_H 3.14 (ddt, *J* = 8.8, 6.0, 4.5 Hz)), one aliphatic methylene (δ_H 2.56 (dd, *J* = 15.3, 4.5) and δ_H 3.35 (dd, *J* = 15.3, 6.0 Hz)) and one methylenedioxy group (δ_H 5.96 (dd, *J* = 6.4, 1.5 Hz)).

The ^1H NMR (Table 4) and ^1H-^1H COSY spectra (Fig. 22) revealed the presence of five proton spin systems suggesting that compound **145** had a podophyllotoxin skeleton.

The olefinic proton resonance which appeared at δ_H 6.11 (qd, J = 7.3, 1.6 Hz) showed HMBC correlations with the methyls at δ_H 1.83 (dd, J = 7.3, 1.6 Hz) and δ_H 1.77 (t, J = 1.6) confirming the presence of angelate moiety. And this moiety was easily assigned to the oxygenated C-2 position. The relative stereochemistry of C-1, C-2, and C-3 was determined from the NOESY correlations (Fig. 23). The negative Cotton effect in the ECD spectrum (Fig. 22) at 289 nm suggested a 1S configuration. Based on this, the configurations at C-2 and C-3 were assigned as R and S, respectively. Therefore, the new compound **145** was characterized as (1S,2R,3S)-2-angeloyloxydeoxy-podophyllotoxin, which is named as erlangerin R.

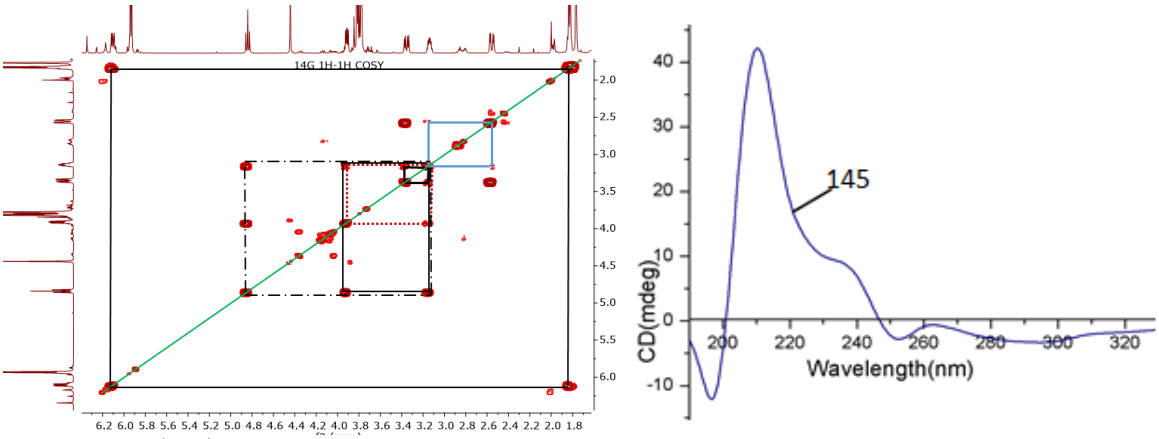

Figure 21: ^{1}H-^{1}H COSY spectra (left) and ECD spectrum (right) of compound **145.**

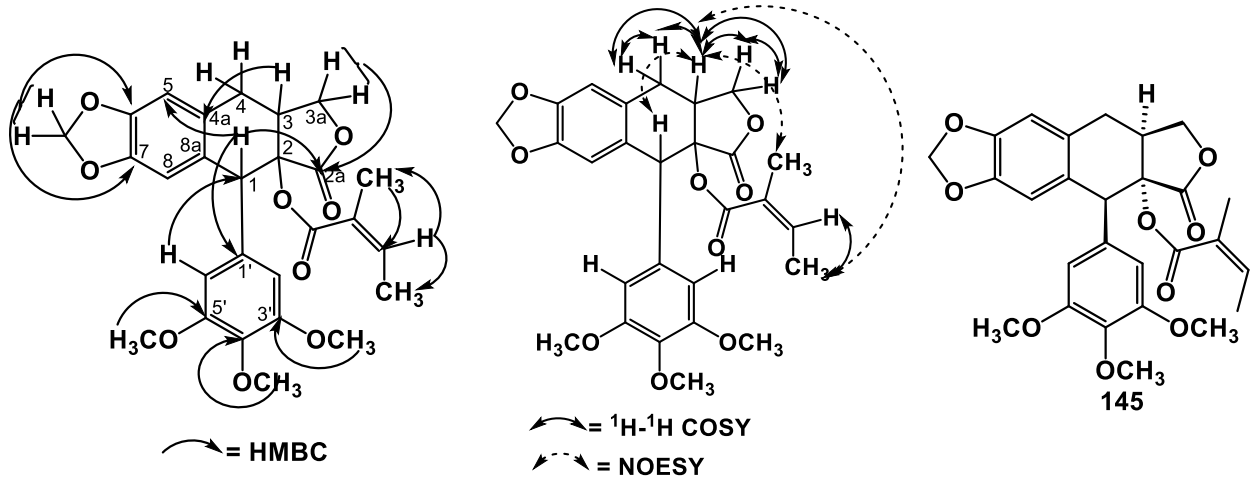

Figure 22: Selected HMBC (left), ^{1}H-^{1}H COSY and NOESY (middle) correlations, and structure (right) of compound **145.**

*Table 4: ^{1}H [ppm, mult., (J in Hz)] and ^{13}C NMR spectroscopic data of compounds **143**, **144**, **152** and **145** in $CDCl_3$*

Position	143		144		152		145	
	δ_C	δ_H	δ_C	δ_H	δ_C	δ_H	δ_C	δ_H
1	46.1	4.68, s	46.6	4.64, s	51.3	4.63, s	51.5	4.44, s
2	80.1	-	77.4	-	80.4	-	81.7	-
2a	171.4	-	171.2	-	175.2	-	175.1	-
3	78.1	-	85.2	-	44.1	3.33, ddd (9.0, 5.5, 3.5)	40.1	3.14, ddt (8.8, 6.0, 4.5)
3a	74.3	4.52, d (9.9) 4.21, d (9.9)	70.0	4.95, d (10.5); 4.35, d (10.5)	67.3	4.58, t (9.0); 4.17, dd (9.0, 3.5)	72.4	4.84, t (8.8); 3.91, dd (8.8, 4.5)
4	71.3	6.27, s	30.0	3.70, d (16.9); 3.35, d (16.9)	69.1	6.52, d (5.5)	33.4	2.56, dd (15.3, 4.5); 3.35, dd (15.3, 6.0)
4a	130.9	-	129.2	-	126.8	-	129.6	
5	106.2	6.73, s	108.8	6.57, s	105.5	6.84, s	109.0	6.72, s
6	147.4	-	146.9	-	148.2	-	147.4	-
7	147.9	-	146.9	-	148.2	-	147.4	-
8	110.2	6.41, s	110.3	6.42, s	110.0	6.71, s	109.8	6.64, s
8a	125.4	-	124.5	-	128.2	-	128.0	-
1’	132.8	-	133.1	-	130.9	-	132.3	-
2’	112.0	7.12, s	112.0	7.22, s	107.8	6.51, s	108.1	6.53, s
3’	152.7	-	152.7	-	152.8	-	152.8	-
4’	137.9	-	138.0	-	137.5	-	137.5	-
5’	152.7	-	152.6	-	152.8	-	152.8	-
6’	107.4	5.97 overlap	107.8	5.99, s	107.8	6.51, s	108.1	6.53, s
OCH_2O	101.7	5.93, d (1.4); 5.97, d (1.4)	101.3	5.91, dd (9.9, 1.4)	101.6	5.98, d (4.1)	101.3	5.93, dd (6.4, 1.5)
3’-OCH_3	56.6	3.65, s	56.3	3.95, s	56.3	3.82 (s, 3H)	-	3.78, s
4’-OCH_3	61.0	3.83, s	61.0	3.84, s	61.0	3.84 (s, 3H)	-	3.82, s
5’-OCH_3	56.3	3.89, s	56.6	3.66, s	56.3	3.82 (s, 3H)	-	3.78, s
Angeloyl	-	-	-	-	166.4	-	166.9	-
	-	-	-	-	126.6	-	126.7	-
	-	-	-	-	141.1	6.24, qd (7.2, 1.5)	141.0	6.11, qd (7.3, 1.6)
	-	-	-	-	16.1	2.02, dd (7.2, 1.5)	15.8	1.83, dd (7.3, 1.6)
	-	-	-	-	20.7	1.99, d (1.6)	20.5	1.77, t (1.6)
Acetate (upper)	171.4		169.6	-	-	-	-	-
	21.0	2.22, s	21.9	1.93, s	-	-	-	-
Acetate (lower)	166.9		166.8	-	-	-	170.1	-
	21.0	1.92, s	20.9	1.87, s	-	-	20.9	2.15, s
3’-OH	-	-	-	-	-	-		3.30, s

Characterization of 146 (Erlangerin M)

Compound **146** was isolated as a white powder, with an optical rotation of $[\alpha]_D^{20}$ +161.0 (*c* 0.10, MeOH). Its molecular formula was assigned to be $C_{24}H_{24}O_9$ from the $[M + H]^+$ peak at m/z 457.1505 in the ESIHRMS spectrum. Its UV spectrum, measured in MeOH displayed absorption bands at 206 and 284 nm.

The ^{1}H NMR spectrum (Table 5) displayed a one-proton doublet at δ_H 6.65 (*J* = 8.0 Hz) and a three-proton multiplet at δ_H 6.59 in the aromatic region. The methylenedioxy group was represented by the two-proton signal at δ_H 5.88. The downfield aliphatic singlet at δ_H 4.86 was due to the benzylic proton at C-1. The other benzylic position (C-4) was occupied by methylene protons resonating at δ_H 3.00 (dd, *J* = 16.3, 10.2 Hz) and 2.76 (dd, *J* = 16.3, 7.3 Hz). The lactone methylene proton resonances appeared at δ_H 4.52 (t, *J* = 9.0 Hz) and 3.36 (t, *J* = 9.0 Hz) and the resonance due to the proton at the lactone ring junction (C-3) appeared at δ_H 3.51 (*J* = 8.4 Hz) as a quintet. The three methoxy groups were represented by three singlets at δ_H 3.89, 3.87 and 3.67. The methyl protons signal at δ_H 1.95 (s) was assigned to an acetate group.

The ^{13}C NMR spectrum (Table 5) of compound **146** showed 24 signals for 24 carbons. The two aromatic ring carbons were represented by twelve signals between δ_C 107.5 – 152.9. The methylenedioxy and oxymethylene carbons appeared at δ_C 101.3 and 72.0, respectively. The two benzylic carbons (C-1 and C-4) and methine carbon (C-3) were represented by signals at δ_C 44.1, 29.9 and 37.1, respectively. The signals due to the three methoxy carbons and the acetate methyl group appeared at δ_C 61.2, 61.0, 56.1, and 21.3, respectively. The carboxylate signals at δ_C 173.9 and 170.0 were due to the lactone and acetate carbonyl carbons, respectively.

Examination of the ^{1}H-^{1}H COSY spectra revealed the presence of five aliphatic proton spin systems (Fig. 24) formed by the methine proton (H-3) and oxymethylene (H-3a) and benzylic (H-4) protons, suggesting that the C-3 was flanked between C-3a and C-4. Detailed analysis of the HMBC spectrum showed that compound **146** had a polygamatin-type skeleton. And also the positions of the three methoxy groups, the methylenedioxy ring, and the acetate group were determined from the HMBC correlations (Fig. 24) of their

respective protons with the carbons they are attached to. Therefore, on the basis of the above spectral data it was determined that compound **146** had the same planar structure as that of **111.**

The *cis* relative configuration of the lactone ring was obtained from the NOESY correlation (Fig. 24) between H-3 and the methyl protons of the acetate group. When the ECD spectrum of **146** was compared with that of **111**, completely opposite Cotton effect was observed (Fig. 24), suggesting that the two compounds might have opposite configurations. The 1S configuration could also be suggested from the negative Cotton effect at 291 nm. Therefore, the new compound **146** was characterized as (1S,2S,3R)-2-acetoxy-6-methoxypolygamatin and designated as erlangerin M.

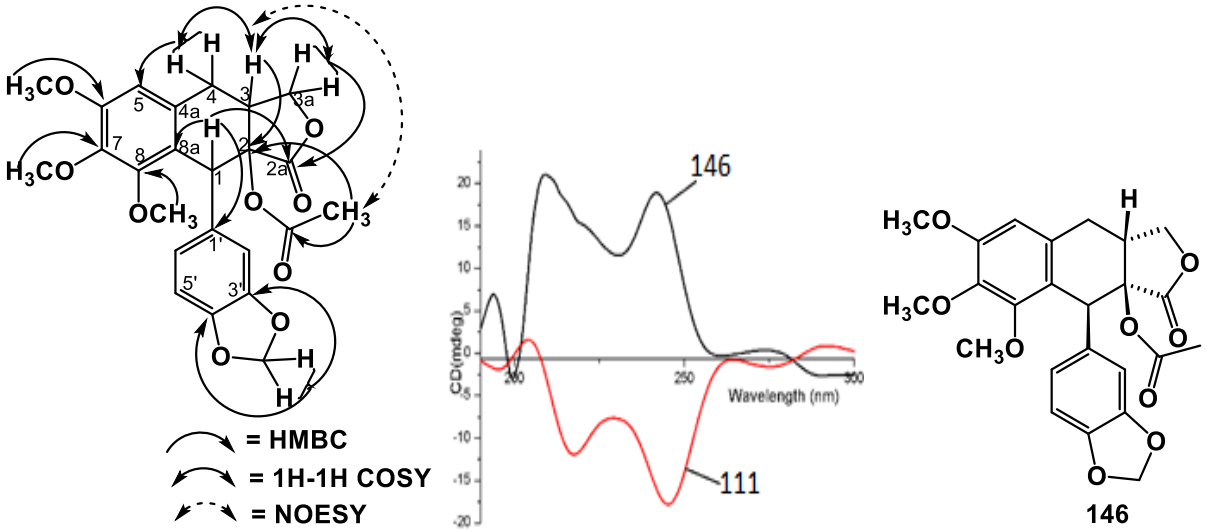

Figure 23: Selected HMBC, ^{1}H-^{1}H COSY and NOESY correlations (left) of compound **146**, overlapped ECD spectra of compounds **146** and **111** (middle), and structure of compound **146** (right).

Characterization of 147 (Erlangerin N)

Compound **147** was isolated as a white powder, with an optical rotation of $[\alpha]_D^{20}$ +197.1 (*c* 0.10, MeOH). Its molecular formula was determined to be $C_{24}H_{24}O_9$ from the $[M + Na]^+$ peak at m/z 437.1211 in the ESIHRMS spectrum. Its UV spectrum, measured in MeOH, displayed absorption bands at 210 and 285 nm.

Analysis of the 1D NMR data of **147** showed similarity with the data generated for **146** (Table 5). The disappearance of signals representing the acetate group in **147** suggested

that it was the hydrolyzed form of **146**. This idea was further supported by the presence of a singlet signal at δ_H 2.85, which was assignable to the OH group. Similar to **146**, the ^{1}H - ^{1}H COSY spectrum of **147** revealed the presence five spin systems (Fig. 25) formed between proton of H-3 with the methylene protons at C-3a and C-4. Such elucidation was further confirmed by detailed analysis of the HMBC spectrum (Fig. 25). The configurations of compound **147** were proposed by comparing its ECD spectrum with that of compounds **146** and **111** (Fig. 25)**.** Hence, compound **147** was identified as (1S,2S,3R)-2-hydroxy-6-methoxypolygamatin, which is named as erlangerin N.

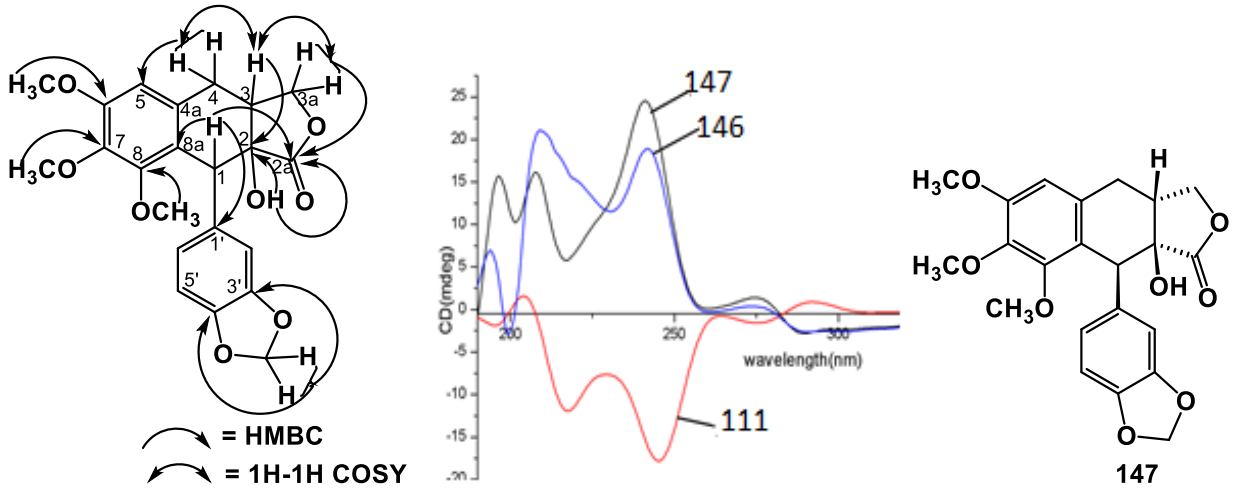

Figure 24: Selected HMBC and ^{1}H-^{1}H COSY correlations of compound **147** (left), overlapped ECD spectra of compounds **147, 146** and **111** (middle), and chemical structure of compound **147** (right).

Characterization of 148 (Erlangerin I)

Compound **148,** obtained as a white powder, was formulated as $C_{22}H_{22}O_8$ from the [M + Na]$^+$ peak at m/z 437.1212 in its ESIMS spectrum. It has an optical rotation of $[\alpha]_D^{20}$ -140.3 (*c* 0.10, MeOH). Its UV spectrum showed absorption maxima at 285 and 207 nm. The IR spectrum displayed absorption bands for OH (3451 cm^{-1}), lactone (1776 cm^{-1}), as well as for aromatic ring (1605 and 1490 cm^{-1}).

Analysis of the NMR data indicated that **148** shares many structural features with **146** (Table 5). The major difference between them was the replacement of the acetate group at C-2 of compound **146** with the OH group in compound **148**. This was evidenced by the absence of acetyl signals (a methyl and a carbonyl signals) in the ^{13}C NMR and a methyl

proton signal in ^{1}H NMR spectra (Table 5). The positions of the methylenedioxy and the methoxy groups were determined from HMBC correlations their proton signals with the respective carbon signals (Fig. 26).

Therefore, based on the above spectroscopic data the planar structure of compound **148** was established as 2-hydroxypolygamatin. The NOESY correlation (Fig. 26) formed between H-1 and H-3 allowed to determine the relative stereochemistry at these two positions. The 1S absolute configuration was established by examination of the ECD spectrum of **148**, which gave a negative Cotton effect at 295 nm (Δε -4.69). The 2R and 3S configurations were obtained from the comparison of its ECD spectrum with that of **146** (Fig. 26)**.** Thus, compound **148** was identified as (1S,2R,3S)-2-hydroxy-6-methoxy-polygamatin and designated as erlangerin I.

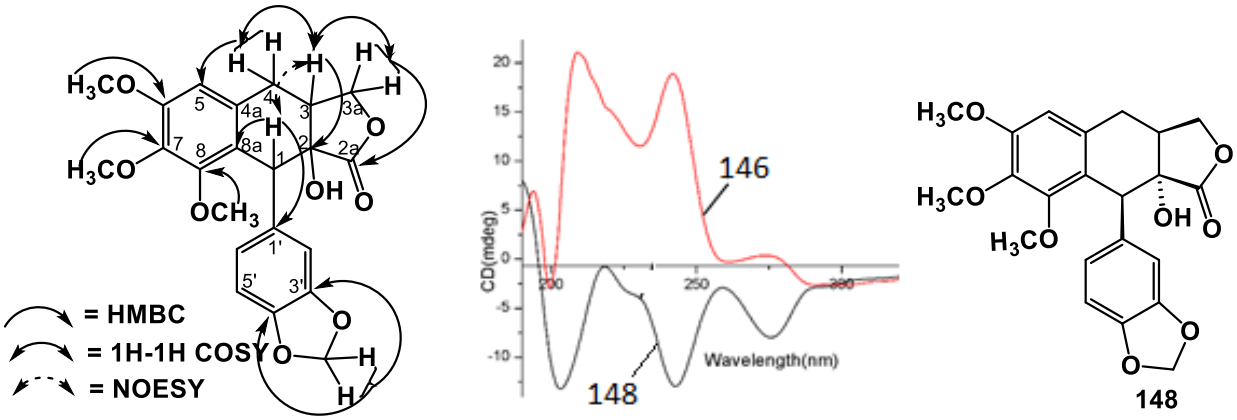

Figure 25: Selected HMBC, ^{1}H-^{1}H COSY, and NOESY correlations of compound **148** (left), overlapped ECD spectra of compounds **146** and **148** (middle)**,** and structure of compound **148** (right).

*Table 5: ^{1}H [ppm, mult., (J in Hz)] and ^{13}C NMR spectroscopic data of compounds **146**, **147** and **148** in $CDCl_3$*

Position	146		147		148	
	δ_C	δ_H	δ_C	δ_H	δ_C	δ_H
1	44.1	4.86, s	47.0	4.71, d (1.9)	46.8	4.69, s
2	84.1	-	78.7	-	75.4	-
2a	173.9	-	179.2	-	175.1	-
3	37.1	3.51, p (8.4)	41.2	3.03, m	35.8	2.86 – 2.75, m
3a	72.0	4.52, t (9.0); 3.36, t (9.0)	71.7	4.34, t (8.9) 3.21, dd (10.5,8.9)	71.2	4.35, d (8.0) 4.24, dd (10.5,8.0)
4	29.9	3.00, dd (16.3,10.2) 2.76, dd (16.3,7.3)	28.3	3.09, dd (15.9,10.3) 2.74, dd (15.9,6.1)	27.1	3.04, dd (15.9,12.3) 2.95, d (6.0)
4a	122.7	-	122.2	-	123.1	-
5	107.5	6.58-6.60 overlap	107.7	6.62, s	107.4	6.54, s
6	152.9	-	153.1	-	152.8	-
7	141.4	-	141.4	-	141.4	-

8	151.9	-	152.3	-	152.4	-
8a	129.8	-	129.9	-	130.0	-
1’	128.0	-	129.5	-	133.7	-
2’	110.2	6.58-6.60 overlap	109.5	6.54, d (1.9)	111.2	6.68, d (1.8)
3’	147.2	-	148.0	-	146.6	-
4’	147.9	-	147.1	-	147.3	-
5’	108.4	6.65, d (8.0)	108.5	6.67, d (8.0)	107.8	6.64, d (8.0)
6’	123.5	6.58-6.60 overlap	122.7	6.56, dd (8.0, 1.9)	124.1	6.60, dd (8.0, 1.8)
OCH_2O	101.3	5.88, d (5.4)	101.3	5.91, m	101.1	5.89, d (1.5) 5.87, d (1.5)
6-OCH_3	56.1	3.89, s	56.2	3.90, s	56.0	3.87, s
7-OCH_3	61.0	3.86, s	61.0	3.86, s	60.8	3.79, s
8-OCH_3	61.2	3.67, s	61.4	3.63, s	60.4	3.36, s
Acetate	170.0	-	-	-	-	-
	21.3	1.95, s	-	-	-	-
2-OH		-	-	2.85, s	-	-

Characterization of 149 (Erlangerin J)

Compound **149** was obtained as a white crystal. Its molecular formula, $C_{29}H_{32}O_{11}$, was determined from the $[M + Na]^+$ peak at m/z 579.1838 in the ESIHRMS spectrum. It showed an optical rotation value of $[\alpha]_D^{20}$ +189.2 (*c* 0.10, MeOH).

The ^1H NMR spectrum of compound **149** (Table 6) revealed the presence of one ABX system at δ_H 6.58 (d, *J*=1.9 Hz), 6.68 (d, *J*=8.1 Hz) and 6.53 (dd, *J*=8.1, 1.9 Hz), respectively, due to a tri-substituted aromatic ring. The spectrum also presented a singlet at δ_H 6.83 due to the 1,2,3,4,5-pentasubstituted aromatic ring. The aliphatic and oxygenated benzylic protons of C-1 and C-4 were represented by signals at δ_H 4.91 (s) and 5.85 (d, *J*=5.4 Hz), respectively. The methine proton and the oxymethylene protons appeared at δ_H 3.33 (tdd, *J*=9.7, 5.5, 1.8 Hz) and 4.63 (d, *J*=9.8 Hz) and 3.62 (t, *J*=9.5, Hz), respectively. The three aromatic methoxy methyls and the acetate methyl protons were represented by singlet signals at δ_H 3.92, 3.90, 3.69 and 1.99, respectively. The two doublets with *J*-value 1.5 Hz at δ_H 5.93 and 5.94 were assignable for the methylenedioxy group. Thus, the above-listed proton signals suggested that **149** had a polygamatin skeleton.

The presence of four spin systems formed by the aliphatic methine proton, oxymethylene protons and aliphatic benzylic proton in the ^1H-^1H COSY spectrum (Fig. 27 and 28), suggested that the methine proton (δ_H 3.33) was positioned in between C-3a and C-4.

The ^{1}H NMR spectrum also presented five proton signals in the aliphatic region at δ_H 0.97 (t, *J* = 7.5 Hz, 3H), 1.56 (m, 1H), 1.28 (d, *J* = 7.0 Hz, 3H), 1.78 (dt, *J* = 13.7, 7.4 Hz, 1H) and 2.55 (h, *J* = 7.0 Hz, 1H). The ^{1}H-^{1}H COSY correlations formed among these protons together with their HMBC correlations (Fig. 28) with the carbonyl signal at δ_C 176.9 (C-1'') and the aliphatic carbons at δ_C 41.1, 26.6, 11.7 and 16.1 confirmed the presence of a 2-methylbutanoyl group. The C-4 position of this substituent was determined from the HMBC correlation of H-4 with C-1'' (Fig. 28). Based on the above spectral data the planar structure of **149** was identified as 2-acetoxy-4-(2-methylbutanoyloxy)-6-methoxy-polygamatin.

The *cis*-configuration of the lactone ring was determined from the NOESY correlation formed between H-3 and the acetyl methyl group (Fig. 28). The NOESY spectrum also enabled to conclude the relative configuration of H-1 and H-4 with respect to the lactone ring. The 1S configuration of **149** was deduced from the negative Cotton effect at 298 nm in the ECD spectrum measured in MeOH (Fig. 29). Based on this the R configuration was assigned for each stereocenter at C-2, C-3, and C-4. The absolute configurations determined were also further confirmed by the X-ray data analysis. Thus, S configuration of the C-2'' of the 2-methylbutanoyl group was obtained from the X-ray analysis. Therefore, the novel compound **149** was identified as (1S,2R,3R,4R)-2-acetoxy-4-((2S)-2-methylbutanoyloxy)-6-methoxypolygamatin, to which the trivial name erlangerin J has been given.

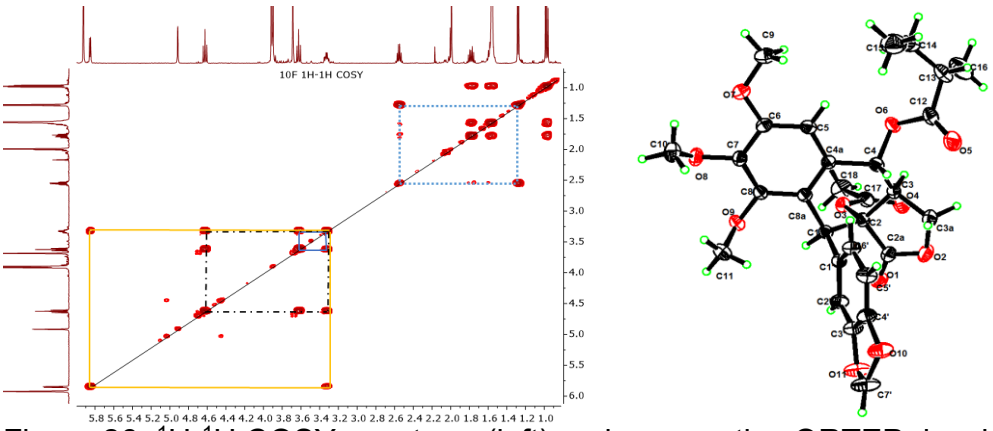

Figure 26: ^{1}H-^{1}H COSY spectrum (left) and perspective ORTEP drawing (right) of compound **149.**

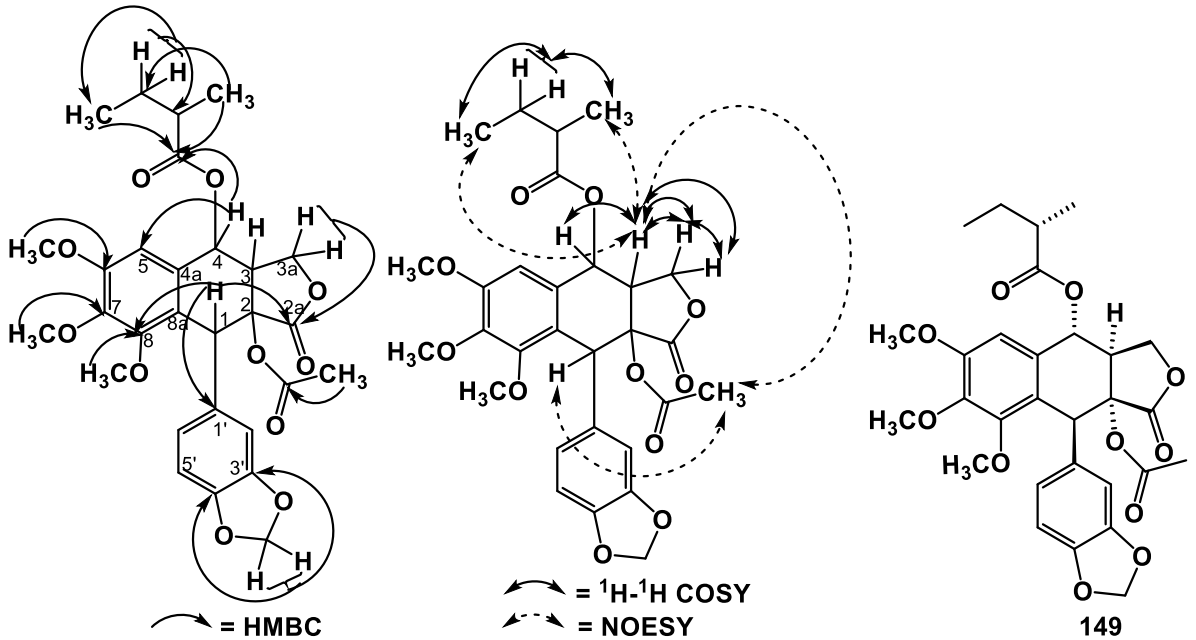

Figure 27: Selected HMBC (left), ^{1}H-^{1}H COSY and NOESY correlations (middle) and chemical structure (right) of compound **149.**

Characterization of 150 (Erlangerin K)

Compound **150,** obtained as a white powder, showed an optical rotation value of $[\alpha]_D^{20}$ +148.5 (*c* 0.10, MeOH). Its molecular formula, $C_{29}H_{30}O_{11}$, was determined from the $[M + Na]^+$ peak at m/z 577.1686 in its ESIHRMS spectrum.

Analysis of the ^{1}H NMR data confirmed that compound **150** (Table 6) contained an ABX system due to a trisubstituted aromatic ring. The singlet at δ_H 6.90 indicated the presence of a 1,2,3,4,5-pentasubstituted aromatic ring. The data also presented four aliphatic spin system formed by H-3/H-3a and H-4. The ^{1}H NMR data also confirmed the presence of three aromatic methoxy groups, an acetate, and a methylenedioxy group. The above ^{1}H NMR data confirmed that **150** had a 2-acetoxy-polgamatin structure similar to **149**. Unlike compound **149,** the ^{1}H NMR data of compound **150** presented an olefinic proton at δ_H 6.25 (qd, *J* = 7.3, 1.5 Hz) and two methyl proton signals at δ_H 2.05 (dd, *J* = 7.3, 1.5 Hz) and δ_H 2.01 (p, *J* = 1.6 Hz) (Table 6). These signals are characteristic proton signals of the angeloyl group. This suggested that **149** was presumably obtained from **150** through reduction of the angeloyl group.

The relative configurations were determined from correlations of proton resonances in the NOESY spectrum (Fig. 30). Similar to **149**, the absolute configuration at each chiral carbon in compound **150** was determined from the negative Cotton effect at 298 nm and by comparing their ECD spectra (Fig. 29). Thus, compound **150** was characterized as (1S,2R,3R,4R)-2-acetoxy-4-angeloxy-6-methoxypolygamatin and designated as erlangerin K.

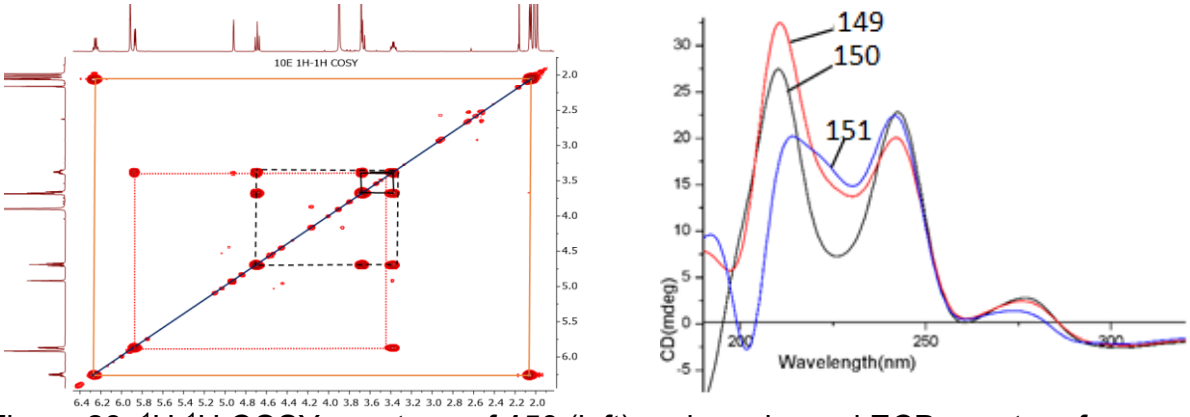

Figure 28: ^{1}H-^{1}H COSY spectrum of **150** (left) and overlapped ECD spectra of compounds **149**, **150** and **151** (right).

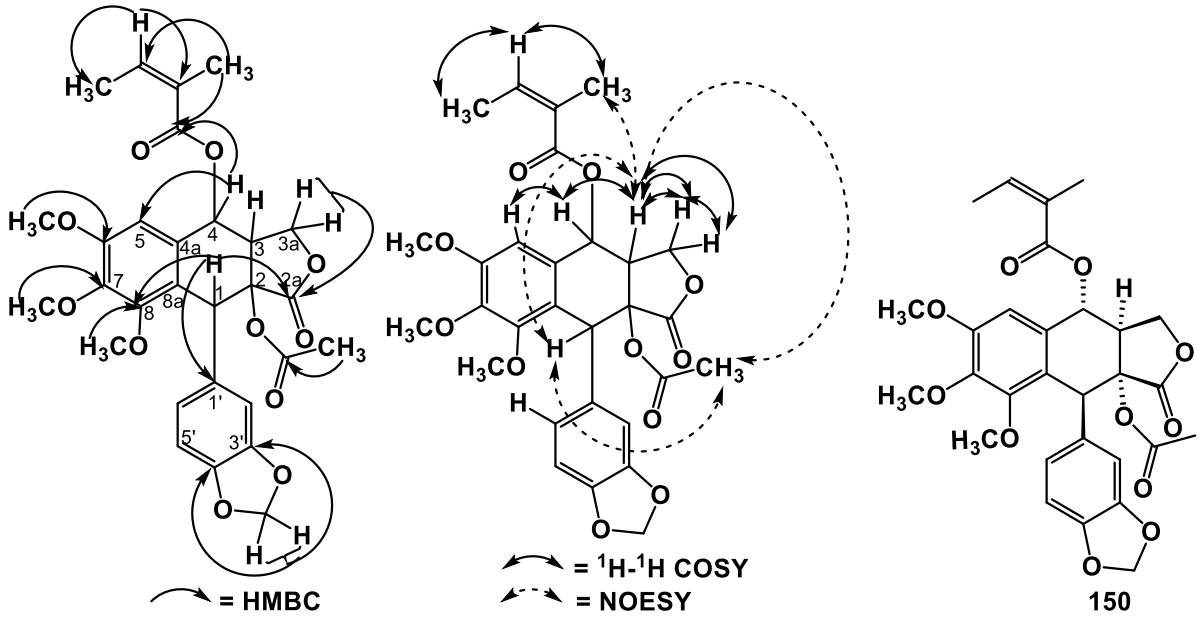

Figure 29: Selected HMBC (left), ^{1}H-^{1}H COSY and NOESY correlations (middle) and chemical structure of compound **150** (right).

Characterization of 151 (Erlangerin L)

Compound **151** was obtained as a white powder and its molecular formula was assigned to be $C_{24}H_{24}O_{10}$ from the $[M + Na]^+$ peak at m/z 495.1260 in the ESIHRMS spectrum. It had an optical rotation of $[\alpha]_D^{20}$ +171.8 (*c* 0.10, MeOH).

Analysis of the ^1H and ^{13}C NMR data (Table 6) indicated that **151** shares many structural features with polygamatins **150** and **149**. The significant differences were the absence of signals representing the angeloyl group in **150** and methylbutanoyl group in **149**. This was evidenced by the upfield chemical shift of the oxymethine proton of H-4 (δ_H 4.90) found in compound **151** with respect to similar H-4 protons found in compounds **150** (δ_H 5.87) and **149** (δ_H 5.85).

Detailed analysis of the 1D and 2D NMR data of **151** enabled the assignment of all the ^1H and ^{13}C NMR signals (Table 6). Its ^1H and ^1H-^1H COSY spectra confirmed the presence of an aliphatic spin system formed by the protons H-3/H-3a/H-4 as observed in **150** and **149** (Fig. 31).

Therefore, the planar structure of compound **151** was characterized as 2-acetoxy-4-hydroxypolygamatin. The relative configuration was determined from its NOESY correlations (Fig. 32). The 1S configuration was obtained from the negative Cotton effect at 296 nm ($\Delta\varepsilon$ -4.01). For the other three chiral centers the R configuration was given on the basis of their NOESY correlations and by comparing the ECD spectrum with that of **149** and **150** (Fig. 29). Therefore, **151** was identified as (1S,2R,3R,4R)-2-Acetoxy-4-hydroxy-6-methoxy-polygamatin, which is named as erlangerin L.

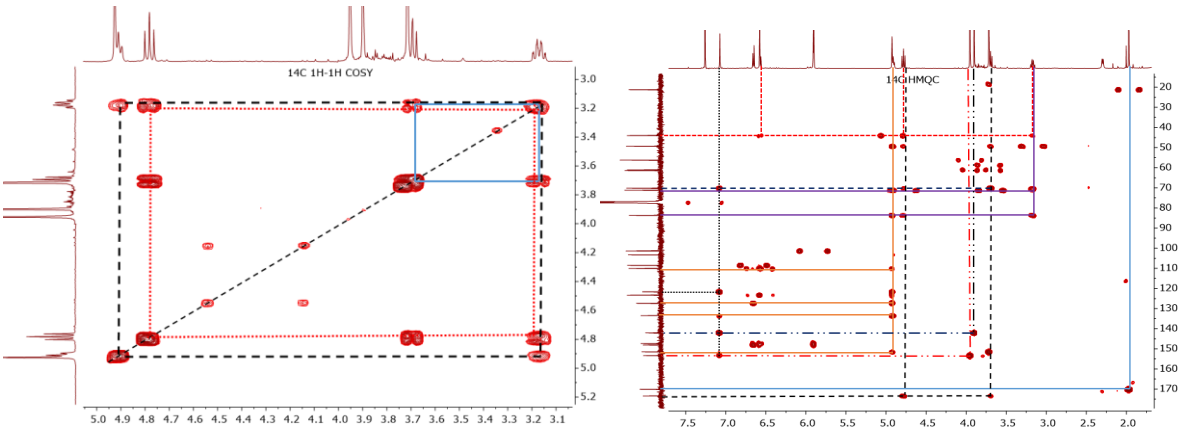

Figure 30: ^1H-^1H COSY (left) and HMBC (right) spectra of compound **151.**

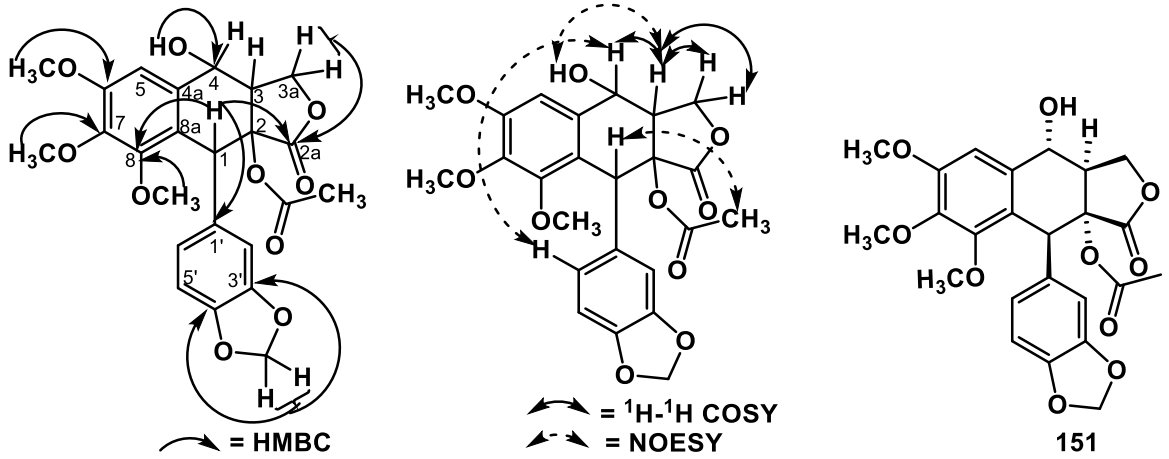

Figure 31: Selected HMBC (left), ^{1}H-^{1}H COSY and NOESY correlations (middle) and chemical structure (right) of compound **151.**

Characterization of 152 (Erlangerin S)

Compound **152** was obtained as a white powder, with an optical rotation of $[\alpha]_D^{20}$ +40.5 (*c* 0.10, MeOH). Its molecular formula $C_{29}H_{30}O_{11}$ was determined from the $[M + Na]^+$ peak at m/z 577.1684 in the ESIMS spectrum. Its UV spectrum showed absorption maxima (λ_{max}) at 292 and 205 nm.

The ^{13}C NMR spectrum (Table 4) displayed occurrence of 26 carbon resonances assignable to three ester groups (δ_C 175.2, 170.1 and 166.4), one trisubstituted double bond (δ_C 141.1 and 126.6), one methylenedioxy group (δ_C 101.6), three methoxy groups (δ_C 56.3 (x2) and 61.0), three aliphatic methine carbons (δ_C 69.1, 51.3 and 44.1), one aliphatic methylene (δ_C 67.3), three aliphatic methyls (δ_C 20.9, 20.7 and 16.1) and twelve aromatic carbons (δ_C 105.0 – 154.0) due to two benzene rings.

Similar to **145**, the ^{1}H NMR spectrum of **152** (Table 4) showed signals due to one unsymmetrical 1,2,4,5-tetrasubstituted (δ_H 6.71 (s) and 6.84 (s)) and one symmetrical 1,3,4,5-tetrasubstituted (δ_H 6.51 (s, 2H)) aromatic rings. The ^{1}H NMR and ^{1}H-^{1}H COSY spectra of **152** displayed the presence of four spin system as in **150**, **149** and **151** which are formed by proton signals at δ_H 3.33 (ddd, *J* = 8.9, 5.5, 3.5 Hz, H-3), 4.58 (t, *J* = 9.0 Hz, H-3a), 4.17 (dd, *J* = 9.2, 3.5 Hz, H-3a) and 6.52 (d, *J* = 5.8 Hz, H-4), suggesting similar substitution pattern at C-2 and C-4. The olefinic proton which appeared at δ_H 6.24 (qd, *J* = 7.2, 1.5 Hz) exhibited ^{1}H-^{1}H COSY correlations with the two methyls at δ_H 2.02 (dd, *J* =

7.1, 1.8 Hz) and 1.99 (d, *J* = 2.6 Hz) confirming the presence of an angelate moiety in **152**. Its position was determined from the HMBC correlation of H-4 with carbonyl of the angelate group (δ_C 166.4) (Fig. 33). HMBC correlation of a methyl (δ_H 2.15) with the carbonyl resonance at δ_C 170.1 suggested that there is an acetyl group in the structure of **152.** The only available position for the acetyl group is the C-2.

The relative stereochemistry at C-1, C-2, and C-3 were determined from the NOESY spectrum whereas the configuration at C-4 was determined by comparing the coupling constant between H-3 and H-4 with the similarly substituted aryltetralin compounds **150** ($J_{H3\text{-}H4}$ = 5.4 Hz) and **149** ($J_{H3\text{-}H4}$ = 5.5 Hz). Since compound **152** has a similar coupling constant ($J_{H3\text{-}H4}$ = 5.5 Hz), the *trans* orientation of H-4 with respect to H-3 was thus confirmed. The 1S configuration was established by examination of ECD spectrum of **152** showing a negative Cotton effect at 290 (Δε -7.64). Thus, the remaining chiral centers at C-2, C-3, and C-4 were assigned the R configuration. Compound **152** was thus identified as (1S,2R,3R,4R)-2-acetoxy-4-angeloxy-podophyllotoxin and named as erlangerin S.

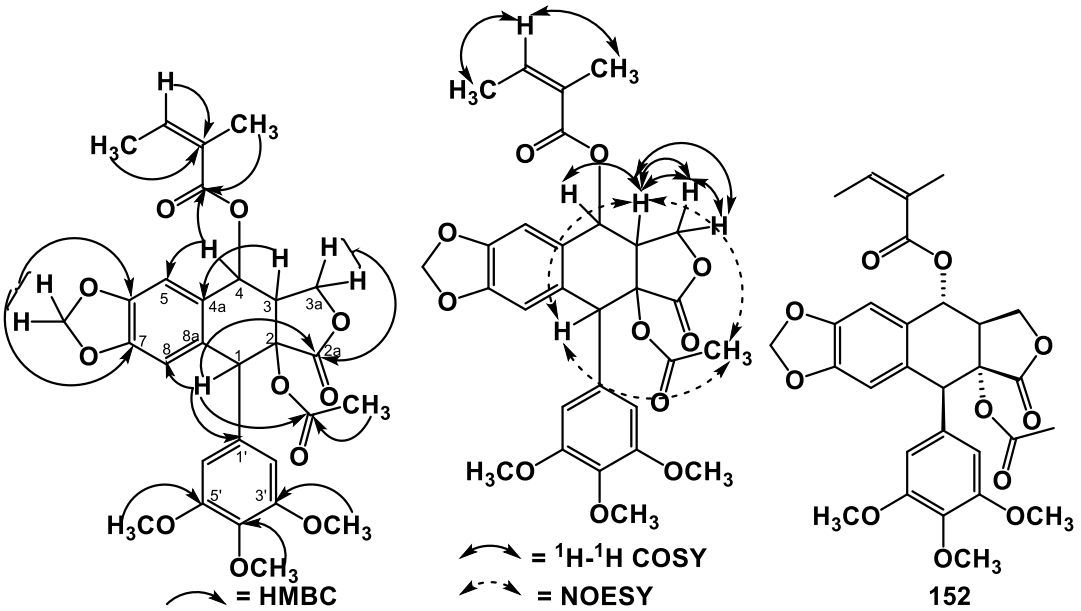

Figure 32: Selected HMBC (left), ^{1}H-^{1}H COSY and NOESY correlations (middle), and chemical structure (right) of compound **152.**

*Table 6: ^{1}H [ppm, mult., (J in Hz)] and ^{13}C NMR spectroscopic data of compounds **151**, **150**, **149**, and **153** in $CDCl_3$*

Position	151		150		149		153	
	δ_C	δ_H	δ_C	δ_H	δ_C	δ_H	δ_C	δ_H
1	44.0	4.93, s	44.0	4.92, s	43.8	4.91, s	41.9	4.33, d (10.0)
2	83.6	-	83.0	-	82.8	-	48.0	2.65, dd (14.5, 10.0)
2a	173.4	-	173.1	-	172.9	-	174.9	-
3	49.3	3.17, dtd (9.8, 7.6, 1.6)	47.0	3.37, tdd (9.7, 5.4, 1.7)	46.6	3.33, tdd (9.7, 5.5, 1.8)	45.5	2.60, m
3a	71.2	4.78, t (9.8); 3.69, d (7.6)	71.2	4.69, t (9.8); 3.68, t (9.8)	70.8	4.63, d (9.8); 3.62, t (9.8)	69.9	4.23, t (9.5); 4.36, dd (9.5, 6.1)
4	70.2	4.90, d (7.4)	70.4	5.87, d (4.9)	70.1	5.85, d (5.4)	72.6	6.18, d (9.7)
4a	121.7	-	128.9	-	128.6	-	131.6	
5	103.3	7.07, s	104.1	6.90, s	103.7	6.83, s	104.0	6.64, s
6	153.3	-	153.2	-	153.1	-	153.0	-
7	142.1	-	142.4	-	142.4	-	142.6	-
8	151.5	-	151.5	-	151.4	-	152.3	-
8a	133.5	-	122.1	-	122.0	-	126.4	-
1’	127.4	-	127.3	-	127.2	-	139.8	-
2’	110.1	6.58, s	110.0	6.58, d (2.0)	109.9	6.58, d (1.9)	108.3	6.72 overlap
3’	147.3	-	147.6	-	147.4	-	146.1	-
4’	148.1	-	148.2	-	148.1	-	147.6	-
5’	108.5	6.66, d (8.6)	108.4	6.68, d (8.1)	108.5	6.68, d (8.1)	108.2	6.72 overlap
6’	123.3	6.57, d (7.5)	123.1	6.54, dd (8.1, 2.0)	123.1	6.53, dd (8.1, 1.9)	121.3	6.72 overlap
OCH_2O	101.4	5.90, m	101.4	5.92, q (1.3)	101.3	5.92, q (1.5)	101.0	5.91, m
6-OCH_3	56.2	3.95, s	55.7	3.90, s	55.9	3.92, s	56.0	3.83, s
7-OCH_3	61.1	3.90, s	61.0	3.90, s	61.0	3.90, s	60.6	3.77, s
8-OCH_3	61.4	3.72, s	61.2	3.69, s	61.2	3.69, s	59.7	3.20, s
	-	-	166.7	-	-	-	168.0	-
	-	-	126.7	-	-	-	127.0	-
Angeloyl	-	-	141.3	6.25, qd (7.2, 1.5)	-	-	140.6	6.23, qd (7.2, 1.5)
	-	-	16.2	2.05, dd (7.2, 1.5)	-	-	16.2	2.06, dq (7.2, 1.5)
	-	-	20.5	2.01, p (1.5)	-	-	20.8	1.99, p (1.5)
	-	-	-	-	176.9	-	-	-
2-Methyl-	-	-	-	-	41.1	2.55, h (7.0)	-	-
butanoyl	-	-	-	-	26.6	1.78, dt (13.7,7.5); 1.56,m	-	-
	-	-	-	-	11.7	0.97, t (7.5)	-	-
	-	-	-	-	16.1	1.28, d (7.0)	-	-
Acetate	170.1	-	170.1	-	169.9	-	-	-
	21.2	1.97, s	21.3	1.99, s	21.2	1.99, s	-	-

Characterization of 153 (Erlangerin O)

Compound **153** was isolated as a white powder, with an optical rotation of $[\alpha]_D^{20}$ -42.3 (*c* 0.10, MeOH). The ^{1}H NMR spectrum of compound **153** showed signals at δ_H 6.23 (qd, *J* = 7.2, 1.4 Hz), 2.03 (qd, *J* = 7.2, 1.6 Hz) and 1.99 (p, *J* = 1.6 Hz) assignable to an angeloyl group. The signals at δ_H 3.83 (s), 3.77 (s) and 3.20 (s), could be assigned to three methoxy groups. A downfield methylene signal at δ_H 5.91 (m, 2H) is a characteristic signal for a methylenedioxy group. A set of geminal-coupled protons resonating at δ_H 4.36 (dd, *J* = 9.2, 6.1 Hz) and 4.23 (t, *J* = 9.5 Hz) represented the oxymethylene protons of the lactone ring.

The ^{1}H-^{1}H COSY spectrum displayed cross-peaks between δ_H 4.23 and 2.60 representing vicinal coupling between methylenic protons with the neighboring methine proton (H-3). The proton at δ_H 4.33 (d, *J* = 10.0 Hz) displayed a cross-peak with a proton at δ_H 2.65 (dd, *J* = 14.5, 10.0 Hz) and was assigned to H-1. The most downfield aliphatic proton at δ_H 6.18 (d, *J* = 9.7 Hz) displayed a cross-peak with a proton at δ_H 2.60 (m) and is assignable to H-4. The three-proton multiplet in the aromatic region of the spectrum between δ_H 6.74-6.66 was assigned to the three aromatic positions found in D-ring.

The ^{13}C NMR spectrum of compound **153** exhibited 27 signals representing 27 carbons. The three methoxy carbons resonating at δ_C 56.0, 60.6 and 59.7 and their methyl protons showed long-range coupling to the aromatic protons at δ_C 153.0, 142.6 and 152.3, respectively in the HMBC spectrum. The other aromatic carbon atom signals resonated at δ_C 104.0, 126.4, 139.8, 108.3, 108.8, 146.1, 147.6 and 121.3. An ester carbonyl carbon (C-2a) resonated at δ_C 174.9, a methylenedioxy carbon appeared at δ_C 101.0 and a downfield methylene carbon resonated at δ_C 69.9. The methine carbons signals at δ_C 41.9, 48.0, 45.5 and 72.6 represented the carbon atoms of B-ring. The singlet at δ_H 6.64 had long-range HMBC interactions with five carbon signals found in A-ring and δ_C 72.6 (C-4). The aromatic protons of ring-D also showed long-range interactions with carbons of ring-E. The above spectroscopic data suggested that compound **153** had a polygamatin-type skeleton. The position of the angeloyl moiety was determined from the HMBC correlation formed between H-4 and the ester carbonyl (δ_C 168.0) (Fig. 34).

Therefore, compound **53** was identified as 4-angeloxy-6-methoxypolygamatin and designated as erlangerin O.

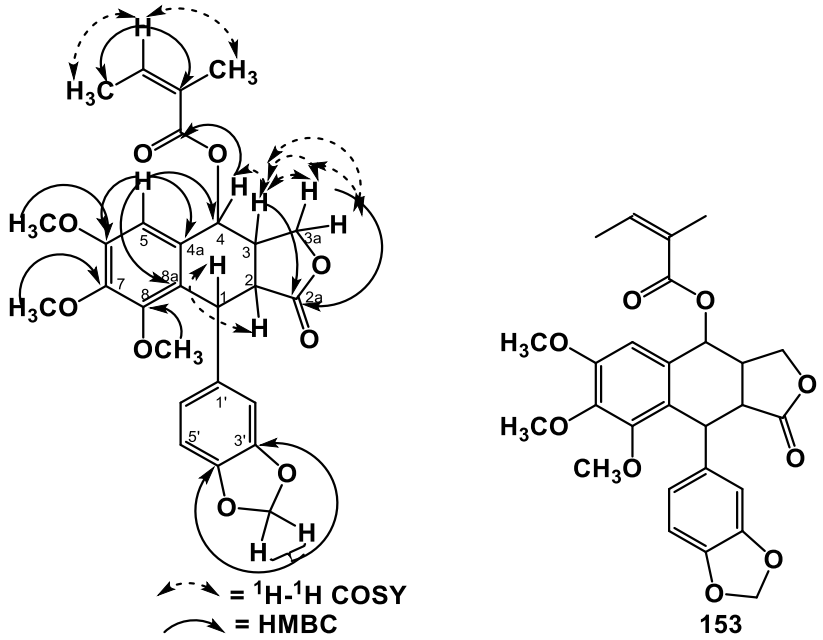

Figure 33: Selected HMBC and ^{1}H-^{1}H COSY correlations (left) and chemical structure (right) of compound **153.**

Characterization of Compound 154 (Erlangerin T)

Compound **154** was isolated as colorless gum, with an optical rotation of $[\alpha]_D^{20}$ -23.0 (*c* 0.10, MeOH). Its molecular formula was determined as $C_{22}H_{24}O_8$ on the basis of the [M + Na]+ peak at *m/z* 439.1370 in the ESIHRMS spectrum. In the UV spectrum, absorption maxima (λ_{max}) were observed at 286 and 205 nm and the IR spectrum included bands at 3476 cm^{-1} (OH), 1773 cm^{-1} (C=O), 1588 and 1506 cm^{-1} (aromatic ring), 1242 cm^{-1} (C-O) and 923 cm^{-1} (OCH_2O).

The ^{1}H NMR spectrum of **154** (Table 7) exhibited the presence of six and three hydrogen singlets at δ_H 3.78 and 3.79 due to three methoxy groups. The three set of signals in the aromatic region at δ_H 6.69 (d, *J* = 1.7 Hz), 6.72 (d, *J* = 8.0 Hz) and 6.76 (dd, *J* = 8.0, 1.7 Hz) were due to one 1,3,4-trisubstituted benzene ring. The other two singlets resonating at δ_H 6.08 confirmed the presence of one symmetrically substituted benzene ring. The two doublets at δ_H 5.95 and 5.97, each integrating for one proton, were assigned to the methylene protons of the methylenedioxy group. The one-proton doublet of doublets at

δ_H 5.28 (*J* = 4.9, 2.9 Hz) was assigned to the methine proton adjacent to the hydroxyl group. The hydroxyl group was represented by a doublet signal resonating at δ_H 2.77 (*J* = 4.9 Hz).

The set of A_2B doublet of doublets resonating at δ_H 3.96 (*J* = 8.9, 5.8 Hz) and 4.36 *(J* = 8.9, 8.0 Hz) was assigned to the α- and *β*-methylene protons of the lactone. While the set of A_2B doublet of doublets resonating at δ_H 2.28 *(J* = 13.6, 7.5 Hz) and 2.44 *(J* = 13.6, 8.0 Hz) was due to the benzylic methylene protons. The one-proton doublet of doublets at δ_H 2.63 *(J* = 6.2*,* 2.9 Hz) was assigned to the methine proton adjacent to the carbonyl group. The multiplet at δ_H 2.82 (*J* = 13.6, 8.0, 6.2 Hz) was due to a methine proton situated in between the two methylene groups.

The ^{13}C NMR spectrum of **154** (Table 7) exhibited 19 signals for 22 carbons including two benzene rings (from δ_C 105.7 to 153.3), a carboxylate group (δ_C 178.3), two oxygenated carbons (a methine (δ_C 71.9) and a methylene (δ_C 72.9)), three aliphatic carbons (two methines (δ_C 36.6 and 52.9) and one methylene (δ_C 40.2)), one methylenedioxy carbon (δ_C 101.5) together with three methoxy carbons (δ_C 56.1 (x 2) and 60.9).

HMBC correlations of the proton signals of the methoxy groups with the respective carbons allowed to assign these groups on the symmetrically substituted benzene ring. The position of the methylenedioxy group on the 1,3,4-trisubstituted benzene ring was determined from the HMBC cross-peaks of the oxymethylene proton signals and C-4' and C-3' (Fig. 35). The presence of the lactone ring was determined from the HMBC correlations between C-2a (δ_C 178.3) and H-2, H-3 and H-3a and correlations between C-3a and H-2 and H-3. The connectivities of the two benzene rings with the lactone ring through oxymethine (C-1) and methylene (C-4) were confirmed by the key correlations between C-1' and H-2', H-5', H-1, and H-2, and correlations between C-4a and H-5, H-4, and H-3.

The relative configuration of **154** was elucidated from NOESY correlations (Fig. 35). It showed strong and weak correlations of H-3/H-$3a_1$ (at δ_H 4.36) and H-3/H-$3a_2$ (at δ_H 3.96), respectively. Correlation of H-2/H-$3a_2$ (at δ_H 3.96) was also observed, which confirmed that H-2 and H-3 are in a *trans* configuration [103, 126, 127]. The ECD spectrum (Fig. 36)

displayed negative Cotton effects at 236 and 279 nm revealing that the absolute configurations at the C-2 and C-3 positions are 2S and 3R, respectively [103, 127]. Regarding the absolute configuration at the C-1 position, it was known that the C-1 proton resonance appeared at δ_H 5.25 (d, *J* = 2.9 Hz) in podorhizol (C-1, S) and at δ_H 4.79 (d, *J* = 7.9 Hz) in *epi*-podorhizol (C-1, R) [126]. In compound **154** the C-1 proton resonance appeared at δ_H 5.28 (*J* = 2.9 Hz), indicating that absolute configuration at the C-1 position is S. From these results, compound **154** was determined to be (1S,2S,3R)-1-hydroxy-3',4'-methylenedioxy-6,7,8-trimethoxydibenzylbutyrolactone and designated as erlangerin T.

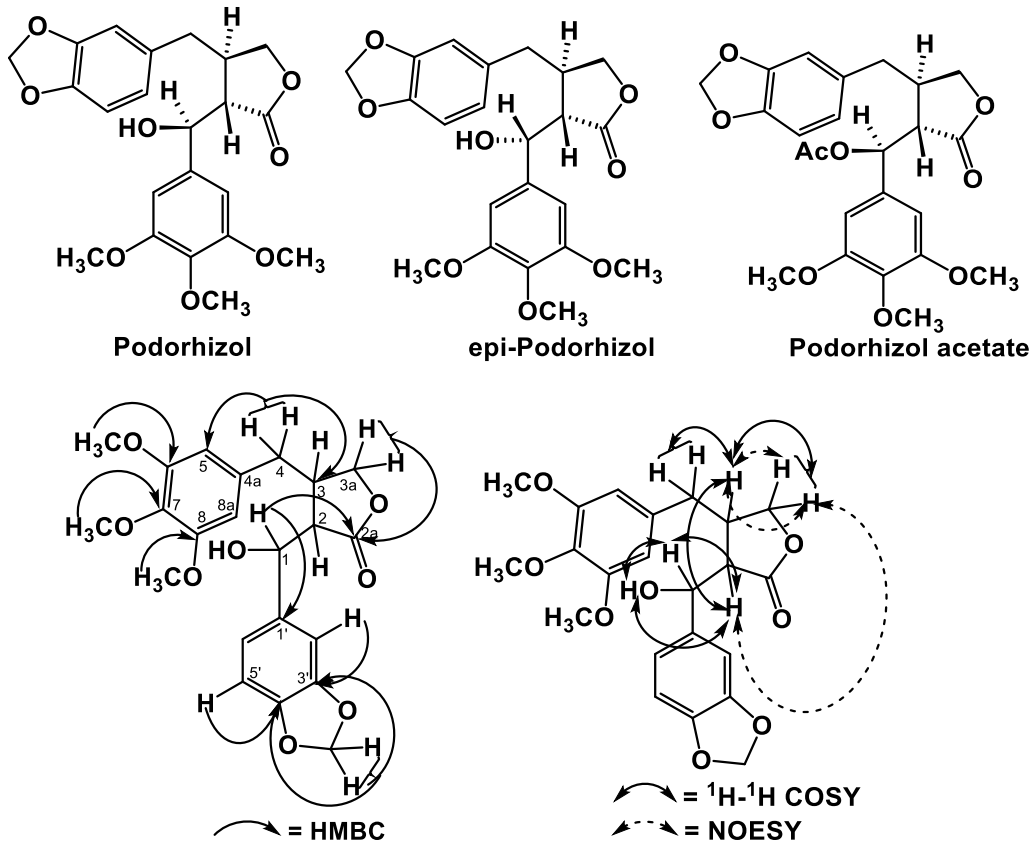

Figure 34: Selected HMBC, ^{1}H-^{1}H COSY (left) and NOESY (right) correlations of compound **154.**

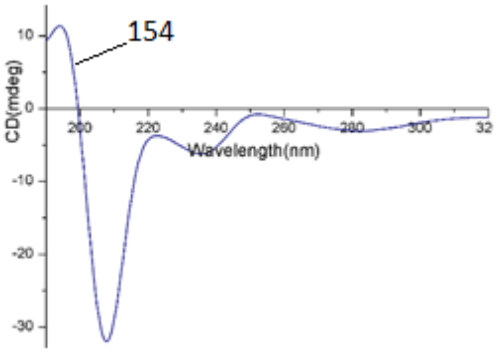

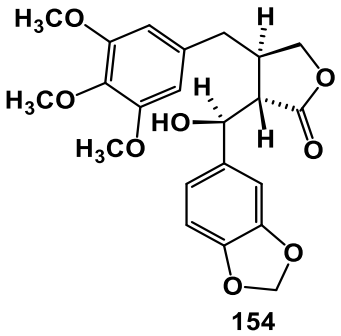

154

Figure 35: ECD spectrum (left) and chemical structure (right) of compound **154.**

Characterization of Compound 155 (Erlangerin U)

Compound **155** was obtained as a white powder, with an optical rotation of $[\alpha]_D^{20}$ -2.0 (*c* 0.10, MeOH). It had the same molecular formula as **154**, which was determined from the $[M + Na]^+$ peak at m/z 439.1377 in its ESIHRMS spectrum. The absorption maxima (λ_{max}) were observed at 286 and 211 nm in the UV spectrum. The IR spectrum showed bands at 3483 cm^{-1} (OH), 1751 cm^{-1} (C=O), 1596 and 1514 cm^{-1} (aromatic ring), 1245 cm^{-1} (C-O) and 923 cm^{-1} (OCH_2O).

The NMR data of **155** (Table 7) were similar to those of compound **154**, which indicated that **155** had a similar planar structure as **154**. The *trans* configuration of the lactone ring was obtained from NOESY correlations (Fig. 37) using the same method that we used for **154** [103]. The 2S and 3R configurations of carbons of the lactone ring were confirmed by the negative Cotton effects at 238 and 278 nm in the ECD spectrum (Fig. 38). The absolute configuration at the oxygenated C-1 position was determined from the coupling constant value of H-1. In *epi*-podorhizol (C-1, R), the H-1 proton signal appeared at δ_H 4.79 (d, *J* = 7.9 Hz) [126]. In compound **155,** the same proton appeared at δ_H 4.79 (*J* = 8.0 Hz), indicating that absolute configuration at the C-1 position is R. Therefore, compound **155** was identified as an *epimer* of **154**, (1R,2S,3R)-1-hydroxy-3',4'-methylenedioxy-6,7,8-trimethoxydibenzylbutyrolactone and named as erlangerin U.

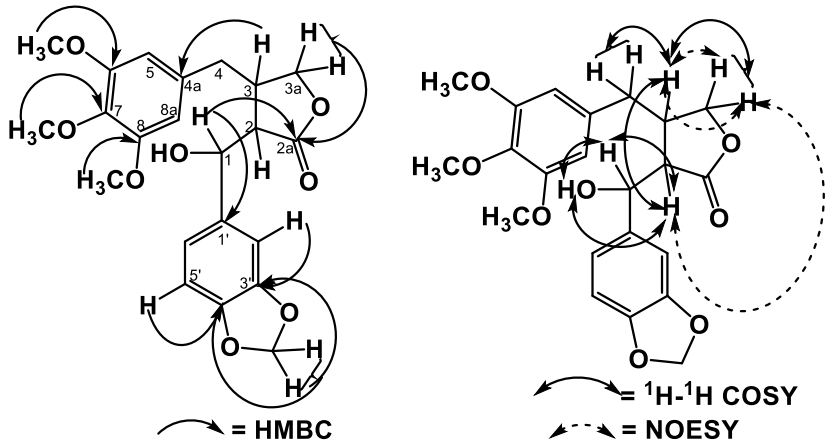

Figure 36: Selected HMBC (left), ^{1}H-^{1}H COSY and NOESY correlations (right) of compound **155.**

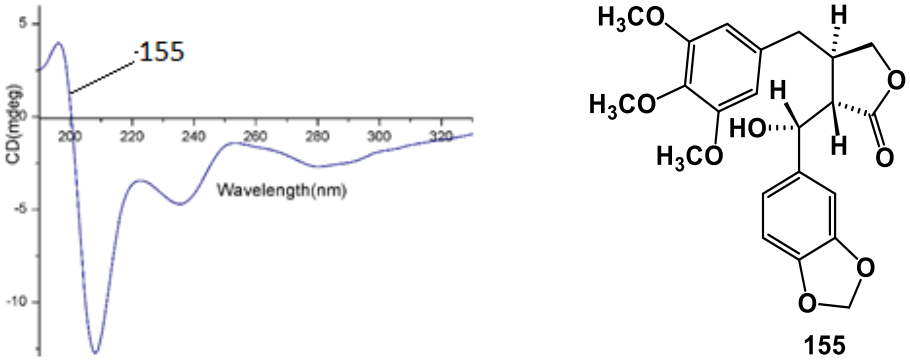

Figure 37: ECD spectrum (left) and chemical structure (right) of compound **155.**

Characterization of Compound 156 (Erlangerin V)

Compound **156** was isolated as a white powder, with a molecular formula of $C_{24}H_{26}O_9$ as established by ESIMS. It had an optical rotation of $[\alpha]_D^{20}$ -38.3 (*c* 0.10, MeOH). The IR spectrum showed bands at 1776 cm^{-1} (lactone C=O), 1742 cm^{-1} (acetate C=O), 1593 and 1504 cm^{-1} (aromatic ring), 1230 cm^{-1} (C-O) and 932 cm^{-1} (OCH_2O).

Detailed investigation of the ^{1}H and ^{13}C NMR spectral data of **156** revealed that it shares many structural features with **154** and **155.** The only significant difference was the presence of an additional acetate group in **156**. This was evidenced by the presence of an additional methyl singlet at δ_H 2.08 and two carbon signals at δ_C 169.0 and 20.8 in **156**. Detailed analysis of the 1D and 2D NMR data of **156** enabled the assignment of all the

^{1}H and ^{13}C NMR signals. The position of the acetate group was determined from the HMBC correlation of H-1 with the acetate carbonyl at δ_C 169.0.

Analysis of the NOESY spectral data (Fig. 39) allowed to assign the *trans* configuration for the lactone ring carbons, C-2 and C-3 [103]. The absolute configurations of the lactone ring carbons were elucidated as 2S and 2R since the ECD spectrum (Fig. 40) exhibited negative Cotton effects at 237 and 279 nm. The 1S configuration was determined by comparing the coupling constant value of H-1 (J = 3.5 Hz) with the value of a similar proton found in **154** (J = 2.9). Therefore, compound **156** was established as (1S,2S,3R)-1-acetoxy-3',4'-methylenedioxy-6,7,8-trimethoxydibenzylbutyrolactone and named as erlangerin V.

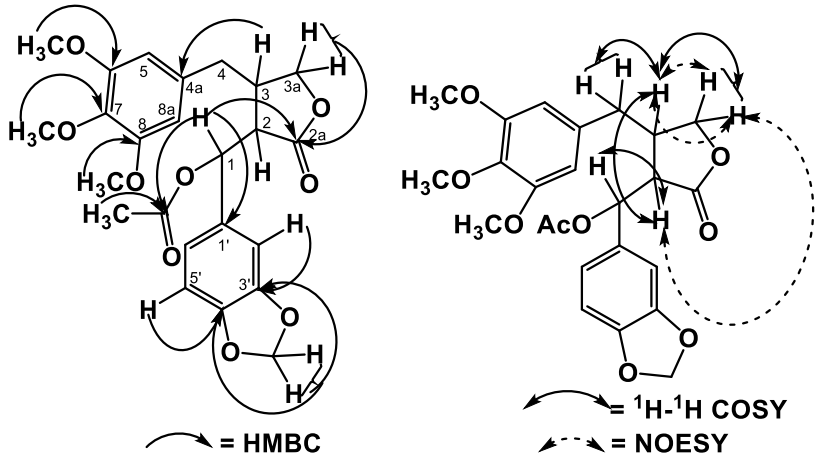

Figure 38: Selected HMBC (left), ^{1}H-^{1}H COSY and NOESY (right) correlations of compound **156.**

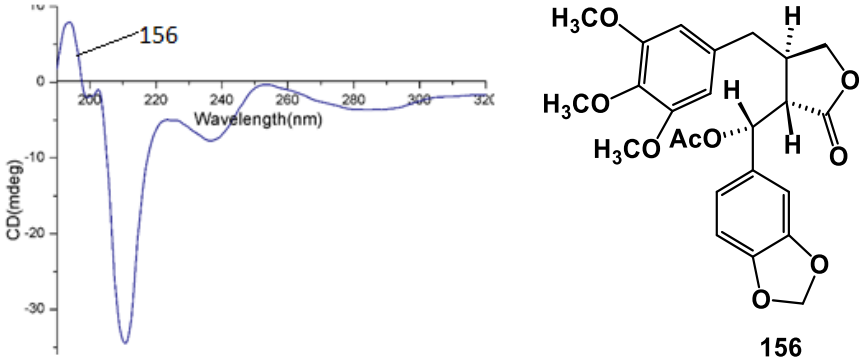

Figure 39: ECD spectrum (left) of chemical structure (right) of compound **156.**

*Table 7: ^{1}H [ppm, mult., (J in Hz)] and ^{13}C NMR spectroscopic data of compounds **154**, **155**, **156**, Podorhizol and epi-Podorhizol in $CDCl_3$*

Position	154		155		156		Podorhizol		*epi*-Podorhizol	
	δ_C	δ_H	δ_C	δ_H	δ_C	δ_H	δ_C	δ_H	δ_C	δ_H
1	71.9	5.28, dd (4.9, 2.9)	74.6	4.79, d (8.0)	73.4	6.11, d (3.5)	72.1	5.25, d (2.9)	74.7	4.79, d (7.9)
2	52.9	2.63, dd (6.2, 2.9)	51.5	2.59, t (8.7)	50.7	2.73, dd (6.5, 3.5)	52.8	2.62, dd (6.1, 2.9)	52.8	2.62, dd (9.1, 7.8)
2a	178.3	-	179.0	-	175.8	-	178.3	-	178.7	-
3	36.6	2.82, m (13.6, 8.0, 6.2)	40.0	2.49, pd (8.4, 5.8)	37.6	2.79, dq (13.6, 7.1)	36.4	2.8, m	38.9	2.50, m
3a	72.9	4.36, dd(8.9, 8.0); 3.96 dd (8.9, 5.8)	72.1	4.19,dd(9.3,7.9); 3.92, t (8.7)	72.0	3.95, dd(9.1, 5.8); 4.28, dd (9.1, 7.6)	72.8	4.39, dd(8.7, 8.0); 3.97, dd (8.7, 8.9)	72.0	4.18, dd(9.3, 7.8); 3.92, dd (9.3, 7.8)
4	40.2	2.44,dd(13.6,8.0); 2.28,dd(13.6, 8.0)	38.9	2.19, m	39.8	2.29,dd(13.6,7.1); 2.44,dd(13.6,7.6)	39.4	2.47,dd(13.7,7.7); 2.25,dd(13.7,8.1)	38.3	2.12,dd(13.7,5.4); 2.20,dd(13.8,8.9)
4a	133.7	-	133.6	-	133.2	-	131.5	-	131.6	-
5	105.7	6.08, s	105.6	6.10, s	105.6	6.08 overlap	108.6	6.22, d (1.5)	108.4	6.33, d (1.7)
6	153.3	-	153.5	-	153.2	-	146.3	-	146.6	-
7	136.8	-	137.0	-	136.7	-	147.9	-	148.1	-
8	153.3	-	153.5	-	153.2	-	107.9	6.59, d (7.7)	108.7	6.66, d (8.2)
8a	105.7	6.08, s	105.6	6.10, s	105.6	6.08 overlap	121.5	6.30, dd (7.8, 1.5)	121.5	6.34, dd (8.2, 1.7)
1’	135.0	-	134.2	-	131.0	-	136.8	-	135.5	-
2’	105.9	6.69, d (1.7)	107.1	6.93, d (1.7)	105.7	6.59, d (1.7)	102.6	6.47, s	104.1	6.65, s
3’	147.2	-	148.0	-	148.1	-	153.4	-	153.8	-
4’	148.1	-	148.1	-	147.2	-	137.6	-	138.7	-
5’	108.1	6.72, d (8.0)	108.2	6.80, d (7.9)	108.1	6.69, d (7.9)	153.4	-	153.8	-
6’	118.4	6.76, dd (8.0, 1.7)	120.4	6.87, dd(7.9,1.7)	118.5	6.63, dd (7.9, 1.7)	102.6	6.47, s	104.1	6.65, s
OCH_2O	101.5	5.97, d(1.5); 5.95, d(1.5)	101.5	5.97, m	101.4	5.91,dd (11.0,1.5)	101.1	5.92, dd (1.4, 1.4)	101.1	5.92, dd (1.4, 1.4)
6-OCH_3	56.1	3.78, s	56.2	3.80, s	56.0	3.75 overlap	-	-	-	-
7-OCH_3	60.9	3.79, s	61.0	3.79, s	60.7	3.75 overlap	-	-	-	-
8-OCH_3	56.1	3.78, s	56.2	3.80, s	56.0	3.75 overlap	-	-	-	-
3’-OCH_3	-	-	-	-	-	-	56.2	3.82, s	56.0	3.88, s
4’-OCH_3	-	-	-	-	-	-	60.8	3.83, s	61.0	3.83, s
5’-OCH_3	-	-	-	-	-	-	56.2	3.82, s	56.0	3.88, s
Acetate	-	-	-	-	169.0	-	-	-	-	-
	-	-	-	-	20.8	2.08. s	-	-	-	-
1-OH	-	2.77, d (4.9)	-	-	-	-	-	-	-	-

Characterization of Compound 157 (Erlangerin W)

Compound **157** was isolated as a white powder, with a molecular formula of $C_{27}H_{30}O_9$ (m/z 521.1785 for $C_{27}H_{30}O_9Na$ in ESIMS). It has an optical rotation $[\alpha]_D^{20}$ -32.0 (***c*** 0.10, MeOH). In the UV spectrum, absorption maxima (λ_{max}) were observed at 287 and 204 nm. The IR spectrum exhibited lactone carbonyl (1774 cm^{-1}), conjugated ester (1722 cm^{-1}), aromatic (1596, 1507 cm^{-1}), C-O (1035 cm^{-1}), methylenedioxy group (938 cm^{-1}).

Analysis of the NMR spectral data of **157** (Table 8) revealed that it contained a dibenzylbutyrolactone lignan skeleton similar to the previous compounds such as **154** and **156** (Table 8). The only structural difference was the presence of angeloyl group at C-1 of **157** in place the OH and acetyl groups found in **154** and **156**, respectively. This was supported by the presence of additional two methyl signals at δ_H 1.95 (p, *J* = 1.5 Hz) and 1.97 (dq, *J* = 7.2, 1.5 Hz); an olefinic proton signal at δ_H 6.14 (qd, *J* = 7.2, 1.5 Hz) and also two quaternary carbon signals at δ_C 165.8 and 126.8 in the ^{13}C NMR spectrum. The position of the angeloyl group was determined from the HMBC correlation of H-1 with carbonyl of the angeloyl at δ_C 165.8.

The relative configuration of H-2 and H-3 was determined to be *trans* through observation of the intensity of correlations of H-1 and H-2 with the methylene protons (H-3a$_\alpha$ and H-3a$_\beta$) in the ROESY spectrum (Fig. 41). The negative Cotton effect at 238 and 276 nm in the ECD spectrum (Fig. 42) established the 2S and 3R configuration for C-2 and C-3, respectively. A relatively small coupling constant value for H-1 (*J* = 3.4 Hz) confirmed the 1S configuration of C-1 in **157** [103]**.** Therefore, the absolute configuration of compound **157** was defined as 1S, 2S, and 3R. Thus, characterized as (1S,2S,3R)-1-angeloxy-3',4'-methylenedioxy-6,7,8-trimethoxydibenzylbutyrolactone and named as erlangerin W.

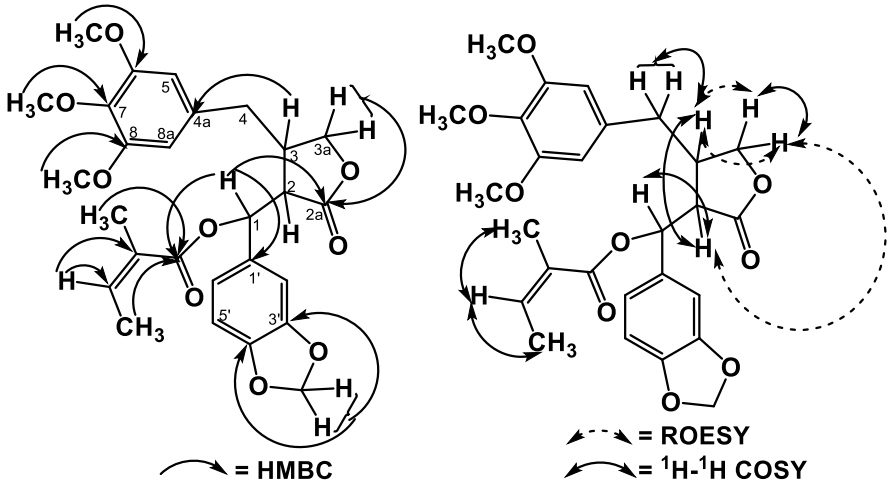

Figure 40: Selected HMBC (left), ^{1}H-^{1}H COSY and ROESY correlations (right) of compound **157.**

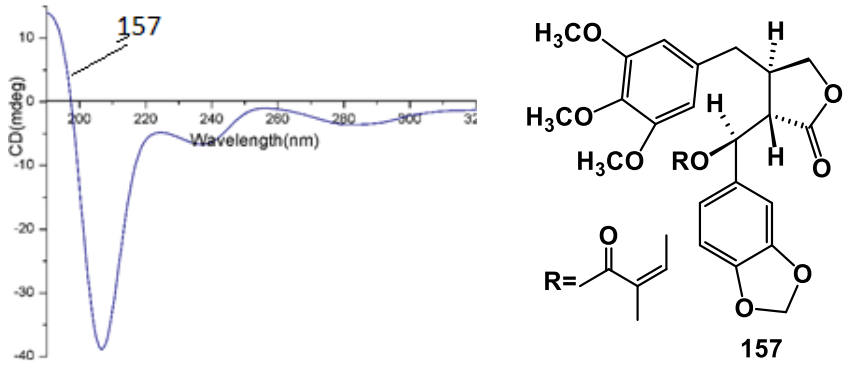

Figure 41: ECD spectrum (left) and chemical structure (right) of compound **157.**

Characterization of Compound 158 (Erlangerin X)

Compound **158**, a white powder, an optical isomer of **157**, displayed spectroscopic features that were similar to those of **157** (Table 8). The molecular formula of $C_{27}H_{30}O_9$ was deduced from the $[M + Na]^+$ peak at m/z 521.1788 in the ESIMS spectrum. It had an optical rotation $[\alpha]_D^{20}$ +35.0 (*c* 0.10, MeOH) and absorption maxima (λ_{max}) at 287 and 204 nm in the UV spectrum. The IR spectrum exhibited lactone carbonyl (1774 cm^{-1}), conjugated ester (1719 cm^{-1}), aromatic (1596, 1502 cm^{-1}), C-O (1035 cm^{-1}), and methylenedioxy group (933 cm^{-1}).

In the NOESY spectrum, correlations of H-3/H-3a_α and H-3/H-3a_β were uncertain because of the signals due to H-3 and one of the H-4 protons overlapped. Nevertheless, the *trans* configuration of the lactone ring could be determined from the negative cotton effect of

the ECD spectrum at 244 and 270 nm. A relatively large J_{H1-H2} value (5.0 Hz) suggested the same configuration at C-1 in **158** and **155**. Therefore, compound **158** was identified as (1R,2S,3R)-1-angeloxy-3',4'-methylenedioxy-6,7,8-trimethoxydibenzylbutyrolactone and designated as erlangerin X.

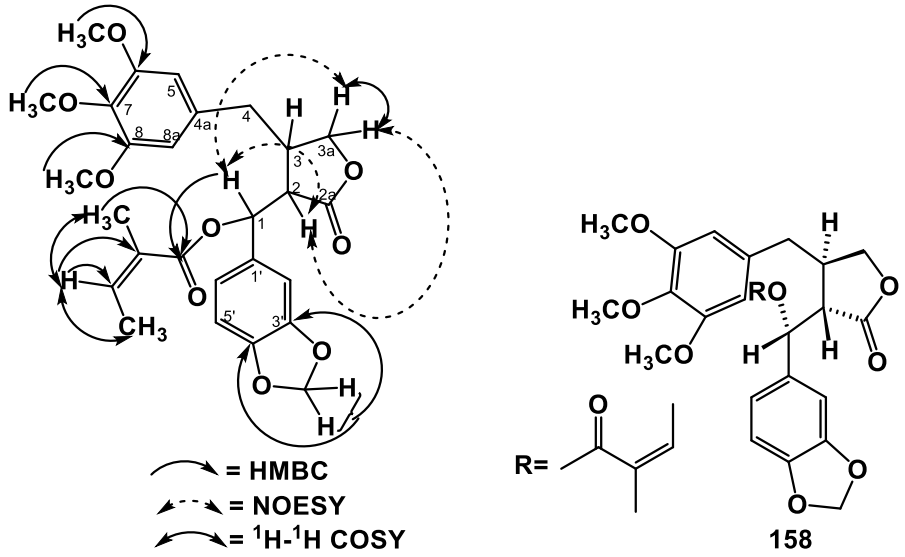

Figure 42: Selected HMBC, ^{1}H-^{1}H COSY, and NOESY (left) correlations and structure (right) of compound **158.**

Characterization of Compound 159

Compound **159** was isolated as a white crystal. Its molecular formula was determined to be $C_{24}H_{28}O_8$ form the $[M + Na]^+$ peak at m/z 467.1690 in the ESIMS spectrum. It has an optical rotation value $[\alpha]_D^{20}$ -32.0 (*c* 0.10, MeOH). In the UV spectrum, absorption maxima (λ_{max}) appeared at 280 and 231 nm. The IR spectrum exhibited lactone carbonyl (1798 cm^{-1}), ester carbonyl (1746 cm^{-1}), aromatic (1593, 1512 cm^{-1}) and C-O (1257 cm^{-1}).

The ^{1}H NMR spectrum of **159** (Table 8) revealed the presence of two ABX systems in the aromatic region at δ_H [6.62 (d, *J* = 2.1 Hz), 6.80 (d, *J* = 8.1 Hz) and 6.67 (dd, *J* = 8.1, 2.1 Hz)] and at δ_H (6.63 (d, *J* = 2.0 Hz), 6.81 (d, *J* = 8.1 Hz) and 6.85 (dd, *J* = 8.1, 2.0 Hz)). Analysis of this spectrum also revealed four overlapping signals attributed to methoxy groups (δ_H 3.89-3.82) and an ester methyl at δ_H 2.05. Furthermore, the spectrum revealed two methylene groups at δ_H 3.27 (d, *J* = 14.3 Hz) and 3.08 (d, *J* = 14.3 Hz) and at δ_H 3.04 (dd, *J* = 13.8, 4.2 Hz) and 2.79 (dd, *J* = 13.8, 9.6 Hz); an oxymethylene protons at δ_H 4.24

(t, *J* = 8.1 Hz) and 3.61 (dd, *J* = 10.7, 8.4 Hz) and a methine proton at δ_H 3.67 (ddd, *J* = 9.2, 7.9, 5.8 Hz). The ^{13}C NMR spectrum of **159** (Table 8) showed 24 carbon signals, of which six could be assigned to the four methoxy groups (δ_C 55.9, 56.0, 56.1 and 56.1) and to the acetyl group (δ_C 169.4 and 21.3). The remaining 18 carbons could be assigned to the lignan skeleton.

Analysis of the 2D NMR spectral data confirmed that **159** had the dibenzylbutyrolactone lignan skeleton. The acetyl group was unambiguously assigned to the oxygenated position (C-2). On the basis of the above analysis, the planar structure of **159** was defined as 2-acetoxy-6,7,3',4'-tetramethoxydibenzylbutyrolactone. The relative configuration of the lactone ring of compound **159** was defined as *cis* from the characteristic correlation of H-3 with protons of the acetyl methyl and the methylene group at C-1 with methylene protons at C-4 in the NOESY spectrum (Fig. 44). The *cis* configuration was also further confirmed from X-ray data (Fig. 45). The 2R and 3S configurations of the lactone ring carbons were deduced from the negative cotton effect of the ECD spectrum (Fig. 47) at 243 and 278 nm. Therefore, compound **159** was characterized as (2R,3S)-2-acetoxy-6,7,3',4'-tetramethoxydibenzylbutyrolactone. The data generated for compound **159** was identical with the data of compound **104** reported from *B. acutifolium* [106].

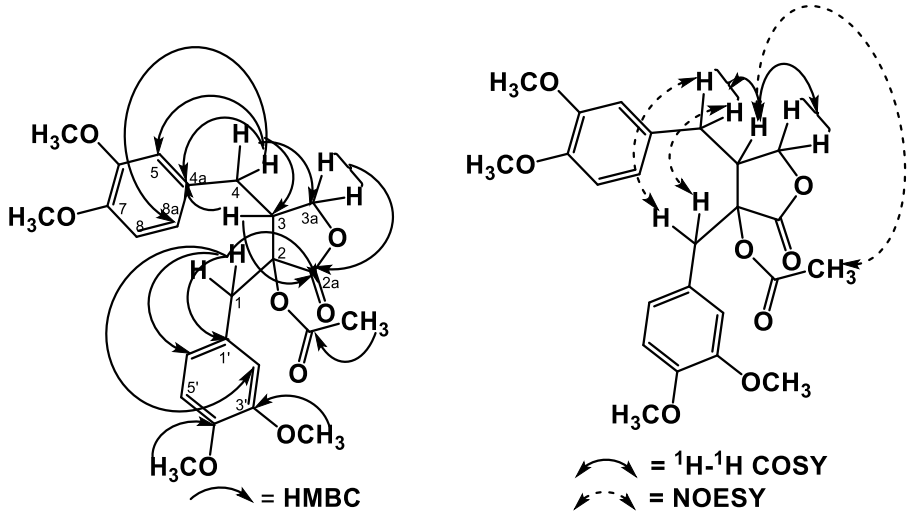

Figure 43: Selected HMBC (right), ^1H-^1H COSY and NOESY correlations (left) of compound **159.**

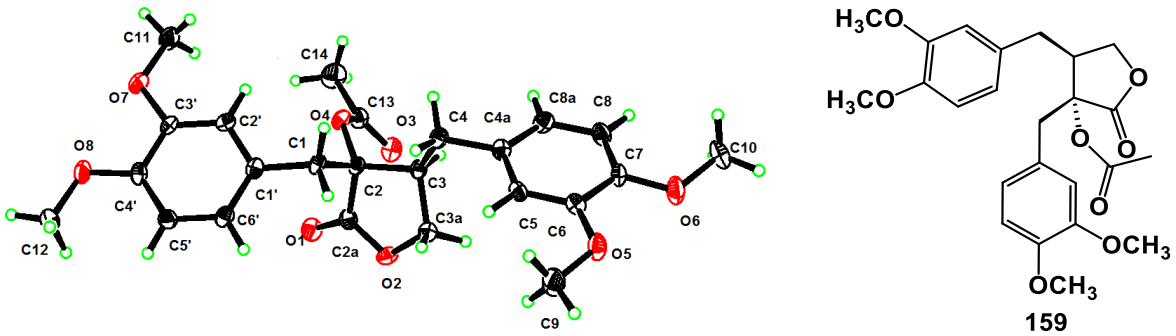

Figure 44: Perspective ORTEP drawing (left) and structure (right) of compound **159.**

Characterization of Compound 160 (Erlangerin Y)

Compound **160** was a white, amorphous powder. The molecular formula of **160** was determined to be $C_{27}H_{33}O_8$ by HREIMS with m/z of 485.2184 $[M + H]^+$. It has an optical rotation value of $[\alpha]_D^{20}$ -15.4 (*c* 0.10, MeOH). In the UV spectrum, absorption maxima (λ_{max}) appeared at 280 and 228 nm.

The ^1H and ^{13}C NMR spectral data of **160** (Table 8) resembled those of **159**. The only observed significant difference between them was the replacement of the acetyl group found in **159** with the angeloyl group. This was supported by the presence of a characteristic olefinic proton signal at δ_H 6.11 (qd, *J* = 7.3, 1.6 Hz, 1H) and two methyl proton resonance at δ_H 1.91 (dq, *J* = 7.3, 1.6 Hz, 3H) and 1.77 (p, *J* = 1.6 Hz, 3H). In the ^{13}C NMR spectrum, the angeloyl group was represented by signals at δ_C 15.9, 20.4, 126.8, 141.0 and 165.9.

Detailed examination of both the 1D and 2D NMR data of compound **160** allowed the assignment of all the signals in ^1H and ^{13}C NMR spectra (Table 8 and Fig. 46). The angeloyl moiety was assigned to the oxygenated position C-2. The *cis* configuration of the lactone ring was determined from the NOESY correlations of the methylene protons at C-1 with the methylene protons at C-4 and the methine proton at C-3 with the methyl protons of the angeloyl group at C-2 (Fig. 46). Based on the above spectral analysis, the structure of **160** was elucidated as 2-angeloxy-6,7,3',4'-tetramethoxydibenzylbutyro-lactone and named as erlangerin Y.

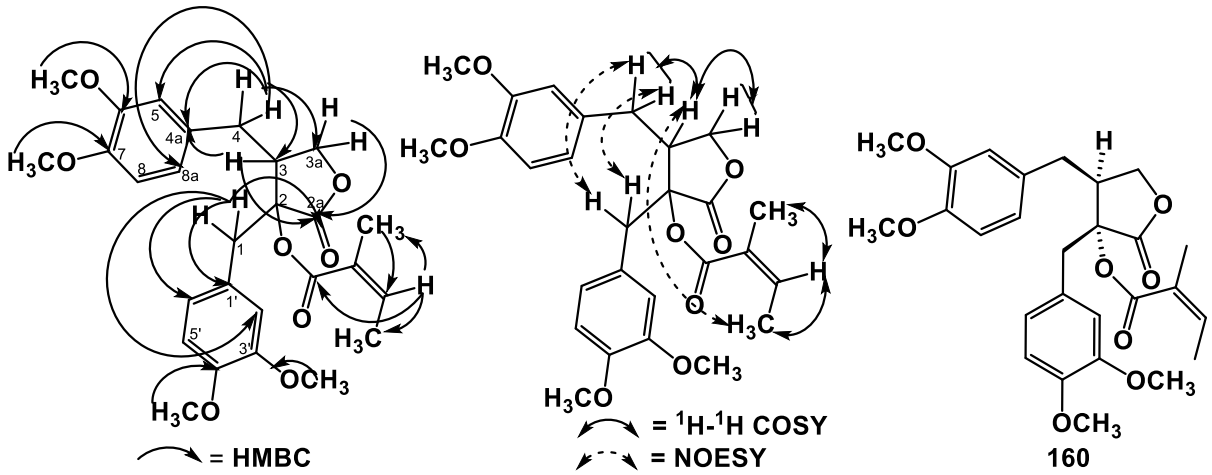

Figure 45: Selected HMBC (left), ^{1}H-^{1}H COSY and NOESY correlations (middle) and chemical structure (right) of compound **160.**

Characterization of Compound 161 (Erlangerin Z1)

The compound was obtained as white, amorphous powder. It has an optical rotation value $[\alpha]_D^{20}$ -100.8 (*c* 0.10, MeOH). The molecular formula $C_{22}H_{24}O_8$ was determined from the $[M + Na]^+$ peak at m/z 439.1367 in its ESIHRMS. The UV spectrum showed absorption maxima (λ_{max}) at 204 and 286 nm and the IR spectral data exhibited absorption bands at 3449 cm^{-1} for OH, 1769 cm^{-1} for lactone carbonyl, 1588 and 1507 cm^{-1} for the aromatic rings, 1040 cm^{-1} for C-O bond, 931 cm^{-1} for methylenedioxy group and 815 cm^{-1} for the 1,2,3-trisubstituted aromatic ring.

The ^{1}H NMR spectrum of compound **161** (Table 9) displayed signals for one symmetrical tetra-substituted aromatic ring at δ_H 6.34 (s, 2H) and one ABX systems at δ_H 6.66 (d, *J* =1.8 Hz, 1H), 6.60 (dd, *J* = 7.9, 1.8 Hz, 1H) and 6.73 (d, *J* = 7.9 Hz, 1H). The spectrum also displayed signals for three methoxy groups at δ_H 3.84 (s, 6H) and 3.82 (s, 3H); two methylene groups at δ_H 3.08 (d, *J* = 13.8 Hz, 1H), 2.92 (m, 2H overlapped), 2.49 (m, 1H); a methine proton multiplet at δ_H 2.52; oxymethylene protons resonance at δ_H 4.02 (d, *J* = 6.6 Hz, 2H) and a signal due to one methylenedioxy group at δ_H 5.93 (s, 2H). The ^{13}C NMR spectrum (Table 9) displayed 19 signals which represent 22 carbon atoms. The overlapped signals include δ_C 56.2 (OCH_3 at C-6 and C-8), δ_C 105.8 (C-5 and C-8a) and δ_C 153.5 (C-6 and C-8). The positions of the three methoxys and the methylenedioxy groups were determined from detailed analysis of the HMBC spectrum. The OH group

was assigned at the C-2 position since in the ^{1}H-^{1}H COSY spectrum the methylene protons at C-1 exhibited no correlation with other protons which revealed that C-2 was quaternary (Fig. 47). The above spectroscopic data revealed that the planar structure of compound **161** had a dibenzylbutyrolactone-type skeleton.

It was difficult to determine the relative configurations at C-2 and C-3 using the NOESY correlations since the benzylic methylenes (H-1 and H-4) were overlapped. Therefore, we used literature information to determine the stereochemistry. Harmatha *et al*. [128] discussed the chemical shifts of the *cis*- and *trans*-dibenzylbutyrolactones. They concluded that in the *cis*-derivatives, the benzylic methylenes and H-2 and H-3 were relatively well-resolved within a broad range (δ_H 2.3-3.3), while the hydrogens of the C-3a-methylene group were almost equivalent in the δ_H 4.0-4.1 range. The ^{1}H NMR spectrum of **161** exhibited the characteristic signals of a *cis*-2,3-dibenzylbutyrolactone lignan, so its relative configuration was determined to be *cis*. The 2R and 3S configurations were determined by overlapping its ECD spectrum with that of **159** (Fig. 47). Therefore, compound **161** was identified as (2R,3S)-2-hydroxy-3',4'-methylenedioxy-6,7,8-trimethoxydibenzyl-butyrolactone and designated as erlangerin Z1.

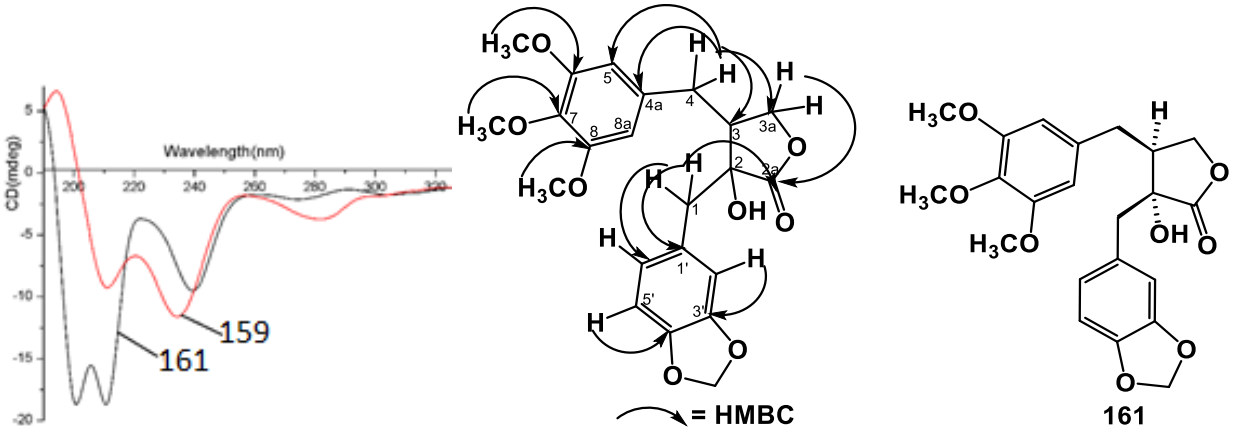

Figure 46: Overlapped ECD spectra of compounds **159** and **161** (left), selected HMBC correlations (middle) and chemical structure (right) of compound **161.**

*Table 8: ^{1}H [ppm, mult., (J in Hz)] and ^{13}C NMR spectroscopic data of compounds **157**, **158**, **159** and **160** in $CDCl_3$*

Position	157		158		159		160	
	δ_C	δ_H	δ_C	δ_H	δ_C	δ_H	δ_C	δ_H
1	73.5	6.20, d (3.4)	73.4	6.16, d (5.0)	37.3	3.27, d (14.3); 3.08, d (14.3)	37.1	3.31, d (14.3); 3.11, d (14.3)
2	51.0	2.81, dd (6.0, 3.4)	50.5	2.92, dd (6.3, 5.0)	81.7	-	81.2	-
2a	175.9		175.0		173.2		173.3	
3	38.0	2.83, ddd (13.0, 7.4, 5.7)	37.9	2.61 overlap	42.9	3.67, ddd (9.2, 7.9, 5.8)	42.5	3.77 (ddt, *J*=10.7, 8.7, 4.5 Hz, 1H)
3a	72.0	4.34, dd (9.0, 7.4); 4.01, dd (9.0, 5.3)	71.4	4.01, dd (9.2, 6.7); 3.90, dd (9.2, 5.4)	69.3	4.24, t (8.1); 3.61, dd (10.7, 8.4)	69.2	4.29, t (8.7); 3.64, dd (10.7, 8.9)
4	40.2	2.38, dd, (13.6, 7.1); 2.52, dd (13.6, 7.4)	39.5	2.80 overlap 2.61 overlap	32.1	3.04, dd (13.8, 4.2); 2.79, dd (13.8, 9.6)	32.0	3.01, dd (14.0, 6.7); 2.79, dd (14.0, 9.2)
4a	133.3		133.5		130.1		130.0	
5	105.7	6.10 overlap	105.8	6.24 overlap	111.6	6.62, d (2.1)	111.3	6.60, d (2.0)
6	153.4	-	153.6	-	149.4	-	149.2	-
7	136.9	-	137.1	-	148.1	-	148.0	-
8	153.4	-	153.6	-	110.0	6.80, d (8.1)	110.8	6.77, d (8.2)
8a	105.7	6.10 overlap	105.8	6.24 overlap	120.5	6.67, dd (8.1, 2.1)	120.5	6.67, dd (8.2, 2.0)
1’	131.4		131.0		125.4	-	125.3	-
2’	106.0	6.62, d (1.8)	107.1	6.80 overlap	113.9	6.83, d (2.0)	113.9	6.79, d (2.1)
3’	147.5	-	147.9	-	148.9	-	148.5	-
4’	148.2	-	148.2	-	148.7	-	148.4	-
5’	108.3	6.72, d (8.0)	108.4	6.76, d (8.4)	111.6	6.81, d (8.1)	111.5	6.78, d (8.2)
6’	118.7	6.66, dd (8.0, 1.8)	120.5	6.80 overlap	123.1	6.85, dd (8.1, 2.0)	123.1	6.82, dd (8.2, 2.1)
OCH_2O	101.6	5.97, dd, (15.0, 1.6)	101.5	5.96 m	-	-	-	-
6-OCH_3	56.1	3.80 overlap	56.2	3.82 overlap	56.1	3.87 overlap	55.9	3.81, s
7-OCH_3	60.9	3.81, s	61.0	3.82 overlap	55.9	3.87overlap	55.8	3.83, s
8-OCH_3	56.1	3.80 overlap	56.2	3.82 overlap	-	-	-	-
3’-OCH_3	-	-	-	-	56.1	3.87 overlap	55.9	3.84 overlap
4’-OCH_3	-	-	-	-	56.0	3.87overlap	56.0	3.84 overlap
	165.8	-	166.2	-	-	-	-	-
	126.8	-	127.0	-	-	-	-	-
Angeloyl	140.6	6.14, qd (7.2, 1.5)	140.5	6.14, dd (7.3, 1.6)	-	-	-	6.11, qd (7.3, 1.6)
	16.0	1.97, dq (7.2, 1.5)	16.0	2.00, dq (7.3, 1.6)	-	-	-	1.91, dq (7.3, 1.6)
	20.7	1.95, p (1.5)	20.7	1.93, p (1.6)	-	-	-	1.77, p (1.6)
Acetate	-	-	-	-	169.4	-	-	-
	-	-	-	-	21.3	2.05, s	-	-

Characterization of Compound 162 (Erlangerin Z)

Compound **162** was isolated as white, amorphous solid, with an optical rotation value of $[\alpha]_D^{20}$ -55.0 (*c* 0.10, MeOH). Its molecular formula was determined to be $C_{26}H_{30}O_{10}$, on the basis of EIMS findings at m/z 502.1836 $[M]^+$. In the UV spectrum, absorption maxima (λ_{max}) appeared at 280 and 232 nm. The IR spectrum exhibited lactone carbonyl (1793 cm^{-1}), ester carbonyl (1751 cm^{-1}), aromatic (1594, 1512 cm^{-1}) and C-O (1262 cm^{-1}).

In the ^1H NMR spectrum (Table 9), the aromatic proton resonances appeared as two sets of ABX system (δ_H 6.68 (d, *J* = 2.1 Hz), 6.69 (d, *J* = 8.1 Hz), 6.71 (dd, *J* = 8.1, 2.1 Hz)). The spectrum also displayed a multiplet signal at δ_H 6.85-6.80 integrated for three protons due to the second aromatic ring. A methine proton resonated at δ_H 3.68 (m, *J* = 11.1, 9.6, 9.1, 7.3 Hz). The proton signals for an oxymethylene group appeared at δ_H 4.37 (t, *J* = 8.9 Hz) and δ_H 3.88 (dd, *J* = 8.9, 1.8 Hz). The two doublet of doublets resonated at δ_H 3.01 (*J* = 14.0, 7.3 Hz) and δ_H 2.70 (*J* = 14.0, 9.1 Hz) were due to a methylene group at C-4. The two acetyl methyl groups and the four methoxy groups were represented by proton signals resonated at δ_H 2.14 and 1.85, and at δ_H 3.86, 3.84, and 3.83.

Examination of both 1D and 2D NMR data (Table 9 and Fig. 48) of compound **162** confirmed that it had dibenzylbutyrolactone-type lignan skeleton. Detailed analysis of the spectroscopic data also showed similarity in planar structure of compound **162** with that of **159**. The only observed significant differences were the presence of additional signals in the ^{13}C NMR spectrum of **162** which represent an acetate group at δ_C 168.7 and 21.3.

The *cis* configuration of the lactone ring of **162** was deduced from its NOESY correlations (Fig. 48) of the H-1 proton with the methylene protons of C-4 and the methyl protons on the acetate (C-1) with H-4a (δ_H 2.70). The 2S and 3R configurations of the lactone ring were obtained by comparing the ECD spectrum of **162** with that of **159** (Fig. 49).

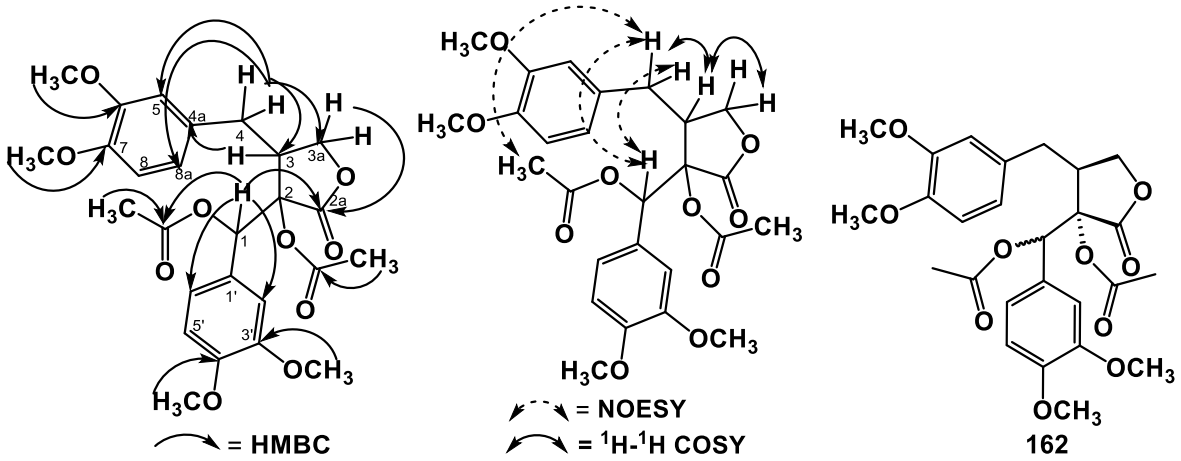

Figure 47: Selected HMBC (left), ^{1}H-^{1}H COSY and NOESY (middle) correlations and structure (right) of compound **162.**

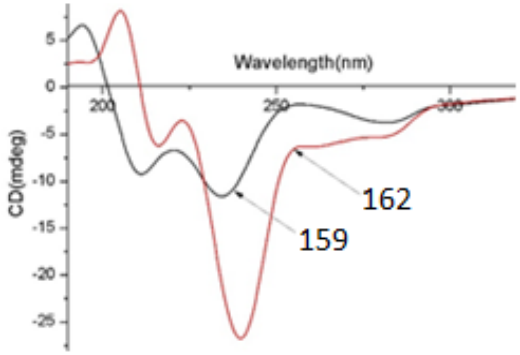

Figure 48: Overlapped ECD spectra of compounds **159** and **162.**

Characterization of Compound 163 (Dimethylmatairesinol)

Compound **163** was obtained as colorless gum, with an optical rotation value $[\alpha]_D^{20}$ -36.7 (*c* 0.10, MeOH). Its molecular formula of was determined to be $C_{22}H_{26}O_8$ from the $[M + H]^+$ peak at m/z 387.1811 in the ESIMS spectrum. The UV spectrum showed absorption maxima (λ_{max}) at 231 and 280 nm and the IR spectral data exhibited absorption bands at 1769 cm^{-1} for the lactone carbonyl, 1591 and 1516 cm^{-1} for the aromatic ring and 1025 cm^{-1} for the C-O bond.

The ^{1}H and ^{13}C NMR spectra (Table 9) of compound **163** were similar to those of the reported compound dimethylmatairesinol (**92**) [100]. The 2R,3R configurations of the lactone ring of compound **163** were deduced from the negative Cotton effect at 233 and

280 nm in the ECD spectrum (Fig. 50). Therefore, compound **163** was elucidated as (2R,3R)-dimethylmatairesinol.

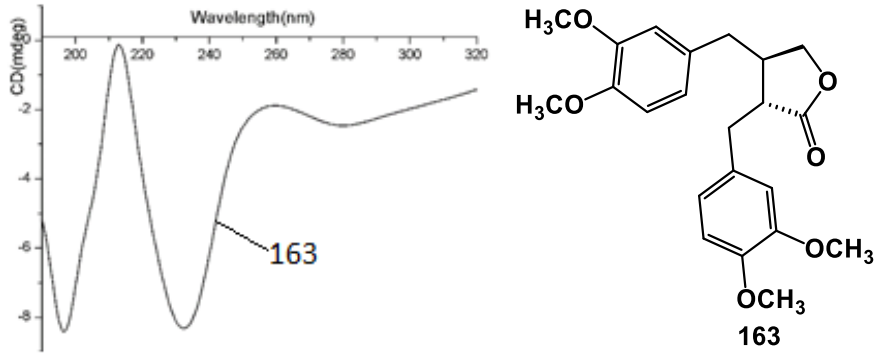

Figure 49: ECD spectrum (left) and structure (right) of compound **163.**

Characterization of Compound 164 (Erlangerin Z2)

Compound **164** was isolated as a colorless gum. Its molecular formula $C_{29}H_{36}O_9$ was determined from the $[M + H]^+$ peak at m/z 529.2440 in its ESIHRMS spectrum. It has an optical rotation value of $[\alpha]_D^{20}$ -5.8 (*c* 0.10, MeOH). In the UV spectrum, the absorption maxima (λ_{max}) were observed at 206 and 286 nm. The IR spectrum displayed bands at 1786, 1734, 1588, 1504, 923 and 840 cm^{-1} assignable for ester carbonyl, conjugated ester carbonyl, aromatic ring, a methylenedioxy group, and 1,2,3-trisubstituted aromatic ring, respectively.

The ^1H NMR spectrum (Table 10) presented three methyl groups [δ_H 2.05 (s, 3H), 2.01 (dq, *J* = 7.3, 1.6 Hz, 3H) and 1.92 (p, *J* = 1.6 Hz, 3H)]; one symmetrical tetrasubstituted aromatic ring [(δ_H 6.27 (s, 2H)]; one unsymmetrical 1,3,5-trisubstituted aromatic ring [δ_H 6.68 (d, *J* = 8.5 Hz, 1H), 6.52 (m, 2H, overlap)]; two set of AA system corresponding to methylene groups (δ_H 2.62 (dt, *J* = 14.0, 8.9 Hz) and 2.68 (ddd, *J* = 14.0, 7.3, 2.6 Hz)); two methine-proton multiplets (δ_H 2.17 and 2.12); two oxymethylene resonances with AB system (δ_H 4.11 (dd, *J* = 11.5, 5.4 Hz, 1H), 4.01 (dd, *J* = 11.3, 5.9 Hz, 1H) and 4.22 (ddd, *J* = 11.3, 6.0, 2.3 Hz, 2H)); three methoxy groups [δ_H 3.79 (s, 6H, overlap) and 3.82 (s, 3H)]; a methylenedioxy group [δ_H 5.91 (s, 2H)] and a characteristic olefinic proton signal for an angeloyl group (δ_H 6.10 (qd, *J* = 7.3, 1.6 Hz, 1H)).

*Table 9: ^{1}H [ppm, mult., (J in Hz)] and ^{13}C NMR spectroscopic data of compounds **161**, **162**, **163** and Dimethylmatairesinol in $CDCl_3$*

Position	161		162		163		Dimethylmatairesinol	
	δ_C	δ_H	δ_C	δ_H	δ_C	δ_H	δ_C	δ_H
1	42.2	3.08, d (13.8); 2.92, m	74.3	6.26, s	34.6	2.95, dd (14.1, 5.4); 2.90 (dd, 14.1, 6.7)	34.5	2.95, dd (14.0, 5.6); 2.91, dd (14.0, 6.3)
2	76.5	-	80.1	-	46.6	2.61 overlap	46.6	2.60, ddd (9.1, 6.3, 5.6)
2a	178.0	-	171.0	-	178.8	-	178.7	-
3	44.1	2.52, m	42.7	3.68, dtd (11.1,9.6,9.1,7.3)	41.2	2.57, m	41.1	2.5, m
3a	70.2	4.06, d (6.6)	70.1	4.37, t (8.8); 3.88, dd (8.9, 1.8)	71.3	4.11, dd (9.1, 7.1); 3.86, dd (9.5, 7.5)	71.2	4.12, dd (8.8, 7.3); 3.89, dd (8.8, 8.2)
4	32.5	2.92 overlap; 2.48, m	32.3	3.01, dd (14.0, 7.2); 2.70, dd (14.0, 9.1)	38.3	2.61 overlap 2.50 overlap	38.2	2.62, dd (13.4, 5.8); 2.50, dd (13.4, 8.0)
4a	128.0	-	129.6	-	130.5	-	130.4	-
5	105.8	6.34, s	111.4	6.68, d (2.1)	112.0	6.47, d (2.0)	111.0	6.49, d (2.1)
6	153.5	-	148.2	-	148.0	-	147.9	-
7	136.4	-	148.1	-	149.1	-	149.0	-
8	153.5	-	110.2	6.79, d (8.1)	112.0	6.74, d (8.1)	111.8	6.78, d (8.1)
8a	105.8	6.34 overlap	120.6	6.71, dd (8.1, 2.1)	120.7	6.54, dd (8.1, 2.0)	120.6	6.55, dd (8.1, 2.1)
1’	134.4	-	126.5	-	130.3	-	130.2	-
2’	110.7	6.66, d (1.8)	111.6	6.82 overlap	112.5	6.67, d (2.0)	112.3	6.69, d (2.0)
3’	147.1	-	149.3	-	148.0	-	147.9	-
4’	148.0	-	149.5	-	149.1	-	149.0	-
5’	108.4	6.73, d (7.9)	111.4	6.82 overlap	112.5	6.76, d (8.1)	111.3	6.76, d (8.3)
6’	123.3	6.60, dd (7.9, 1.8)	120.9	6.82 overlap	121.4	6.64, dd (8.1, 2.0)	121.3	6.66, dd (8.3, 2.0)
OCH_2O	101.2	5.93, s	-	-	-	-	-	-
6-OCH_3	56.2	3.84 overlap	56.0	3.86 overlap	55.9	3.84 overlap	55.9	3.87, s
7-OCH_3	61.0	3.82, s	55.8	3.86 overlap	55.9	3.80, s	55.9	3.83, s
8-OCH_3	56.2	3.84 overlap	-	-	-	-	-	-
3’-OCH_3	-	-	56.0	3.83, s	55.9	3.84 overlap	55.8	3.86, s
4’-OCH_3	-	-	56.0	3.84, s	55.9	3.82 overlap	55.9	3.84, s
5’-OCH_3	-	-	-	-	-	-	-	-
Acetate	-	-	168.7	2.19, s	-	-	-	-
	-	-	21.3	-	-	-	-	-
Acetate	-	-	168.8	1.85, s	-	-	-	-
	-	-	21.0	-	-	-	-	-

The ^{13}C NMR spectrum (Table 10) of compound **164** exhibited signals for 29 carbon atoms including two benzene rings (from δ_C 105.9 to 153.2), an acetyl group (δ_C 171.1, 21.1), an angeloyl group (δ_C 169.9, 127.6, 138.9, 16.0, 20.8), three methoxy groups (δ_C 56.1, 61.0), a methylenedioxy group (δ_C 101.0), two aliphatic methine carbons (δ_C 40.0, 40.2) and two oxymethylene carbons (δ_C 63.9, 64.0).

Detailed analysis of ^{1}H-^{1}H COSY and HMBC spectra (Fig. 51) revealed that compound **164** is a dibenzylbutane-type lignan. The connectivity between an acetyl and an angeloyl group was obtained from the HMBC correlations (Fig. 51) of H-2a and H-3a with acetate carbonyl (δ_C 171.1) and angeloyl carbonyl (δ_C 167.9), respectively. Therefore, the structure of compound **164** was elucidated as 9'-acetoxy-9-angeloxy-3,4-methylene-dioxy-3',4',5'-trimethoxydibenzylbutane and named as erlangerin Z2.

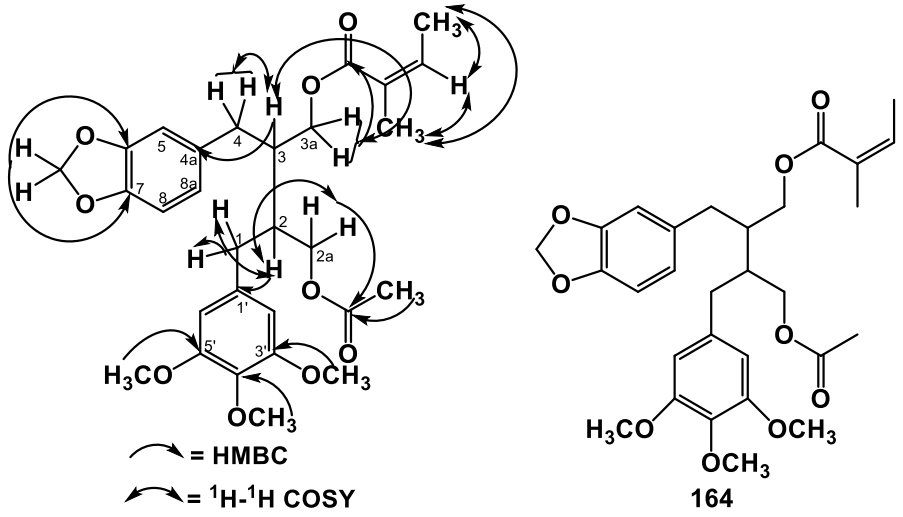

Figure 50: Selected HMBC and ^{1}H-^{1}H COSY (left) and correlations chemical structure (right) of compound **164.**

Characterization of Compound 165 (Erlangerin Z3)

Compound **165** was isolated as a white powder, with an optical rotation value $[\alpha]_D^{20}$ -14.0 (*c* 0.10, MeOH). The molecular formula $C_{29}H_{38}O_9$ obtained from EIMS ($[M]^+$, m/z 530.2518). In the UV spectrum, the absorption maxima (λ_{max}) were observed at 205 and 285 nm.

The ^{1}H and ^{13}C NMR spectra of compound **165** (Table 10) revealed close similarity with that of **164**. The most important difference was the olefinic proton signal at δ_H 6.10 and

carbon signals at δ_C 127.6 and 138.9 found in **164** were replaced with aliphatic proton and carbon resonances. The ^1H and ^{13}C NMR spectral data of the 2-methylbutanoyl group found in **165** showed similarity in terms of chemical shift and coupling constant values with those of **149**. On the basis of detailed analysis of both the 1D and 2D NMR data (Table 10 and Fig. 52), the structure of compound **165** was proposed as 9'-acetoxy-9-(2-methylbutanoyloxy)-3,4-methylenedioxy-3',4',5'-trimethoxydibenzylbutane and designated as erlangerin Z3.

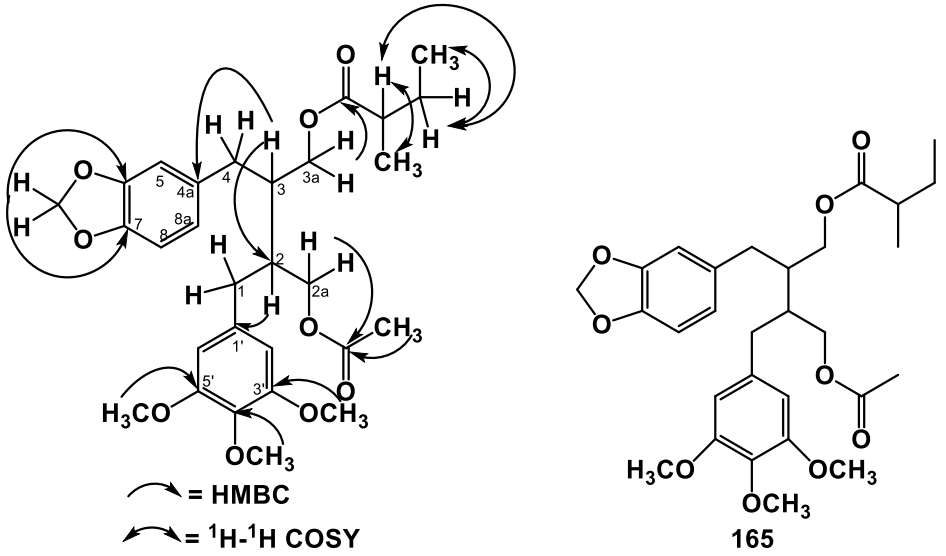

Figure 51: Selected HMBC and ^{1}H-^{1}H COSY correlations (left) and chemical structure (right) of compound **165.**

Characterization of Compound 166 (Erlangerin Z4)

Compound **166** was isolated as white, amorphous powder, with an optical rotation value $[\alpha]_D^{20}$ -55.2 (*c* 0.10, MeOH). Its molecular formula $C_{26}H_{30}O_7$ was deduced from the $[M + Na]^+$ peak at m/z 477.1880 in the ESIHRMS spectrum.

Its ^1H NMR spectrum (Table 10) exhibited signals for a symmetrical tetrasubstituted benzene ring [(δ_H 6.38 (s, 2H); an unsymmetrical 1,3,5-trisubstituted aromatic ring [(δ_H 6.86 (d, *J* = 1.1 Hz, 1H), 6.73 (d, *J* = 1.1 Hz, 2H, overlap)]; a methylenedioxy group [δ_H 5.94 (s, 2H)]; two olefinic protons (δ_H 6.30 (d, *J* = 15.1 Hz, 1H) and 5.92 (m, 1H)); one angeloyl olefinic proton (δ_H 6.07 (qd, *J* = 7.2, 1.5 Hz, 1H)), oxymethylene protons (δ_H 4.17 (d, *J* = 6.2 Hz, 2H)); three methoxy groups (δ_H 3.80 (s, 6H) and 3.82 (s, 3H)); methylene protons (δ_H 2.78 (dd, *J* = 13.6, 6.6 Hz, 1H) and 2.73 (dd, *J* = 13.5, 7.5 Hz, 1H)); a methine

proton (δ_H 2.85 (h, *J* = 6.6 Hz, 1H)) and two angeloyl methyl groups (δ_H 1.98 (dq, *J* = 7.2, 1.5 Hz, 3H) and 1.85 (p, *J* = 1.5 Hz, 3H)).

The ^{13}C NMR spectrum (Table 10) of compound **166** exhibited 23 signals for 26 carbon atoms. These include two benzene rings (from δ_C 105.6 to 153.2), an angeloyl group (δ_C 168.1, 138.2, 128.0, 16.0, 20.8), two olefinic carbons (δ_C 131.5, 128.5), a methylenedioxy group (δ_C 101.2), an oxymethylene (δ_C 66.4), three methoxy groups (δ_C 56.2 (2C), 61.0), an aliphatic methine (δ_C 43.9) and an aliphatic methylene (δ_C 38.9).

The HMBC correlations (Fig. 53) of H-4 and H-3 with C-4a, C-2, C-1; H-2 and H-1 with C-1', C-2', C-6' and H-3 and H-4 with C-1, C-2 revealed the connectivity of the two aromatic rings via four carbon atoms (C-1 to C-4). HMBC correlations also helped to deduce the positions of the three methoxys, methylenedioxy and angeloyl groups (Fig. 53). Therefore, based on the above spectroscopic data, the structure of compound **166** was characterized as 9'-angeloxy-3,4-methylenedioxy-3',4',5'-trimethoxydibenzylbutene and named as erlangerin Z4.

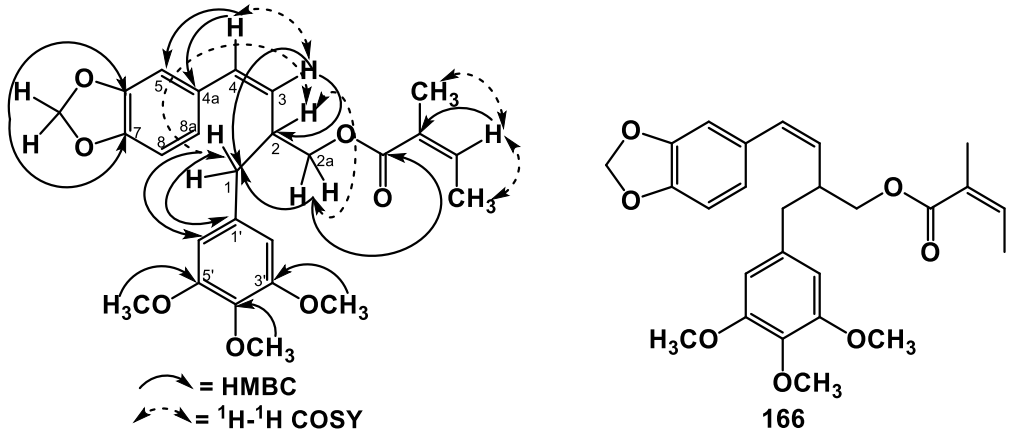

Figure 52: Selected HMBC and ^1H-^1H COSY correlations (left) and chemical structure (right) of compound **166.**

*Table 10: ^{1}H [ppm, mult., (J in Hz)] and ^{13}C NMR spectroscopic data of compounds **164**, **165**, and **166** in $CDCl_3$*

Position	164		165		166	
	δ_C	δ_H	δ_C	δ_H	δ_C	δ_H
1	35.1	2.62, dt (14.0, 8.9)	35.1	2.65, dt (14.0, 7.1); 2.60, ddd (14.0, 7.8, 3.9)	38.9	2.78, dd (13.6, 6.6); 2.73, dd (13.6, 7.5)
2	40.0	2.12, m	40.0	2.11 overlap	43.9	2.85, h (6.6)
2a	63.9	4.22, ddd(11.3,6.0,2.3); 4.01, dd(11.3, 5.9)	64.1	4.00, ddd (14.4, 11.5, 5.6); 4.22, ddd (11.5, 5.9, 1.6)	66.4	4.17, d (6.2)
3	40.2	2.17, m	40.2	2.11 overlap	128.5	5.92, m
3a	64.4	4.22, ddd(11.3,6.0,2.3); 4.11, dd(11.3, 5.4)	64.4	4.00, ddd (14.4, 11.5, 5.6); 4.22, ddd (11.5, 5.9, 1.6)	-	-
4	35.9	2.68, ddd(14.0,7.3,2.6)	35.8	2.65, dt (14.0, 7.1); 2.60, ddd (14.0, 7.8, 3.9)	131.5	6.30, d (15.1)
4a	133.5	-	133.6	-	131.9	-
5	109.2	6.52, s	109.3	6.52, m	105.9	6.86, d (1.1)
6	146.0	-	146.1	-	147.2	-
7	147.8	-	147.8	-	148.1	-
8	108.2	6.68, d (8.5)	108.2	6.69, d (8.2)	108.4	6.73, d (1.1)
8a	122.0	6.52, s	122.0	6.52, m	120.7	6.73, d (1.1)
1’	135.6	-	135.5	-	135.0	-
2’	105.9	6.27, s	106.0	6.26, s	106.4	6.38, s
3’	153.2	-	153.3	-	153.2	-
4’	136.4	-	136.6	-	136.6	-
5’	153.2	-	153.3	-	153.2	-
6’	105.9	6.27, s	106.0	6.26, s	106.4	6.38, s
OCH_2O	101.0	5.91, s	101.0	5.92, s	101.2	5.94, s
3’-OCH_3	56.1	3.79, s	56.2	3.80, s	56.2	3.80, s
4’-OCH_3	61.0	3.82, s	61.0	3.83, s	61.0	3.82, s
5’-OCH_3	56.1	3.79, s	56.2	3.80, s	56.2	3.80, s
	167.9	-	-	-	168.1	-
	127.6	-	-	-	128.0	-
Angeloyl	138.9	6.10, qd (7.3, 1.6)	-	-	138.2	6.07, qd (7.2, 1.5)
	16.0	2.01, dq (7.3, 1.6)	-	-	16.0	1.98, dq (7.2, 1.5)
	20.8	1.92, p (1.6)	-	-	20.8	1.89, p (1.5)
	-	-	176.8	-	-	-
2-Methyl-	-	-	41.3	2.40, h (6.9)	-	-
butanoyl	-	-	27.0	1.70, dt (13.8, 7.6); 1.55, ddd (13.8, 7.6, 6.5)	-	-
	-	-	11.8	0.93, t (7.6)	-	-
	-	-	16.8	1.17, d (6.9)	-	-
Acetate	171.1	-	171.1	-	-	-
	21.1	2.05, s	21.2	2.06, s	-	-

Characterization of Compound 168 (Erlangerin Z5)

Compound **168** was isolated as white gummy like material, with an optical rotation value $[\alpha]_D^{20}$ 0.0 (*c* 0.10, MeOH). The molecular formula $C_{30}H_{38}O_8$ was determined from the $[M + Na]^+$ peak at m/z 549.2471 in its ESIHRMS spectrum.

The ^1H NMR spectrum (Table 11) displayed signals for a methylene group (δ_H 2.70 (dd, *J* = 14.0, 7.2 Hz) and 2.62 (dd, *J* = 13.9, 7.6 Hz)), an oxymethylene group (δ_H 4.29 (dd, *J* = 11.4, 6.1 Hz) and 4.11 (dd, *J* = 11.4, 5.3 Hz)), a methine group (δ_H 2.17 (m)). An ABX system in the aromatic region (δ_H 6.78 (d, *J* = 8.0 Hz), 6.57 (dd, *J* = 8.0, 2.0 Hz) and δ_H 6.49 (d, *J* = 2.0 Hz)) revealed the presence of a trisubstituted aromatic ring. Besides, signals due to a methoxy group (δ_H 3.78 (s)), an aromatic hydroxyl group (δ_H 5.47 (s)) and an angeloyl group (δ_H 6.09 (qd, *J* = 7.3, 1.6 Hz), 2.00 (dq, *J* = 7.3, 1.6 Hz) and 1.91 (p, *J* = 1.6 Hz)) were observed.

The ^{13}C NMR spectrum (Table 11) of **168** displayed only 15 carbon signals. Out of these six signals could be assigned to six aromatic carbon atoms (δ_C 111.3, 114.3, 121.8, 131.8, 144.1, 146.6) and the signal at δ_C 55.8 was assigned to a methoxy carbon. The angeloyl moiety was represented by signals at δ_C 168.0, 127.8, 138.6, 20.8 and 16.0. The carbon signals at δ_C 35.0, 40.1 and 64.1 were assignable to a methylene, a methine and an oxymethylene carbon atoms, respectively. The ^1H-^1H COSY correlations (Fig. 54) of H-8 with the methylene groups (H-7 and H-9) revealed that H-8 was in between H-7 and H-9. This relationship was further confirmed by the HMBC correlation of H-8 with C-7 and C-9. The connectivity of C-7 with the aromatic ring was confirmed from the HMBC correlations (Fig. 54) of H-7 with C-1, C-2, and C-6. The attachment of C-9 with the angeloyl group was also obtained from HMBC correlations of H-9 with the carbonyl group (δ_C 168.0). The HMBC correlations of a methoxy and a hydroxyl proton with C-3 and C-4 suggested the respective positions of these groups. Partial structure **167** could be deduced based on the above spectroscopic data. This proposed structure (**167**) corresponds to a molecular formula of $C_{15}H_{19}O_4$ which is half of the molecular formula of **168**. Presumably, compound **168** is a dimer of **167** where the two fragments are joined at C-8 and C-8'. This assumption was also confirmed by the presence of HMBC correlation

of the proton signal of H-8/H-8' with the carbon signal of C-8/C-8'. Therefore, based on the above analysis compound **168** was characterized as 9,9'-diangeloxy-4,4'-dihydroxy-3,3'-dimethoxydibenzylbutane and named as erlangerin Z5.

*Table 11: ^{1}H [ppm, mult., (J in Hz)] and ^{13}C NMR spectroscopic data of compound **168** in $CDCl_3$*

Position	δ_C	δ_H
1 & 1'	131.8	-
2 & 2'	111.3	6.49, d (2.0)
3 & 3'	146.6	-
4 & 4'	144.1	-
5 & 5'	114.3	6.78, d (8.0)
6 & 6'	121.8	6.57, dd (8.0, 2.0)
7 & 7'	35.0	2.70, dd (14.0, 7.2); 2.62 (14.0, 7.6)
8 & 8'	40.1	2.17, m
9 & 9'	64.1	4.29, dd (11.4, 6.1); 4.11 (11.4, 5.3)
3 & 3'-OCH_3		3.78, s
	168.0	-
	127.8	-
Angeloyl	138.6	6.09, qd (7.2, 1.6)
	16.0	2.00, dq (7.2, 1.6)
	20.8	1.91, p (1.6)
5 & 5' OH		5.47

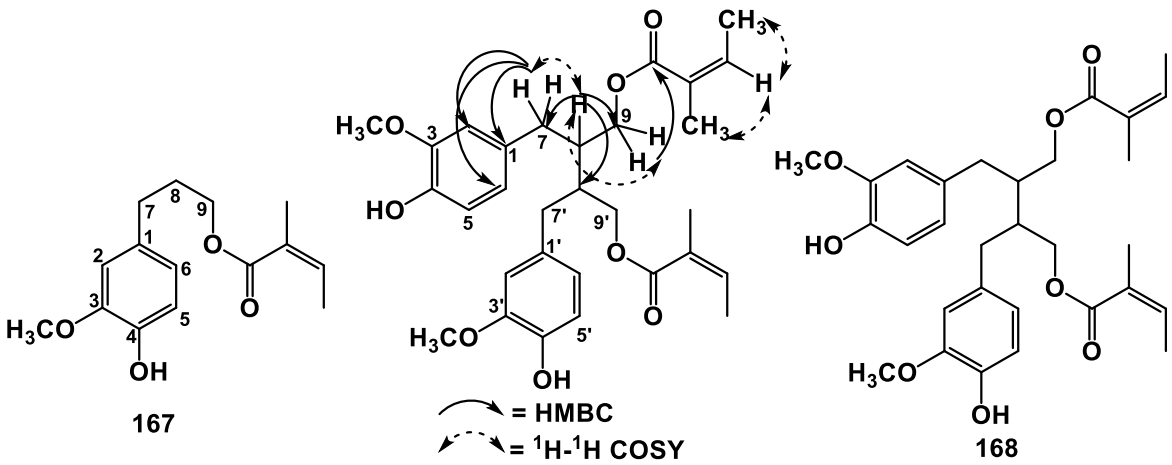

Figure 53: Structure of compound **167** (left), selected HMBC and ^{1}H-^{1}H COSY correlations (middle) and chemical structure (right) of compound **168.**

Characterization of Compound 169 (Erlangerin Z6)

Compound **169** was isolated as a white powder. The molecular formula $C_{26}H_{28}O_9$ was determined from its EIMS spectrum ([M^+], m/z 484.1727).

Its ^{1}H NMR spectrum (Table 12) showed signals for an unsymmetrical tetrasubstituted aromatic ring (δ_H 6.57 (s, 1H) and 6.62 (s, 1H)); a symmetrical tetrasubstituted aromatic ring [δ_H 6.74 (s)); an oxybenzylic proton (δ_H 5.13 (s)); a methine group (δ_H 4.31 (ddt, *J* =

11.2, 6.6, 4.2 Hz)); benzylic methylene protons (δ_H 3.34 (dd, *J* = 16.2, 7.3 Hz) and 2.56 (dd, *J* = 16.3, 11.0 Hz)); a methylenedioxy group (δ_H 5.96 (d, *J* = 1.3 Hz) and 5.94 (d, *J* = 1.3 Hz)); an oxymethylene group (δ_H 4.38 (dd, *J* = 10.5, 8.7 Hz) and 4.21 (dd, *J* = 10.5, 4.6 Hz)) and three methoxy groups (δ_H 3.87 (s, 6H) and 3.83 (s, 3H)). The angeloyl group was represented by signals at δ_H 5.97 (qd, *J* = 7.2, 1.6 Hz, 1H), 1.75 (dq, *J* = 7.3, 1.6 Hz, 3H) and 1.58 (s, 3H).

The ^{13}C NMR spectrum (Table 12) exhibited 23 signals. The signals due to the aromatic carbons appeared from δ_C 102.9 to 153.6. The most downfield signal at δ_C 208.6 was assigned to a ketone carbonyl. A methine, an oxymethylene, and a methylenedioxy group were represented by signals at δ_C 43.1, 62.6, and 101.8, respectively. The signal at δ_C 91.8 must be assigned to an oxybenzylic carbon and the other methylene carbon resonance at δ_C 31.9 to an aliphatic benzylic carbon. The three methoxy carbons were represented by two signals at δ_C 56.3 (x2) and 60.9. The angeloyl group was represented by four signals at δ_C 167.6, 127.3, 139.0, 15.7, and 20.3.

Table 12: ^{1}H [ppm, mult., (J in Hz)] and ^{13}C NMR spectroscopic data of compound **169** in $CDCl_3$.

Position	**δ_C**	**δ_H**
1	91.8	5.13, s
2	208.6	
3	43.1	4.31, ddt (11.2, 6.6, 4.2)
3a	62.6	4.38, dd (10.5, 8.7); 4.21, dd (10.5, 4.6)
4	31.9	3.34, dd (16.0, 7.3); 2.56, dd (16.0 11.0)
4a	121.3	
5	109.3	6.57, s
6	147.2	
7	145.2	
8	104.1	6.62, s
8a	150.7	
1’	130.0	
2’	102.9	6.74 overlap
3’	153.6	
4’	138.3	
5’	153.6	
6’	102.9	6.74 overlap
OCH_2O	101.8	5.96, d (1.3); 5.94, d (1.3)
3’-OCH_3	56.3	3.87 overlap
4’-OCH_3	60.9	3.83, s
5’-OCH_3	56.3	3.87 overlap
	167.6	
	127.3	
Angeloyl	138.9	5.97, qd (7.2, 1.6)
	15.7	1.75, dd (7.2, 1.6)
	20.3	1.58, s

The most important correlations observed from the ^{1}H-^{1}H COSY spectrum were: correlations of H-3/H-3a(δ_H 3.34) and H-3/H-4(δ_H 4.38) and allylic coupling between H-1/H-2' and H-1/H-6'. The HMBC spectrum exhibited long-range correlations of an oxybenzylic proton (H-1) with C-3, C-2'/C-6', C-1', C-8a and C-2 and the methine proton (H-3) with C-4, C-1''and C-2. The benzylic protons (H-4) also showed HMBC correlations with C-3, C-1'', C-1, C-5, C-4a, C-8a, and C-2. The above spectroscopic data agreed with the fact that the two aromatic rings were joined by a seven-membered ring (oxepanone). The position of the angeloyl group was deduced from the HMBC correlation of H-1'' with its ester carbonyl. The NOESY spectrum showed a correlation of H-1 and H-2'/H-6' suggesting the trimethoxy-substituted aromatic ring is connected to C-1 and the angeloyl group must be attached to the oxymethylene moiety at C-3a. On the basis of the spectral data, the novel compound **169** was elucidated as shown below and designated as erlangerin Z6.

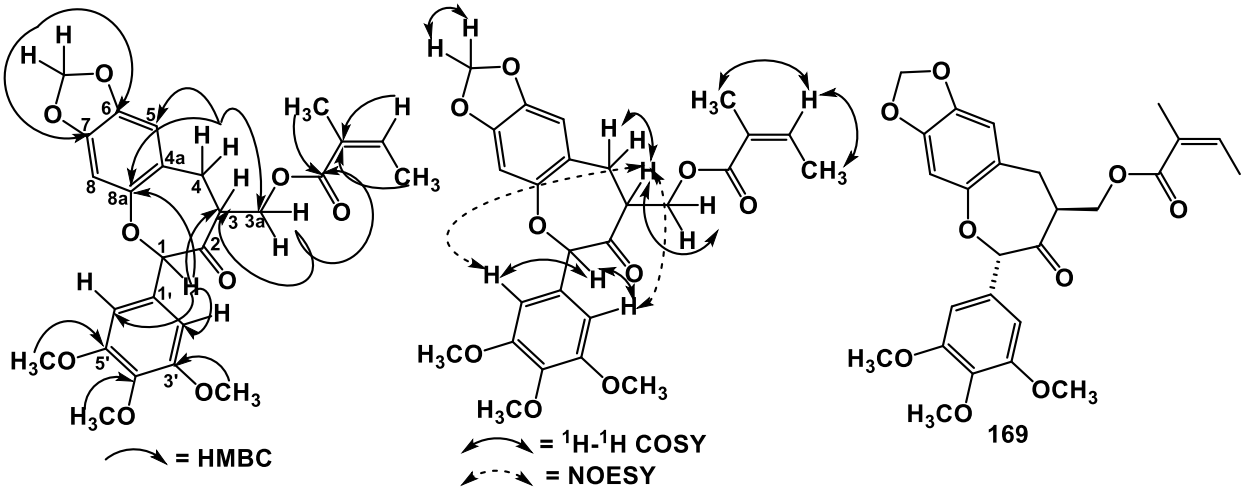

Figure 54: Selected HMBC (left), ^{1}H-^{1}H COSY and NOESY correlations (middle) and chemical structure (right) of compound **169.**

The above proposed structure was further confirmed by the observation in the mass spectrum fragment ions at m/z 384, 217, 181, and 157, which were derived from the loss of an angeloyl group, an oxepanone ring with attached aromatic ring, a trimethoxy substituted aromatic ring, and an aromatic ring with methylenedioxy group, respectively (Fig. 56).

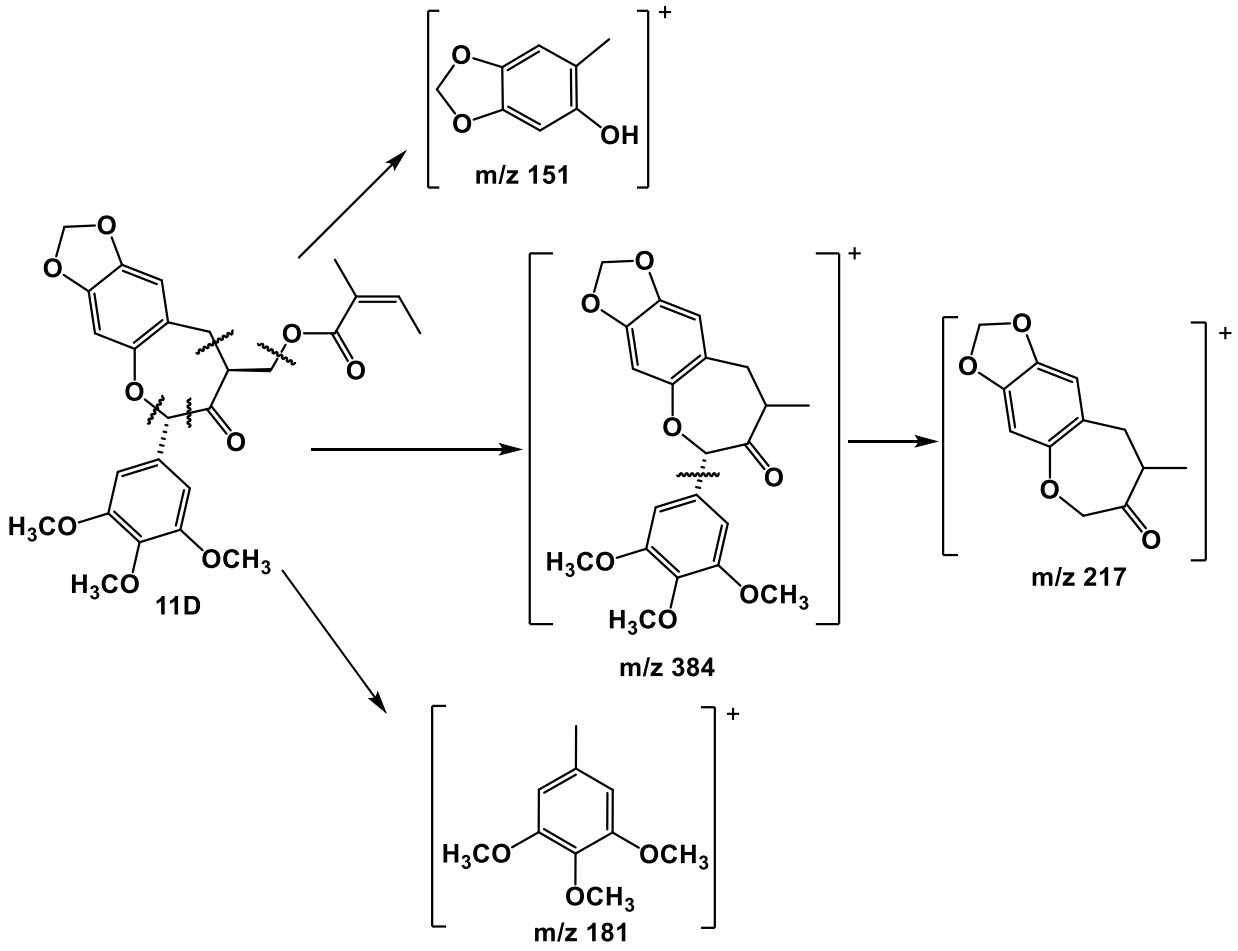

Figure 55: Mass spectral fragmentation pathway for compound **169.**

1.2.2 Proposed Biosynthetic Pathways for Lignans of *C. erlangeriana* resin

Figure 57 shows that the dibenzylbutyrolactone lignan, matairesinol (**163**), could be derived from matairesinol (**119**) by methylation of the aromatic hydroxyl group. Compound **163** might be the precursor for compounds **160**, **159** and **162**. Compound **163** could also be the precursor for the intermediate compound **170**, which can act as the precursor for all 3',4'-methylenedioxy-6,7,8-trimethoxydibenzylbutyro- lactone lignans (**161**, **154**, **155**, **156**, **158,** and **157**). Compound **170** could be also the precursor for all 6-methoxy-polygamatin-type skeleton (**171**), which could be transformed into aryltetralin lignans **153**, **148** and **147.** Again these can be immediate precursors for others aryltetralin lignans. Through series of hydroxylation, methylation, and addition of angeloyl group, compounds **153**, **148** and **147** possibly will be transformed into compounds **150**, **149**, **151**, **146**, **142**, **139**, **140,** and **141**. The aryltetralin lignan (-)-deoxypodophyllotoxin (**124**) could be

changed to compounds **143**, **145**, **152** and **144** upon hydroxylation, methylation, and addition of angeloyl group. The dibenzylbutane lignan secoisolariciresinol (**118**) may possibly be a common precursor for compounds **168** and **164**, which could be considered as precursors for compounds **166** and **165**.

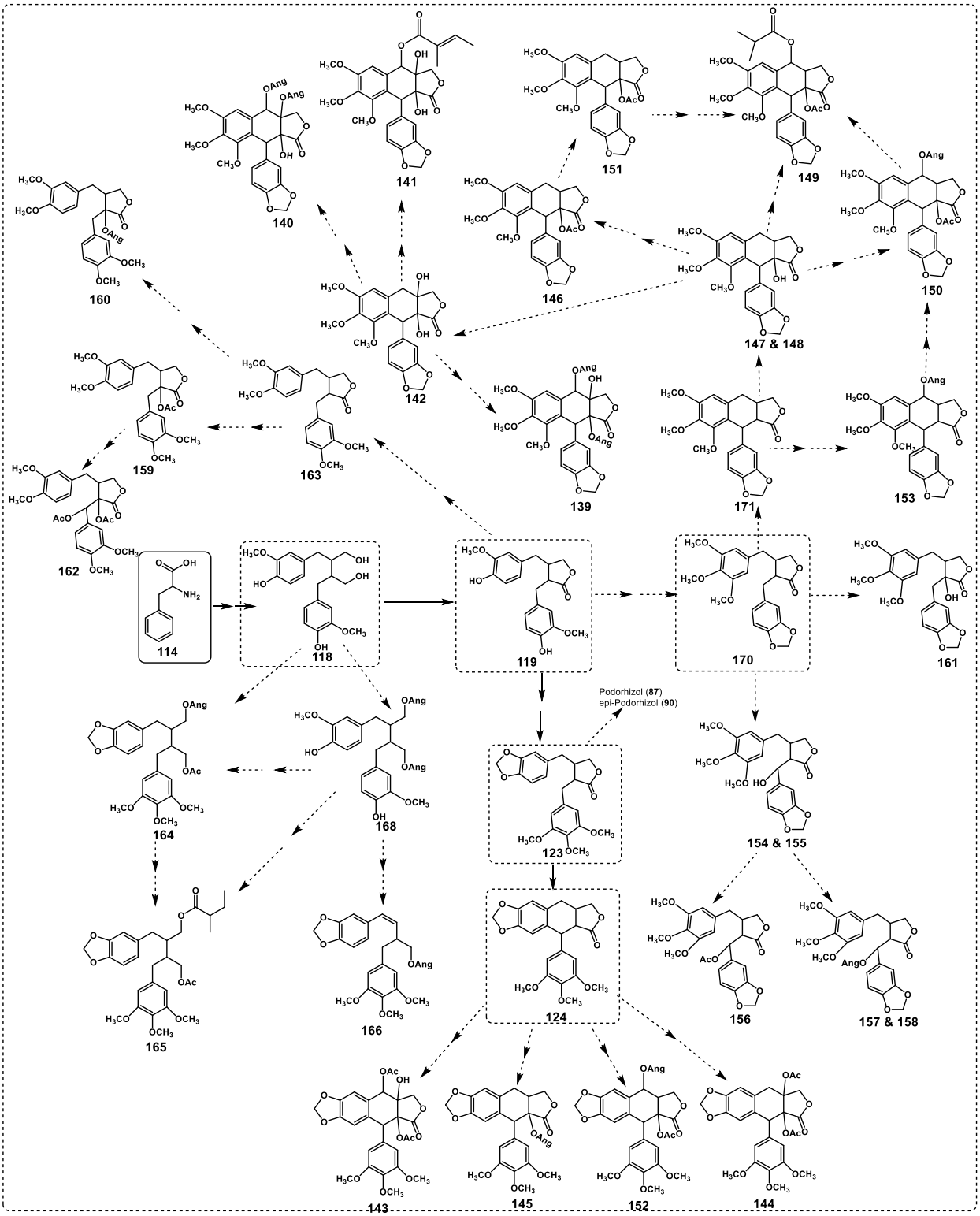

Figure 56: Possible biosynthetic pathways for various types of lignans isolated from C. erlangeriana resin

1.3 Experimental

1.3.1 General

TLC experiments were carried out on pre-coated silica gel 60 F254 25 Aluminum sheets (Merck KGaA, Darmstadt, Germany) and the TLC spots were viewed at 254 nm and visualized with 5% H_2SO_4 in EtOH containing 10 mg/mL vanillin. Macroporous resin AB-8 gel (Shan-dong Lu Kang Chemical Industrials, Jinan, Shandong, China), ODS (YMC Co., Ltd., Japan), and Sephadex LH-20 (Pharmacia Biotech AB, Uppsala, Sweden) were used for column chromatography (CC).

Analytical HPLC was applied on a Waters 2695 instrument (Milford, MD, USA) coupled with a 2998 PDA, a Waters 2424 ELSD, and a Waters 3100 MS detector. Preparative HPLC was performed on a Varian PrepStar instrument with an Alltech 3300 ELSD detector (Columbia, MD, USA) using a Waters Sunfire RP C18, 5 mm, 30 x 150 mm column.

Optical rotations were measured on a Rudolph Autopol VI Automatic polarimeter (Hackettstown, NJ, USA). IR spectra were recorded on a Nicolet Magna FT-IR 750 spectrophotometer (Waltham, MA, USA) using KBr disks. ECD spectra were recorded on a JASCO J-810 spectrometer. ESIMS and ESIHRMS data were recorded on Waters 2695-3100 LC-MS and Agilent G6520 Q-TOF mass spectrometers (Santa Clara, CA, USA), respectively. NMR spectra were recorded on a Bruker Avance III (Bruker) 500 and 600 MHz NMR spectrometer with TMS as an internal standard.

All solvents used for column chromatography were of at least analytical grade (Shanghai Chemical Reagents Co., Ltd., Shanghai, China), and solvents used for HPLC were of HPLC grade (Merck KGaA, Darmstadt, Germany).

1.3.2 Plant material

For plant material collection, identification and ethnobotanical information see references [109, 129].

1.3.3 Extraction and Isolation of Compounds from *C. erlangeriana*

The powdered resin of *C. erlangeriana* (150 g) was extracted with MeOH and EtOAc (1:1) by stirring on a magnetic plate for 6 h. Removal of the solvent gave reddish gummy material (75 g, 50%).

The extract was adsorbed on coarse silica gel (100-200 mesh, 150 g) and applied to silica gel column (200-300 mesh, 1.5 kg) then eluted successively with PE, PE/EA (20:1 to 1:10) and Ac to yield seventeen fractions (A-Q) as shown in Table 13 below.

Table 13: Summary of Column Chromatography of MeOH/EtOAc (1:1) extract of C. erlangeriana resin

Combined Fractions	Solvent system	Solvent volume (Lit)	Amount (mg)	Given Code	Major Compound Isolated
1-7	PE:EA (1:0)	4.5	800	A	
8-13	PE:EA (20:1)	4.5	140	B	
14-22	PE:EA (15:1)	4.5	235	C	
23-31	PE:EA (10:1)	4.5	360	D	
32-39	PE:EA (8-1)	4	250	E	
40-46	PE:EA (8:1 & 6-1)	3.5	270	F	
47-55	PE:EA (6:1 & 5-1)	4.5	570	G	
56-59	PE:EA (4:1)	2	960	H	**140**
60-68	PE:EA (4:1 & 3-1)	4.5	6,100	I	**139**
69-70	PE:EA (3:1)	1	1,400	J	
71-74	PE:EA (3:1 & 2-1)	2	4,000	K	**110**
75-79	PE:EA (2:1)	2.5	27,000	L	**110**
80-85	PE:EA (2:1 & 1-1)	3	17,500	M	**111**
86-89	PE:EA (1:1)	2	7,500	N	**111**
90-97	PE:EA (1:2)	4	12,000	O	**112**
98-99	PE:EA (1:2)	1	1,200	P	**112**
100-106	Ac	4.5	1,800	Q	**113**

Fraction H was recrystallized with absolute EtOH to give a white powder **140** (40 mg). The liquid part (900 mg) was further fractionated by column chromatography (silica gel, 300-400 mesh) and eluted with PE/EtOAc (15:1 to 9:1) to yield six subfractions (H_1-H_6). H_3 was purified by using preparative HPLC to give **166** (2 mg).

Fraction I was subjected to column chromatography packed with silica gel (300-400 mesh). Elution was done by using PE/Ac (10:1 to 1:2) and Ac to give eight subfractions

(I_1-I_8). I_3 (70 mg), I_5 (100 mg) and I_6 (80mg) were injected into preparative HPLC to give **168** (5 mg), **153** (2 mg) and **165** (4 mg); **164** (15 mg); and **150** (30 mg) and **149** (7 mg), respectively. Recrystallization of 3 g of the last subfraction with 95% EtOH gives a white crystal **139** (2.5 g).

Fractions K and L were purified and concentrated to give **110** (25 g). Fraction M was recrystallized with $CHCl_3$/MeOH (4:1) to yield 1.1 g of **111**. Part of the liquid part of M (14 g) was adsorbed on MCI gel powder and applied on column chromatography packed with MCI gel (300 g). Elution was done by using a different percentage of EtOH in H_2O (50% to 95%) to give six subfractions (M_1-M_6).

Subfraction M_1 (250 mg) was purified by passing over Sephadex LH-20 ($CHCl_3$:MeOH=1:1) to afford **148** (15 mg). The second subfraction (M_2, 1.6 g) was further fractionated into eight fractions (M_{2A}-M_{2H}) by applying on ODS column packed with 120 g of ODS gel. This was eluted with different percentage of MeOH in H_2O (50% to 100%). M_{2B} (54 mg) and M_{2F} (124 mg) were purified by preparative HPLC to give **161** (10 mg) and **145** (8 mg) respectively. M_{2G} (270 mg) was chromatographed over silica. nH_2O column and eluted with PE/EtOAc (5:1 to 5:2) to yield two fractions (M_{2G1} and M_{2G2}). The second fraction (M_{2G2}) was further purified by preparative TLC ($CHCl_3$:Ac = 9:1) to give **157** (30 mg) and **141** (50 mg).

Subfraction M_6 was further fractionated on silica gel (300-400 mesh) column and eluted with PE/EtOAc (10:1 to 5:2) to yield four fractions (M_{6A}-M_{6D}). M_{6A} (50 mg) was purified by preparative TLC with $CHCl_3$:Ac (9:1) to give **167** (3 mg). M_{6B} (140 mg) was also purified by preparative HPLC to give **158** (14 mg) and **152** (36 mg).

Fraction N and O were recrystallized with $CHCl_3$:MeOH (4:1) to yield **111** (3 g) and **112** (5 g) respectively. The liquid part (9 g) was fractionated into ten subfractions (O_1-O_{10}) by subjecting to silica gel (300-400 mesh) column with PE/EtOAc (5:1 to 2:1). The subfraction O_5 (800 mg) was further chromatographed over silica gel (300-400 mesh) column with eluting solvents PE/$CHCl_3$ (3:2 to 1:4) and $CHCl_3$ to give five fractions (O_{5A}-O_{5E}). Fraction O_{5D} (230 mg) was purified by preparative HPLC to give **146** (80 mg) and **160** (45 mg).

The subfraction O_6 (3.3 g) was further fractionated into ten fractions (O_{6A}-O_{6I}) by applying on silica gel (300-400 mesh) column with solvents PE/Ac (20:3 to 2:1) and Ac. Fraction O_{6D} (140 mg) was purified by preparative HPLC to give **163** (30 mg).

Fraction O_{6F} (2.6 g) was chromatographed over ODS column and eluted with MeOH in H_2O (50% to 100%) to yield seven fractions (O_{6F1}- O_{6F7}). 200 mg of the first fraction (O_{6F1}) was purified by preparative TLC ($CHCl_3$: Ac= 9:1) to give **156** (50 mg), **155** and **154** (12 mg). The third fraction (O_{6F3}) was also purified by preparative TLC ($CHCl_3$: Ac= 95:5) to afford **144**.

The subfraction O_7 (1.2 g) was fractionated into two fractions (O_{7A} and O_{7B}) over ODS column. The first fraction (O_{7A}) was purified by preparative TLC ($CHCl_3$: Ac= 9:1) to yield **147** (6 mg). The subfraction O_{10} was also purified by preparative TLC ($CHCl_3$: Ac= 88:12) to give **159** (50 mg).

Fraction P was allowed to recrystallize with MeOH:$CHCl_3$ (4:1) to yield **112** (130 mg). After concentrating the liquid part, the solid was fractionated into ten subfractions (P_1-P_{10}) by chromatographing over silica gel (300-400 mesh) column and eluting with PE/Ac (10:1 to 2:1) and Ac.

The subfraction P_5 (150 mg) was purified by preparative HPLC to afford **142** (17 mg). The subfraction P_8 (80 mg) was purified by chromatographed over silica.nH_2O column and eluted with PE/EtOAc (10:1 to 1:1) to yield **162**. The white crystal **143** (40 mg) was obtained from the subfraction P_{10} (70 mg) after purified by preparative HPLC. The last fraction (Fraction Q) was recrystallized with $CHCl_3$ and MeOH (3:2) to yield **113** (400 mg).

Compound 140: White powder; $[\alpha]\frac{20}{D} + 95.2$ (0.10, MeOH); **ECD** (MeOH) ($\Delta\varepsilon$) 302 (0.87), 278 (2.76), 243 (10.98), 209 (10.25); **^{1}H NMR** (Chloroform-*d*, 500 MHz) and **^{13}C NMR** ($CDCl_3$, 126 MHz) see table 3.

Compound 139: White crystal; $[\alpha]\frac{20}{D} + 86.0$ (0.10, MeOH); **ECD** (MeOH) ($\Delta\varepsilon$) 296 (-3.07), 276 (3.05), 243 (45.38), 210 (41.92); **^{1}H NMR** (Chloroform-*d*, 600 MHz) and **^{13}C NMR** ($CDCl_3$, 151 MHz) see table 3.

Compound 141: White powder; $[\alpha]\frac{20}{D} + 57.0$ (0.20, MeOH); **ECD** (MeOH) (Δε) 295 (-5.06), 276 (2.82), 243 (38.99), 209 (11.66); **^{1}H NMR** (Chloroform-*d*, 500 MHz) and **^{13}C NMR** ($CDCl_3$, 126 MHz) see table 3.

Compound 143: White crystal; $[\alpha]\frac{20}{D} + 88.0$ (0.10, MeOH); **ECD** (MeOH) (Δε) 289 (7.72), 271 (-4.30), 249 (-16.41), 230 (49.78), 216 (90.61), 200 (-97.30); **^{1}H NMR** (Chloroform-*d*, 500 MHz) and **^{13}C NMR** ($CDCl_3$, 126 MHz) see table 4.

Compound 142: White powder; $[\alpha]\frac{20}{D} + 207.0$ (0.10, MeOH); **ECD** (MeOH) (Δε) 290 (-4.47), 275 (4.37), 240 (39.16), 197 (31.15); **^{1}H NMR** (Chloroform-*d*, 500 MHz) and **^{13}C NMR** ($CDCl_3$, 126 MHz) see table 3.

Compound 144: White powder; $[\alpha]\frac{20}{D} + 38.0$ (0.10, MeOH); **ECD** (MeOH) (Δε) 289 (7.04), 271 (-4.08), 249 (-10.38), 230 (35.01), 216 (75.39), 200 (-64.14); **^{1}H NMR** (Chloroform-*d*, 500 MHz) and **^{13}C NMR** ($CDCl_3$, 126 MHz) see table 4.

Compound 145: White powder; $[\alpha]\frac{20}{D} + 132.7$ (0.10, MeOH); **ECD** (MeOH) (Δε) 289 (-6.45), 253 (-5.31), 235 (17.95), 211 (83.88), 196 (-24.16); **^{1}H NMR** (Chloroform-*d*, 500 MHz) and **^{13}C NMR** ($CDCl_3$, 126 MHz) see table 4.

Compound 148: White powder; $[\alpha]\frac{20}{D} - 140.3$ (0.10, MeOH); **ECD** (MeOH) (Δε) 295 (-4.69), 276 (-13.29), 243 (-21.54), 203 (-21.85); **^{1}H NMR** (Chloroform-*d*, 500 MHz) and **^{13}C NMR** ($CDCl_3$, 126 MHz) see table 5.

Compound 151: White powder; $[\alpha]\frac{20}{D} + 171.8$ (0.10, MeOH); **ECD** (MeOH) (Δε) 296 (-4.01), 275 (2.77), 242 (42.55), 213 (38.26); **^{1}H NMR** (Chloroform-*d*, 500 MHz) and **^{13}C NMR** ($CDCl_3$, 126 MHz) see table 6.

Compound 150: White powder; $[\alpha]\frac{20}{D} + 148.5$ (0.10, MeOH); **ECD** (MeOH) (Δε) 298 (-5.83), 276 (6.13), 243 (50.70), 210 (61.05); **^{1}H NMR** (Chloroform-*d*, 500 MHz) and **^{13}C NMR** ($CDCl_3$, 126 MHz) see table 6.

Compound 149: White powder; $[\alpha]\frac{20}{D} + 189.2$ (0.10, MeOH); **ECD** (MeOH) (Δε) 298 (-4.68), 276 (5.27), 243 (44.83), 210 (72.39); **^{1}H NMR** (Chloroform-*d*, 500 MHz) and **^{13}C NMR** ($CDCl_3$, 126 MHz) see table 6.

Compound 152: White powder; $[\alpha]\frac{20}{D} + 40.5$ (0.10, MeOH); **ECD** (MeOH) (Δε) 290 (-7.64), 252 (-12.82), 235 (3.96), 212 (37.34), 199 (-45.03); **^{1}H NMR** (Chloroform-*d*, 500 MHz) and **^{13}C NMR** ($CDCl_3$, 126 MHz see table 4.

Compound 153: White powder; $[\alpha]\frac{20}{D} - 42.3$ (0.10, MeOH); **ECD** (MeOH) (Δε) 291 (-5.83), 276 (0.95), 259 (-1.89), 243 (16.64), 217 (-32.53), 203 (41.17); **^{1}H NMR** (Chloroform-*d*, 500 MHz) and **^{13}C NMR** ($CDCl_3$, 126 MHz) see table 6.

Compound 154: White powder; $[\alpha]\frac{20}{D} - 23.0$ (0.10, MeOH); **ECD** (MeOH) (Δε) 281 (-5.21), 236 (-10.65), 207 (-53.41); **^{1}H NMR** (Chloroform-*d*, 500 MHz) and **^{13}C NMR** ($CDCl_3$, 126 MHz) see table 7.

Compound 155: White powder; $[\alpha]\frac{20}{D} - 2.0$ (0.10, MeOH); **ECD** (MeOH) (Δε) 281 (-4.58), 236 (-7.81), 208 (-21.33); **^{1}H NMR** (Chloroform-*d*, 500 MHz) and **^{13}C NMR** ($CDCl_3$, 126 MHz) see table 7.

Compound 156: White powder; $[\alpha]\frac{20}{D} - 38.3$ (0.10, MeOH); **ECD** (MeOH) (Δε) 279 (-6.91), 237 (-14.15), 210 (-62.82); **^{1}H NMR** (Chloroform-*d*, 500 MHz) and **^{13}C NMR** ($CDCl_3$, 126 MHz) see table 7.

Compound 157: White powder; $[\alpha]\frac{20}{D} - 32.0$ (0.10, MeOH); **ECD** (MeOH) (Δε) 282 (-6.98), 236 (-13.66), 207 (-77.11); **^{1}H NMR** (Chloroform-*d*, 600 MHz) and **^{13}C NMR** ($CDCl_3$, 151 MHz) see table 8.

Compound 158: White powder; $[\alpha]\frac{20}{D} + 35.0$ (0.10, MeOH); **ECD** (MeOH) (Δε) 278 (-4.16), 243 (-3.38), 222 (2.65), 208 (-7.78); **^{1}H NMR** (Chloroform-*d*, 500 MHz) and **^{13}C NMR** ($CDCl_3$, 126 MHz) see table 8.

Compound 159: White powder; $[\alpha]_D^{20} - 32.0$ (0.10, MeOH); **ECD** (MeOH) ($\Delta\varepsilon$) 282 (-6.78), 235 (-20.78), 211 (-16.52); **^{1}H NMR** (Chloroform-*d*, 500 MHz) and **^{13}C NMR** ($CDCl_3$, 126 MHz) see table 8.

Compound 160: White powder; $[\alpha]_D^{20} - 15.4$ (0.20, MeOH); **^{1}H NMR** (Chloroform-*d*, 600 MHz) and **^{13}C NMR** ($CDCl_3$, 151 MHz) see table 8.

Compound 161: White powder; $[\alpha]_D^{20} - 100.8$ (0.10, MeOH); **ECD** (MeOH) ($\Delta\varepsilon$) 275 (-3.56), 239 (-15.89), 210 (-31.25); **^{1}H NMR** (Chloroform-*d*, 600 MHz) and **^{13}C NMR** ($CDCl_3$, 151 MHz) see table 9.

Compound 162: White powder; $[\alpha]_D^{20} - 55.0$ (0.10, MeOH); **ECD** (MeOH) ($\Delta\varepsilon$) 283 (-10.49), 239 (-53.78), 216 (-12.87); **^{1}H NMR** (Chloroform-*d*, 500 MHz) and **^{13}C NMR** ($CDCl_3$, 151 MHz) see table 9.

Compound 163: White powder; $[\alpha]_D^{20} - 36.7$ (0.10, MeOH); **ECD** (MeOH) ($\Delta\varepsilon$) 280 (-4.00), 233 (-14.42), 204 (-7.69); **^{1}H NMR** (Chloroform-*d*, 500 MHz) and **^{13}C NMR** ($CDCl_3$, 126 MHz) see table 9.

Compound 164: White powder; $[\alpha]_D^{20} - 5.8$ (0.10, MeOH); **^{1}H NMR** (Chloroform-*d*, 600 MHz) and **^{13}C NMR** ($CDCl_3$, 151 MHz) see table 10.

Compound 165: White powder; $[\alpha]_D^{20} - 14.0$ (0.10, MeOH); **^{1}H NMR** (Chloroform-*d*, 600 MHz) and **^{13}C NMR** ($CDCl_3$, 126 MHz) see table 10.

Compound 166: White powder; $[\alpha]_D^{20} - 55.2$ (0.10, MeOH); **^{1}H NMR** (Chloroform-*d*, 500 MHz) and **^{13}C NMR** ($CDCl_3$, 126 MHz) see table 10.

Compound 168: White powder; $[\alpha]_D^{20} 0.0$ (0.10, MeOH); **^{1}H NMR** (Chloroform-*d*, 500 MHz) and **^{13}C NMR** ($CDCl_3$, 126 MHz) see table 11.

Compound 169: White powder; $[\alpha]\frac{20}{D} - 1.0$ (0.20, MeOH); **^{1}H NMR** (Chloroform-*d*, 500 MHz) and **^{13}C NMR** ($CDCl_3$, 126 MHz see table 12.

References

1. Coppen, J.J.W., *Gums, Resins and Latexes of Plant Origin.* **1995**, Rome: Food and Agriculture Organization of the United Nations. 1-152.
2. Langenheim, J.H. *Plant Resins Chemistry, Evolution, Ecology, and Ethnobotany*. 2003, Hong Kong: Timber Press Portland, Cambridge.
3. https://medical-dictionary.thefreedictionary.com/resin.
4. Giri, S.R., Prasad, N., Pandey, S.K., Prasad, M., and Baboo, B. *Natural Resins and Importance Gums of Commercial - At a Glanee*. **2008**, Indian Institute of Natural Resins and Gums., India. p. 1-43.
5. https://medical-dictionary.thefreedictionary.com/gum.
6. *Ethiopian Revenue and Custom Authority (ERCA): Import and Export Information.*
7. Tadesse, W., Desalegn, G., and Alia, R. *Natural Gum and Resin Bearing Species of Ethiopia and their Potential Applications.* Sist Recur For, **2007**, 16(3), 211-221.
8. Adem, M., Worku, A., Lemenih, M., Tadesse, W., and Pretzsch, J. *Diversity, Regeneration Status and Population Structure of Gum- and Resin-Bearing Woody Species in South Omo Zone, Southern Ethiopia.* Journal of Forestry Research (Harbin, China), **2014,** 25(2), 319-328.
9. Mekonnen, Z., Worku, A., Yohannes, T., Bahru, T., Mebratu, T., and Teketay, D. *Economic Contribution of Gum and Resin Resources to Household Livelihoods in Selected Regions and the National Economy of Ethiopia.* Ethnobotany Research & Applications, **2013**, 11, 273-288.
10. Lemenih, M., and Kassa, H. *Gums and resins of Ethiopia.* Brief, **2011,** 3, 1-4.
11. Friis, I., Demissew, S., and Breugel, P. *Atlas of the Potential Vegetation of Ethiopia*. **2010**, Denmark: The Royal Danish Academy of Sciences and Letters.
12. Mahr, D., *Commiphora: An Introduction to the Genus.* Cactus and Succulent Journal, **2012**, 84(3), 140-154.
13. Shoemaker, M., Hamilton, B., Dairkee, S.H., Cohen, I., and Campbell, M.J. *In vitro Anticancer Activity of Twelve Chinese Medicinal Herbs.* Phytotherapy Research, **2005**, 19, 649-651.
14. Shen, T., Li, G., Wang, X., and Lou, H. *The Genus Commiphora: A Review of its Traditional Uses, Phytochemistry and Pharmacology.* Journal of Ethnopharmacology, **2012**, 142(2), 319-330.
15. Lemenih, M., and Teketay, D., *Frankincense and Myrrh Resources of Ethiopia: II. Medicinal and Industrial Uses.* Sinet: Ethiop. J. Sci., **2003**, 26(2), 161-172.
16. Su, S., Wang, T., Chen, T., Duan, J., Yu, L., and Tang, Y. *Cytotoxicity Activity of Extracts and Compounds from Commiphora myrrha Resin Against Human Gynecologic Cancer Cells.* Journal of Medicinal Plants Research, **2011**, 5(8), 1382-1389.
17. Dut, N.J., Choudhary, J. Sharama, P., Sharma, N., and Joshi, S.J. *A Review on Bioactive Compounds and Medicinal Uses of Commiphora mukul.* Journal of Plant Sciences, **2012**, 7(4), 113-137.
18. Kimura, I., Yoshikawa, M., Kobayashi, S., Sugihara, Y., Suzuki, M., Oominami, H., Murakami, T., Matsuda, H., and Doiphode, V.V. *New Triterpenes, Myrrhanol A and Myrrhanone A, from Guggul-Gum Resins, and Their Potent Anti-Inflammatory*

Effect on Adjuvant-Induced Air-Pouch Granuloma of Mice. Bioorganic and Medicinal Chemistry Letters, **2001**, 11(8), 985-989.

19. Sallau, M.S. *Phytochemical and Pharmacological Studies of the Leaves of Commiphora kerstingii Engl (Burseraceae)*, in *Pharmaceutical and Medicinal Chemistry*. **2009**, Ahmadu Bello University: Zaria-Nigeria. p. 181.
20. Singh, B.B., Mishra, L.C., Vinjamury, S.P., Aquilina, N., Singh, V.J., and Shepard, N. *The Effectiveness of Commiphora mukul for Osteoarthritis of the Knee.* Alternative Therapies in Health and Medicine, **2003**, 9, 74-79.
21. Matsuda, H., Morikawa, T., Ando, S., Oominami, H., Murakami, T., Kimura, I., and Yoshikawa, M. *Absolute Stereostructures of Polypodane- and Octanordammarane-type Triterpenes with Nitric Oxide Production Inhibitory Activity from Guggul-Gum Resins.* Bioorganic Medicinal Chemistry, **2004a**, 12, 3037-3046.
22. Meselhy, M.R. *Inhibition of LPS-induced NO Production by the Oleogum Resin of Commiphora wightii and its Constituents.* Phytochemistry, **2003**, 62, 213-218.
23. Tariq, M., Ageel, A.M., Al-Yahya, M.A., Mossa, J.S., Al-Saro, M.S., and Parmar, N.S. *Anti-inflammatory Activity of Commiphora molmol.* Agents and Actions, **1985**, 17, 318-382.
24. Tipton, D.A., Lyle, B., Babich, H., and Dabbous, M.K. *In vitro Cytotoxic and Antiinflammatory Effects of Myrrh Oil on Human Gingival Fbroblasts and Epithelial Cells.* Toxicology in Vitro, **2003**, 17, 301-310.
25. Paraskeva, M.P., Vuuren, S.F., Zyl, R.L., Davids, H., and Viljoen, A.M. *The In Vitro Biological Activity of Selected South African Commiphora Species.* Journal of Ethnopharmacology, **2008**, 119, 673-679.
26. Abbas, M.S., and Abd-Elkhalik, A. H. *Analgesic, Anti-inflammatory and Anti-hyperlipidemic Activities of Commiphora molmol extract (Myrrh).* J. Intercult Ethnopharmacol, **2014**, 3(2).
27. Annu, W., Latha, P.G., Shaji, J., Anuja, G.I., Sujia, S.R., Sini, S., Shyamal, S., Shine, V.J., Shikha, P., and Rajiasekharan, S. *Anti-inflammatory, Analgesic and Anti-lipid Peroxidation Studies on Leaves of Commiphora caudata (Wight & Arn.) Engl.* Journal of Indian Natural Products and Resources, **2010**, 1, 44-48.
28. Fraternale, D., Sosa, S., Ricci, D., Genovese, S., Messina, F., Tomasini, S., Montanari, F., and Marcotullio, M.C. *Anti-inflammatory, Antioxidant and Antifungal Furanosesquiterpenoids Isolated from Commiphora erythraea (Ehrenb.) Engl. resin.* Fitoterapia, **2011**, 82, 654-661.
29. Dolara, P., Luceri, C., Ghelardini, C., Monserrat, C., Aiolli, S., Luceri, F., Lodovici, M., Menichetti, S., and Novella, M. R. *Analgesic effects of myrrh.* Nature, **1996**, 379, 29.
30. Banso, A., and Mann, A. *Antimicrobial Alkaloid Fraction from Commiphora africana.* Journal of Pharmacy & Bioresources, **2006**, 3(2), 98-102.
31. Gbolade, A.A., and Adeyemi, A.A. *Anthelmintic Activities of Three Medicinal Plants from Nigeria.* Fitoterapia, **2008**, 79(3), 223-225.
32. Ma, J., Jones, S.H., and Hecht, S.N. *A Dihydroflavonol Glucoside from Commiphora africana that Mediates DNA Strand Scission.* Journal of Natural Products, **2005**, 68(1), 115-117.

33. Chandrasekar, K., Rajan, V., Raj, C.D., and Gowrishankar, N.L. *Antiulcerogenic Activity of Commiphora caudata Bark Extract Against Ethanol-Induced Gastric Ulcer in Rats.* Journal of Pharmacy Research, **2009**, 2(24), 701-703.
34. Nanthakumar, R., Ambrose, S.S., Sriram, E., Babu, G., Chitra, K., and Reddy, U.C. *Effect of Bark Extract and Gum Exudate of Commiphora caudata on Aspirin Induced Ulcer in Rats.* Pharmacognosy Research, **2009**, 11(6), 375-380.
35. Carroll, J.F., Maradufu, A., and Warthen, J.D. *An Extract of Commiphora erythraea: A Repellent and Toxicant Against Ticks.* Entomol. Exp. Appl., **1989**, 53, 111-116.
36. Birkett, M.A., Al-Bassi, S., Krober, T., Chamberlain, K., Hooper, A. M., Guerin, P. M., Pettersson, J., Pickett, J. A., Slade, R., and Wadhams, L. J. *Antiectoparasitic Activity of the Gum Resin, Gum Haggar, from the East African plant, Commiphora holtziana.* Phytochemistry, **2008**, 69(8), 1710-1715.
37. Duwiejua, M., Zeitlin, I.J., Waterman, P.G., Chapman, J., Mhango, G.J., and Provan, G.J. *Anti-inflammatory Activity of Resins from some Species of the Plant Family Burseraceae.* Planta Med., **1993**, 59(1), 12-16.
38. Al-Howiriny, T.A., Al-Sohaibani, M.O., Al-Said, M.S., Al-Yahya, M.A., El-Tahir, K. H., and Rafatullah, S. *Hepatoprotective Properties of Commiphora opobalsamum ("Balessan"), a Traditional Medicinal Plant of Saudi Arabia.* Drugs Exp Clin Res, **2004a**, 30(56), 213-220.
39. Shankar, G.L., Manavalan, R., Venkappayya, D., and Raj, D. C. *Hepatoprotective and Antioxidant effects of Commiphora berryi (Arn) Engl Bark Extract Against CCl(4)-Induced Oxidative Damage in Rats.* Food and Chemical Toxicology, **2008**, 46, 3182-3185.
40. Ashry, K.M., El-Sayed, Y.S., Khamiss, R.M., and El-Ashmawy, I.M. *Oxidative Stress and Immunotoxic Effects of Lead and their Amelioration with Myrrh (Commiphora molmol) Emulsion.* Food and Chemical Toxicology, **2010**, 48, 236-241.
41. Mothana, R.A., and Lindequist, U. *Antimicrobial Activity of Some Medicinal Plants of the Island Soqotra.* J. Ethnopharmacol, **2005**, 96(1-2), 177-181.
42. Claeson, P., Andersson, R., and Samuelsson, G. *T-cadinol: A Pharmacologically Active Constituent of Scented Myrrh: Introductory Pharmacological Characterization and High Field ^{1}H- and ^{13}C- NMR Data.* Planta Medica, **1991**, 57, 352-356.
43. Habtemariam, S. *Cytotoxic and Cytostatic Activity of Erlangerins from Commiphora erlangeriana.* Toxicon, **2003**, 41, 723-727.
44. Mekonnen, Y., Dekebo, D., and Dagne, E. *Toxicity Study in Mice of Resins of Three Commiphora Species.* SINET: Ethiop. J. Sci., **2003**, 26(2), 151-153.
45. Al-Mathal, E.M., and Fouad, M.A. *Effect of Commiphora Molmol on Adults, Egg Masses and Egg-Deposition of Biomphalaria Arabica Under Laboratory Conditions.* J. Egypt Soc Parasitol, **2006**, 36(1), 305-314.
46. Cunha, N.L., Teixeira, G.M., Martins, T.D., Souza, A.R., Oliveira, P.F., Simaro, G.V., Rezende, K.C., Goncalves, N.S., Souza, D.G., and Tavares, D.C. *(-)-Hinokinin Induces G2/M Arrest and Contributes to the Antiproliferative Effects of Doxorubicin in Breast Cancer Cells.* Planta Medica, **2016**, 82(6), 530-538.

47. Gnabre, J., Bates, R., and Chih, R.H. *Creosote Bush Lignans for Human Disease Treatment and Prevention: Perspectives on Combination Therapy.* Journal of Traditional and Complementary Medicine, **2015**, 5, 119-126.
48. Gordaliza, M., García, P. A., Miguel del Corral, J. M., Castro, M. A., and Gómez-Zurita, M. A. *Podophyllotoxin: Distribution, Sources, Applications and New Cytotoxic Derivatives.* Toxicon, **2004**, 44(4), 441-459.
49. Fazary, E.A., Alfaifi, Y.M., Saleh, A.K., Alshehri, A.M., and Eldin, S.E. *Bioactive Lignans: A Survey Report on their Chemical Structures?* Natural Products Chemistry & Research, **2016**, 04(04), 1-15.
50. Donald W. M.; Neil, G.H. *Biological Activities of Lignans.* Phytochemistry, **1984**, 23(6), 1207-1220.
51. Gordaliza, M., Castro, M.A., Corral, J.M., and Feliciano, S.A. *Antitumor Properties of Podophyllotoxin and Related Compounds.* Current Pharmaceutical Design, **2000**, 6, 1811-1839.
52. Hazra, S., and Chattopadhyay, S. *An Overview of Lignans with Special Reference to Podophyllotoxin, a Cytotoxic Lignan.* Chem. Biol. Lett, **2016**, 3(1), 1-8.
53. Karuppaiya, P., and Tsay, H.S. *Therapeutic Values, Chemical Constituents and Toxicity of Taiwanese Dysosma pleiantha.* Toxicol Lett., **2015**, 236(2), 90-97.
54. Hajra, S., Garai, S., and Hazra, S. *Catalytic Enantioselective Synthesis of (-)-Podophyllotoxin.* Org Lett., **2017**, 19(24), 6530-6533.
55. Konuklugil, B. *The Importance of Aryltetralin (Podophyllum) Lignans and Their Distribution in The Plant Kingdom.* J. Fac. Pharm. Ankara, **1995**, 24(2), 109-125.
56. Gunjan, M., Rameshwar, J.N., Rillera, R.M., and Saad, N.M. *Need of an Ancient Roots to Modern Medicine in the Treatment of Cancer- A review*, in *International Journal of Phytomedicine*, **2017**.
57. Stevenson, R. *Some Aspects of the Chemistry of Lignans.* Studies in Natural Products Chemistry, **1995**, 17, 311-356.
58. Ionkova, I. *Anticancer Compounds from In Vitro Cultures of Rare Medicinal Plants.* Pharmacogn. Rev., **2009**, 2(4), 206-218.
59. Sun, Y.J., Li, Z.L., Chen, H., Liu, X.Q., Zhou, W., and Hua, H.M. *Three New Cytotoxic Aryltetralin Lignans from Sinopodophyllum emodi.* Bioorganic & Medicinal Chemistry Letters, **2011**, 21, 3794-3797.
60. Mikame, K., Sakakibara, N., Umezawa, T., and Shimada, M. *Lignans of Linum flavum var. compactum.* J Wood Sci, **2002**, 48, 440-445.
61. Udino, L., Abaulr, J., Bourgeois, P., Gorrichon, L., Duran, H., and Zedde, C. *Lignans from the Seeds of Hernandia sonora.* Planta Medica, **1999**, 65, 279-281.
62. Bruschi, M., Orlandi, M., Rindone, M., Rindone, B., Saliua, F., Suarez-Bertoa, R., Liisa, E.T., and Zoia, L. *Podophyllotoxin and Antitumor Synthetic Aryltetralines. Toward a Biomimetic Preparation Learning from Nature*. **2010**.
63. Zhao, C., Nagastu, A., Hatano, K., Shirai, N., Kato, S., and Ogihara, Y. *New Lignan Glycosides from Chinese Medicinal Plant, Sinopodophillum emodi.* Chem. Pharm. Bull., **2003**, 51(3), 255-261.
64. Parvaiz, H.Q., Rashid, A., and Sami, A.S. *"Podophyllum hexandrum" - A Versatile Medicinal Plant.* Int. J. Pharm Pharm Sci., **2011**, 3(5), 261-268.
65. Broomhead, A.J., and Dewick, P.M. *Aryltetralin Lignans from Linum flavum and Linum capitatum.* Phytochemistry, **1990**, 29(12), 3839-3844.

66. Ylj, P., Wang, L., and Chen, Z. *A New Podophyllotoxin-Type Lignan from Dysosma verslpellls Var. tomentosa.* Journal of Natural Products, **1991**, 54(5), 1422-1424.
67. León, A., Mauricio, A.R., Luisa, M.V., and Alvarez, L. *Aryldihydronaphthalene-type Lignans from Bursera fagaroides var. fagaroides and their Antimitotic Mechanism of Action.* RSC Adv, **2016**, 6, 4950-4959.
68. Oliva, A., Moraes, R.M., Watson, S.B., Duke, S.O., and Dayan, F.E. *Aryltetralin Lignans Inhibit Plant Growth by Affecting the Formation of Mitotic Microtubular Organizing Centers.* Pesticide Biochemistry and Physiology, **2002**, 72(1), 45-54.
69. San, A.F., Jose, M.M., Gordaliza, M., and Angeles, C. *Lignans from Juniperus sabina.* Phytochemistry, **1990**, 29(4), 1335-1338.
70. Gigliarelli, G., Zadra, C., Cossignani, L., Enrique, R.R., Rascón-Valenzuela, L.A., Velázquez-Contreras, C.A., and Carla, M.M. *Two New Lignans from the Resin of Bursera microphylla A. Gray and their Cytotoxic Activity.* Natural Product Research, **2017**.
71. Saleem, M., Ja, H.K., Shaiq, M.A. and Sup, Y.L. *An Update on Bioactive Plant Lignans.* Nat. Prod. Rep., **2005**, 22**,** 696-716.
72. Thi, T.T., Cuong, V.P., Doan, T.H., Litaudon, M., Guéritte, F., Hung, V.N., and Minh, V.C. *Cytotoxic Aryltetralin Lignans from Fruits of Cleistanthus indochinensis.* Planta Med., **2014**, 80, 695-702.
73. Tran, T.D., Pham, N.B., Booth, R., Forster, P.I., and Quinn, R.J. *Lignans from the Australian Endemic Plant Austrobaileya scandens.* J. Nat. Prod., **2016**, 79(6), 1514-1523.
74. Broomhead, A.J., and Dewick, M.P. *Tumour-Inhibitory Aryltetralin Lignans In Podophyllum versipelle, Diphylleia Cymosa and Diphylleia Grayi* Phytochemistry, **1990**, 29(12), 3831-3837.
75. Gerard, C.H. *The Lignans Of Polygala polygama (Polygalaceae): Deoxypodophyllotoxis and Three New Lignan Lactones.* J. Nat. Prod., **1979**, 42(4), 378-384.
76. Solyomvary, A., Beni, S., and Boldizsar, I. *Dibenzylbutyrolactone Lignans - A Review of Their Structural Diversity, Biosynthesis, Occurrence, Identification and Importance.* Mini-Reviews in Medicinal Chemistry, **2017**, 17(12), 1053-1074.
77. Mao, J., Yu, N., Yang, Y., and Zhao, Y. *Research Progress on Biological Activities of Dibenzylbutyrolactone Lignans.* Guoji Yaoxue Yanjiu Zazhi, **2014**, 41(3), 275-281.
78. Lee, J.Y., Cho, B.J., Park, T.W., Park, B.E., Kim, S.J., Sim, S.S., and Kim, C.J. *Dibenzylbutyrolactone Lignans from Forsythia koreana Fruits Attenuate Lipopolysaccharide-Induced Inducible Nitric Oxide Synthetase and Cyclooxygenase-2 Expressions through Activation of Nuclear Factor-kB and Mitogen-Activated Protein Kinase in RAW264.7 Cells.* Biol. Pharm. Bull, **2010**, 33(11), 1847-1853.
79. Umezawa, T., Okunishi, T., and Shimada, M. *Stereochemical Differences in Lignan Biosynthesis Between Arctium lappa, Wikstroemia sikokiana, and Forsythia spp*. in *ACS Symposium Series; ACS*. **1998**. Washington, DC.
80. Lee, J.H., Lee, J.Y., Kim, T.D., and Kim, C.J. *Antiasthmatic Action of Dibenzylbutyrolactone Lignans from Fruits of Forsythia viridissima on Asthmatic*

Responses to Ovalbumin Challenge in Conscious Guinea-Pigs. Phytother Res, **2011**, 25(3), 387-395.

81. Cho, M.K., Jang, Y.P., Kim, Y.C., and Kim, S.G. *Arctigenin, a Phenylpropanoid Dibenzylbutyrolactone Lignan, Inhibits MAP Kinases and AP-1 Activation via Potent MKK Inhibition: the Role in TNF-alpha Inhibition.* Int. Immunopharmacol, **2004**, 4(10-11), 1419-29.
82. Kyung, C.M., Weon, P. J., Pyo, Y. J., Choong, K. Y., and Geon, S. K. *Potent Inhibition of Lipopolysaccharide-Inducible Nitric Oxide Synthase Expression by Dibenzylbutyrolactone Lignans Through Inhibition of I-kB Phosphorylation and of p65 Nuclear Translocation in Macrophages.* International Immunopharmacology, **2002**, 2, 105-116.
83. Badheka, L.P., Pralihu, B.R., and Mulchandani, N.B. *Dibenzylbutyrolactone Lignans from Piper cubeba.* Phytochemistry, **1986**, 25(2), 487-489.
84. Su, B.N., Jones, W.P., Cuendet, M., Kardono, L.B., Ismail, R., Riswan, S., Fong, H.H., Farnsworth, N.R., Pezzuto, J.M., and Kinghorn, A.D. *Constituents of the Stems of Macrococculus pomiferus and Their Inhibitory Activities Against Cyclooxygenases-1 and -2.* Phytochemistry, **2004**, 65(21), 2861-6.
85. Pyo, Y.J., Ra, S.K., and Choong, Y.K. *Neuroprotective Dibenzylbutyrolactone Lignans of Torreya nucifera.* Planta Med, **2001**, 67, 470-472.
86. Piccinelli, A.L., Mahmood, N., Mora, G., Poveda, L., De Simone, F., and Rastrelli, L. *Anti-HIV Activity of Dibenzylbutyrolactone-Type Lignans from Phenax Species Endemic in Costa Rica.* Journal of Pharmacy and Pharmacology, **2005**, 57, 1109-1115.
87. Lima, O.A., and Braz-Filho, R. *Dibenzylbutyrolactone Lignans and Coumarins from Ipomoea cairica.* J. Braz. Chem. Soc., **1997**, 8(3), 235-238.
88. Kim, S.H., Jang, Y. P., Sung, Y. P., Kim, C. J., Kim, J. W., and Kim, Y. C. *Hepatoprotective Dibenzylbutyrolactone Lignans of Torreya nucifera against CCl4-Induced Toxicity in Primary Cultured Rat Hepatocytes.* Biol. Pharm. Bull., **2003**, 26(8), 1202-1205.
89. Willfor, S.M., Ahotupa, M.O., Hemming, J.E., Reunanen, M.H.T., Eklund, P.C., Sjoholm, R.E., Eckerman, C.S., Pohjamo, S.P., and Holmbom, B.R. *Antioxidant Activity of Knotwood Extractives and Phenolic Compounds of Selected Tree Species.* J. Agric. Food Chem., **2003**, 51, 7600-7606.
90. Huo, C., Liang, H., Zhao, Y., Wang, B., and Zhang, Q. *Neolignan Glycosides from Symplocos caudata.* Phytochemistry, **2008**, 69, 788-795.
91. Kawamura, F., Ohira, T, and Kikuchi, Y. *Constituents from the Roots of Taxus cuspidata.* J. Wood Sci, **2004**, 50, 548-551.
92. Yang, Y., Huang, X., Feng, Z., Jiang, J., and Zhang, P. *Hepatoprotective Activity of Twelve Novel 7'-Hydroxy Lignan Glucosides from Arctii fructus.* Journal of Agricultural and Food Chemistry, **2014**, 62(37), 9095-9102.
93. Harmatha, J., Budesinsky, M., and Trka, A. *The Structure of Yatein. Determination of The Positions, and Configurations of Benzyl Groups in Lignans of the 2,3-Dibenzylbutyrolactone Type.* Collection Czechoslovak Chern. Commun., **1982**, 47, 644-663.
94. Lucia, M.X., Yoshida, M., and Otto, R. G. *Dibenzylbutyrolactone Lignans from Virola sebifera.* Phytochemistry, **1983**, 22(6), 1516-1518.

95. Jairo, K.B., Otto, R.G., Silvio, J.S., and David, S. F. *Isolation of Lignans and Sesquiterpenoids from Leaves of Zanthoxylum naranjillo.* Nutural Product Letters, **1996**, 9, 65-70.
96. Takaku, N., Choi, D., Mikame, K., Okunishi, T., Suzuki, S., Ohashi, H., Umezawa, T., and Shimada, M. *Lignans of Chamaecyparis obtusa.* J. Wood Sci, **2001**, 47, 476-482.
97. Ito, C., Itoigawa, M., Ogata, M., Mou, X.Y., Tokuda, H., Nishino, H., and Furukawa, H. *lignan as Anti-Tumor-Promotor from the Seed of Hernandia ovigera.* Planta Med., **2001**, 67, 166-168.
98. Kuhnt, M., Rimpler, H., and Heinrich, M. *Lignans and Other Compounds from the Mixe Indian Medicinal Plant Hyptis verticillata.* Phytochemistry, **1994**, 36(2), 485-479.
99. Bernas, H., Plomp, A.J., Bitter, J.H., and Murzin, D.Y. *Influence of Reaction Parameters on the Hydrogenolysis of Hydroxymatairesinol Over Carbon Nanofibre Supported Palladium Catalysts.* Catalysis Letters, **2008**, 125(1-2), 8-13.
100. Tanabe, H., Fukutomi, R., Yasui, K., Kaneko, A., Imai, S., Nakayama, A., and Isemura, M. *Identification of Dimethylmatairesinol as an Immunoglobulin E-suppressing Component of the Leaves of Cinnamomum camphora.* Journal of Health Science, **2011**, 57(2), 184-187.
101. Min, B., Na, M., Oh, S., Ahn, K., Jeong, G., Li, G., Lee, S., Joung, H., and Lee, H. *New Furofuran and Butyrolactone Lignans with Antioxidant Activity from the Stem Bark of Styrax japonica.* J. Nat. Prod., **2004**, 67, 1980-1984.
102. Bai, M., Yao, G., Liu, S., Wang, D., Liu, Q., Huang, X., and Song, S. *Lignans from a Wild Vegetable (Patrinina villosa) able to Combat Alzheimer's Disease.* Journal of Functional Foods, **2017**, 28, 106-113.
103. Sub, C.K., Subedi, L., Wook, O.K., Bong, H.P., Yeou, S.K., Un, S.C., and Ro, K.L. *Wasabisides A−E, Lignan Glycosides from the Roots of Wasabia japonica.* J. Nat. Prod., **2016**, 79, 2652-2657.
104. Chang, C., Lien, Y., Karin, C.S., Liu, C., and Lee, S. *Lignans from Phyllanthus urinaria.* Phytochemistry, **2003**, 63, 825-833.
105. Li, N., Wu, J., Sakai, J., and Ando, M. *Dibenzylbutyrolactone and Dibenzylbutanediol Lignans from Peperomia duclouxii.* J. Nat. Prod., **2003**, 66, 1421-1426.
106. Barrero, A.F., Herrador, M. M., Akssira, M., Arteaga, P., and Luis, J. R. *Lignans and Polyacetylenes from Bupleurum acutifolium.* J. Nat. Prod., **1999**, 62, 946-948.
107. Cho, J.Y., Park, J., Kim, P.S., Yoo, E.S., Baik, K.U., and Park, M.H. *Savinin, a Lignan from Pterocarpus santalinus Inhibits Tumor Necrosis Factor-Production and T Cell Proliferation.* Biol. Pharm. Bull., **2001**, 24(2), 167-171.
108. Hanus, L.O., Rezanka, T., Moussaieff, A., and Valery, M.D. *Myrrh – Commiphora Chemistry.* Biomed. Papers, **2005**, 149(1), 3-28.
109. Dekebo, A., Lang, M., Polborn, K., Dagne, E., and Steglich, W. *Four Lignans from Commiphora erlangeriana.* J. Nat. Prod., **2002**, 65, 1252-1257.
110. Okunishi, T., Umezawa, T., and Shimada, M. *Enantiomeric Compositions and Biosynthesis of Wikstroemia sikokiana Lignans.* J. Wood Sci., **2000**, 46, 234-242.
111. Umezawa, T., Ragamustari, S.K., Nakatsubo, T., Wada, S., Li, L., Yamamura, M., Sakakibara, N., Hattori, T., Suzuki, S., and Chiang, V.L. *A lignan O-*

Methyltransferase Catalyzing the Regioselective Methylation of Matairesinol in Carthamus tinctorius. Plant Biotechnology, **2013**, 30(2), 97-109.
112. Jung, H.K., Ono, E., Morimoto, K., Yamagaki, T., Okazawa, A., Kobayashi, A., and Honoo, S. *Metabolic Engineering of Lignan Biosynthesis in Forsythia Cell Culture.* Plant Cell Physiol., **2009**, 50(12), 2200-2209.
113. Umezawa, T., Laurence, B.D., Yamamoto, E., David, G.I., and Norman, G.L. *Lignan Biosynthesis in Forsythia Species.* J. Chem. Soc., Chem. Commun., **1990**, 1405-1408.
114. Maiada, M.A., Dewick, P.M., Jackson, D.E., and Lucas, J.A. *Biosynthesis of Lignans In Forsythia Intermedia.* Phytochemistry, **1990**, 29(6), 1841-1846.
115. Broomhead, A.J., Rahman, M.A., Dewick, P.M., Jackson, D.E., and Lucas, J.A. *Matairesinol as Precursor of Podophyllum Lignans.* Phytochemistry, **1991**, 30(5), 1489-1492.
116. Lau, W., and Sattely, E.S. *Six Enzymes from Mayapple that Complete the Biosynthetic Pathway to the Etoposide Aglycone.* Science, **2015**, 349(6253), 1224-1228.
117. Canel, C., Moraes, M.R., Franck, E.D., and Ferreira, D. *Podophyllotoxin.* Phytochemistry, **2000**, 54, 115-120.
118. Kamal, A., Mohammed, S.A., Rahim, A., and Riyaz, S. *Podophyllotoxin Derivatives: A Patent Review (2012 - 2014)*, L. Informa UK, Editor. **2015**, India.
119. María, A.C., Pablo, A.G., Ángela, P.H., and Díezb, D. *An Overview on Heterocyclic Podophyllotoxin Derivatives,* **2016**, 19, 28-61.
120. Giri, A.M., and Lakshmi, M.N. *Production of Podophyllotoxin from Podophyllum hexandrum: a Potential Natural Product for Clinically useful Anticancer Drugs.* Cytotechnology, **2000**, 34, 17-26.
121. Liu, J., Cao, B., Gao, Y., Bai, M., Mei, X., Chen, H., Jiang, Y., and Huang, D. *Design, Synthesis, and Antitumor Activity of Novel Podophyllotoxin Derivatives as Potent Anticancer Agents.* Journal of Asian Natural Products Research, **2013**, 15(9), 985-992.
122. Yang, J., Bogni, A., Schuetz, E.G., Ratain, M., Dolan, M.E., McLeod, H., Gong, L., Thorn, C., Relling, M.V., Klein, T.E., and Altman, R.B., *Etoposide pathway.* Pharmacogenet Genomics, **2009**, 19(7), 552-553.
123. Yu, P., Wang, L., and Chen, Z. *A New Podophyllotoxin-Type Lignan from Dysosma verslpellls Var. tomentosa.* J. Nat. Prod., **1991**, 54(5), 1422-1424.
124. Thanh, V.T., Pham, V.C., Mai, H.D., Litaudon, M., Gueritte, F., Retailleau, P., Nguyen, V.H., and Chau, V.M. *Cytotoxic Lignans from Fruits of Cleistanthus indochinensis: Synthesis of Cleistantoxin Derivatives.* J. Nat. Prod., **2012**, 75(9), 1578-83.
125. Robert, R.F., *Long-Range Coupling Constants in the NMR Spectra of Olefines.* Can. J. Chem., **1960**, 38, 549-553.
126. Atta-ur-Rahman. *Studies in Natural Products Chemistry: Stereoselective Synthesis (Part K)*. Vol. 18, **2005**, Amsterdam, The Netherlands: Elsevier.
127. Trazzi, G., Fabiano, M. A., and Coelho, F. *Diastereoselective Synthesis of β-Piperonyl-γ-Butyrolactones from Morita-Baylis-Hillman Adducts. Highly Efficient Synthesis of (±)-Yatein, (±)-Podorhizol and (±)-epi-Podorhizol.* J. Braz. Chem. Soc., **2010**, 21(12), 2327-2010.

128. Harmatha, J., Budesinsky, M., and Trka, A. *The Structure of Yatein: Determination of The Positions, and Configurations of Benzyl Groups in Lignans of the 2,3-Dibenzylbutyrolactone Type.* Collect. Czech. Chem. Commun., **1982**, 47, 644-663.
129. Dekebo, A. *Chemical Studies of The Resins of Some Boswellia and Commiphora Species*, in *AAU, Chemistry Department*, **2002**, AAU.

Appendices

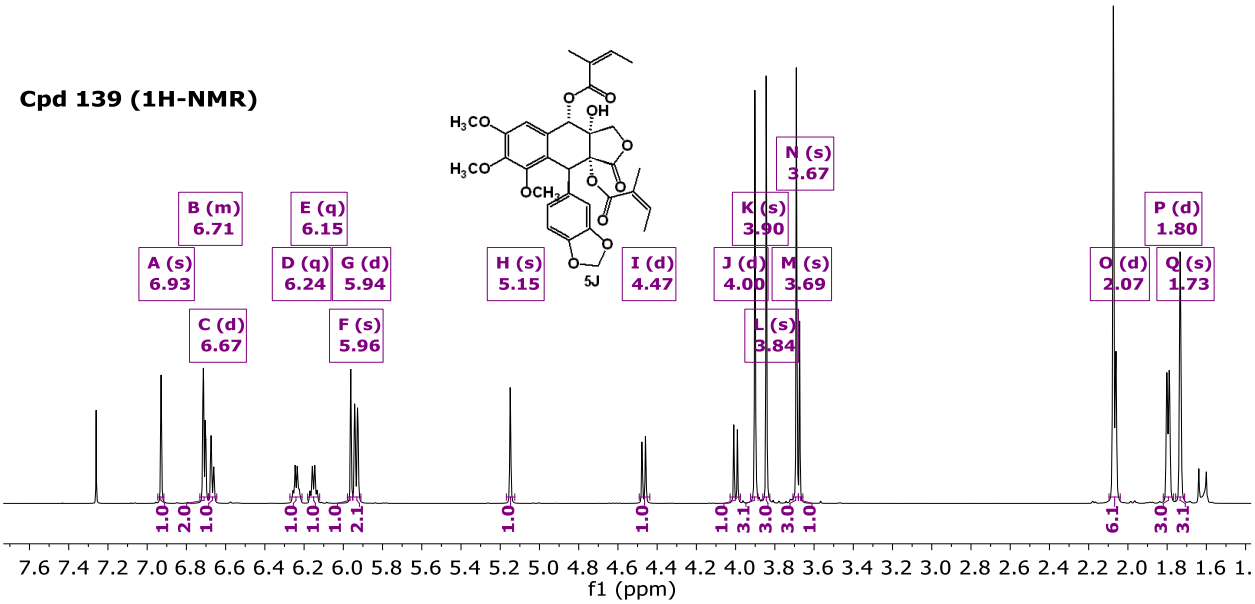
Cpd 139 (1H-NMR)
A (s) 6.93
B (m) 6.71
C (d) 6.67
D (q) 6.24
E (q) 6.15
F (s) 5.96
G (d) 5.94
H (s) 5.15
I (d) 4.47
J (d) 4.00
K (s) 3.90
L (s) 3.84
M (s) 3.69
N (s) 3.67
O (d) 2.07
P (d) 1.80
Q (s) 1.73
f1 (ppm)

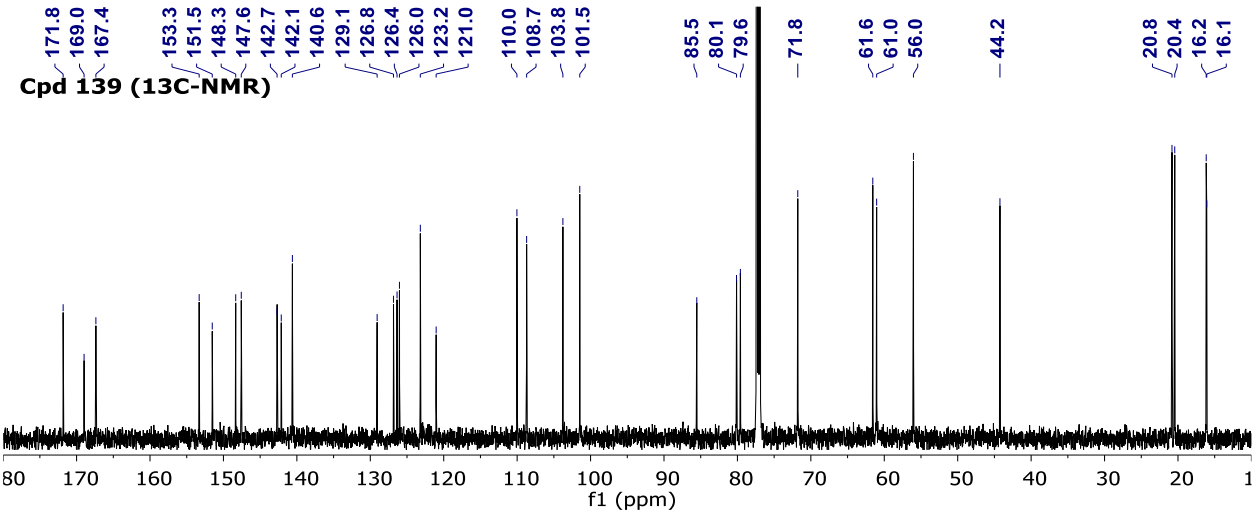
Cpd 139 (13C-NMR)
171.8
169.0
167.4
153.3
151.5
148.3
147.6
142.7
142.1
140.6
129.1
126.8
126.4
126.0
123.2
121.0
110.0
108.7
103.8
101.5
85.5
80.1
79.6
71.8
61.6
61.0
56.0
44.2
20.8
20.4
16.2
16.1
f1 (ppm)

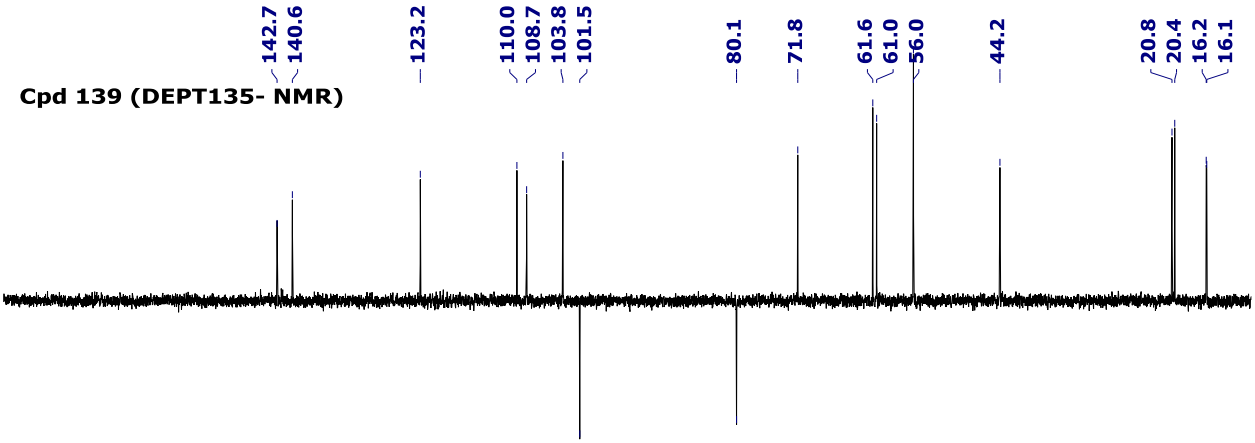
Cpd 139 (DEPT135- NMR)
142.7
140.6
123.2
110.0
108.7
103.8
101.5
80.1
71.8
61.6
61.0
56.0
44.2
20.8
20.4
16.2
16.1

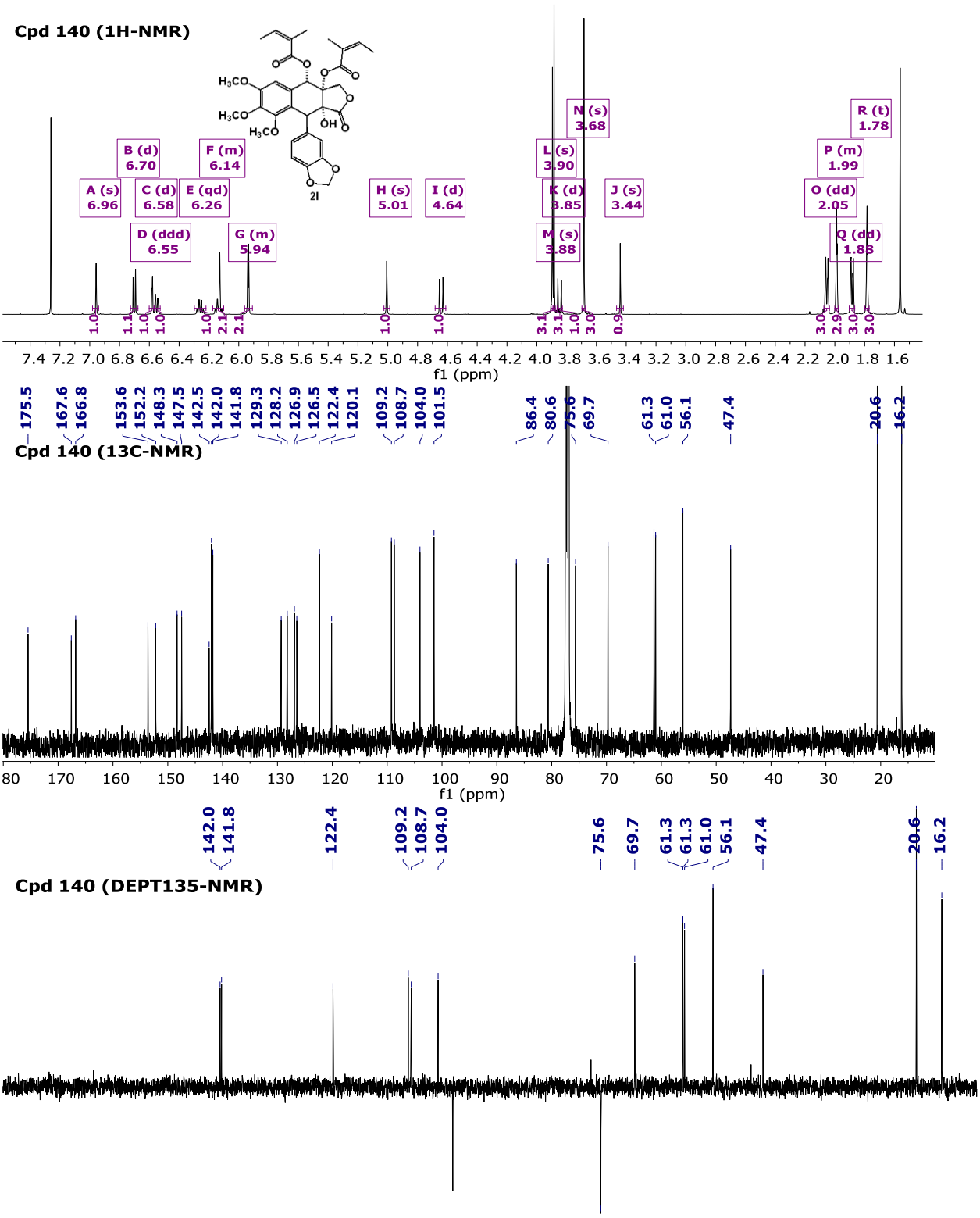
Cpd 140 (1H-NMR)
A (s) 6.96
B (d) 6.70
C (d) 6.58
D (ddd) 6.55
E (qd) 6.26
F (m) 6.14
G (m) 5.94
H (s) 5.01
I (d) 4.64
J (s) 3.44
K (d) 3.85
L (s) 3.90
M (s) 3.88
N (s) 3.68
O (dd) 2.05
P (m) 1.99
Q (dd) 1.88
R (t) 1.78
f1 (ppm)
Cpd 140 (13C-NMR)
175.5
167.6
166.8
153.6
152.2
148.3
147.5
142.5
142.0
141.8
129.3
128.2
126.9
126.5
122.4
120.1
109.2
108.7
104.0
101.5
86.4
80.6
75.6
69.7
61.3
61.0
56.1
47.4
20.6
16.2
f1 (ppm)
Cpd 140 (DEPT135-NMR)
142.0
141.8
122.4
109.2
108.7
104.0
75.6
69.7
61.3
61.3
61.0
56.1
47.4
20.6
16.2

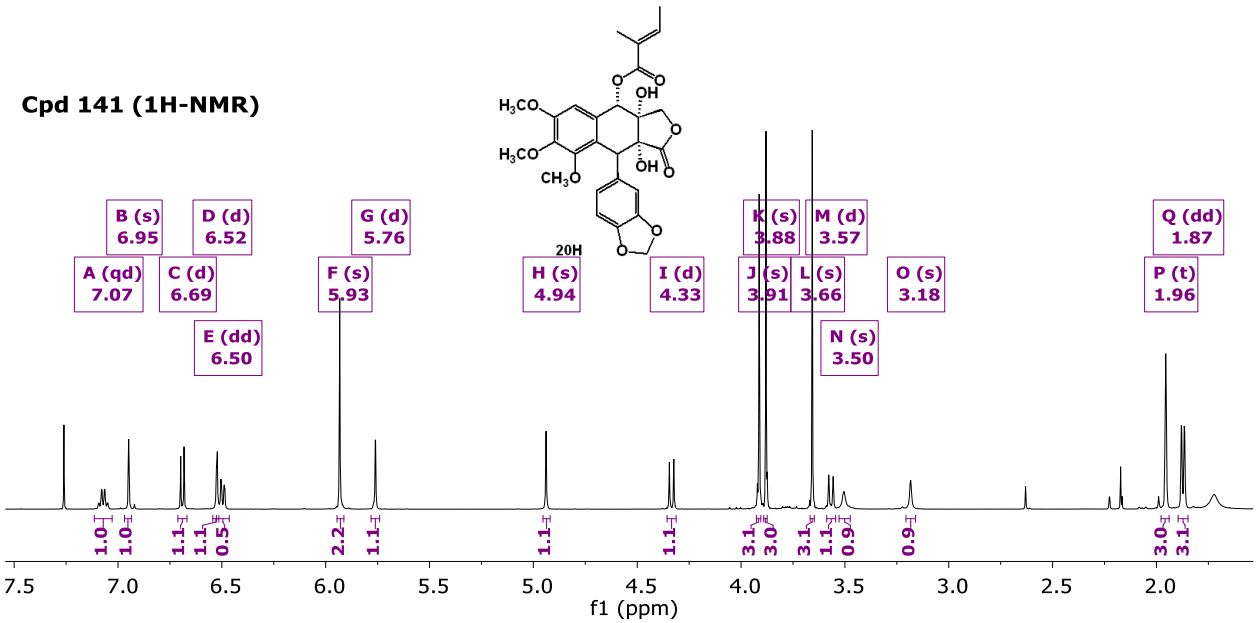
Cpd 141 (1H-NMR)
B (s) 6.95
D (d) 6.52
G (d) 5.76
K (s) 3.88
M (d) 3.57
Q (dd) 1.87
A (qd) 7.07
C (d) 6.69
F (s) 5.93
H (s) 4.94
I (d) 4.33
J (s) 3.91
L (s) 3.66
O (s) 3.18
P (t) 1.96
E (dd) 6.50
N (s) 3.50
1.0 1.0 1.1 1.1 0.5 2.2 1.1 1.1 1.1 3.1 3.0 3.1 1.1 0.9 0.9 3.0 3.1
7.5 7.0 6.5 6.0 5.5 5.0 4.5 4.0 3.5 3.0 2.5 2.0
f1 (ppm)

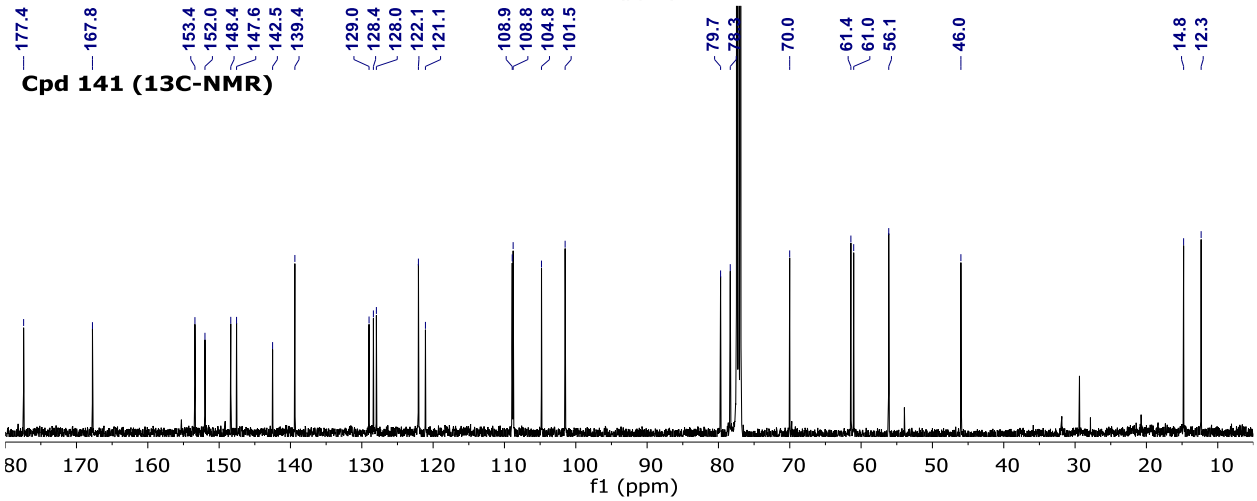
177.4 167.8 153.4 152.0 148.4 147.6 142.5 139.4 129.0 128.4 128.0 122.1 121.1 108.9 108.8 104.8 101.5 79.7 78.3 70.0 61.4 61.0 56.1 46.0 14.8 12.3
Cpd 141 (13C-NMR)
80 170 160 150 140 130 120 110 100 90 80 70 60 50 40 30 20 10
f1 (ppm)

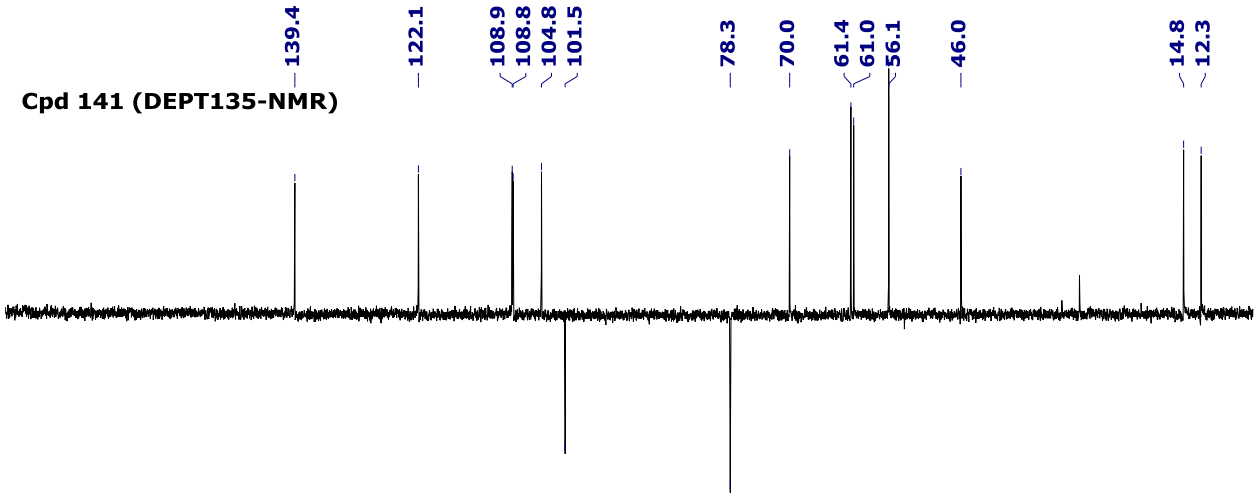
139.4 122.1 108.9 108.8 104.8 101.5 78.3 70.0 61.4 61.0 56.1 46.0 14.8 12.3
Cpd 141 (DEPT135-NMR)

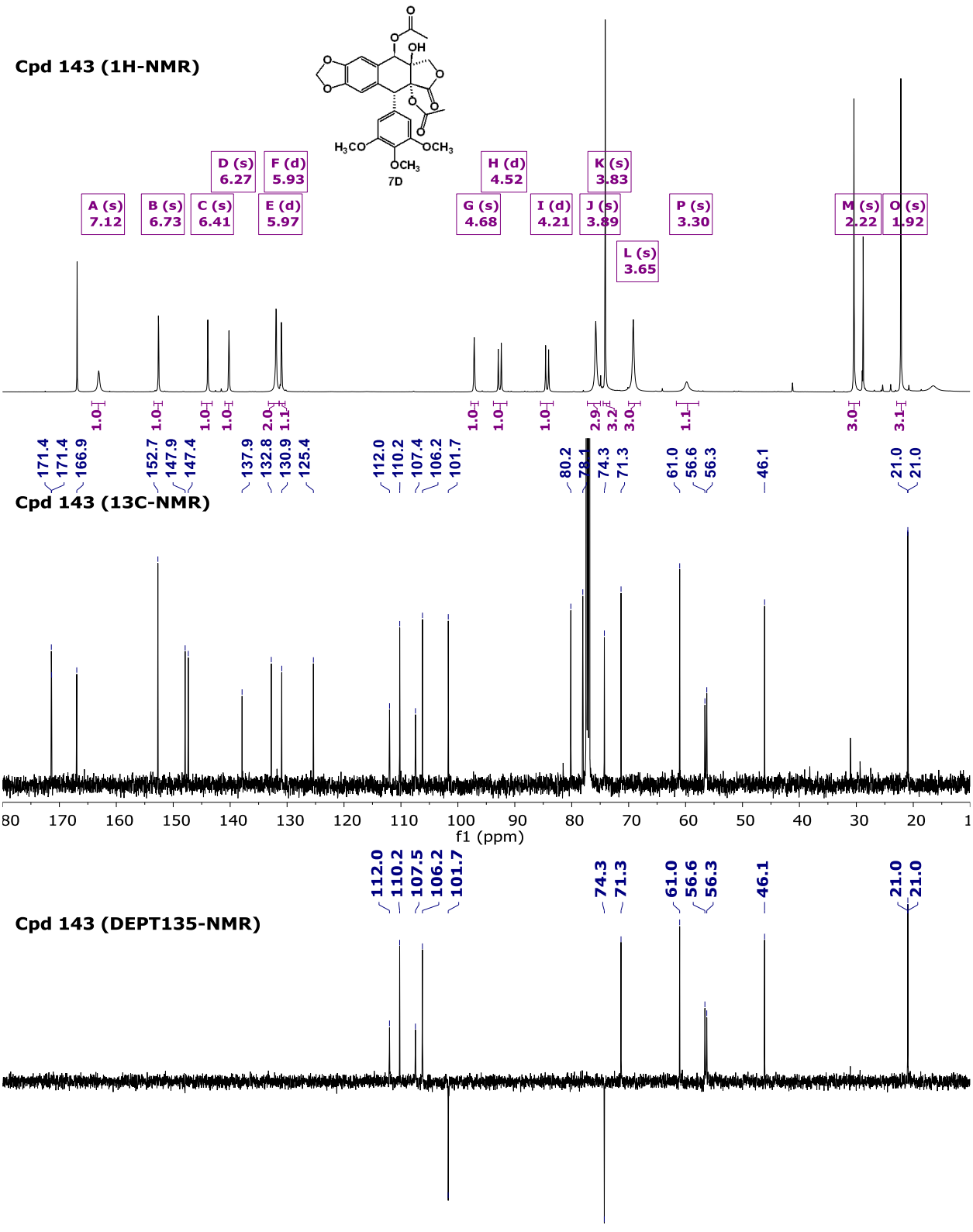
Cpd 143 (1H-NMR)
7D
A (s) 7.12
B (s) 6.73
C (s) 6.41
D (s) 6.27
E (d) 5.97
F (d) 5.93
G (s) 4.68
H (d) 4.52
I (d) 4.21
J (s) 3.89
K (s) 3.83
L (s) 3.65
P (s) 3.30
M (s) 2.22
O (s) 1.92
1.0 1.0 1.0 1.0 2.0 1.1 1.0 1.0 1.0 2.9 3.2 3.0 1.1 3.0 3.1
171.4 171.4 166.9 152.7 147.9 147.4 137.9 132.8 130.9 125.4 112.0 110.2 107.4 106.2 101.7 80.2 78.1 74.3 71.3 61.0 56.6 56.3 46.1 21.0 21.0
Cpd 143 (13C-NMR)
80 170 160 150 140 130 120 110 100 90 80 70 60 50 40 30 20 1
f1 (ppm)
112.0 110.2 107.5 106.2 101.7 74.3 71.3 61.0 56.6 56.3 46.1 21.0 21.0
Cpd 143 (DEPT135-NMR)

Cpd 142 (1H-NMR)

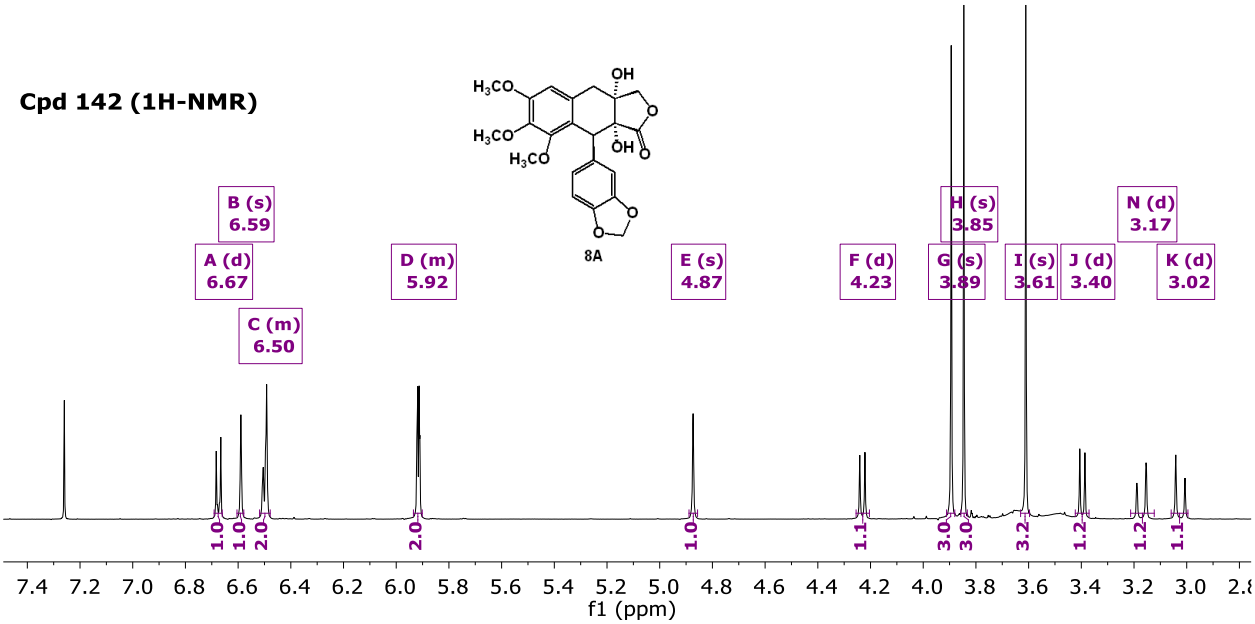

8A

Cpd 142 (13C-NMR)

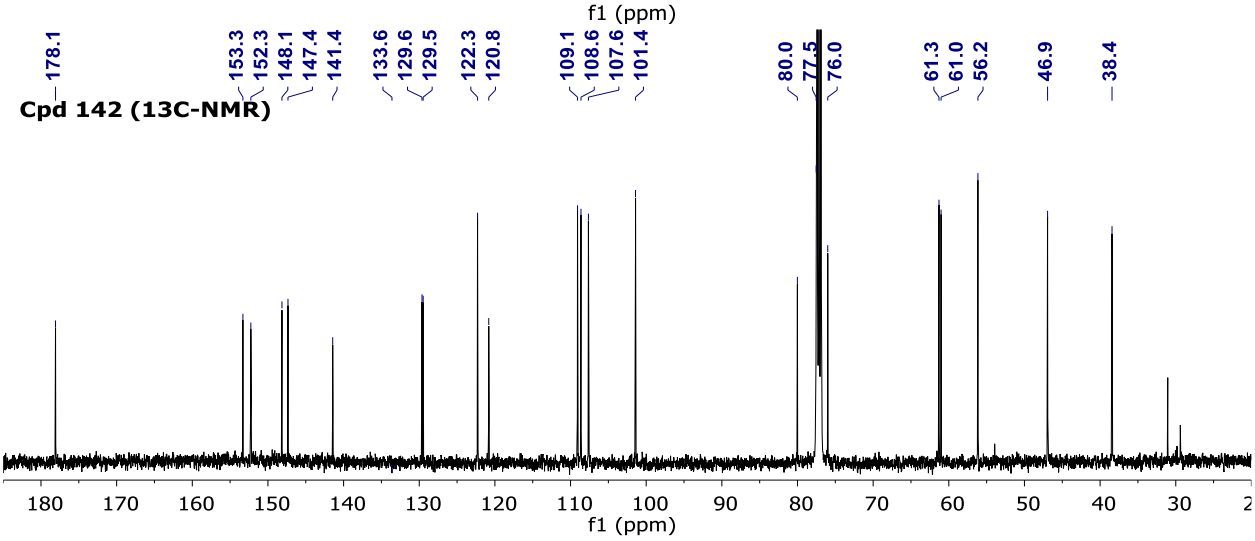

Cpd 142 (DEPT135-NMR)

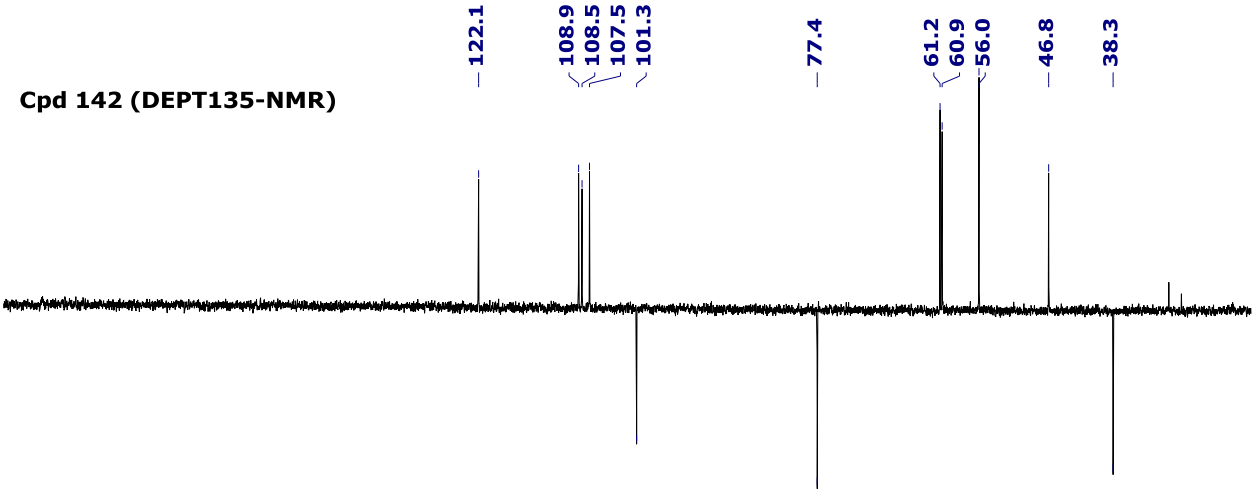

Cpd 144 (1H-NMR)

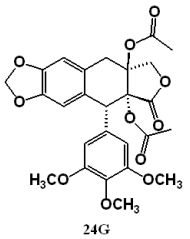

Cpd 144 (13C-NMR)

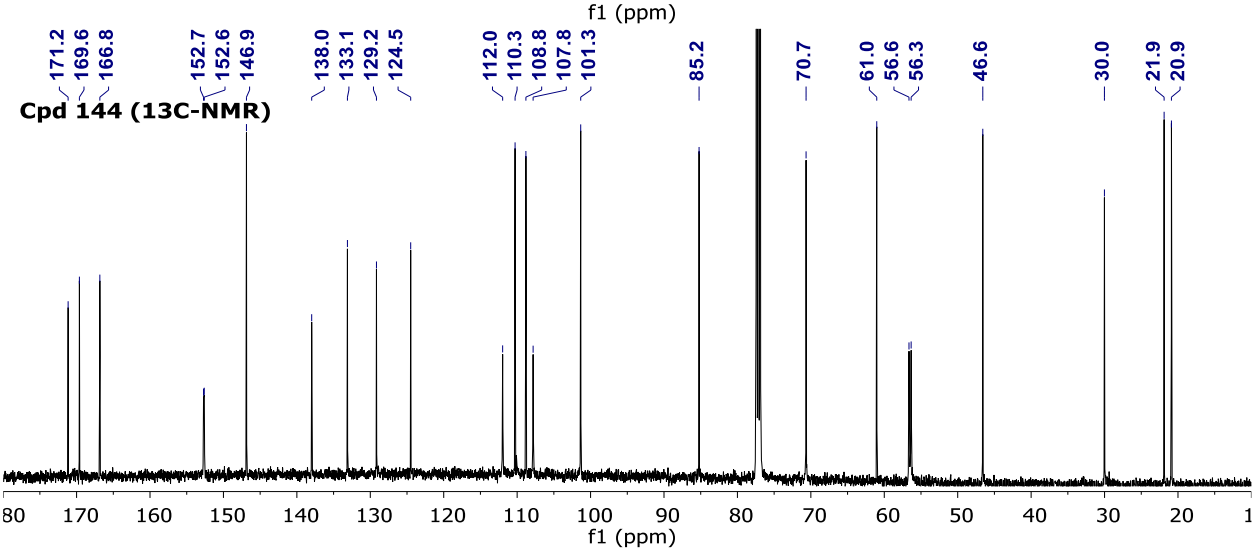

Cpd 144 (DEPT135-NMR)

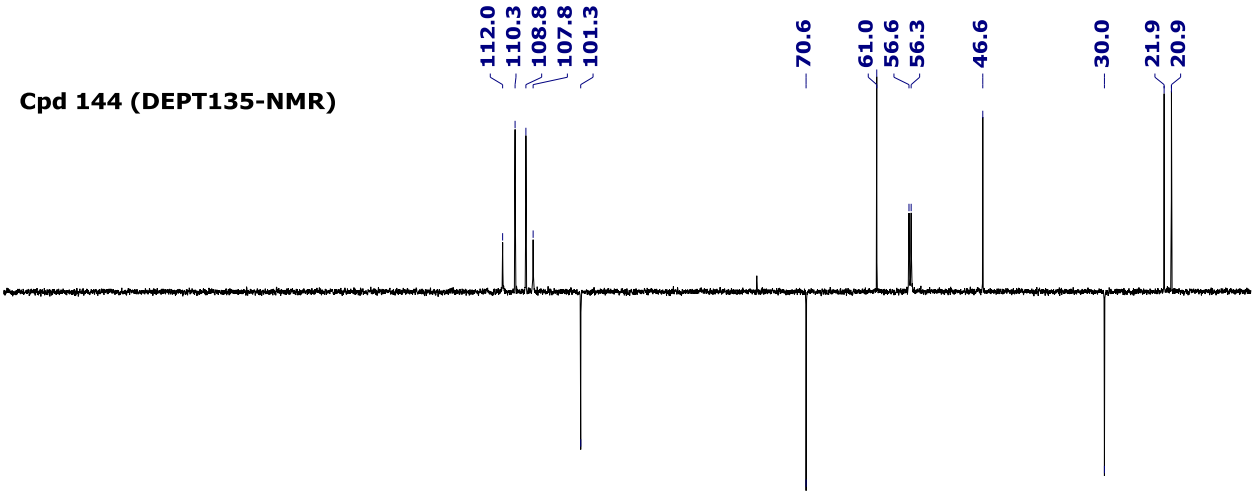

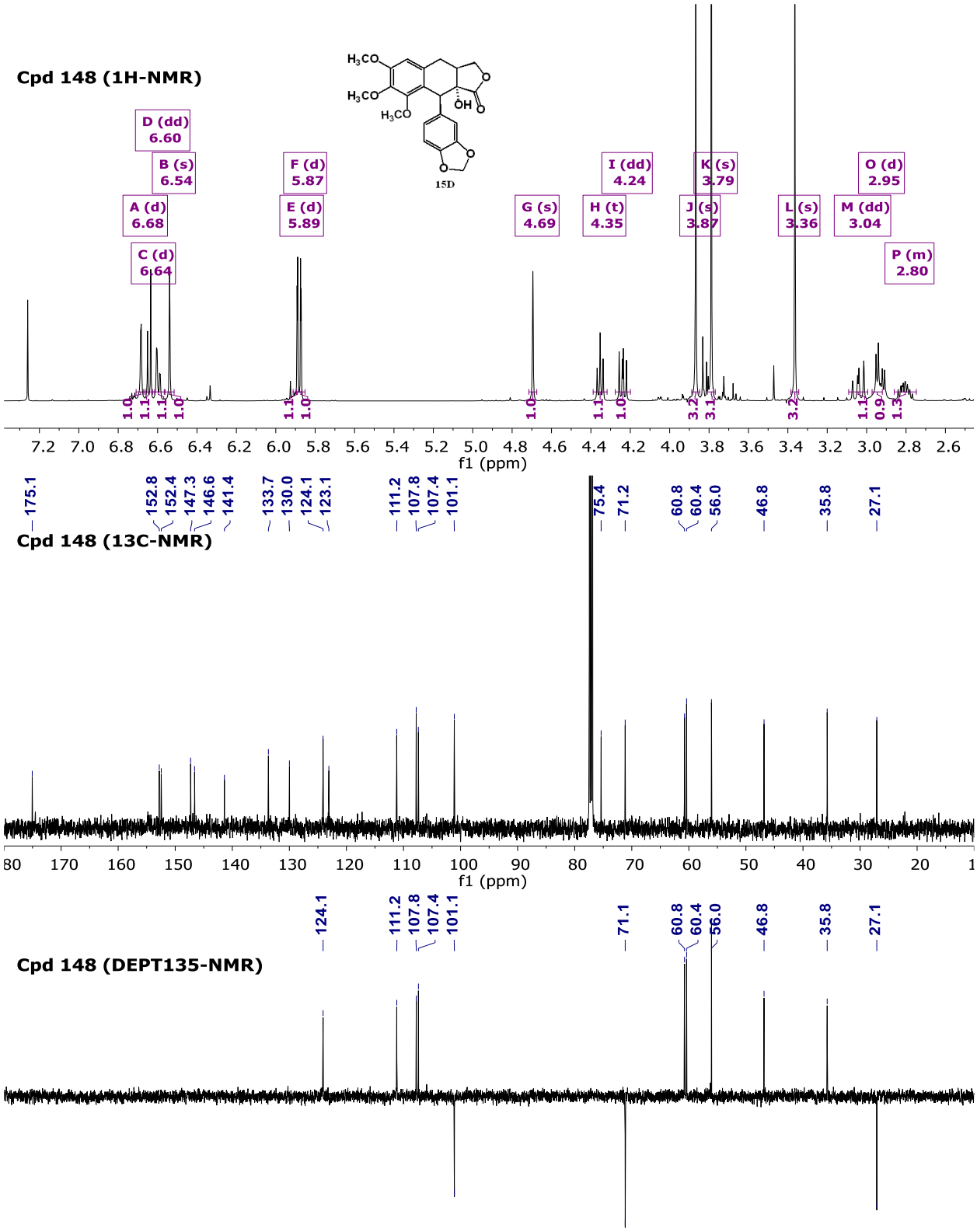
Cpd 148 (1H-NMR)
D (dd) 6.60
B (s) 6.54
A (d) 6.68
C (d) 6.64
F (d) 5.87
E (d) 5.89
G (s) 4.69
I (dd) 4.24
H (t) 4.35
K (s) 3.79
J (s) 3.87
L (s) 3.36
O (d) 2.95
M (dd) 3.04
P (m) 2.80
15D
f1 (ppm)
Cpd 148 (13C-NMR)
175.1
152.8
152.4
147.3
146.6
141.4
133.7
130.0
124.1
123.1
111.2
107.8
107.4
101.1
75.4
71.2
60.8
60.4
56.0
46.8
35.8
27.1
f1 (ppm)
Cpd 148 (DEPT135-NMR)
124.1
111.2
107.8
107.4
101.1
71.1
60.8
60.4
56.0
46.8
35.8
27.1

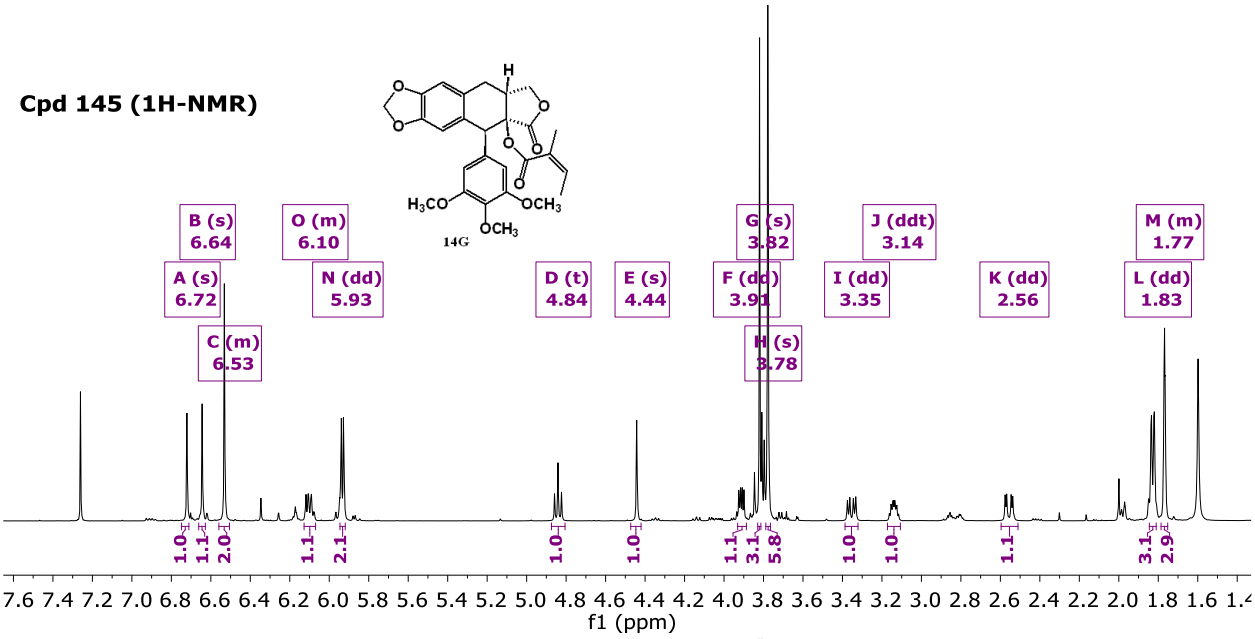
Cpd 145 (1H-NMR)
B (s) 6.64
A (s) 6.72
C (m) 6.53
O (m) 6.10
N (dd) 5.93
D (t) 4.84
E (s) 4.44
G (s) 3.82
F (dd) 3.91
H (s) 3.78
I (dd) 3.35
J (ddt) 3.14
K (dd) 2.56
M (m) 1.77
L (dd) 1.83
1.0 1.1 2.0 1.1 2.1 1.0 1.0 1.1 3.1 5.8 1.0 1.0 1.1 3.1 2.9
7.6 7.4 7.2 7.0 6.8 6.6 6.4 6.2 6.0 5.8 5.6 5.4 5.2 5.0 4.8 4.6 4.4 4.2 4.0 3.8 3.6 3.4 3.2 3.0 2.8 2.6 2.4 2.2 2.0 1.8 1.6
f1 (ppm)

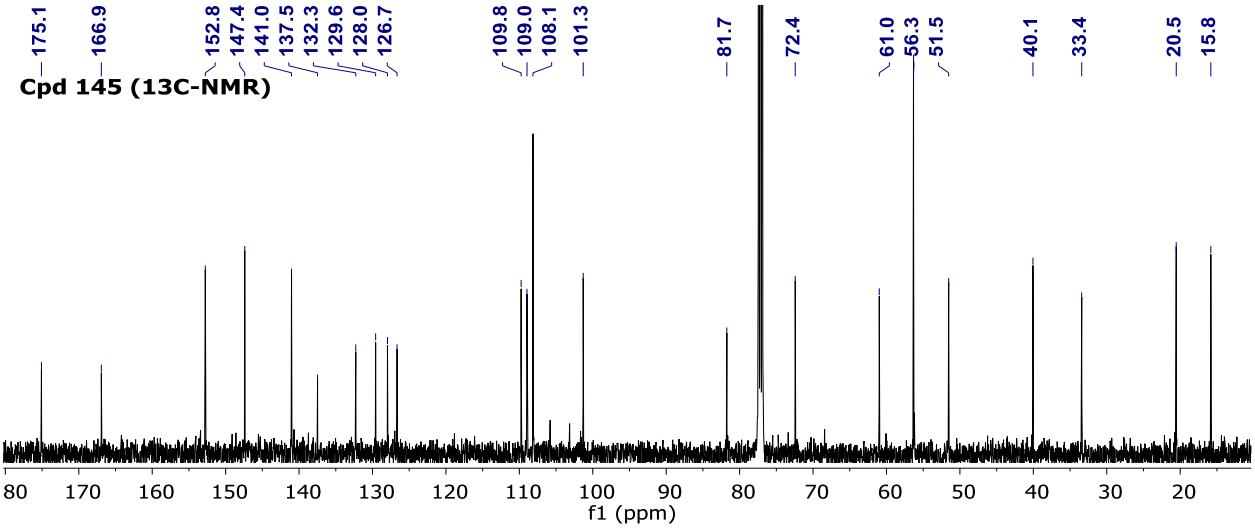
175.1 166.9 152.8 147.4 141.0 137.5 132.3 129.6 128.0 126.7 109.8 109.0 108.1 101.3 81.7 72.4 61.0 56.3 51.5 40.1 33.4 20.5 15.8
Cpd 145 (13C-NMR)
80 170 160 150 140 130 120 110 100 90 80 70 60 50 40 30 20
f1 (ppm)

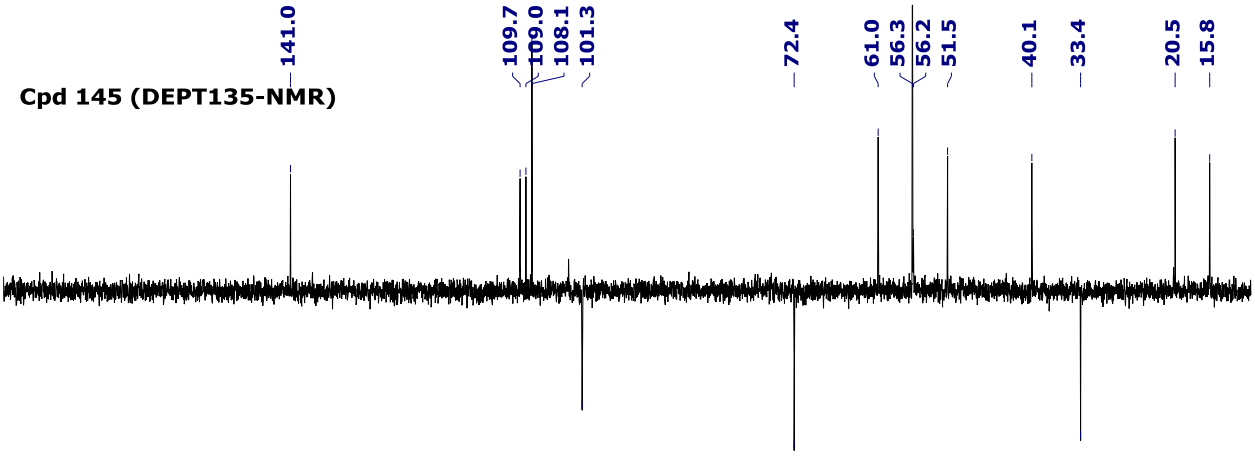
141.0 109.7 109.0 108.1 101.3 72.4 61.0 56.3 56.2 51.5 40.1 33.4 20.5 15.8
Cpd 145 (DEPT135-NMR)

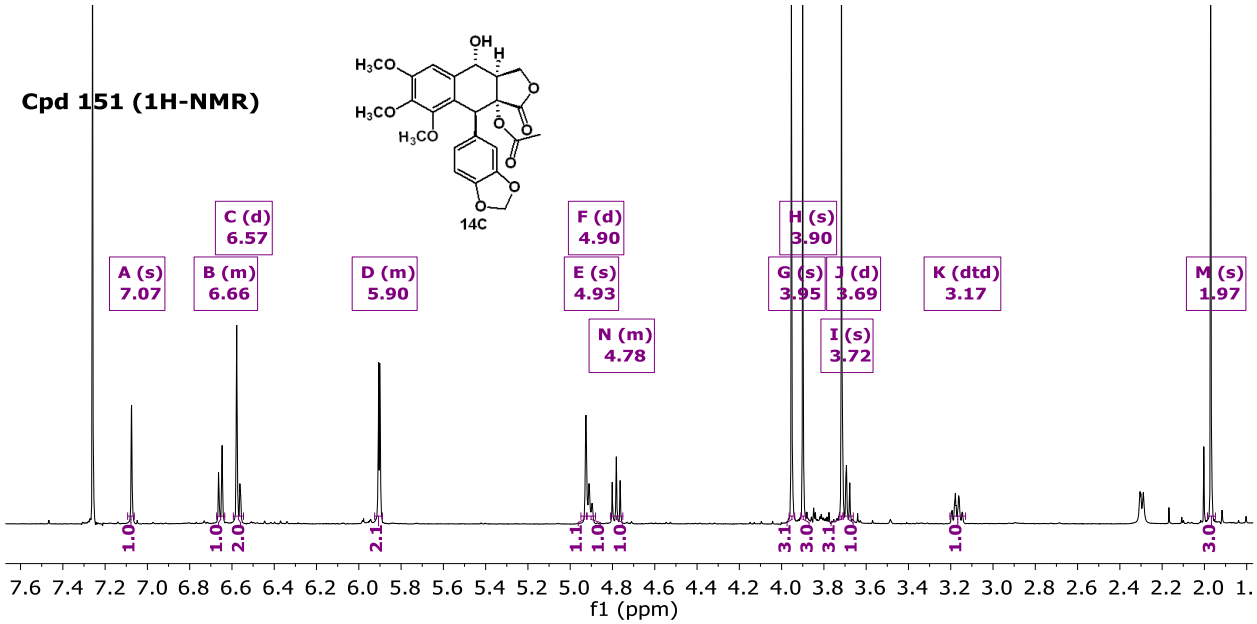
Cpd 151 (1H-NMR)
OH
H
H3CO
H3CO
H3CO
O
O
O
O
O
14C
A (s) 7.07
B (m) 6.66
C (d) 6.57
D (m) 5.90
E (s) 4.93
F (d) 4.90
N (m) 4.78
G (s) 3.95
H (s) 3.90
J (d) 3.69
I (s) 3.72
K (dtd) 3.17
M (s) 1.97
1.0
1.0
2.0
2.1
1.1
1.0
1.0
3.1
3.0
3.1
1.0
1.0
3.0
7.6 7.4 7.2 7.0 6.8 6.6 6.4 6.2 6.0 5.8 5.6 5.4 5.2 5.0 4.8 4.6 4.4 4.2 4.0 3.8 3.6 3.4 3.2 3.0 2.8 2.6 2.4 2.2 2.0 1.
f1 (ppm)

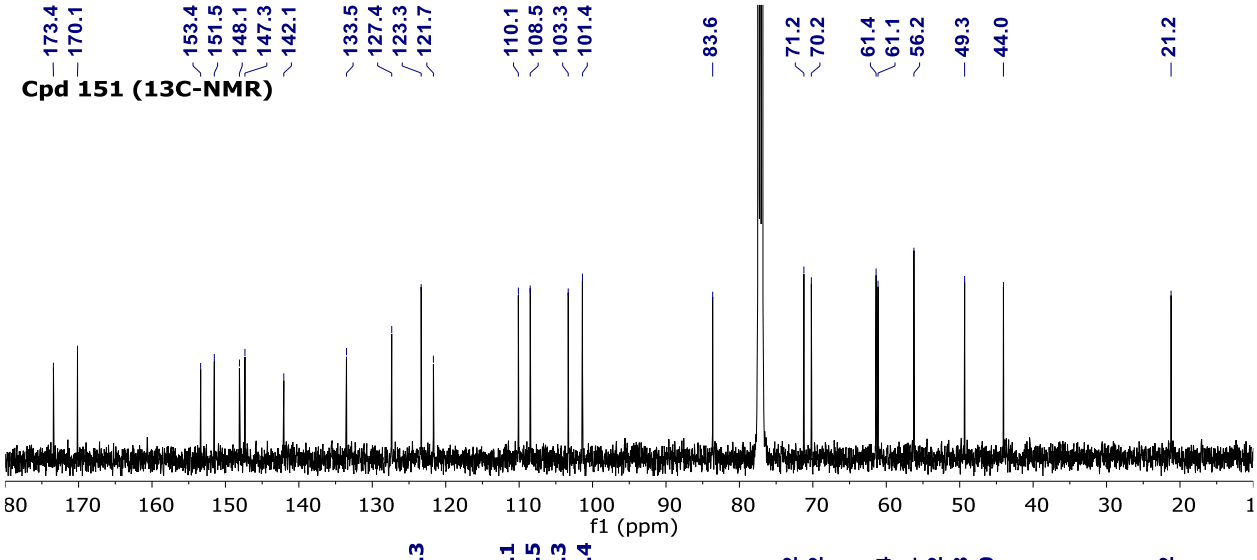
173.4
170.1
153.4
151.5
148.1
147.3
142.1
133.5
127.4
123.3
121.7
110.1
108.5
103.3
101.4
83.6
71.2
70.2
61.4
61.1
56.2
49.3
44.0
21.2
Cpd 151 (13C-NMR)
80 170 160 150 140 130 120 110 100 90 80 70 60 50 40 30 20 1
f1 (ppm)

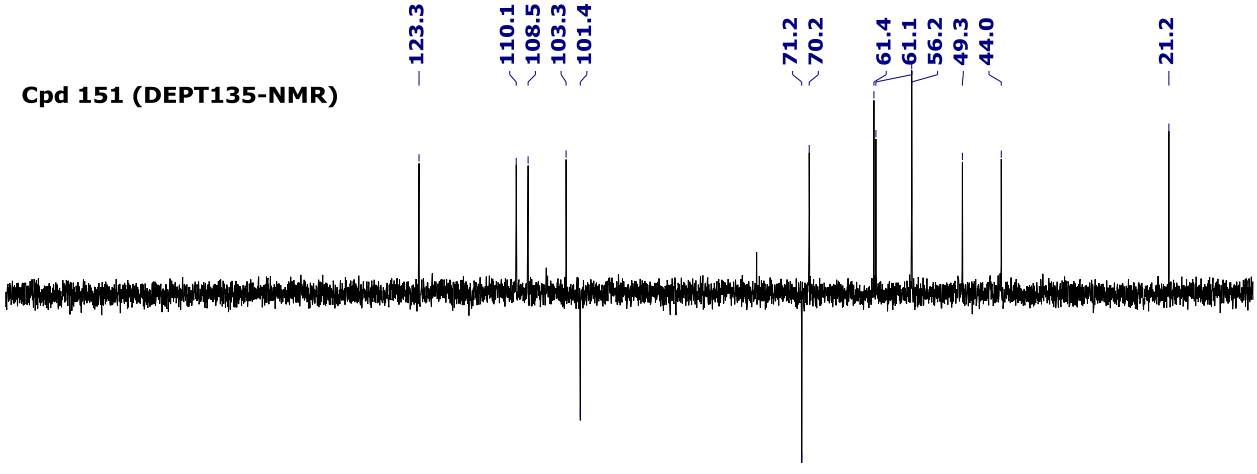
123.3
110.1
108.5
103.3
101.4
71.2
70.2
61.4
61.1
56.2
49.3
44.0
21.2
Cpd 151 (DEPT135-NMR)

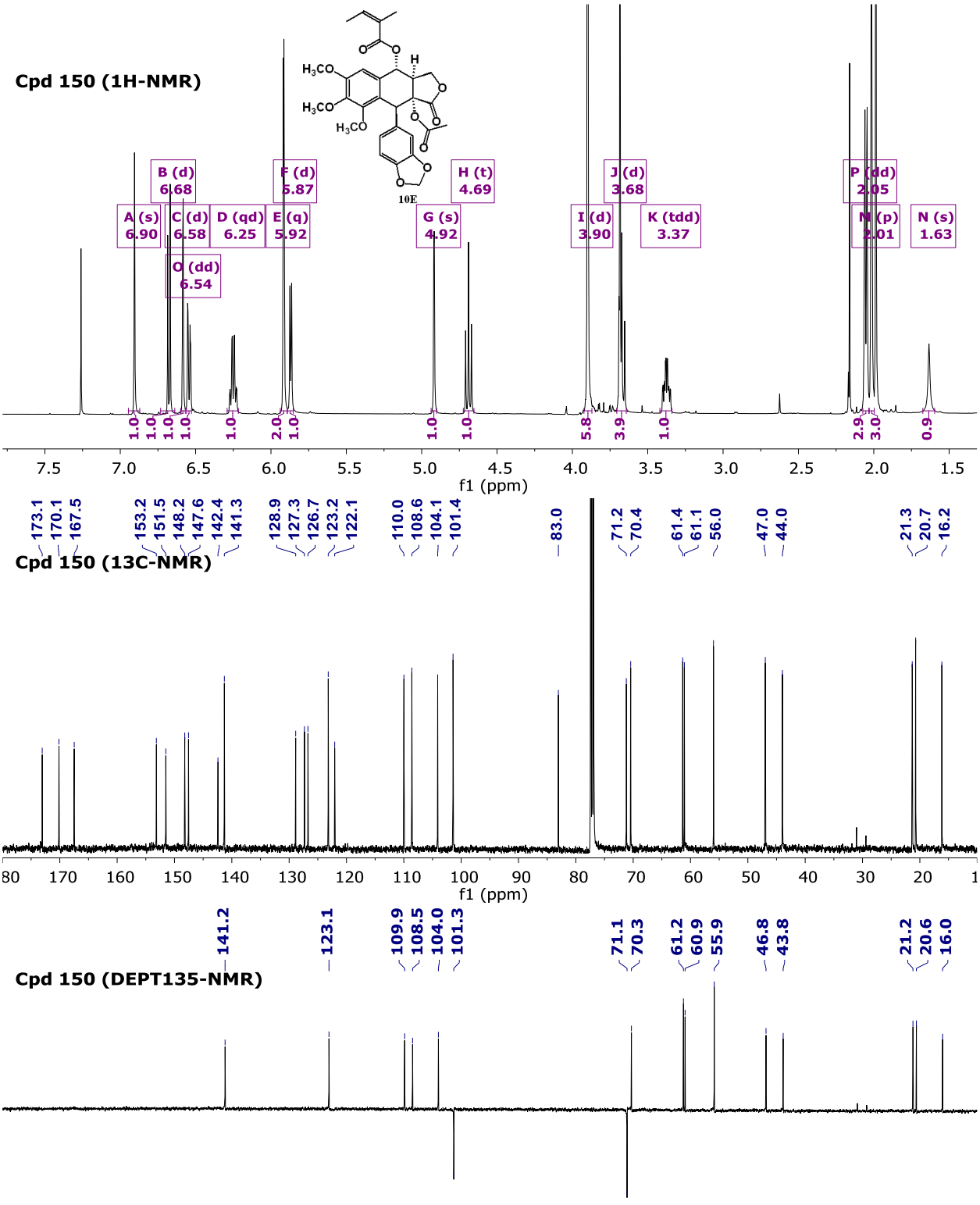
Cpd 150 (1H-NMR)
A (s) 6.90
B (d) 6.68
C (d) 6.58
D (qd) 6.25
E (q) 5.92
F (d) 5.87
G (s) 4.92
H (t) 4.69
I (d) 3.90
J (d) 3.68
K (tdd) 3.37
O (dd) 6.54
P (dd) 2.05
N (p) 2.01
N (s) 1.63
1.0 1.0 1.0 1.0 1.0 2.0 1.0 1.0 1.0 5.8 3.9 1.0 2.9 3.0 0.9
7.5 7.0 6.5 6.0 5.5 5.0 4.5 4.0 3.5 3.0 2.5 2.0 1.5
f1 (ppm)
Cpd 150 (13C-NMR)
173.1 170.1 167.5 153.2 151.5 148.2 147.6 142.4 141.3 128.9 127.3 126.7 123.2 122.1 110.0 108.6 104.1 101.4 83.0 71.2 70.4 61.4 61.1 56.0 47.0 44.0 21.3 20.7 16.2
80 170 160 150 140 130 120 110 100 90 80 70 60 50 40 30 20 1
f1 (ppm)
Cpd 150 (DEPT135-NMR)
141.2 123.1 109.9 108.5 104.0 101.3 71.1 70.3 61.2 60.9 55.9 46.8 43.8 21.2 20.6 16.0

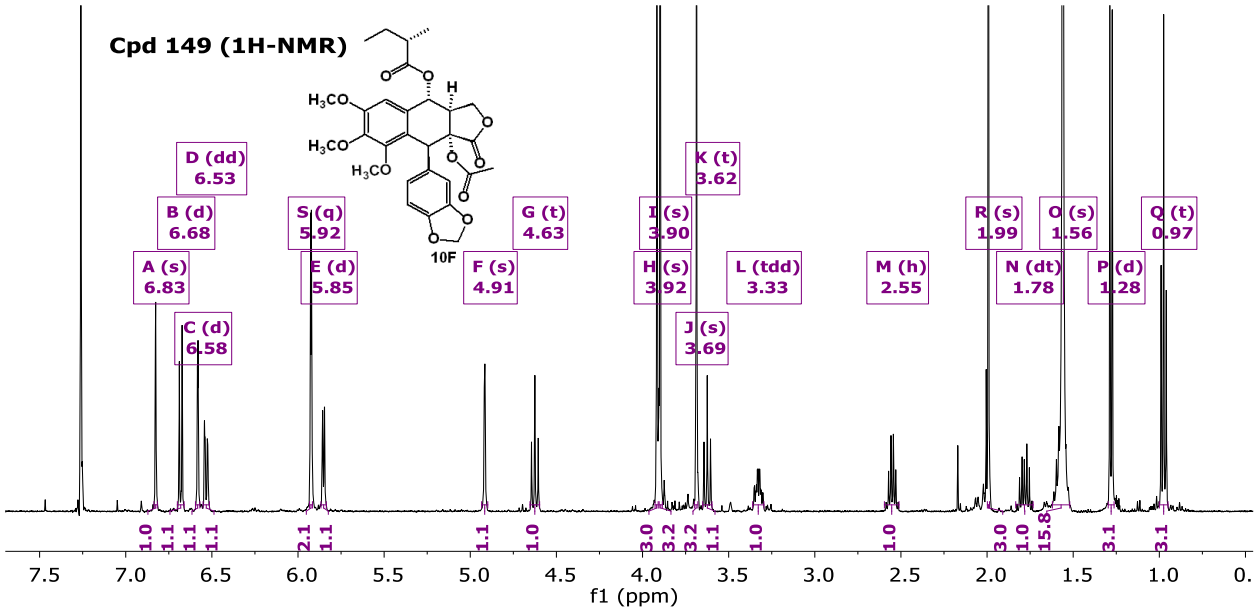
Cpd 149 (1H-NMR)
D (dd) 6.53
B (d) 6.68
A (s) 6.83
C (d) 6.58
S (q) 5.92
E (d) 5.85
G (t) 4.63
F (s) 4.91
K (t) 3.62
I (s) 3.90
H (s) 3.92
J (s) 3.69
L (tdd) 3.33
M (h) 2.55
R (s) 1.99
N (dt) 1.78
O (s) 1.56
P (d) 1.28
Q (t) 0.97
10F
f1 (ppm)

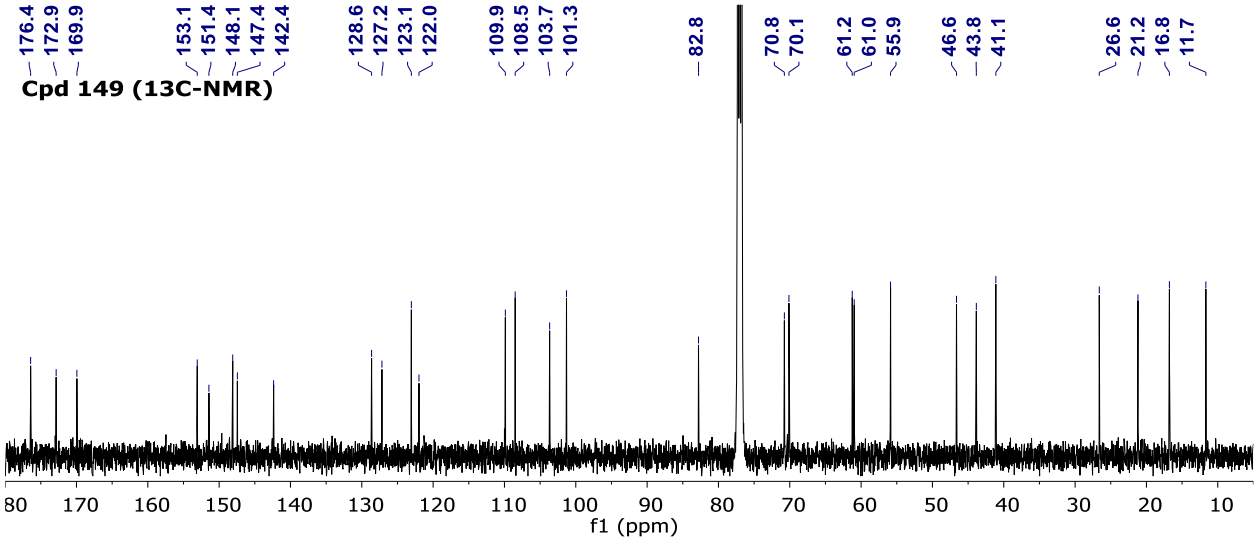
Cpd 149 (13C-NMR)
176.4
172.9
169.9
153.1
151.4
148.1
147.4
142.4
128.6
127.2
123.1
122.0
109.9
108.5
103.7
101.3
82.8
70.8
70.1
61.2
61.0
55.9
46.6
43.8
41.1
26.6
21.2
16.8
11.7
f1 (ppm)

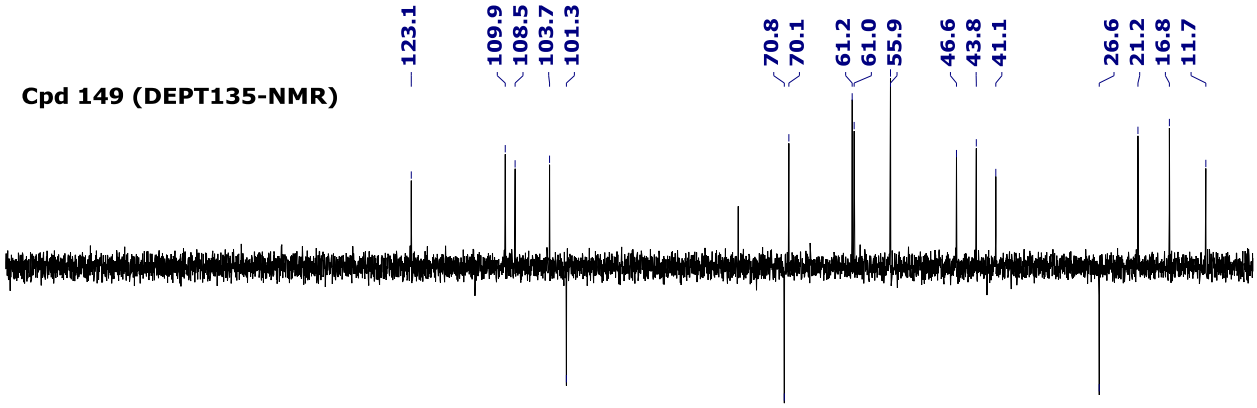
Cpd 149 (DEPT135-NMR)
123.1
109.9
108.5
103.7
101.3
70.8
70.1
61.2
61.0
55.9
46.6
43.8
41.1
26.6
21.2
16.8
11.7

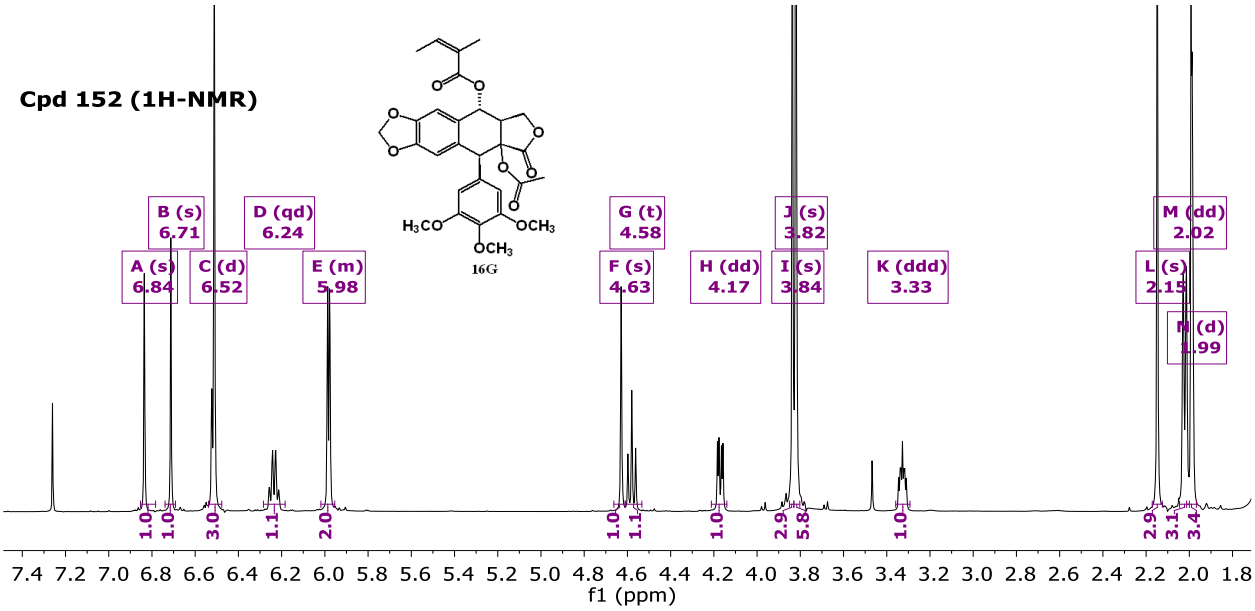
Cpd 152 (1H-NMR)
A (s) 6.84
B (s) 6.71
C (d) 6.52
D (qd) 6.24
E (m) 5.98
F (s) 4.63
G (t) 4.58
H (dd) 4.17
I (s) 3.84
J (s) 3.82
K (ddd) 3.33
L (s) 2.15
M (dd) 2.02
N (d) 1.99
1.0 1.0 3.0 1.1 2.0 1.0 1.1 1.0 2.9 5.8 1.0 2.9 3.1 3.4
7.4 7.2 7.0 6.8 6.6 6.4 6.2 6.0 5.8 5.6 5.4 5.2 5.0 4.8 4.6 4.4 4.2 4.0 3.8 3.6 3.4 3.2 3.0 2.8 2.6 2.4 2.2 2.0 1.8
f1 (ppm)

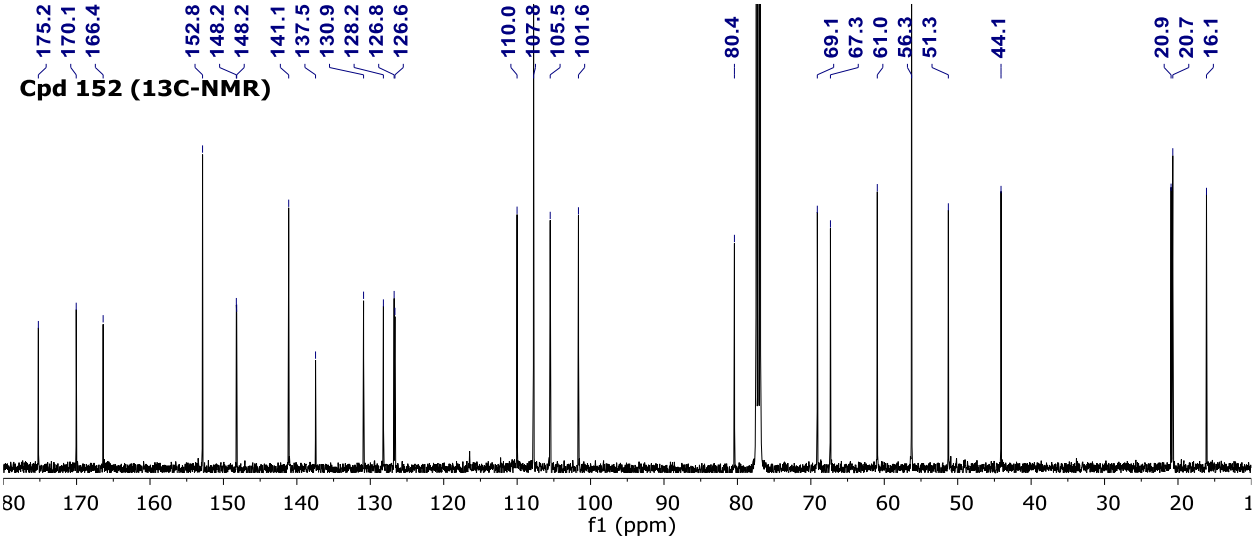
Cpd 152 (13C-NMR)
175.2 170.1 166.4 152.8 148.2 148.2 141.1 137.5 130.9 128.2 126.8 126.6 110.0 107.8 105.5 101.6 80.4 69.1 67.3 61.0 56.3 51.3 44.1 20.9 20.7 16.1
80 170 160 150 140 130 120 110 100 90 80 70 60 50 40 30 20 1
f1 (ppm)

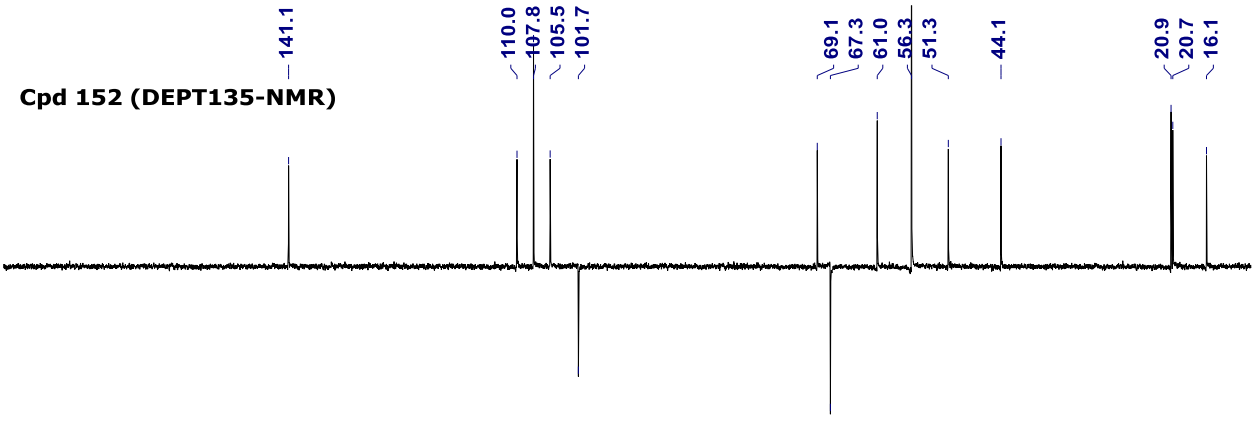
Cpd 152 (DEPT135-NMR)
141.1 110.0 107.8 105.5 101.7 69.1 67.3 61.0 56.3 51.3 44.1 20.9 20.7 16.1

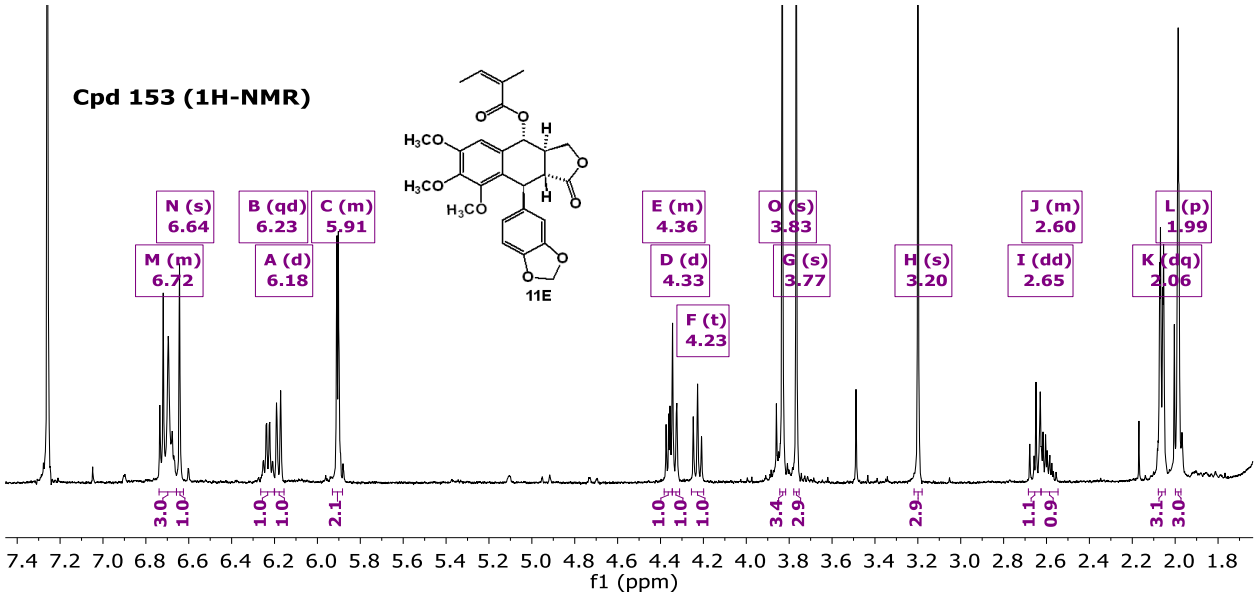
Cpd 153 (1H-NMR)
N (s) 6.64
M (m) 6.72
B (qd) 6.23
A (d) 6.18
C (m) 5.91
E (m) 4.36
D (d) 4.33
F (t) 4.23
O (s) 3.83
G (s) 3.77
H (s) 3.20
J (m) 2.60
I (dd) 2.65
L (p) 1.99
K (dq) 2.06
11E
f1 (ppm)

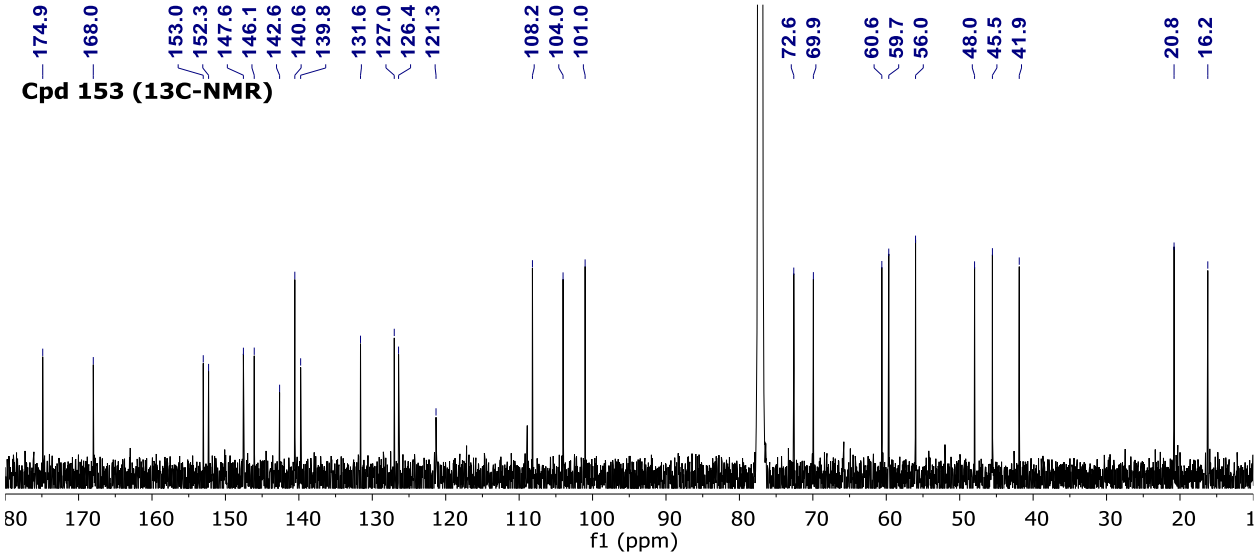
174.9
168.0
153.0
152.3
147.6
146.1
142.6
140.6
139.8
131.6
127.0
126.4
121.3
108.2
104.0
101.0
72.6
69.9
60.6
59.7
56.0
48.0
45.5
41.9
20.8
16.2
Cpd 153 (13C-NMR)
f1 (ppm)

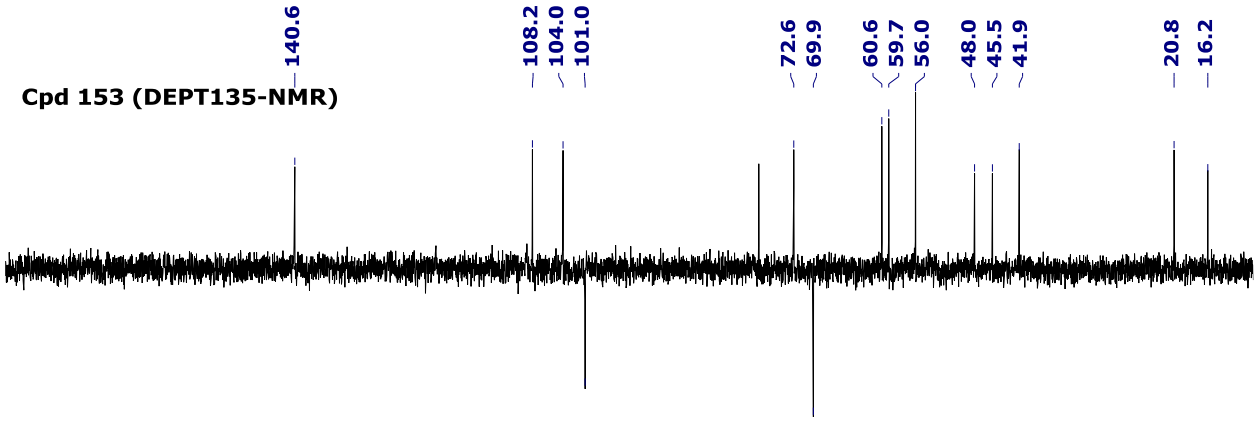
140.6
108.2
104.0
101.0
72.6
69.9
60.6
59.7
56.0
48.0
45.5
41.9
20.8
16.2
Cpd 153 (DEPT135-NMR)

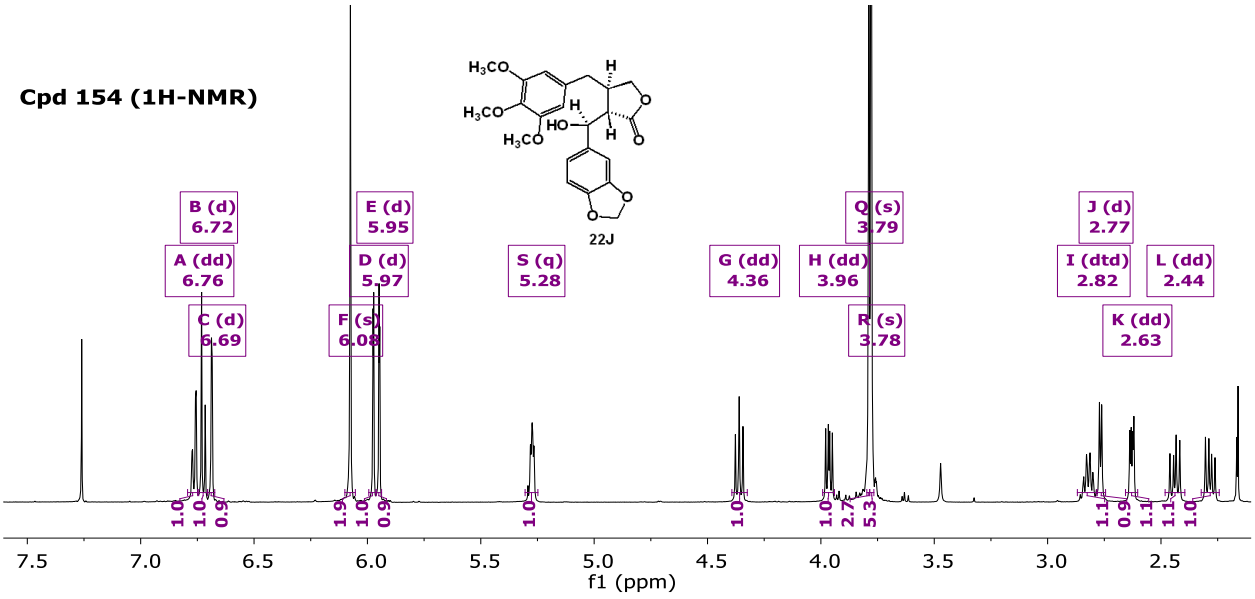
Cpd 154 (1H-NMR)
22J
B (d) 6.72
A (dd) 6.76
C (d) 6.69
E (d) 5.95
D (d) 5.97
F (s) 6.08
S (q) 5.28
G (dd) 4.36
H (dd) 3.96
Q (s) 3.79
R (s) 3.78
J (d) 2.77
I (dtd) 2.82
L (dd) 2.44
K (dd) 2.63
1.0 1.0 0.9 1.9 1.0 0.9 1.0 1.0 2.7 5.3 1.1 0.9 1.1 1.1 1.0
7.5 7.0 6.5 6.0 5.5 5.0 4.5 4.0 3.5 3.0 2.5
f1 (ppm)

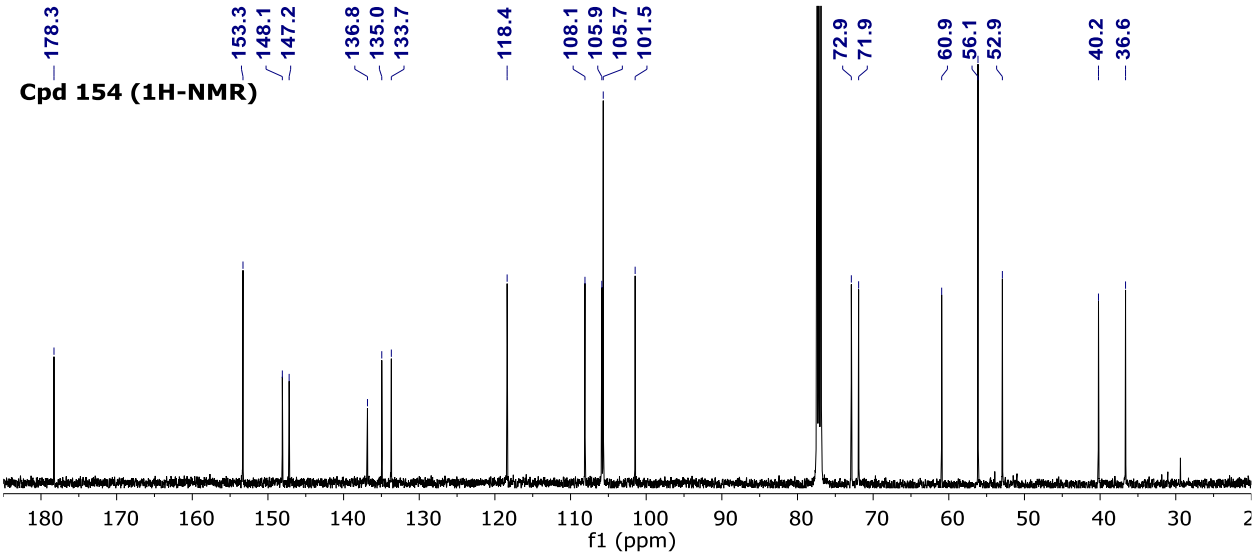
Cpd 154 (1H-NMR)
178.3
153.3 148.1 147.2
136.8 135.0 133.7
118.4
108.1 105.9 105.7 101.5
72.9 71.9
60.9 56.1 52.9
40.2 36.6
180 170 160 150 140 130 120 110 100 90 80 70 60 50 40 30
f1 (ppm)

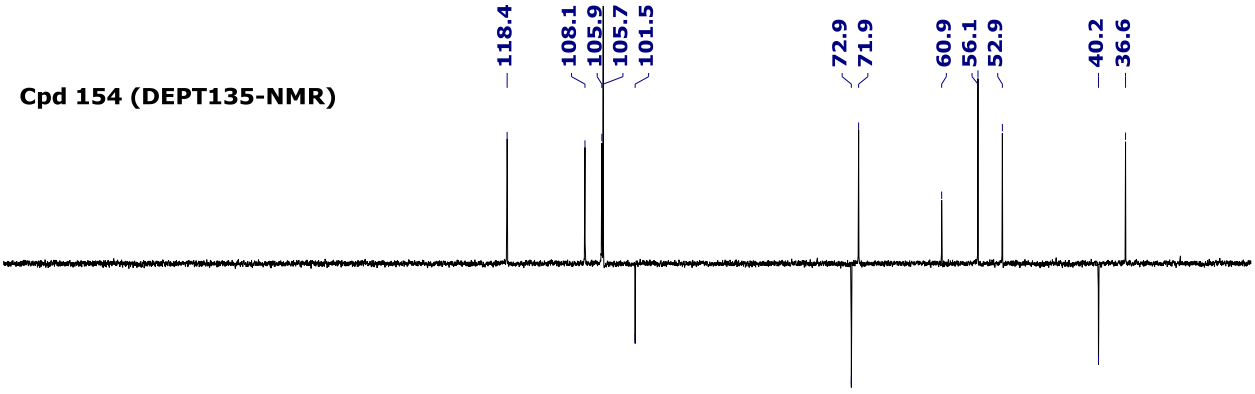
Cpd 154 (DEPT135-NMR)
118.4
108.1 105.9 105.7 101.5
72.9 71.9
60.9 56.1 52.9
40.2 36.6

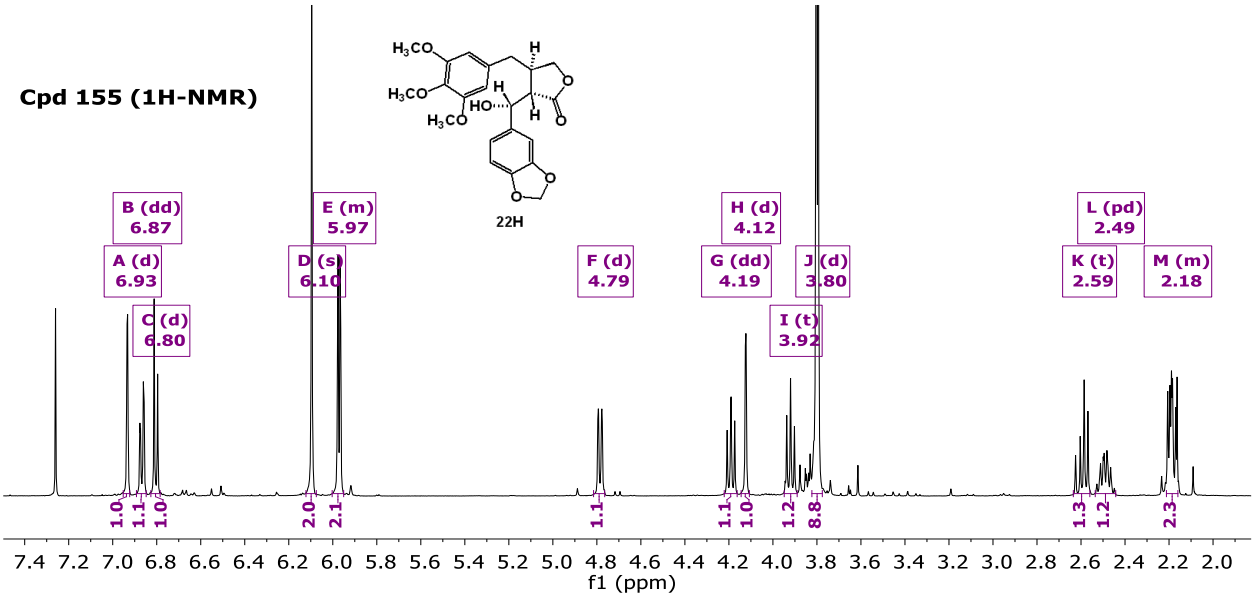
Cpd 155 (1H-NMR)
22H
B (dd) 6.87
A (d) 6.93
C (d) 6.80
E (m) 5.97
D (s) 6.10
F (d) 4.79
H (d) 4.12
G (dd) 4.19
J (d) 3.80
I (t) 3.92
L (pd) 2.49
K (t) 2.59
M (m) 2.18
1.0
1.1
1.0
2.0
2.1
1.1
1.1
1.0
1.2
8.8
1.3
1.2
2.3
7.4 7.2 7.0 6.8 6.6 6.4 6.2 6.0 5.8 5.6 5.4 5.2 5.0 4.8 4.6 4.4 4.2 4.0 3.8 3.6 3.4 3.2 3.0 2.8 2.6 2.4 2.2 2.0
f1 (ppm)

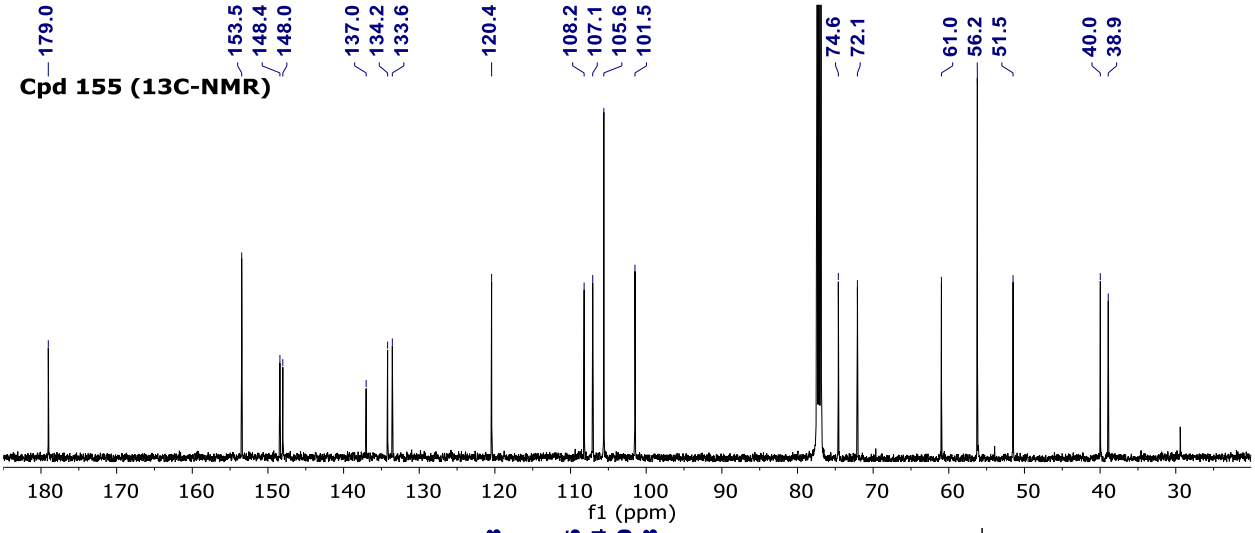
Cpd 155 (13C-NMR)
179.0
153.5
148.4
148.0
137.0
134.2
133.6
120.4
108.2
107.1
105.6
101.5
74.6
72.1
61.0
56.2
51.5
40.0
38.9
180 170 160 150 140 130 120 110 100 90 80 70 60 50 40 30
f1 (ppm)

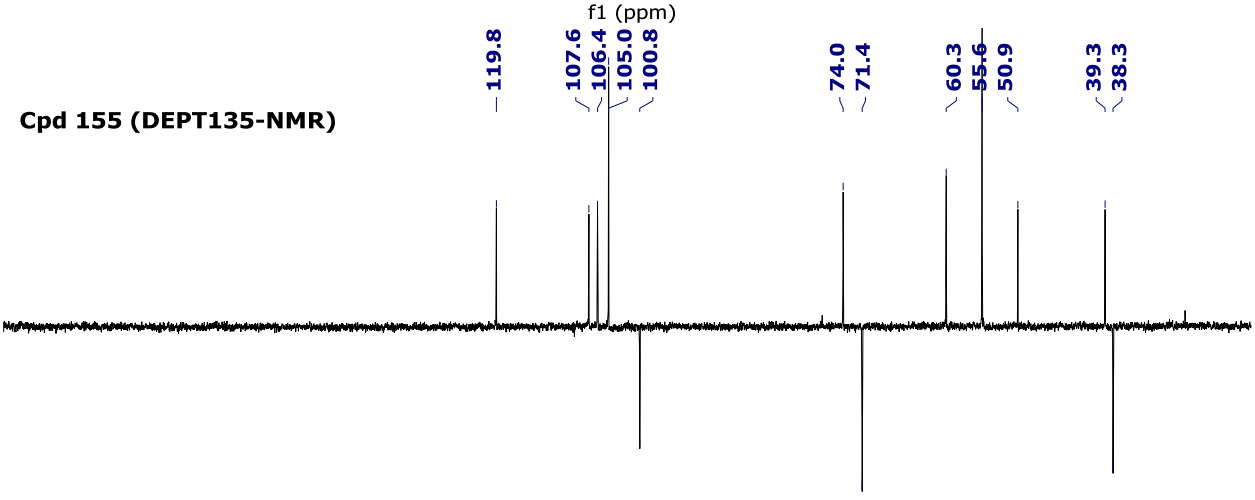
Cpd 155 (DEPT135-NMR)
119.8
107.6
106.4
105.0
100.8
74.0
71.4
60.3
55.6
50.9
39.3
38.3

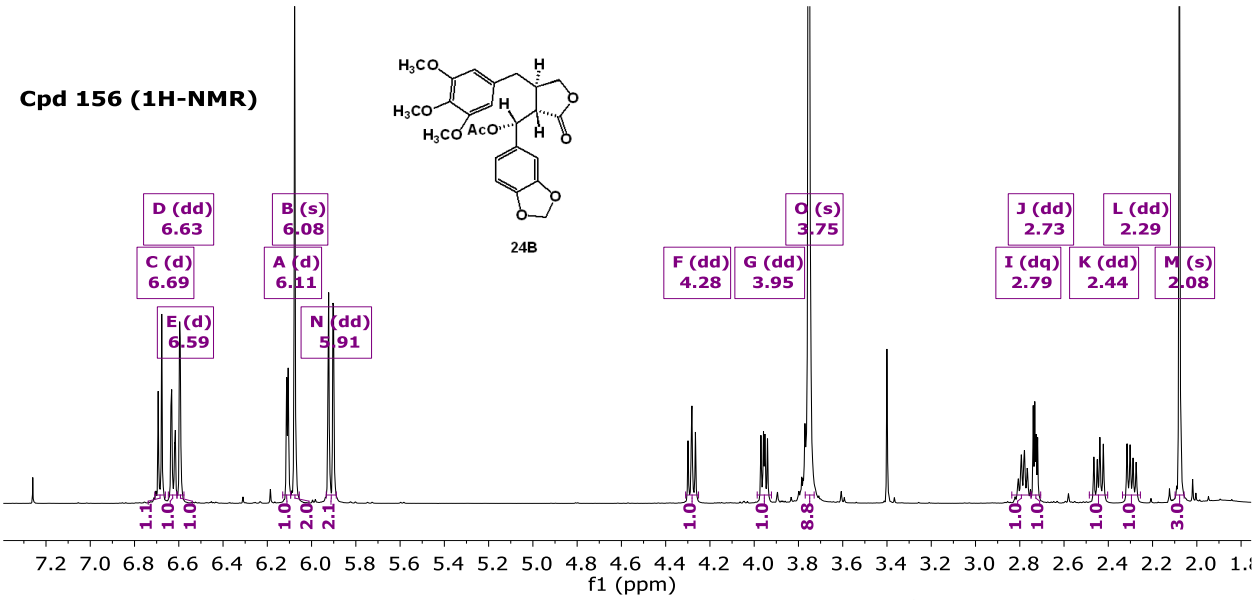
Cpd 156 (1H-NMR)
24B
D (dd) 6.63
C (d) 6.69
E (d) 6.59
B (s) 6.08
A (d) 6.11
N (dd) 5.91
F (dd) 4.28
G (dd) 3.95
O (s) 3.75
J (dd) 2.73
I (dq) 2.79
K (dd) 2.44
L (dd) 2.29
M (s) 2.08
f1 (ppm)

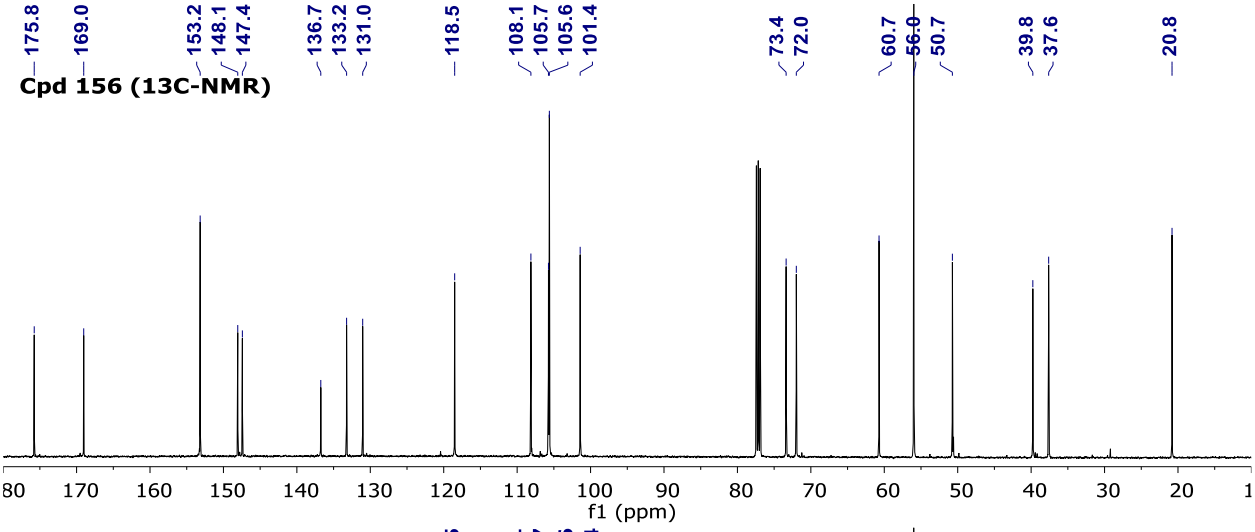
Cpd 156 (13C-NMR)
175.8
169.0
153.2
148.1
147.4
136.7
133.2
131.0
118.5
108.1
105.7
105.6
101.4
73.4
72.0
60.7
56.0
50.7
39.8
37.6
20.8
f1 (ppm)

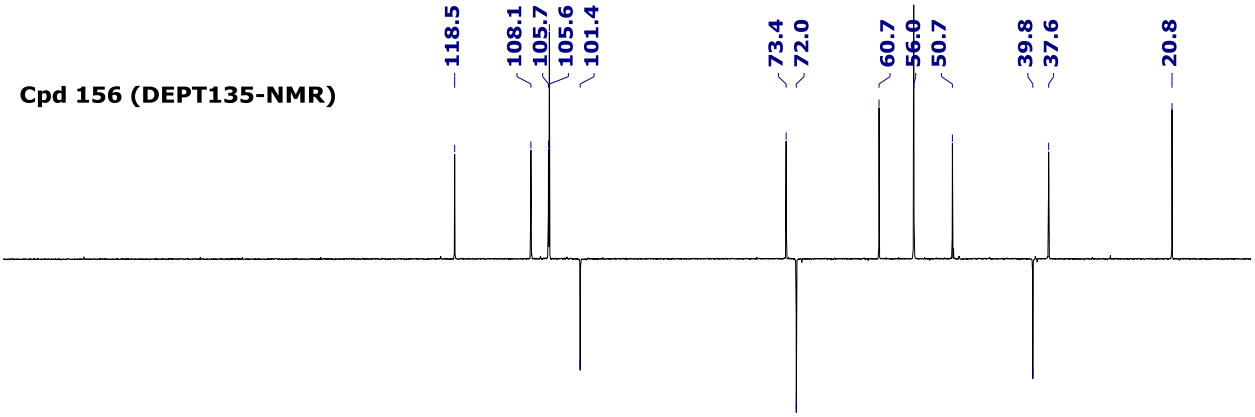
Cpd 156 (DEPT135-NMR)
118.5
108.1
105.7
105.6
101.4
73.4
72.0
60.7
56.0
50.7
39.8
37.6
20.8

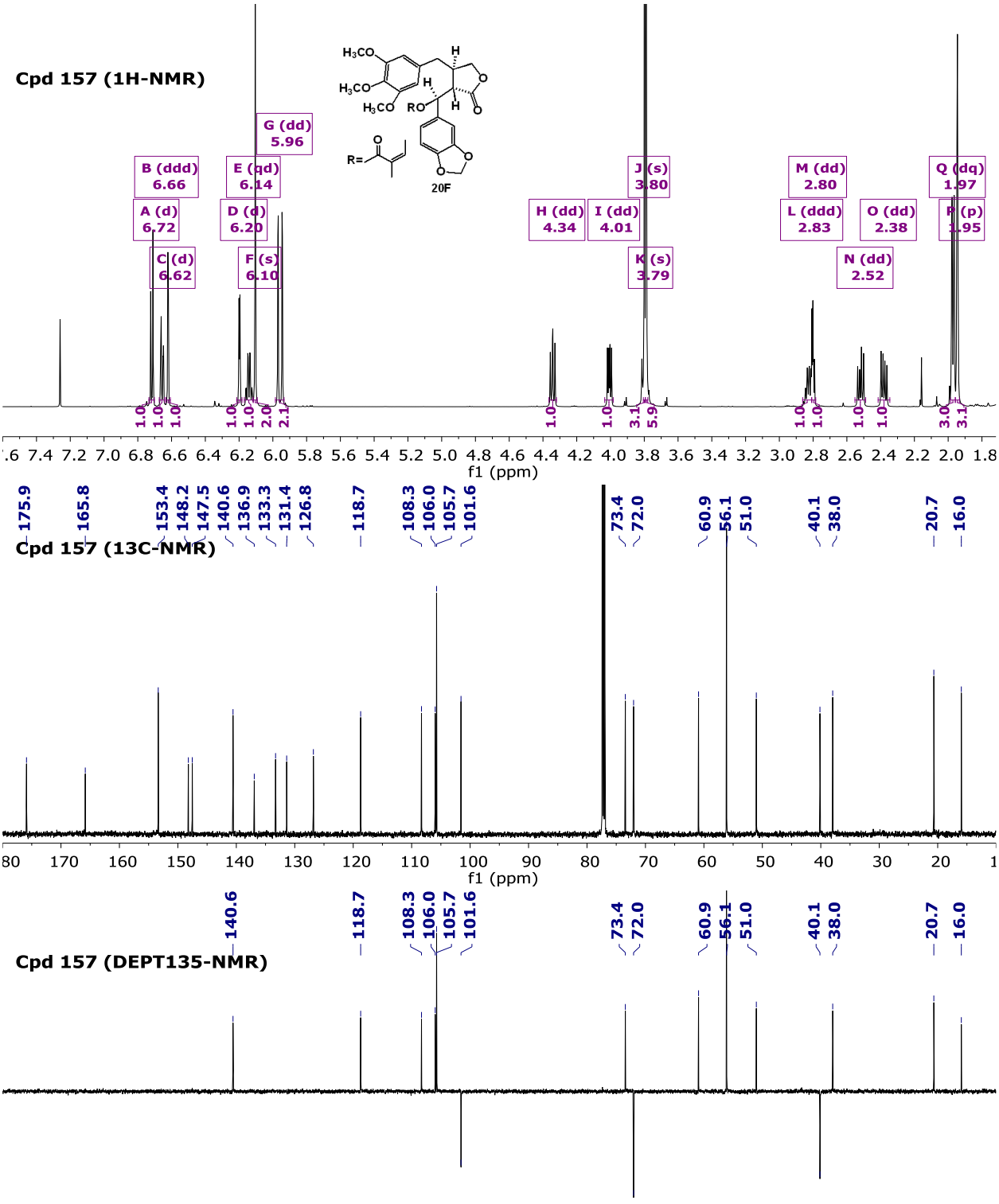
Cpd 157 (1H-NMR)
20F
A (d) 6.72
B (ddd) 6.66
C (d) 6.62
D (d) 6.20
E (qd) 6.14
F (s) 6.10
G (dd) 5.96
H (dd) 4.34
I (dd) 4.01
J (s) 3.80
K (s) 3.79
L (ddd) 2.83
M (dd) 2.80
N (dd) 2.52
O (dd) 2.38
Q (dq) 1.97
f1 (ppm)
Cpd 157 (13C-NMR)
175.9
165.8
153.4
148.2
147.5
140.6
136.9
133.3
131.4
126.8
118.7
108.3
106.0
105.7
101.6
73.4
72.0
60.9
56.1
51.0
40.1
38.0
20.7
16.0
f1 (ppm)
Cpd 157 (DEPT135-NMR)
140.6
118.7
108.3
106.0
105.7
101.6
73.4
72.0
60.9
56.1
51.0
40.1
38.0
20.7
16.0

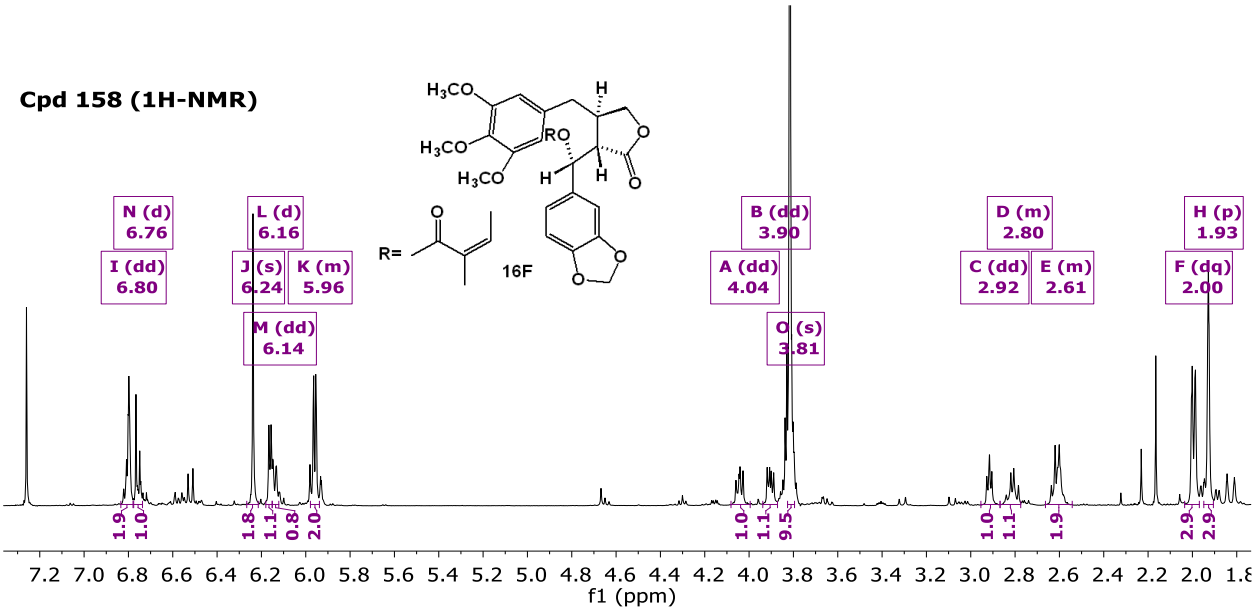
Cpd 158 (1H-NMR)
N (d) 6.76
I (dd) 6.80
L (d) 6.16
J (s) 6.24
K (m) 5.96
M (dd) 6.14
B (dd) 3.90
A (dd) 4.04
O (s) 3.81
D (m) 2.80
C (dd) 2.92
E (m) 2.61
H (p) 1.93
F (dq) 2.00
R=
16F
f1 (ppm)

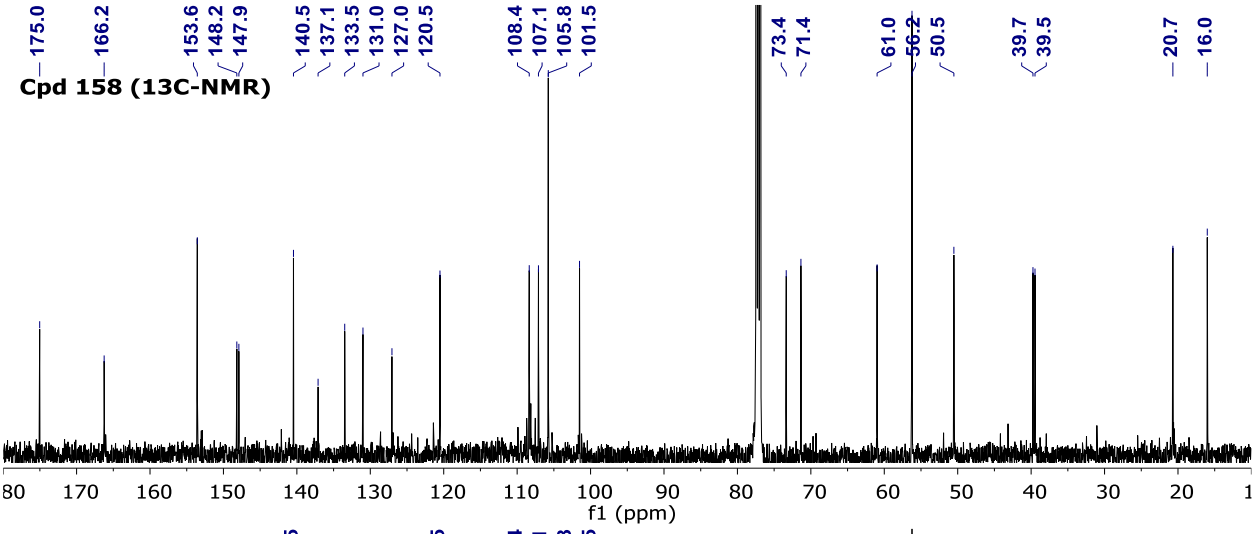
Cpd 158 (13C-NMR)
175.0
166.2
153.6
148.2
147.9
140.5
137.1
133.5
131.0
127.0
120.5
108.4
107.1
105.8
101.5
73.4
71.4
61.0
56.2
50.5
39.7
39.5
20.7
16.0
f1 (ppm)

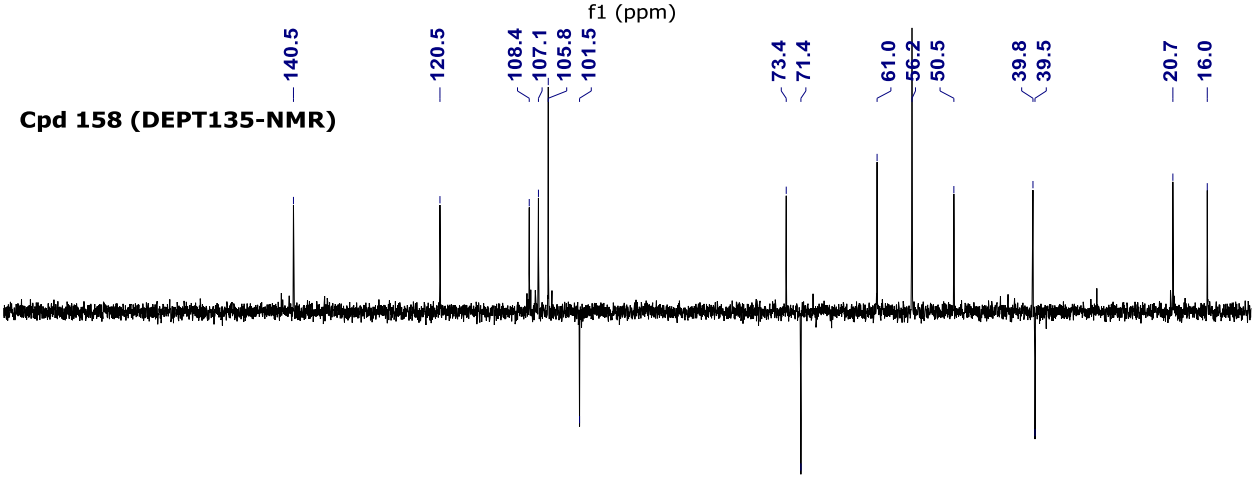
Cpd 158 (DEPT135-NMR)
140.5
120.5
108.4
107.1
105.8
101.5
73.4
71.4
61.0
56.2
50.5
39.8
39.5
20.7
16.0

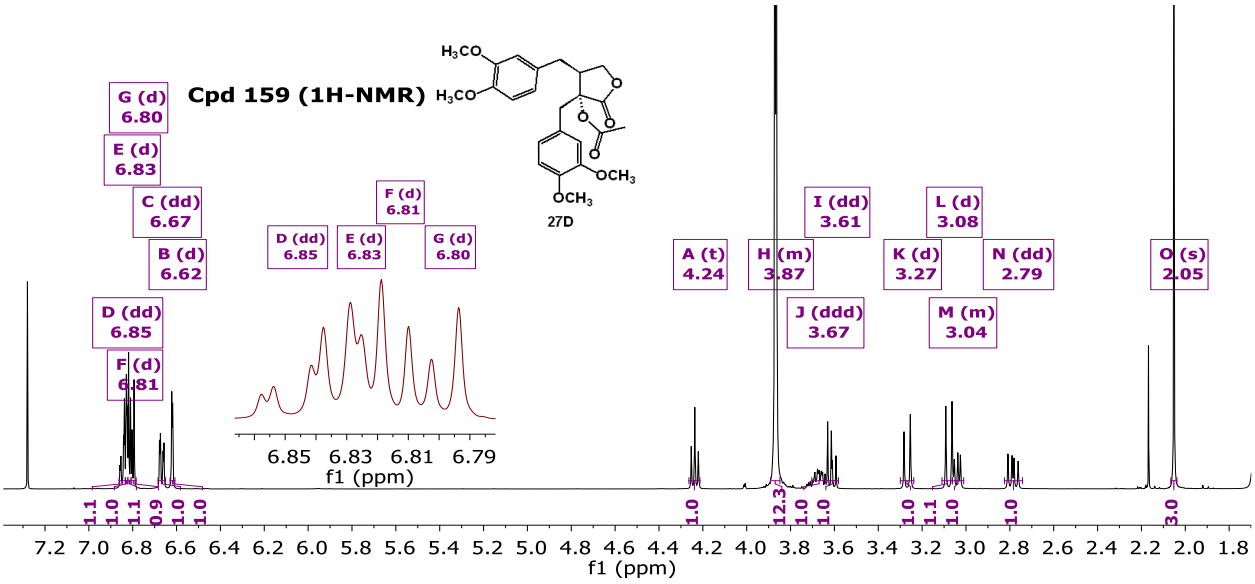
Cpd 159 (1H-NMR)
27D
G (d) 6.80
E (d) 6.83
C (dd) 6.67
B (d) 6.62
D (dd) 6.85
F (d) 6.81
A (t) 4.24
H (m) 3.87
I (dd) 3.61
J (ddd) 3.67
K (d) 3.27
L (d) 3.08
M (m) 3.04
N (dd) 2.79
O (s) 2.05
f1 (ppm)

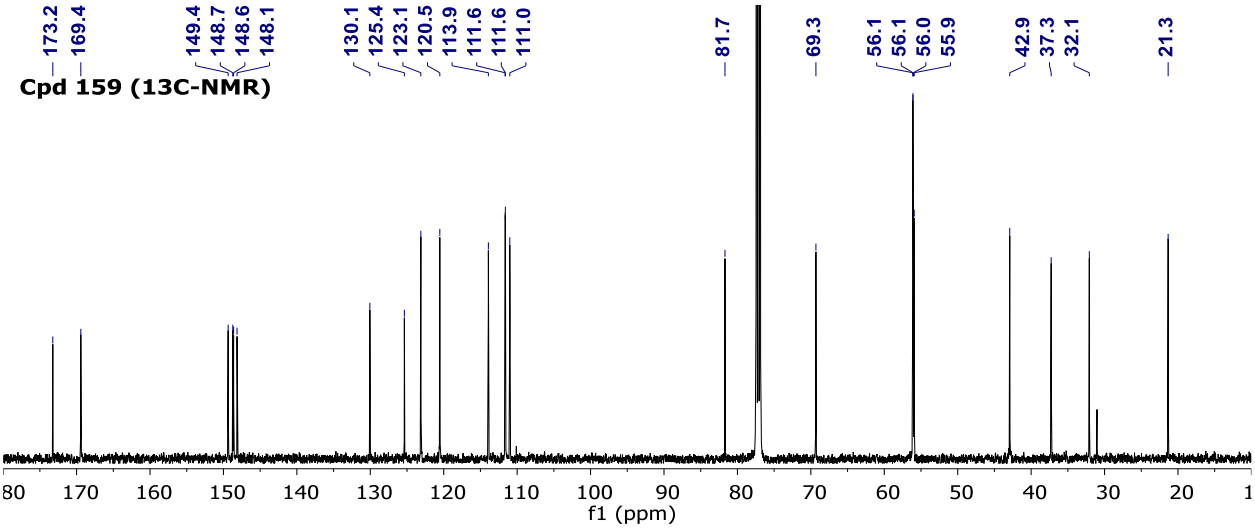
Cpd 159 (13C-NMR)
173.2
169.4
149.4
148.7
148.6
148.1
130.1
125.4
123.1
120.5
113.9
111.6
111.6
111.0
81.7
69.3
56.1
56.1
56.0
55.9
42.9
37.3
32.1
21.3
f1 (ppm)

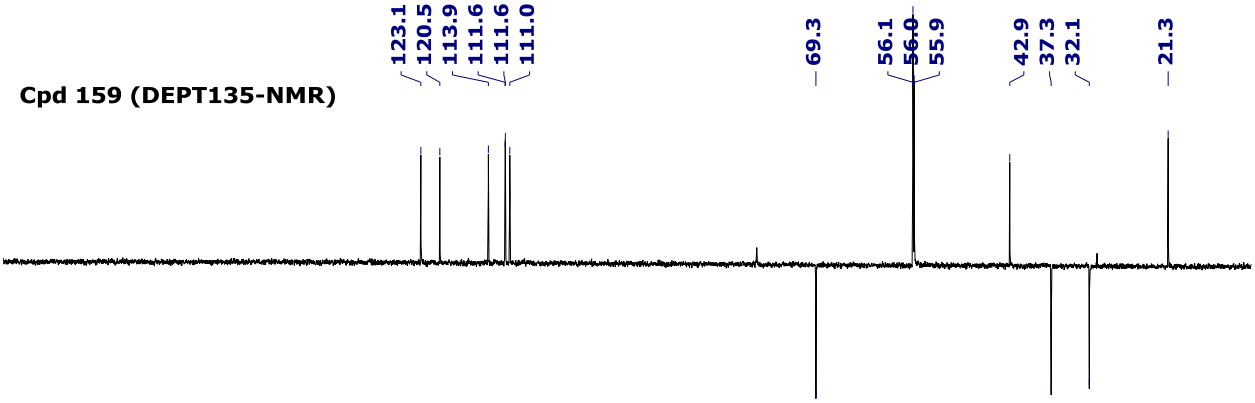
Cpd 159 (DEPT135-NMR)
123.1
120.5
113.9
111.6
111.6
111.0
69.3
56.1
56.0
55.9
42.9
37.3
32.1
21.3

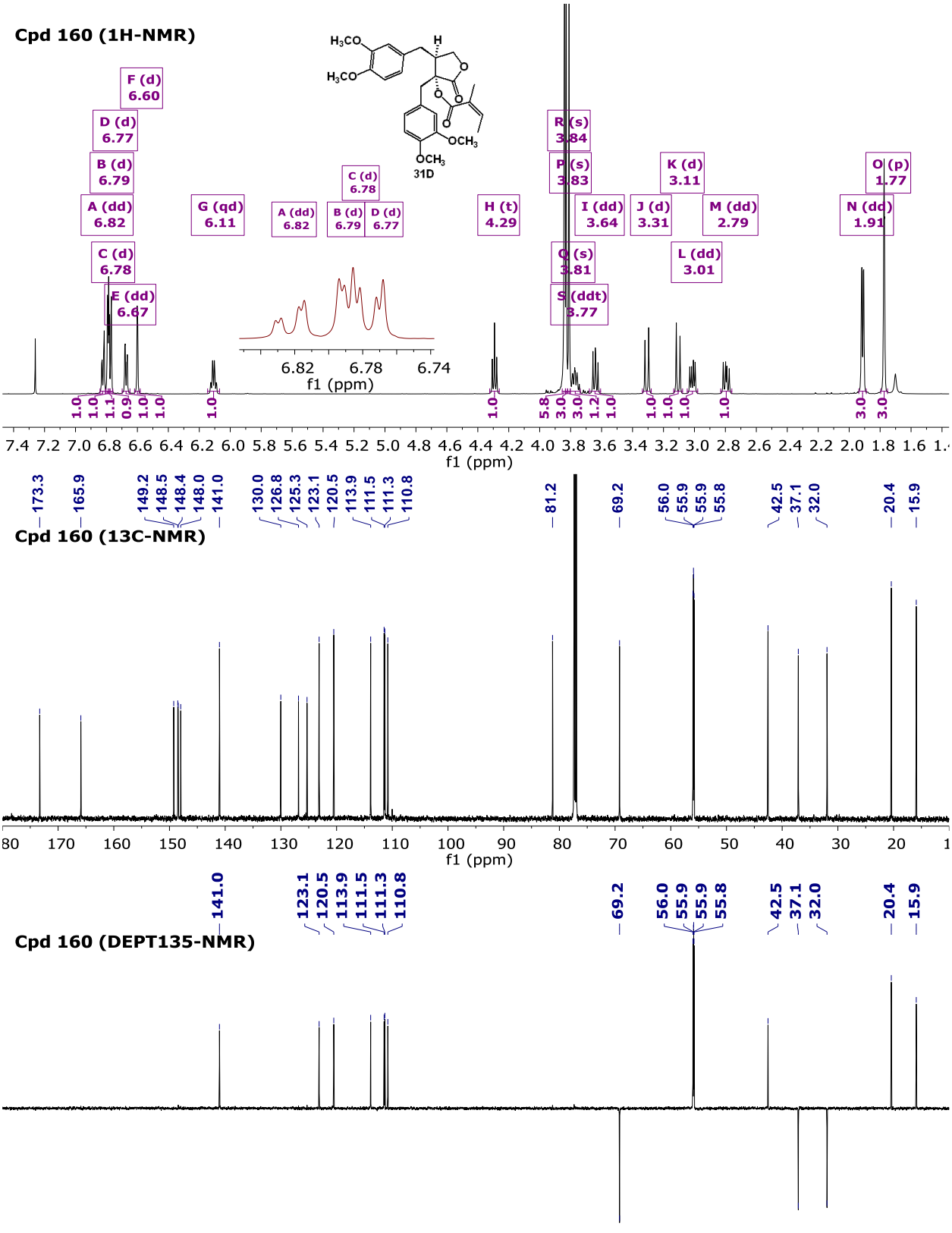
Cpd 160 (1H-NMR)
F (d) 6.60
D (d) 6.77
B (d) 6.79
A (dd) 6.82
C (d) 6.78
E (dd) 6.67
G (qq) 6.11
A (dd) 6.82
C (d) 6.78
B (d) 6.79
D (d) 6.77
H (t) 4.29
R (s) 3.84
P (s) 3.83
I (dd) 3.64
Q (s) 3.81
S (ddt) 3.77
J (d) 3.31
K (d) 3.11
L (dd) 3.01
M (dd) 2.79
O (p) 1.77
N (dd) 1.91
31D
6.82 6.78 6.74
f1 (ppm)
7.4 7.2 7.0 6.8 6.6 6.4 6.2 6.0 5.8 5.6 5.4 5.2 5.0 4.8 4.6 4.4 4.2 4.0 3.8 3.6 3.4 3.2 3.0 2.8 2.6 2.4 2.2 2.0 1.8 1.6
f1 (ppm)
Cpd 160 (13C-NMR)
173.3 165.9 149.2 148.5 148.4 148.0 141.0 130.0 126.8 125.3 123.1 120.5 113.9 111.5 111.3 110.8 81.2 69.2 56.0 55.9 55.9 55.8 42.5 37.1 32.0 20.4 15.9
80 170 160 150 140 130 120 110 100 90 80 70 60 50 40 30 20
f1 (ppm)
Cpd 160 (DEPT135-NMR)
141.0 123.1 120.5 113.9 111.5 111.3 110.8 69.2 56.0 55.9 55.9 55.8 42.5 37.1 32.0 20.4 15.9

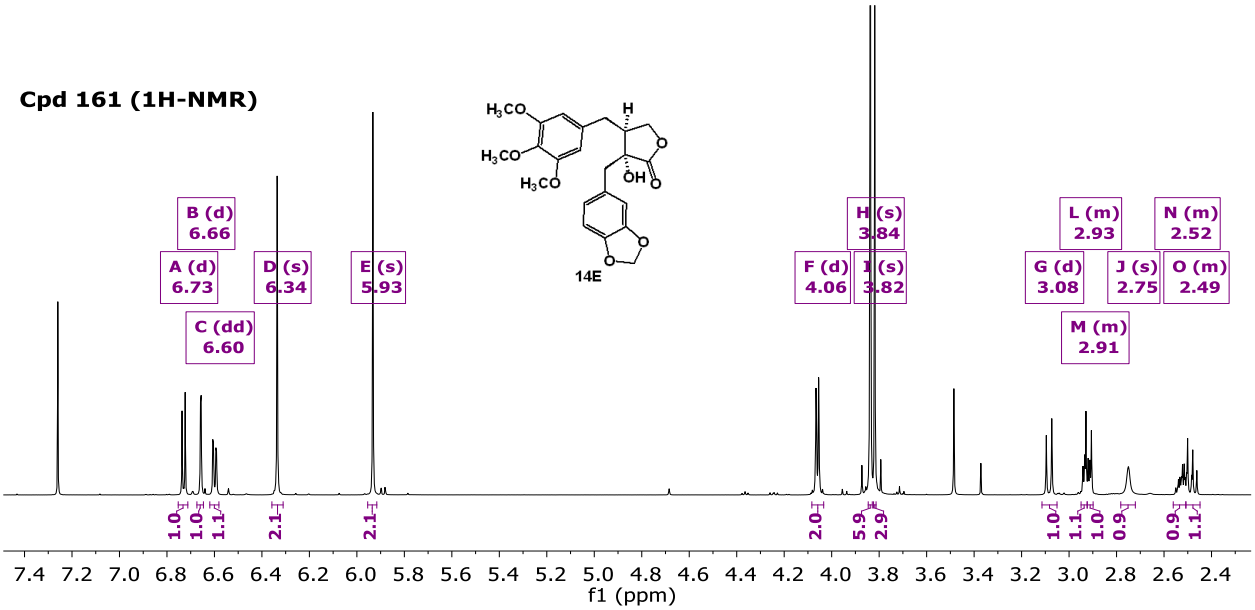
Cpd 161 (1H-NMR)
14E
B (d) 6.66
A (d) 6.73
C (dd) 6.60
D (s) 6.34
E (s) 5.93
F (d) 4.06
H (s) 3.84
I (s) 3.82
G (d) 3.08
L (m) 2.93
M (m) 2.91
J (s) 2.75
N (m) 2.52
O (m) 2.49
f1 (ppm)

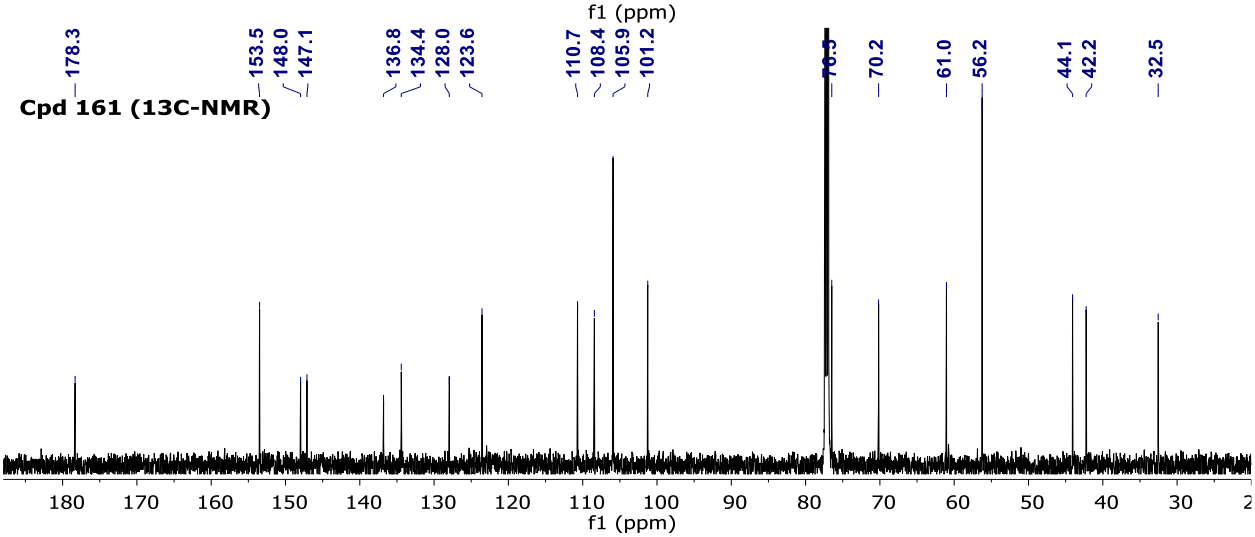
Cpd 161 (13C-NMR)
178.3
153.5
148.0
147.1
136.8
134.4
128.0
123.6
110.7
108.4
105.9
101.2
70.3
70.2
61.0
56.2
44.1
42.2
32.5
f1 (ppm)

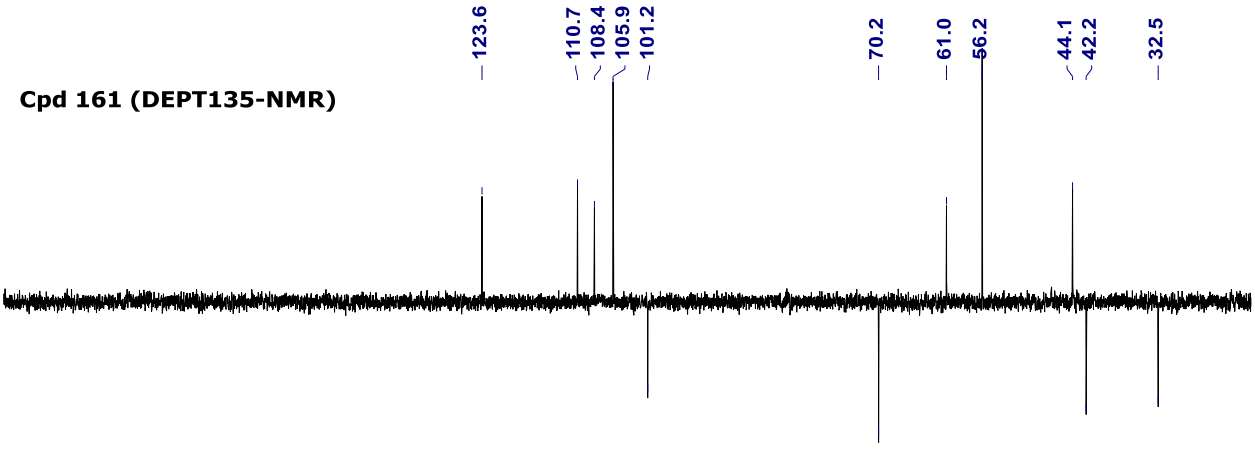
Cpd 161 (DEPT135-NMR)
123.6
110.7
108.4
105.9
101.2
70.2
61.0
56.2
44.1
42.2
32.5

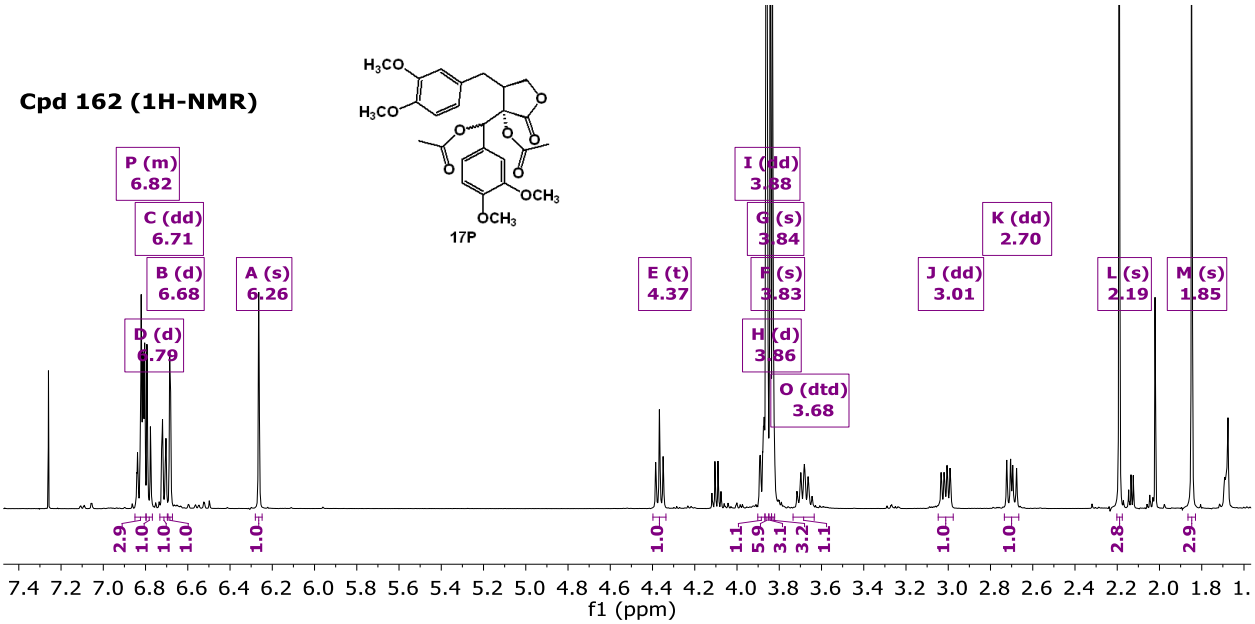
Cpd 162 (1H-NMR)
17P
P (m) 6.82
C (dd) 6.71
B (d) 6.68
D (d) 6.79
A (s) 6.26
E (t) 4.37
I (dd) 3.88
G (s) 3.84
F (s) 3.83
H (d) 3.86
O (dtd) 3.68
J (dd) 3.01
K (dd) 2.70
L (s) 2.19
M (s) 1.85
2.9 1.0 1.0 1.0 1.0 1.0 1.1 5.9 3.1 3.2 1.1 1.0 1.0 2.8 2.9
7.4 7.2 7.0 6.8 6.6 6.4 6.2 6.0 5.8 5.6 5.4 5.2 5.0 4.8 4.6 4.4 4.2 4.0 3.8 3.6 3.4 3.2 3.0 2.8 2.6 2.4 2.2 2.0 1.8 1.
f1 (ppm)

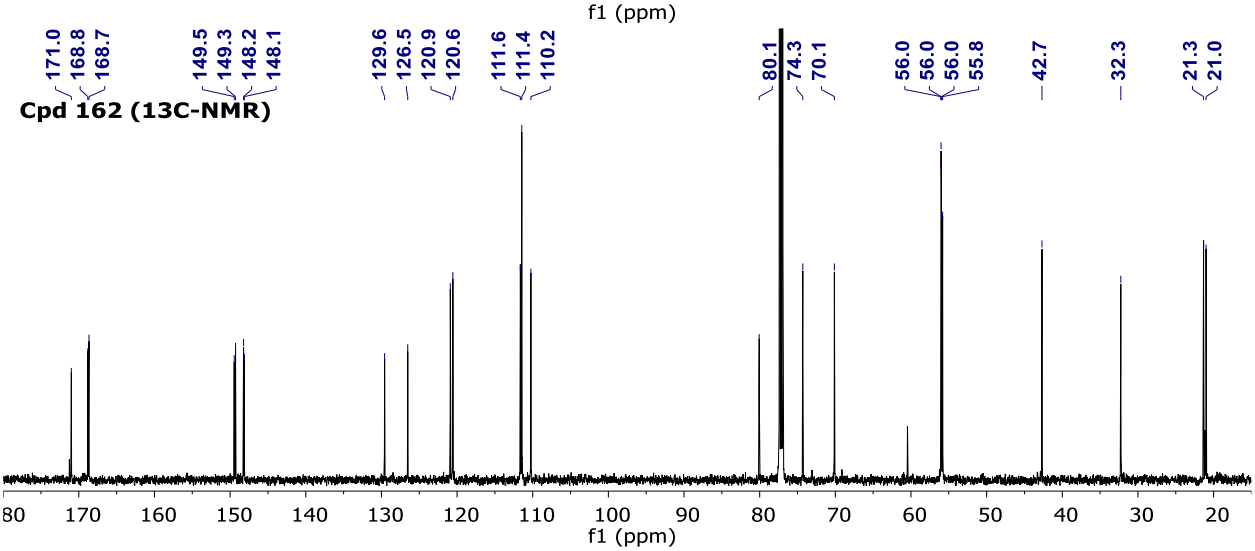
Cpd 162 (13C-NMR)
171.0 168.8 168.7 149.5 149.3 148.2 148.1 129.6 126.5 120.9 120.6 111.6 111.4 110.2 80.1 74.3 70.1 56.0 56.0 56.0 55.8 42.7 32.3 21.3 21.0
80 170 160 150 140 130 120 110 100 90 80 70 60 50 40 30 20
f1 (ppm)

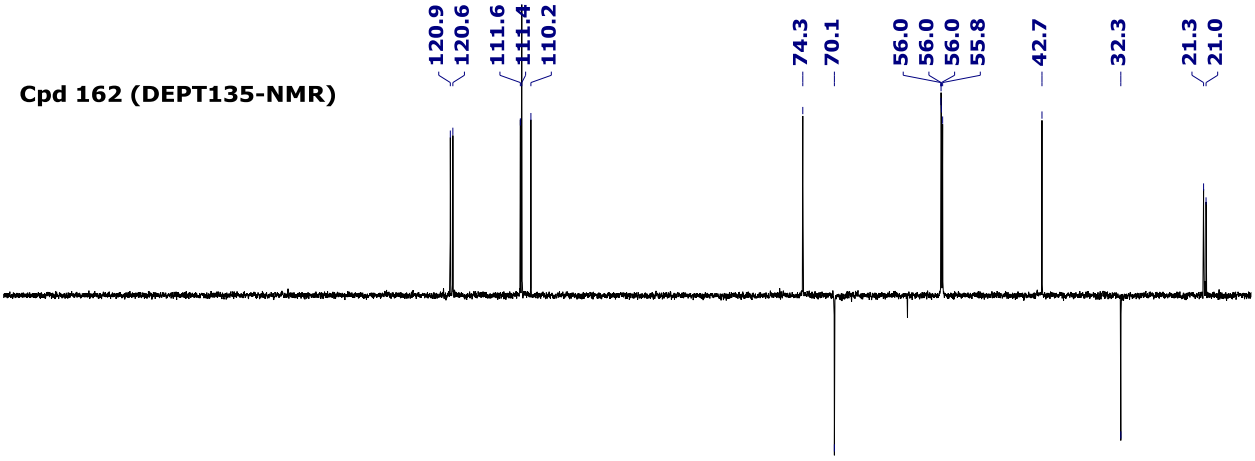
Cpd 162 (DEPT135-NMR)
120.9 120.6 111.6 111.4 110.2 74.3 70.1 56.0 56.0 56.0 55.8 42.7 32.3 21.3 21.0

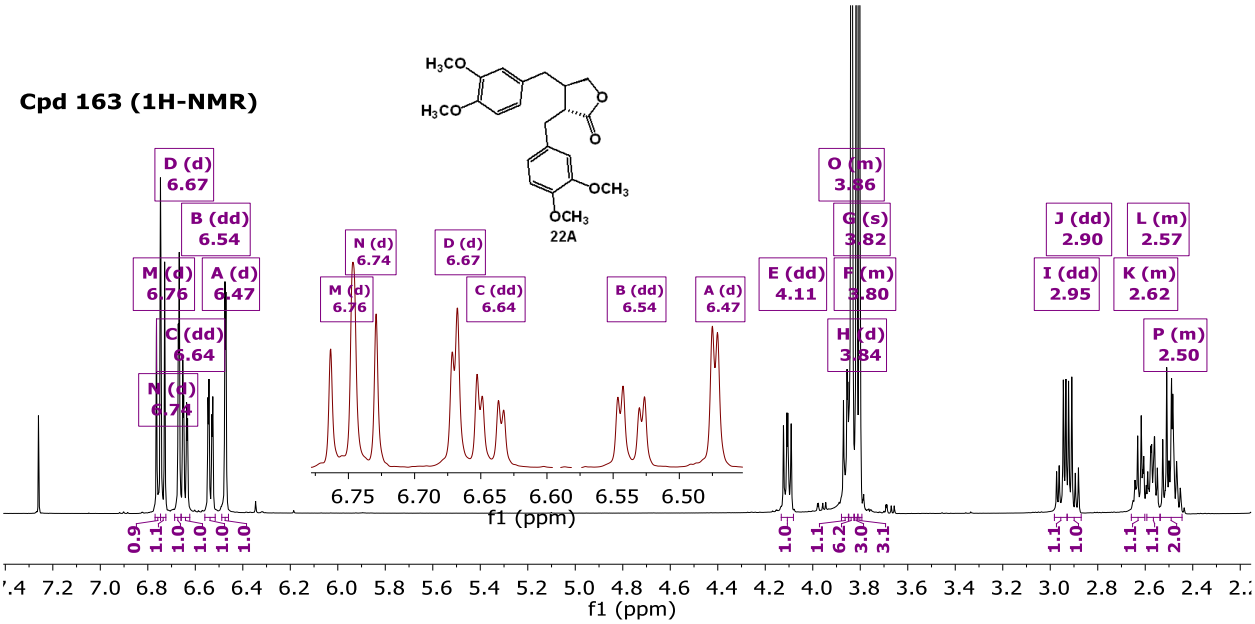
Cpd 163 (1H-NMR)
22A
D (d) 6.67
B (dd) 6.54
M (d) 6.76
A (d) 6.47
C (dd) 6.64
N (d) 6.74
O (m) 3.86
G (s) 3.82
E (dd) 4.11
F (m) 3.80
H (d) 3.84
J (dd) 2.90
L (m) 2.57
I (dd) 2.95
K (m) 2.62
P (m) 2.50
f1 (ppm)

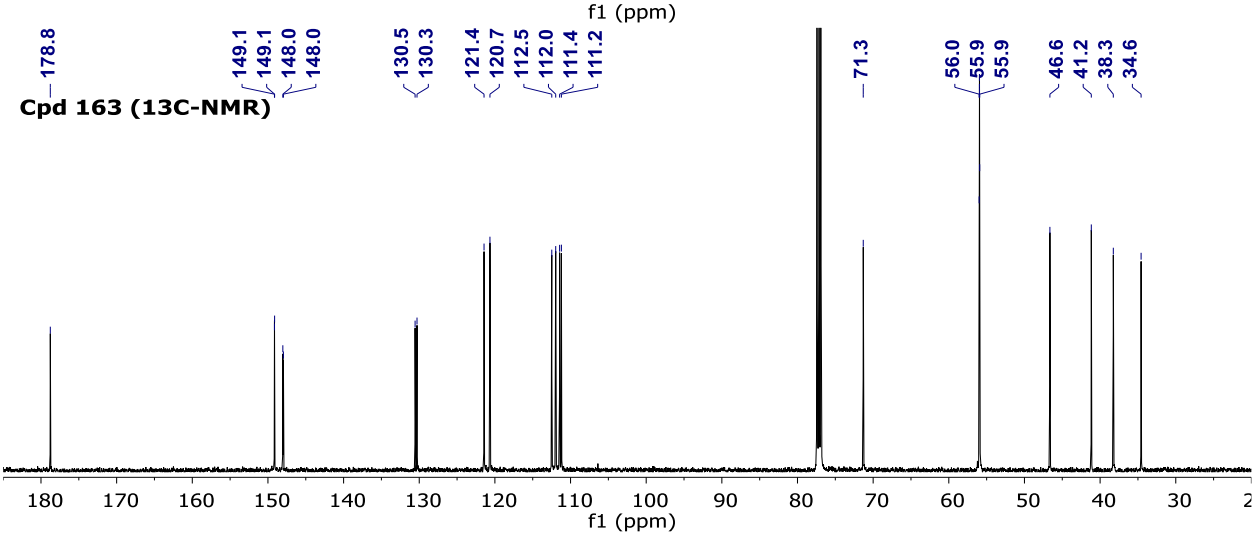
Cpd 163 (13C-NMR)
178.8
149.1
149.1
148.0
148.0
130.5
130.3
121.4
120.7
112.5
112.0
111.4
111.2
71.3
56.0
55.9
55.9
46.6
41.2
38.3
34.6
f1 (ppm)

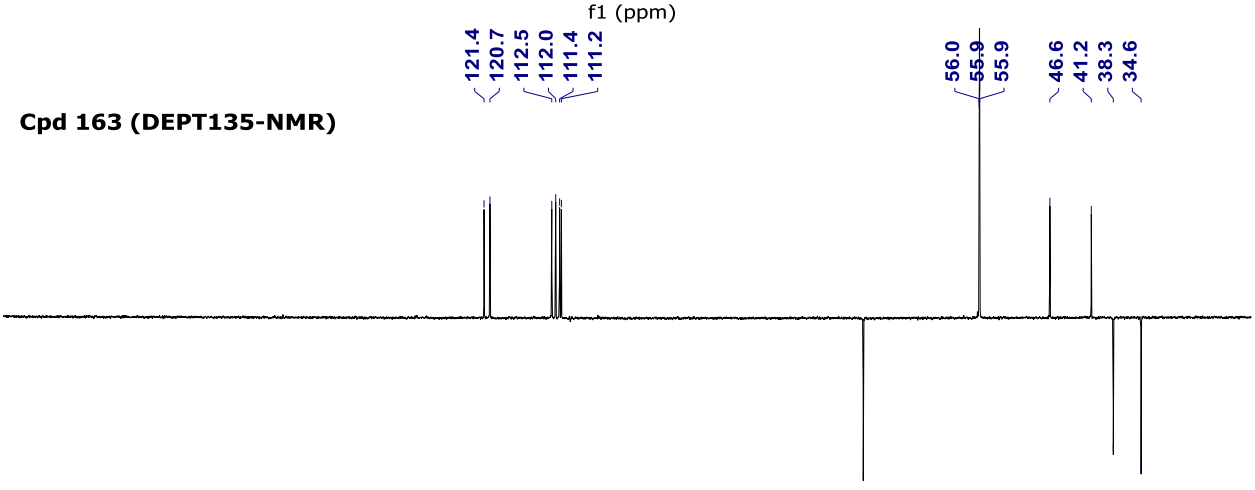
Cpd 163 (DEPT135-NMR)
121.4
120.7
112.5
112.0
111.4
111.2
56.0
55.9
55.9
46.6
41.2
38.3
34.6

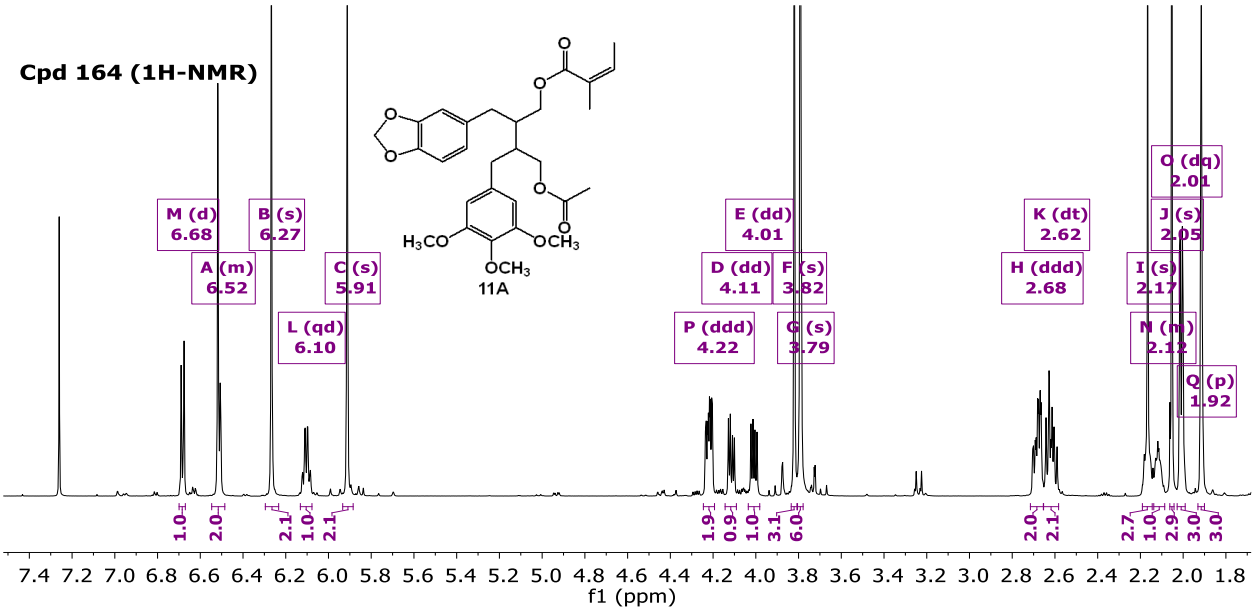
Cpd 164 (1H-NMR)
M (d) 6.68
B (s) 6.27
A (m) 6.52
C (s) 5.91
L (qd) 6.10
E (dd) 4.01
D (dd) 4.11
F (s) 3.82
P (ddd) 4.22
G (s) 3.79
K (dt) 2.62
H (ddd) 2.68
O (dq) 2.01
J (s) 2.05
I (s) 2.17
N (m) 2.12
Q (p) 1.92
11A
1.0 2.0 2.1 1.0 2.1 1.9 0.9 1.0 3.1 6.0 2.0 2.1 2.7 1.0 2.9 3.0 3.0
7.4 7.2 7.0 6.8 6.6 6.4 6.2 6.0 5.8 5.6 5.4 5.2 5.0 4.8 4.6 4.4 4.2 4.0 3.8 3.6 3.4 3.2 3.0 2.8 2.6 2.4 2.2 2.0 1.8
f1 (ppm)

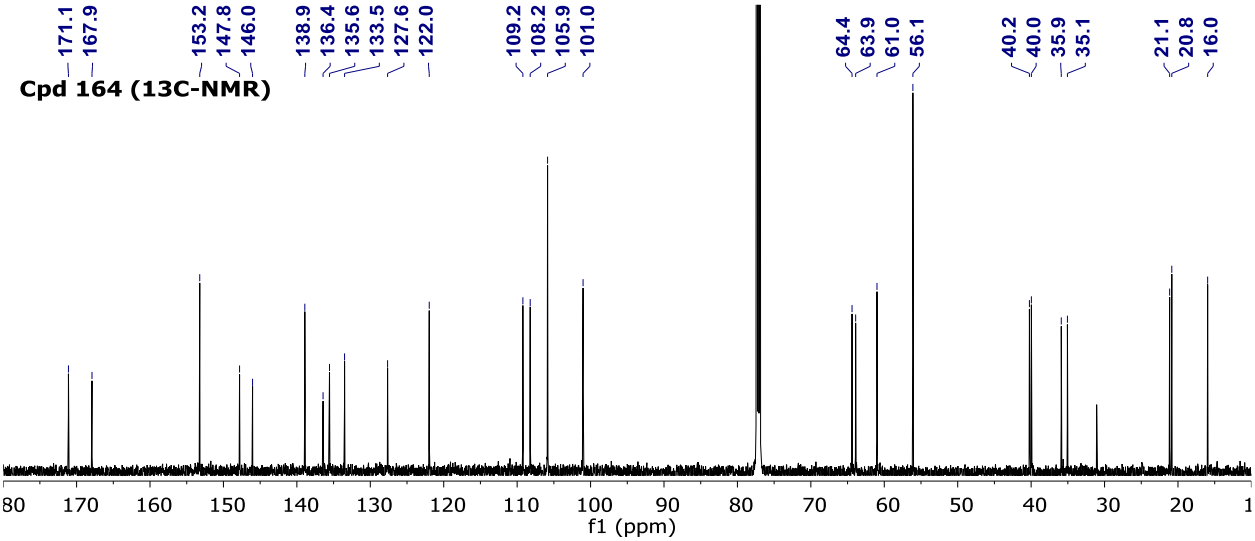
171.1 167.9 153.2 147.8 146.0 138.9 136.4 135.6 133.5 127.6 122.0 109.2 108.2 105.9 101.0 64.4 63.9 61.0 56.1 40.2 40.0 35.9 35.1 21.1 20.8 16.0
Cpd 164 (13C-NMR)
80 170 160 150 140 130 120 110 100 90 80 70 60 50 40 30 20 1
f1 (ppm)

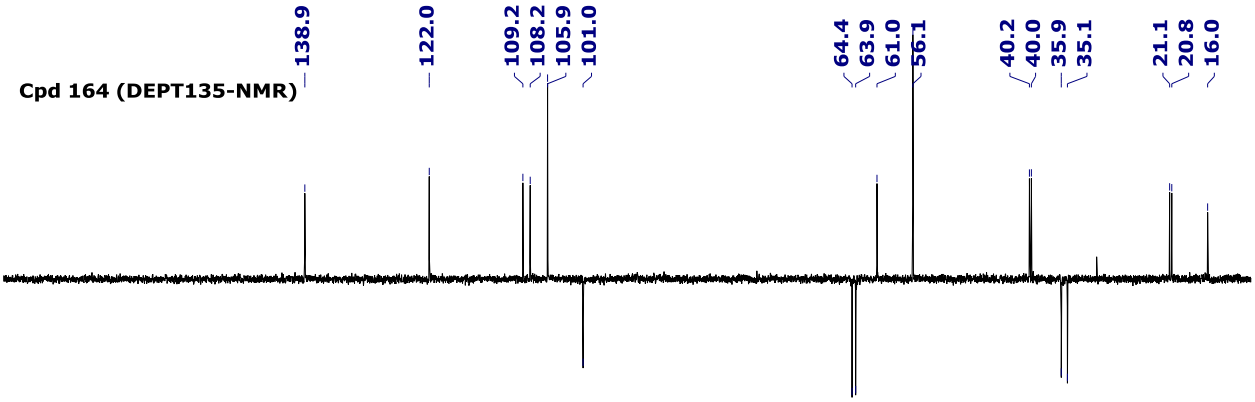
138.9 122.0 109.2 108.2 105.9 101.0 64.4 63.9 61.0 56.1 40.2 40.0 35.9 35.1 21.1 20.8 16.0
Cpd 164 (DEPT135-NMR)

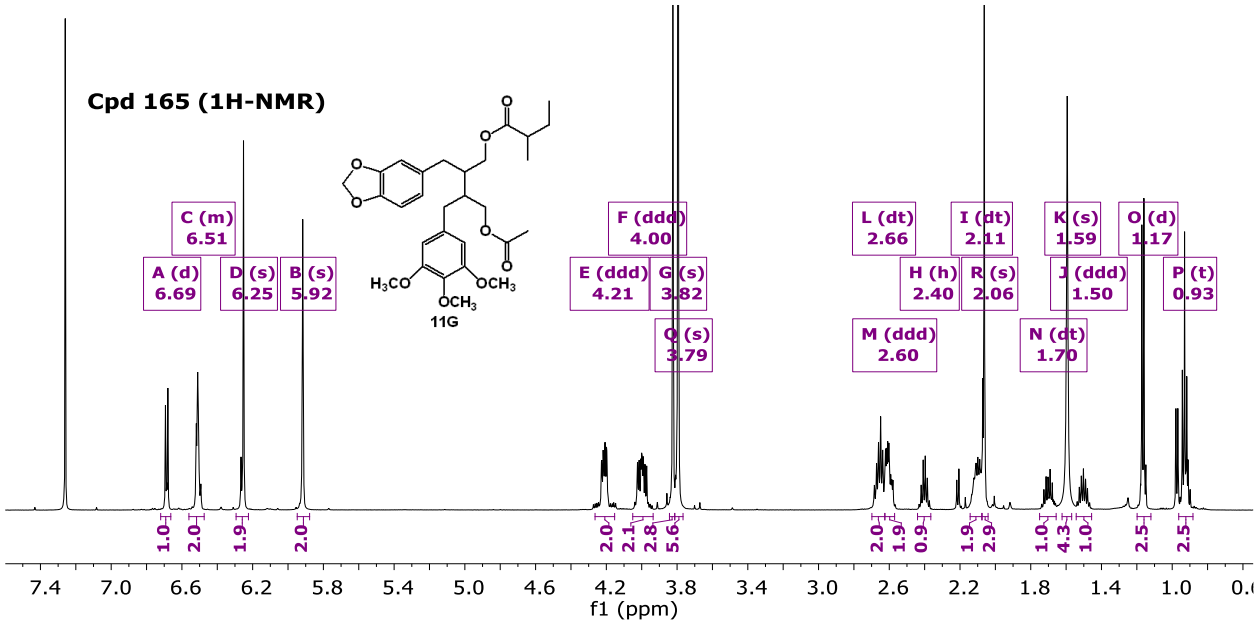
Cpd 165 (1H-NMR)
A (d) 6.69
B (s) 5.92
C (m) 6.51
D (s) 6.25
E (ddd) 4.21
F (ddd) 4.00
G (s) 3.82
H (h) 2.40
I (dt) 2.11
J (ddd) 1.50
K (s) 1.59
L (dt) 2.66
M (ddd) 2.60
N (dt) 1.70
O (d) 1.17
P (t) 0.93
Q (s) 3.79
R (s) 2.06
11G
f1 (ppm)

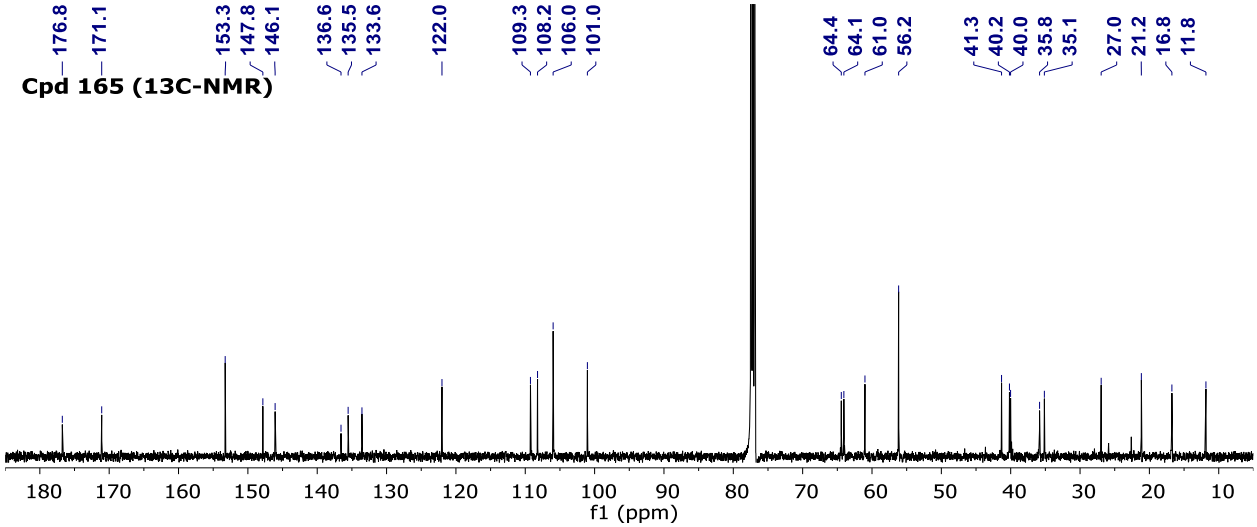
Cpd 165 (13C-NMR)
176.8
171.1
153.3
147.8
146.1
136.6
135.5
133.6
122.0
109.3
108.2
106.0
101.0
64.4
64.1
61.0
56.2
41.3
40.2
40.0
35.8
35.1
27.0
21.2
16.8
11.8
f1 (ppm)

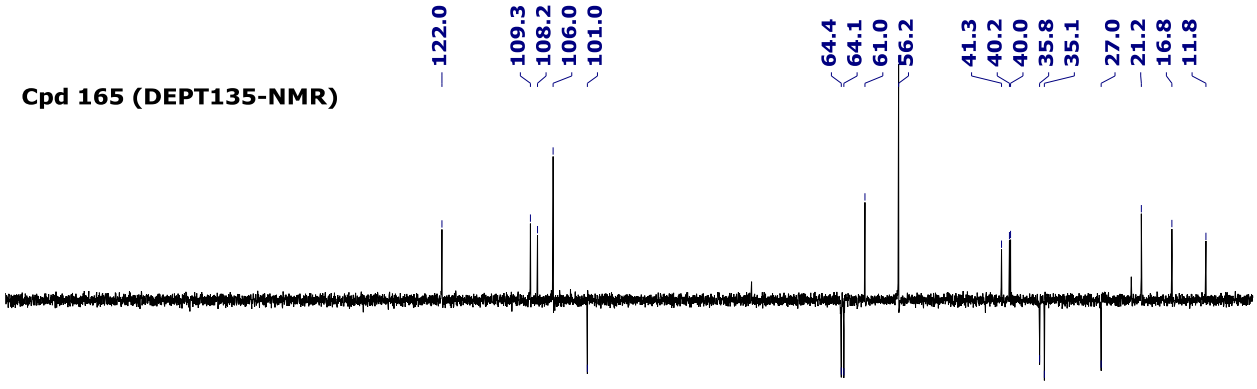
Cpd 165 (DEPT135-NMR)
122.0
109.3
108.2
106.0
101.0
64.4
64.1
61.0
56.2
41.3
40.2
40.0
35.8
35.1
27.0
21.2
16.8
11.8

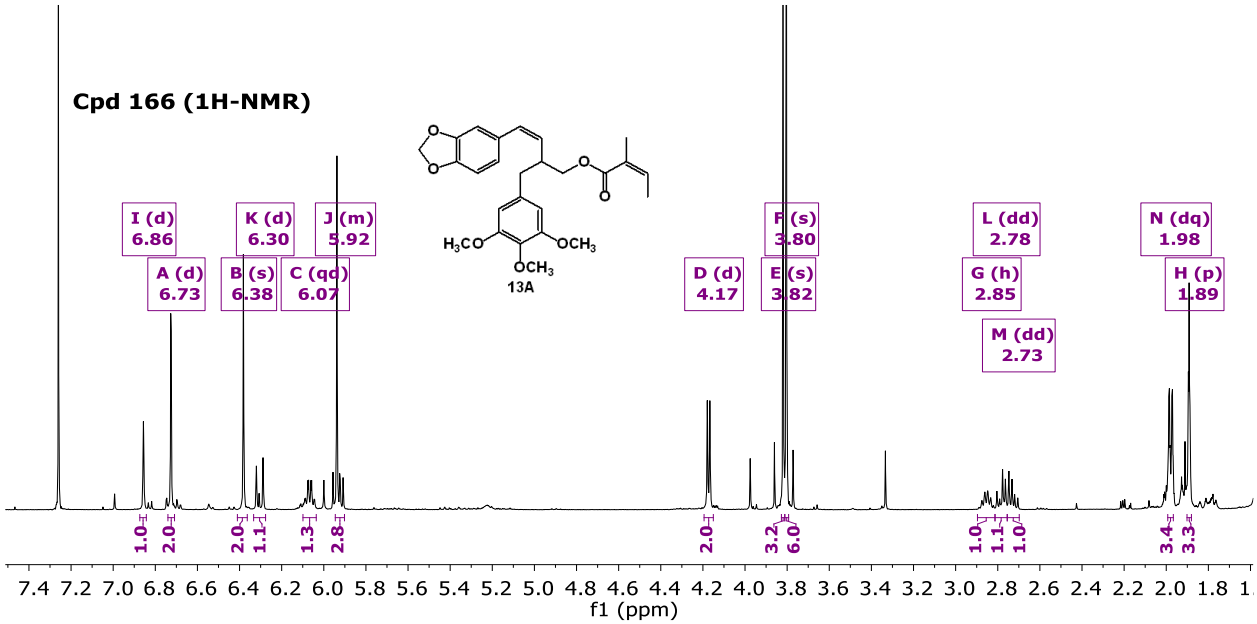
Cpd 166 (1H-NMR)
I (d) 6.86
A (d) 6.73
K (d) 6.30
B (s) 6.38
C (qd) 6.07
J (m) 5.92
D (d) 4.17
F (s) 3.80
E (s) 3.82
L (dd) 2.78
G (h) 2.85
M (dd) 2.73
N (dq) 1.98
H (p) 1.89
13A
1.0 2.0 2.0 1.1 1.3 2.8 2.0 3.2 6.0 1.0 1.1 1.0 3.4 3.3
7.4 7.2 7.0 6.8 6.6 6.4 6.2 6.0 5.8 5.6 5.4 5.2 5.0 4.8 4.6 4.4 4.2 4.0 3.8 3.6 3.4 3.2 3.0 2.8 2.6 2.4 2.2 2.0 1.8 1
f1 (ppm)

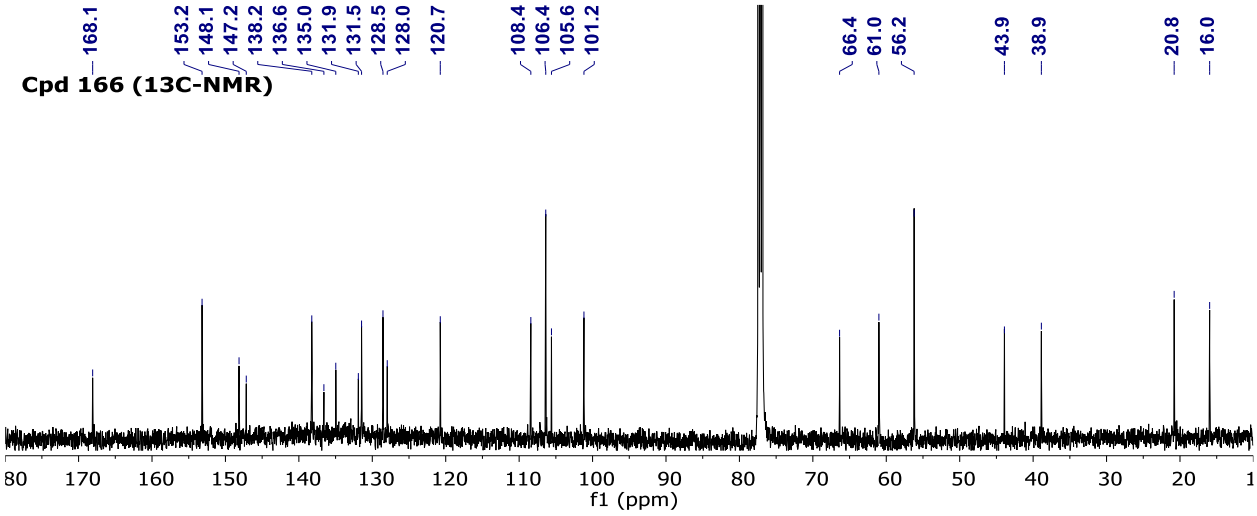
168.1
153.2 148.1 147.2 138.2 136.6 135.0 131.9 131.5 128.5 128.0 120.7
108.4 106.4 105.6 101.2
66.4 61.0 56.2
43.9 38.9
20.8 16.0
Cpd 166 (13C-NMR)
80 170 160 150 140 130 120 110 100 90 80 70 60 50 40 30 20 1
f1 (ppm)

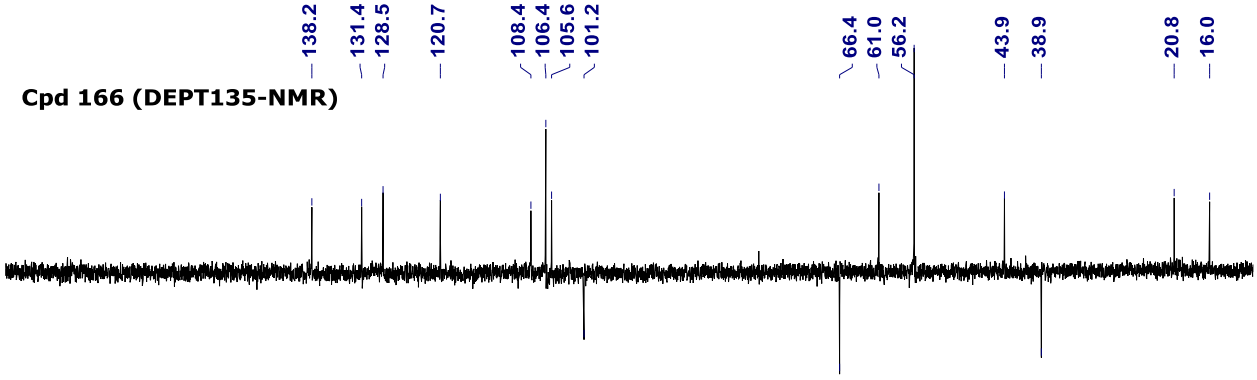
138.2 131.4 128.5 120.7
108.4 106.4 105.6 101.2
66.4 61.0 56.2
43.9 38.9
20.8 16.0
Cpd 166 (DEPT135-NMR)

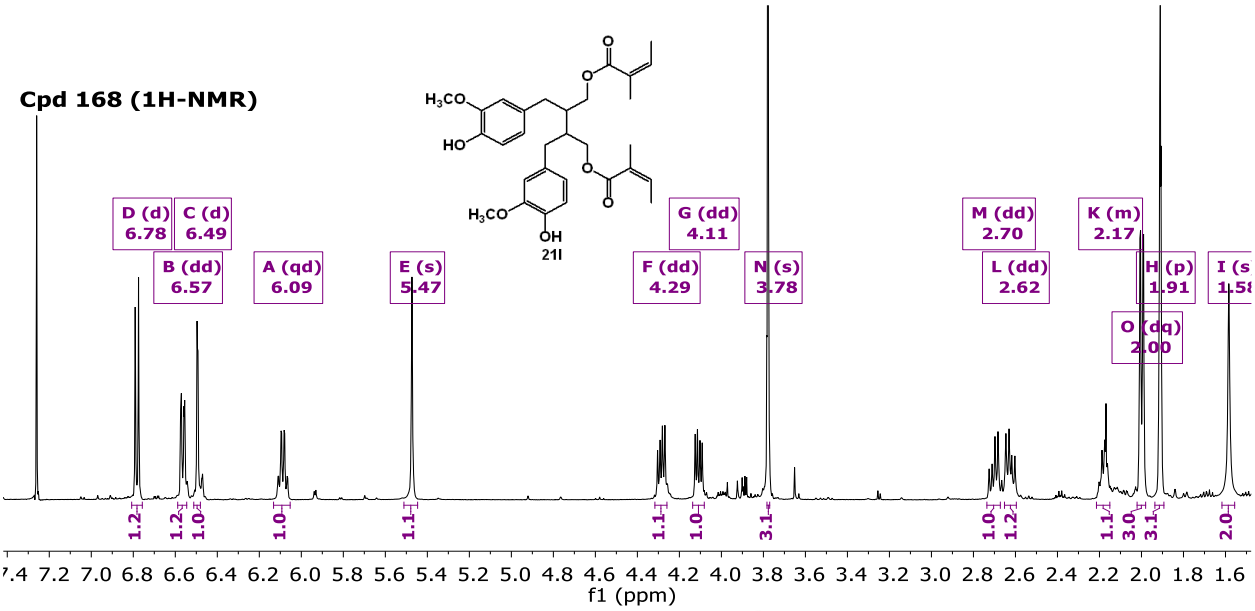
Cpd 168 (1H-NMR)
D (d) 6.78
C (d) 6.49
B (dd) 6.57
A (qd) 6.09
E (s) 5.47
G (dd) 4.11
F (dd) 4.29
N (s) 3.78
M (dd) 2.70
L (dd) 2.62
K (m) 2.17
H (p) 1.91
O (dq) 2.00
I (s
1.2
1.2
1.0
1.0
1.1
1.1
1.0
3.1
1.0
1.2
1.1
3.0
3.1
2.0
f1 (ppm)

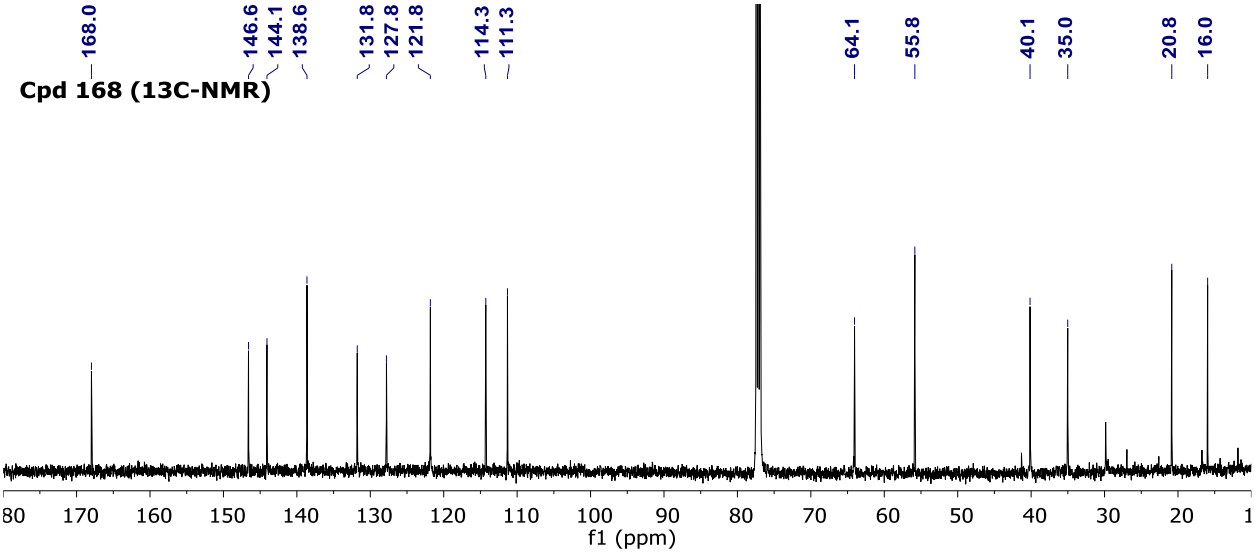
168.0
146.6
144.1
138.6
131.8
127.8
121.8
114.3
111.3
64.1
55.8
40.1
35.0
20.8
16.0
Cpd 168 (13C-NMR)
f1 (ppm)

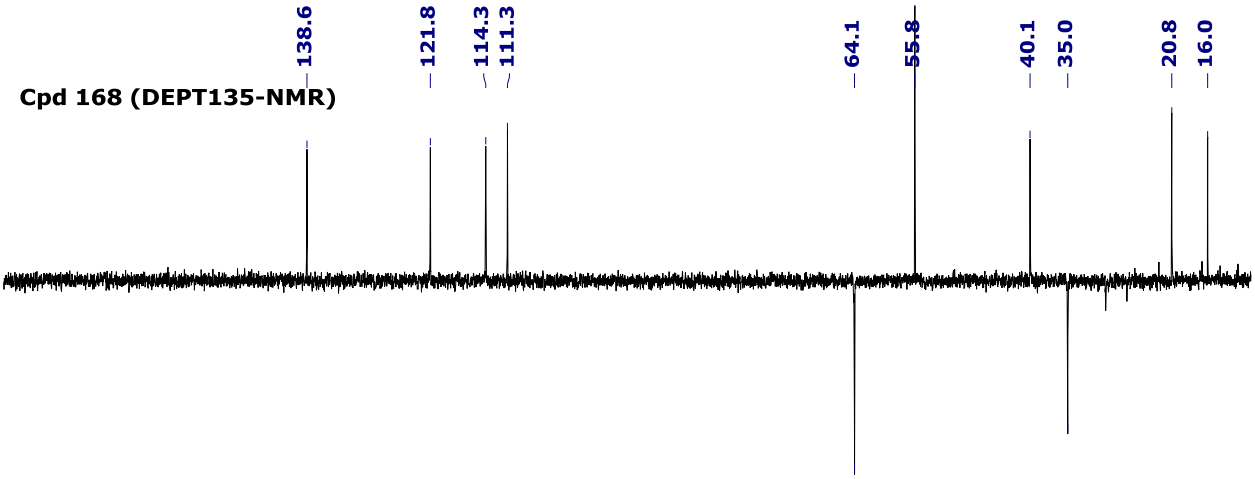
138.6
121.8
114.3
111.3
64.1
55.8
40.1
35.0
20.8
16.0
Cpd 168 (DEPT135-NMR)

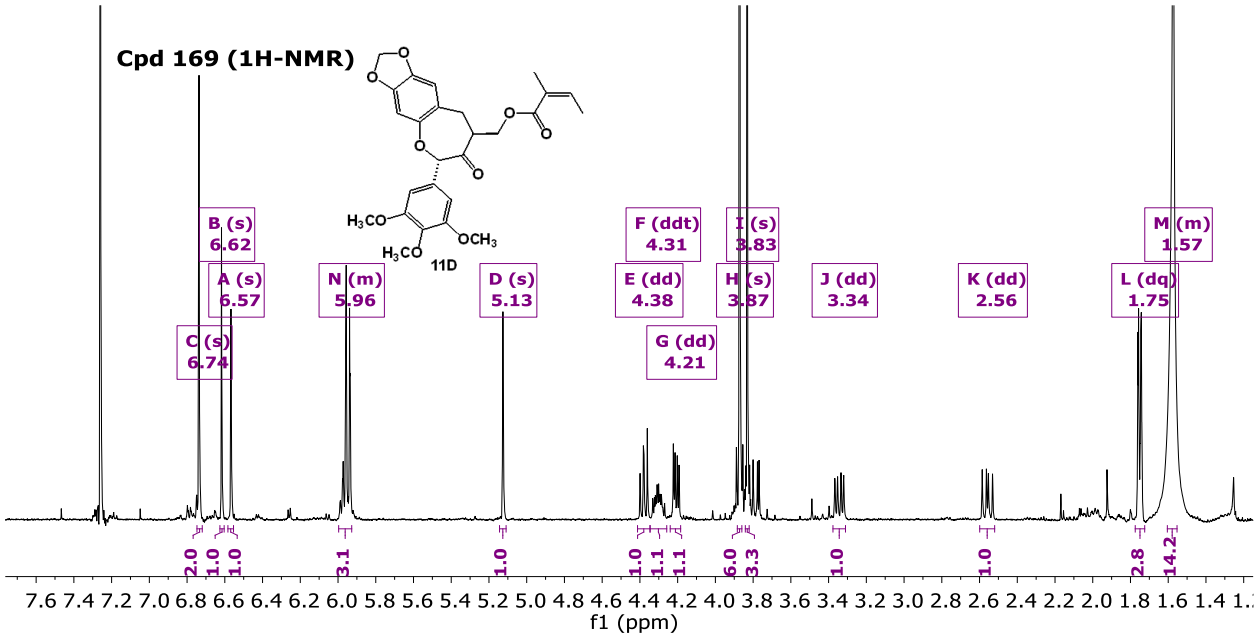
Cpd 169 (1H-NMR)
B (s) 6.62
A (s) 6.57
C (s) 6.74
N (m) 5.96
D (s) 5.13
F (ddt) 4.31
E (dd) 4.38
G (dd) 4.21
I (s) 3.83
H (s) 3.87
J (dd) 3.34
K (dd) 2.56
M (m) 1.57
L (dq) 1.75
11D
2.0 1.0 1.0 3.1 1.0 1.0 1.1 6.0 3.3 1.0 1.0 2.8 14.2
7.6 7.4 7.2 7.0 6.8 6.6 6.4 6.2 6.0 5.8 5.6 5.4 5.2 5.0 4.8 4.6 4.4 4.2 4.0 3.8 3.6 3.4 3.2 3.0 2.8 2.6 2.4 2.2 2.0 1.8 1.6 1.4
f1 (ppm)

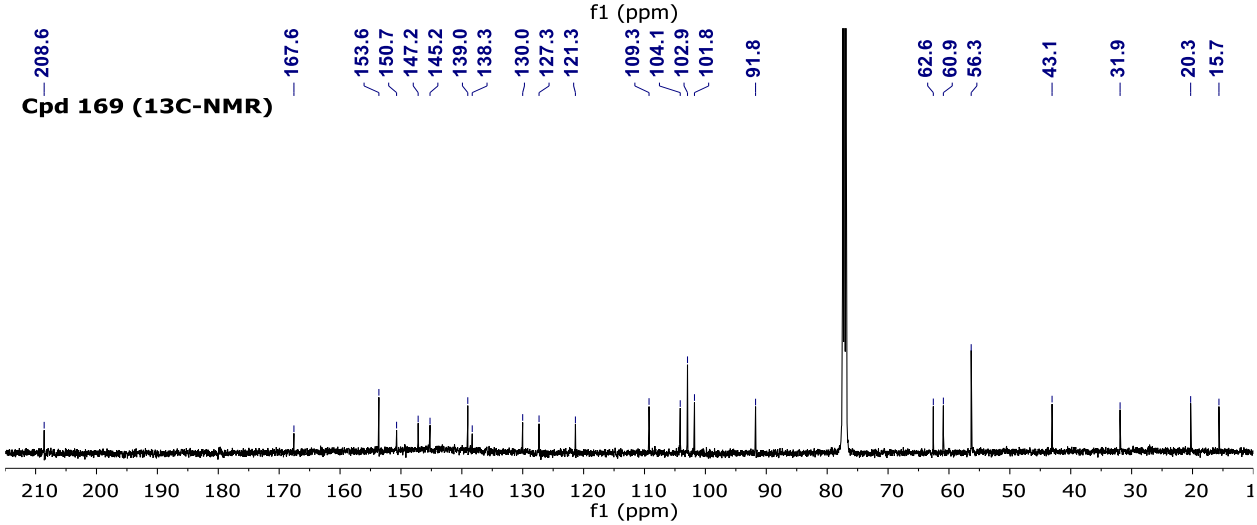
208.6
167.6
153.6
150.7
147.2
145.2
139.0
138.3
130.0
127.3
121.3
109.3
104.1
102.9
101.8
91.8
62.6
60.9
56.3
43.1
31.9
20.3
15.7
Cpd 169 (13C-NMR)
210 200 190 180 170 160 150 140 130 120 110 100 90 80 70 60 50 40 30 20
f1 (ppm)

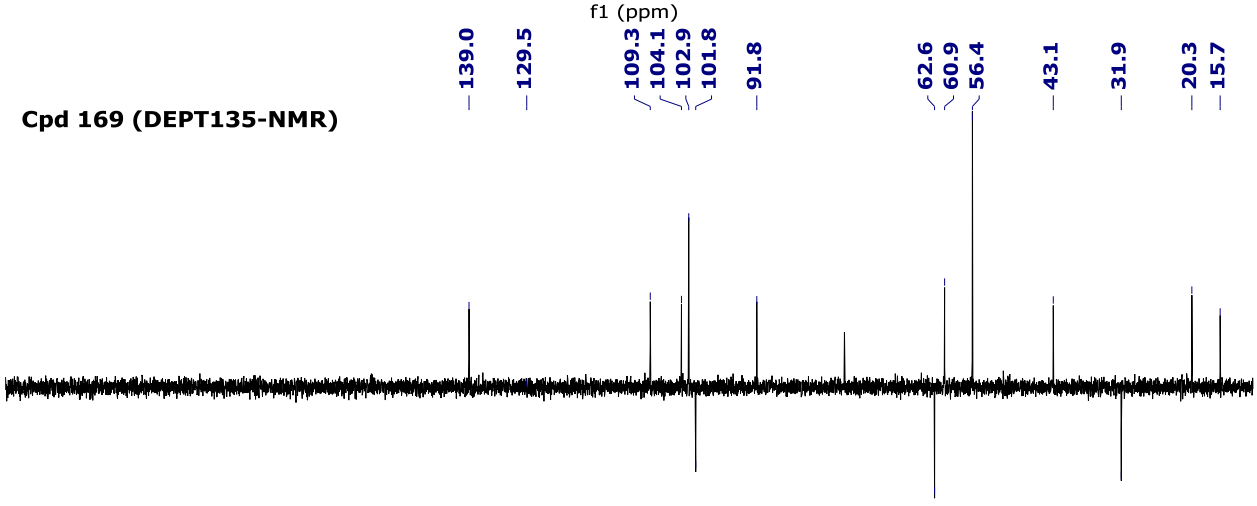
139.0
129.5
109.3
104.1
102.9
101.8
91.8
62.6
60.9
56.4
43.1
31.9
20.3
15.7
Cpd 169 (DEPT135-NMR)

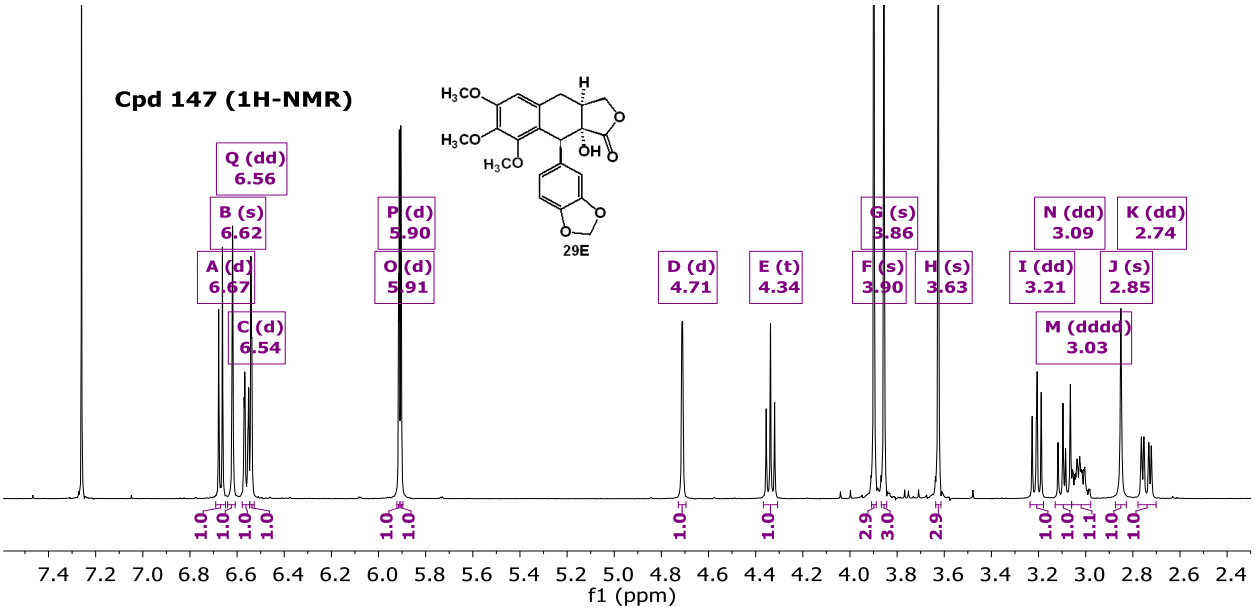
Cpd 147 (1H-NMR)
29E
Q (dd) 6.56
B (s) 6.62
A (d) 6.67
C (d) 6.54
P (d) 5.90
O (d) 5.91
D (d) 4.71
E (t) 4.34
G (s) 3.86
F (s) 3.90
H (s) 3.63
N (dd) 3.09
K (dd) 2.74
I (dd) 3.21
J (s) 2.85
M (dddd) 3.03
1.0 1.0 1.0 1.0 1.0 1.0 1.0 1.0 2.9 3.0 2.9 1.0 1.0 1.1 1.0 1.0
7.4 7.2 7.0 6.8 6.6 6.4 6.2 6.0 5.8 5.6 5.4 5.2 5.0 4.8 4.6 4.4 4.2 4.0 3.8 3.6 3.4 3.2 3.0 2.8 2.6 2.4
f1 (ppm)

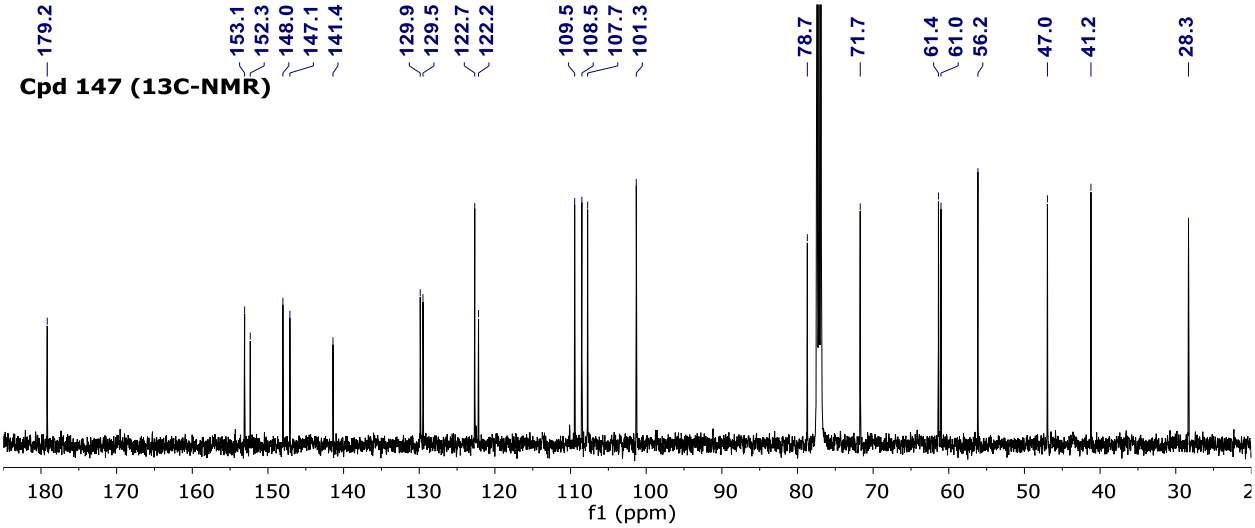
Cpd 147 (13C-NMR)
179.2 153.1 152.3 148.0 147.1 141.4 129.9 129.5 122.7 122.2 109.5 108.5 107.7 101.3 78.7 71.7 61.4 61.0 56.2 47.0 41.2 28.3
180 170 160 150 140 130 120 110 100 90 80 70 60 50 40 30
f1 (ppm)

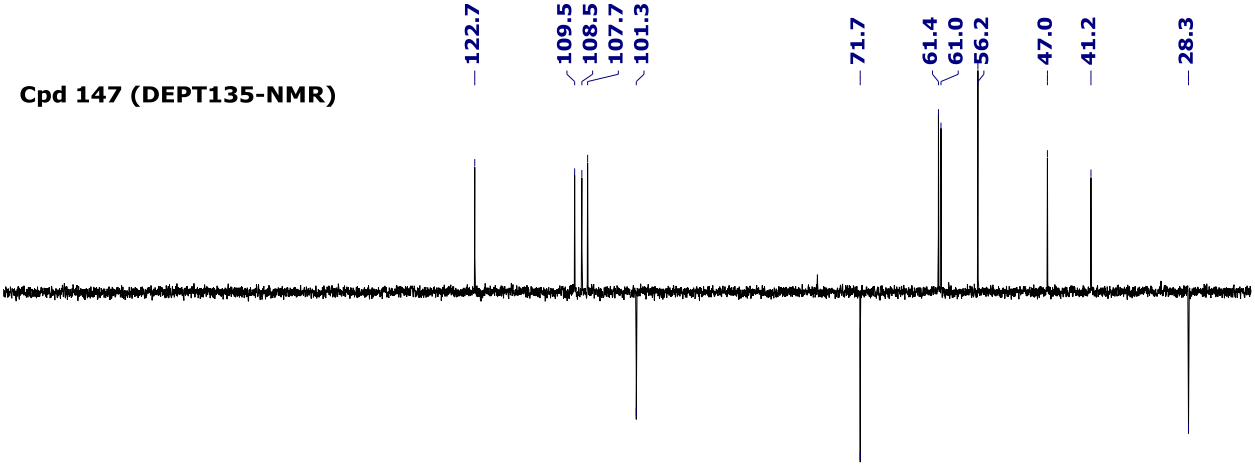
Cpd 147 (DEPT135-NMR)
122.7 109.5 108.5 107.7 101.3 71.7 61.4 61.0 56.2 47.0 41.2 28.3

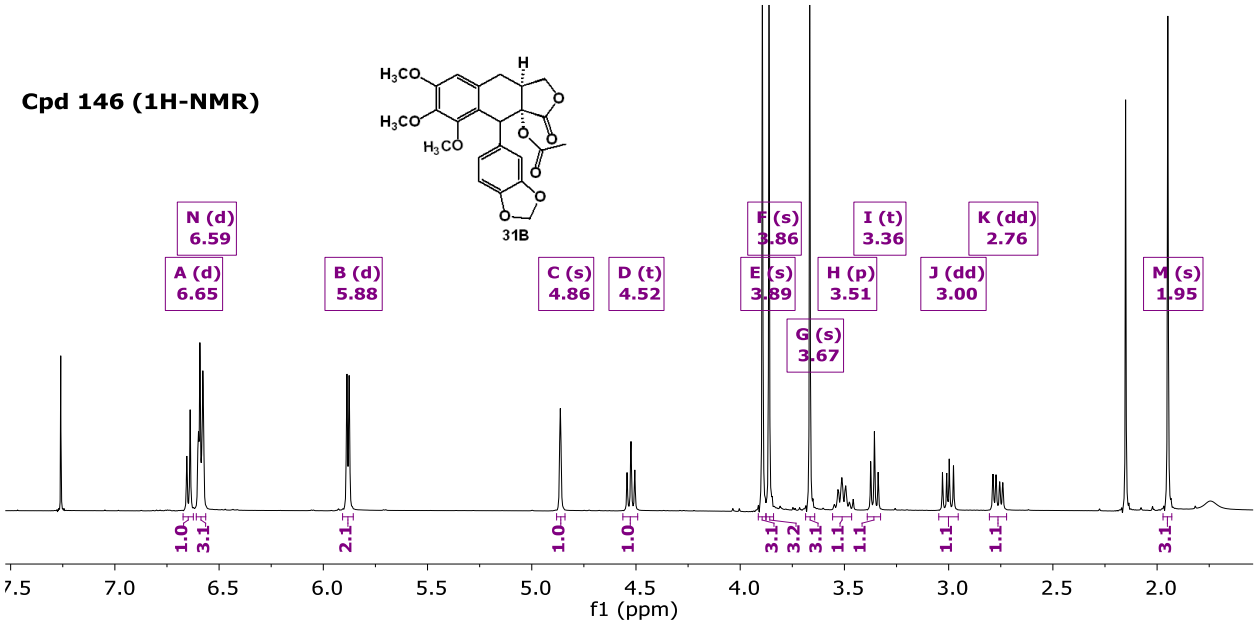
Cpd 146 (1H-NMR)
31B
N (d) 6.59
A (d) 6.65
B (d) 5.88
C (s) 4.86
D (t) 4.52
F (s) 3.86
E (s) 3.89
G (s) 3.67
H (p) 3.51
I (t) 3.36
J (dd) 3.00
K (dd) 2.76
M (s) 1.95
1.0
3.1
2.1
1.0
1.0
3.1
3.2
3.1
1.1
1.1
1.1
1.1
3.1
7.5
7.0
6.5
6.0
5.5
5.0
4.5
4.0
3.5
3.0
2.5
2.0
f1 (ppm)

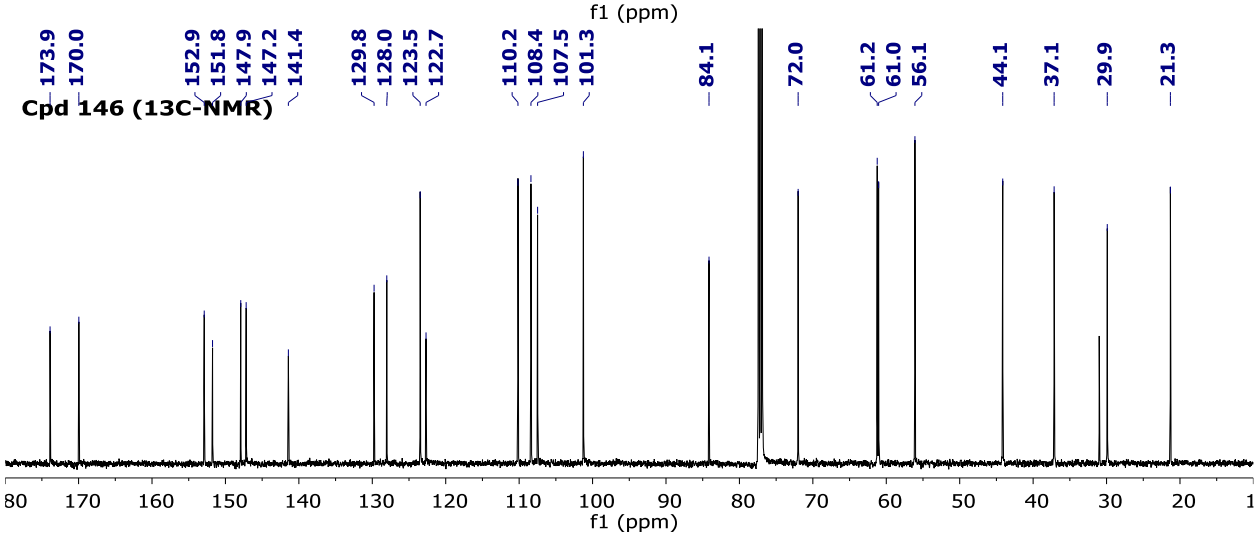
Cpd 146 (13C-NMR)
173.9
170.0
152.9
151.8
147.9
147.2
141.4
129.8
128.0
123.5
122.7
110.2
108.4
107.5
101.3
84.1
72.0
61.2
61.0
56.1
44.1
37.1
29.9
21.3
80
170
160
150
140
130
120
110
100
90
80
70
60
50
40
30
20
1
f1 (ppm)

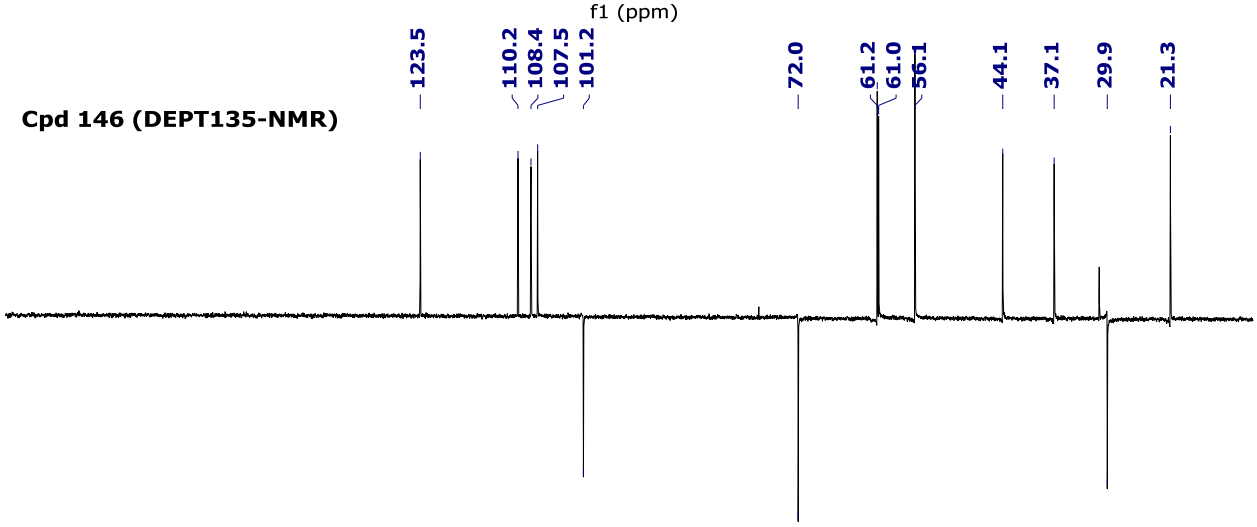
Cpd 146 (DEPT135-NMR)
123.5
110.2
108.4
107.5
101.2
72.0
61.2
61.0
56.1
44.1
37.1
29.9
21.3

Part 2: Chemical Studies of Some Plants in Yayu Nature Reserve

2.1 Introduction

2.1.1 Forest as a Source of Medicinal Plants

Forests, cover approximately 30% of the Earth's land surface, serve as a habitat for a wide range of flora and fauna with significant carbon stock [1, 2]. Historical sources indicate that about 35% of Ethiopia's land area was once covered with forest [3]. In the early 1950's forests covered 19 million hectares or 16% of the land area. However, in the 1980's the coverage was reduced to 3.6% and by 1989 to 2.7 % [4, 5]. In order to conserve the ecosystem and the various species, United Nations Educational, Scientific and Cultural Organization (UNESCO) has recognized 651 biosphere reserves worldwide.

Biosphere reserves are areas of terrestrial and coastal ecosystems promoting solutions to reconcile the conservation of biodiversity with its sustainable use. They are internationally recognized, nominated by national governments and remain under independent authority of the states where they are located. They serve in some ways as 'living laboratories' for testing out and demonstrating integrated management of land, water and biodiversity [6, 7].

Taking this into account UNESCO has recognized four biodiversity areas of Ethiopia in its global list of biosphere reserves. These are Yayu coffee forest (2010), Kafa forest (2010), Sheka forest (2012) and Lake Tana (2015) [6, 7].

High biodiversity forests are recognized by their large number of species and biochemical diversity. They contain valuable medicinal resources and serves as natural laboratories for studying biochemical diversity [8]. Therefore, chemical research conducted on forest plants may lead to the discovery of new drugs and new chemical leads [9].

For this research work field trip was made three times to Yayu nature reserve. This nature reserve is found in Ilubabor zone of Oromia regional state at about 564 kilometers southwest of Addis Ababa (Fig. 58).

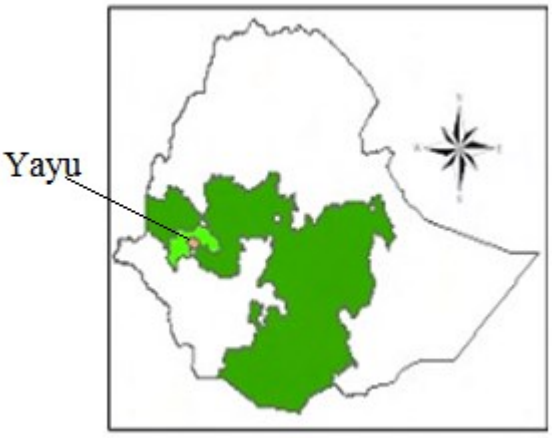

Figure 57: Map of the Yayu Coffee forest, South-west, Oromia region
(Source: http://www.cepf.net/SiteCollectionDocuments/eastern_afromontane)

Twenty plants were collected on the basis of information obtained from local botanist (Mr. Dese Olana) and literature reports on their medicinal value [10, 11]. Ethnomedicinal reports of the collected plants and parts used are summarized in table below.

Table 14: List of medicinal plants and their traditional uses collected from Yayu forest.

Species (Family)	Local Name (Oro)	Traditional Uses
Allophylus abyssinicus (Sapindaceae)	Tatessa	for cold, worms and venereal diseases (Leaf)
Clematis longicauda (Ranunculaceae)	Bagee	for ear disease and eczema, itching skin, toothache and local wound (Leaf)
Clematis simensis (Ranunculaceae)	Fiti	Medicinal (Leaf)
Combretum paniculatum (Combretaceae)	Bagee	for conjunctivitis and other eye ailments and leprosy (Leaf)
Cynoglossum amplifolium (Boraginaceae)	Maxanee	for eye infection, wound, headache michi and evil eye for diarrhoeal. mixed with a little water to make an extract, which is drunk or put in the nose to treat colds. (Leaf)
Ehretia cymosa (Boraginaceae)	Ulagaa	for venereal diseases, pneumonia, dry cough, malaria, tonsils, mental problems, asthma, typhoid, wounds, aphrodisiac stomach ulcer and toothache (Leaf)
Galinsoga parviflora (Asteraceae)	Rafu sibiroo	Medicinal (Leaf)

Morus mesozygia (Moraceae)	Sachoo	for *rheumatic* diseases, dermal diseases, stomach trouble, malnutrition, venereal disease, malaria and syphilis also as a pain killer (Leaf)
Olea welwitschii (Oleaceae)	Baha	for house fumigating, toothache (Leaf)
Plectranthus longipes (Lamiaceae)	Yeroo	for stomach ache, amoebiasis and diarrhea (Leaf)
Sida tenuicarpa (Malvaceae)	Karabba	for wound (Leaf)
Vernonia leopoldi (Asteraceae)	Soyomaa adi	for dressing wounds and gastric disorders (Leaf)
Vernonia sp. (Asteraceae)	Soyomaa guracha	Medicinal (Leaf)
Vernonia sp. (Asteraceae)	Reji	Medicinal (Leaf)
Cyperus longibracteatus (Cyperaceae)	Kuni	Medicinal (Root)
Tragia brevipes (Euphorbiaceae)	Gurgubee	Viral disease, purgative and in the treatment of stomach, rheumatism (Leaf)
*Rhoicissus revoilii (*Vitaceae*)*	Hida refa	Medicinal (Leaf)
*Ritchiea albersii (*Capparaceae*)*	Deqo qalame	Medicinal (Leaf)

From the collected plant materials three plants namely *Clematis longicauda, Ehretia cymosa and Vernonia leopoldi* were selected for chemical studies.

2.1.2 Brief Review on Traditional Uses, Chemistry and Pharmacological Properties of the Genus Clematis, Vernonia and Ehretia

2.1.2.1 The Genus *Clematis*

Clematis is the second largest genus in the family Ranunculaceae comprising more than 300 species worldwide and numerous are garden hybrids [12, 13]. The word '*Clematis*' comes from the Greek word '*vine shoot*' on account of its climbing habit. Most species are known as Clematis in English. *Clematis* species are often referred to as the queen of the flowering plants because of their sepals [14].

Four species namely *C. burgensis, C. hirsute, C. longicauda* and *C. simensis* are known from the Ethiopian flora and the first three are endemic. They are known by their local

name as *Yeazo Hareg* and *Nech Yeazo Hareg* (in Amharic), *Feetii* and *Bagee* (in Oromo) [15].

Clematis species are the common medicinal plants in Ethiopia. The air dried powder leaf of *C. simensis* is used to dress wounds, to treat eczema, ringworm and tropical ulcers, whereas its seed is used for rheumatic pain and to reduce fever. The leaves of *C. longicauda* and *C. hirsute* are used for eye infection and to reduce toothache, respectively [16, 17, 18, 19, 20].

In Kenya, Tanzania, and South Africa the leaf of *C. brachiate* is used for headache, malaria and other febrile illnesses, abdominal disorders, skin disorders and to prevent saddle sores [21, 22].

In traditional Chinese medicine, 68 *Clematis* species are listed in 34 Chinese herbal preparations mainly to treat inflammatory conditions. They are also used to promote urination, to help menses, to treat tetanus, for acute hepatitis, to treat calculus in the urinary tract and gall bladder and hemorrhoids [23, 24, 25].

In Europe and Eastern Asia, *Clematis* species are used as diuretic, antimalarial, antidote in snake bites, anti-dysentery and to treat rheumatic pain, eye infections, gonorrheal symptoms, bone illnesses, chronic skin disorders and varicosity [26].

In Aboriginal medicine in Australia, freshly crushed leaves of *C. glycinoides* and *C. pickeringii* are inhaled to reduce headache and cold and their stems are used for asthma, arthritis, rheumatism, oedema infections and for other related inflammatory diseases [27].

Clematis species have a wide range of chemical constituents such as triterpenes, flavonoids, lignans, coumarins, alkaloids, volatile oils, steroids, organic acids, macrocyclic compounds, polyphenols, etc. Among these, triterpenoid saponins, flavonoids and lignans constitute major classes of chemical constituents. Triterpenoid saponins found in *Clematis* are mainly oleanolic (**1**) and hederagenin type (**2**) [28, 29, 30, 31].

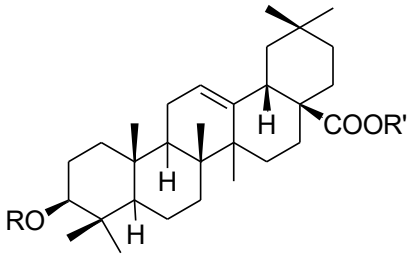

1

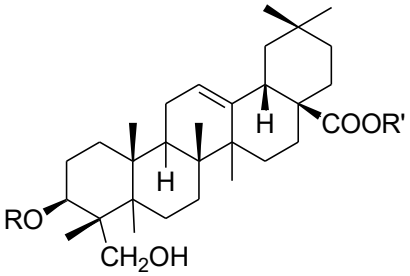

2

Reported flavonoids from *Clematis* species are mainly naringenin (**3**), genistein (**4**), apigenin (**5**), kaempferol (**6**), luteolin (**7**) and quercetin (**8**) [32, 33, 34].

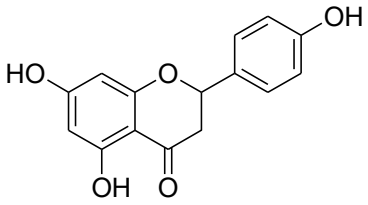

3

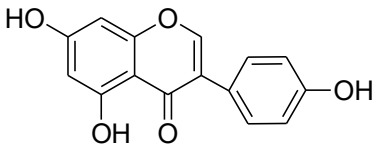

4

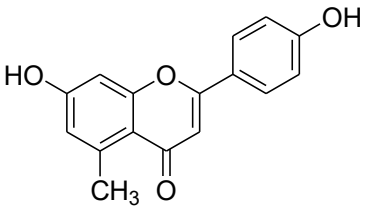

5

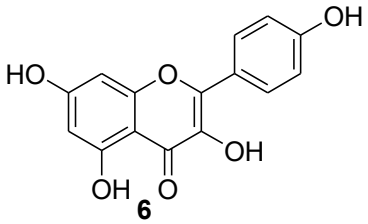

6

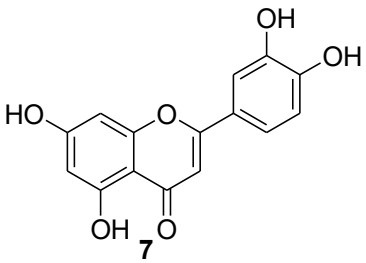

7

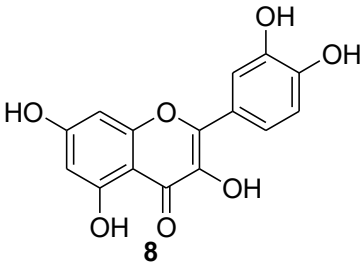

8

Several classes of lignans were reported from *Clematis* including clemastatin A (**9**) and clemastatin B (**10**) [35].

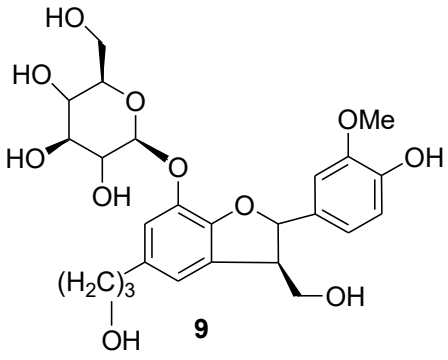

9

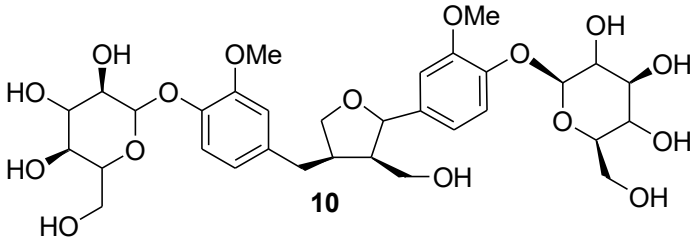

10

Anemonin (**11**) and protoanemonin (**12**) are also reported from several *Clematis* species. Protoanemonin is unstable and can conjugate to form anemonin. Ranunculin (**13**), the glycoside of protoanemonin, is also isolated from some plants [36].

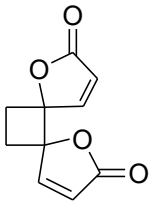

11

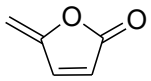

12

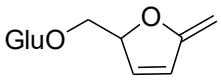

13

Stigmasterol (**14**), β-sitosterol (**15**), α-amyrin (**16**) and β-amyrin (**17**) are among reported steroids from *Clematis* species [37, 38, 39].

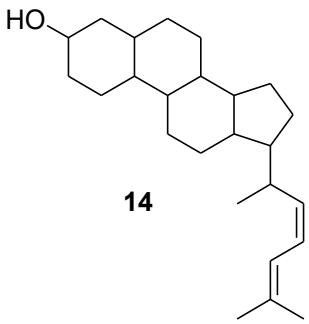

14

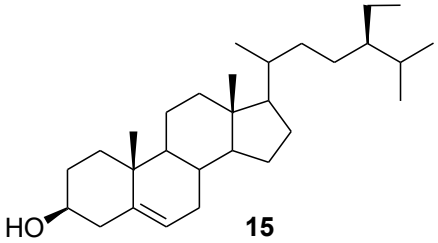

15

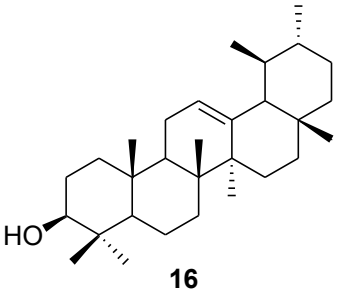

16

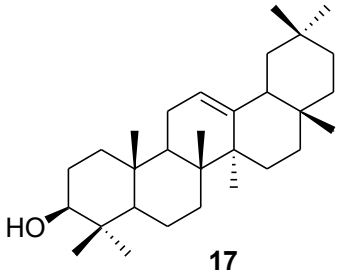

17

Clematis species exhibit different biological activities: antitumor [40], anti-inflammatory [41], antibacterial and antifungal [42] *and broad* spectrum activity against pathogenic yeast [43].

2.1.2.2 The Genus *Vernonia*

The genus *Vernonia,* belongs to Asteraceae family, consists of about 1000 species of shrubs found mainly in tropical and warmer parts of North and South America, tropical

Africa, Madagascar and South East Asia. It is named after William Vernon, an English botanist who collected and identified this genus in Maryland in the late 1600s [44]. Forty-nine *Vernonia* species are recorded from the flora of Ethiopia [45, 46].

V. amygdalina is the most studied member of the genus [47]. The leaves have characteristic odour and bitter taste, which can be reduced by boiling or soaking and washing in water. The bitter taste is due the presence of alkaloids, saponins, tannins and glycosides. In addition to these, *V. amygdalina* is rich in nutrients such as aminoacids, minerals and vitamins [48].

In different parts of the world, people use *Vernonia* species for various therapeutic purposes such as anthelmintic, stomachic, diuretic, sedative and for the treatment of various diseases such as hepatitis, diabetes, malaria, skin infections, kidney problems, eczema, wounds, venereal diseases, sore throat, cold, tooth aches, rheumatism aches, asthma and bronchitis [49, 50].

In Ethiopian, the root of *V. adoensis* is chewed with honey for menstrual disorders; the leaves extract of *V. amygdalina* is used for tonsillitis, as an antifertility agent and to control tick [51]. In Kenya and Uganda, infusion of leaf and root of *V. brachycalyx, V. lasiopus* and *V. auriculifera* are taken to treat malaria [52]. In Nigeria *V. amygdalina* is used to cure malaria and helminthes infection [53].

From *Vernonia* species several classes of compounds such as triterpenoids, steroids, lignoid coumarins and sucrose ester have been reported. However, sesquiterpene lactones and flavonoids are the most common compounds [44]. The lactone ring is responsible for most of the biological activities exhibited by sesquiterpene lactones [54]. Reported sesquiterpene lactones include zaluzanin D (**18**) [55]**,** glaucolides D (**19**) and E (**20**) [56], vernolides A (**21**), B (**22**), D (**23**), vernolide (**24**) and vernolepin (**25**) [57, 58].

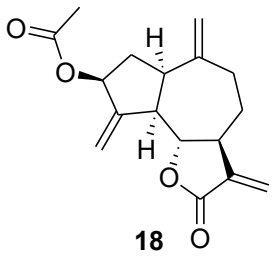

18

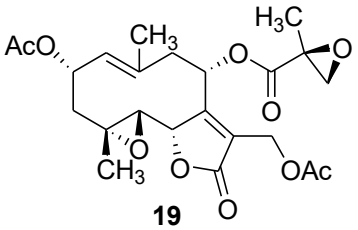

19

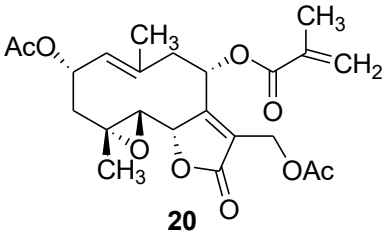

20

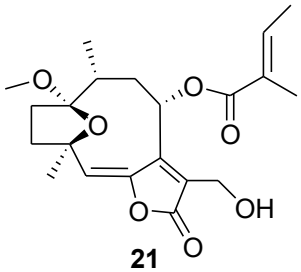

21

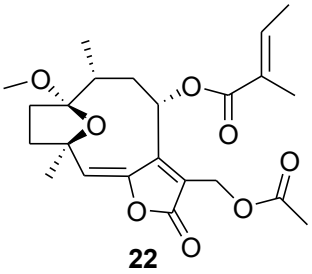

22

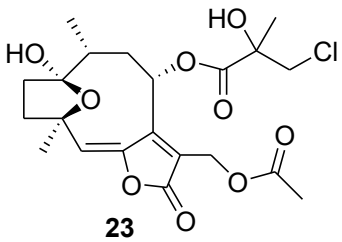

23

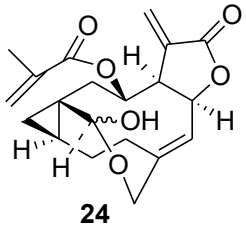

24

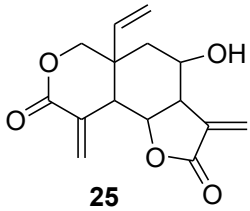

25

Reported biological activities from *Vernonia* species include wound-healing [59], antibacterial and antifungal [60, 61, 62], antitumor [63] and blood glucose lowering [64].

2.1.2.3 The Genus *Ehretia*

The genus *Ehretia* (Boraginaceae), contains 50 species, mainly distributed in tropical Asia and Africa [65]. In Ethiopia, the genus *Ehretia* is represented by two indigenous species namely *E. cymosa* (Local Name: *Mukerba*) and *E. obtusifolia.*

In Ethiopia, the fresh leaves of *E. cymosa* is chewed to get relief from toothache [66]. In Kenya, the roots and leaves are used to treat venereal diseases, pneumonia, dry cough, malaria, tonsils, mental problems, asthma, typhoid, wounds and aphrodisiac [67].

Reported compounds from *Ehretia* species include sterols, phenolic acids, flavonoids, benzoquinones and fatty acids [65]. Some of these compounds are: allomicrophyllone

(**26**), bauerenol (**27**), [88], ehreticoumarin (**28**), ehretiamide (**29**), ehretiquinone (**30**) [69], ehretianone (**31**) [70] and lewisone (**31**) [71].

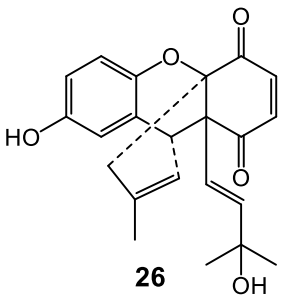

26

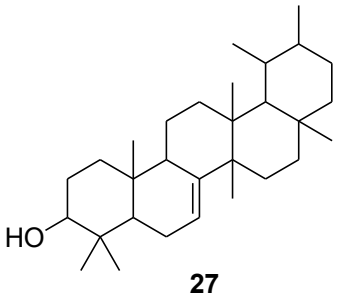

27

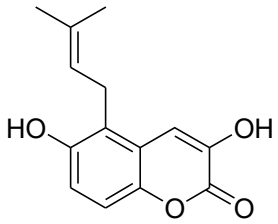

28

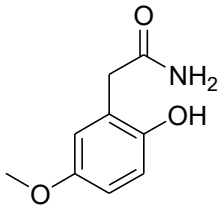

29

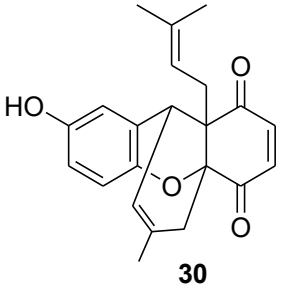

30

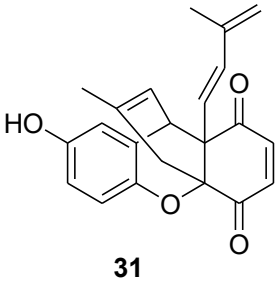

31

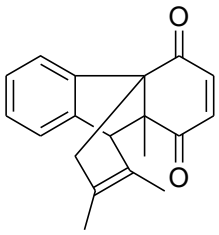

32

2.2 Objectives

The objectives of this work was to:

- study the chemistry of some plants occurring in Yayu nature reserve
- isolate compounds from some plants of Yayu nature reserve
- elucidate the structures of the isolated compounds using different spectroscopic techniques

2.3 Materials and Methods

2.3.1 Place of collection and plant materials

Three plants namely *C. longicauda, E. cymosa* and *V. leopoldi* collected from Yayu nature reserve were prepared for further chemical investigations.

2.3.2 Extraction and Isolation

Sun-dried grounded 50 g of leaves *C. longicauda, V. leopoldi* and *E. cymosa* were separately extracted with ethanol by placing on shaker for 12 h. These were filtered and concentrated to give ethanol extracts.

Isolation of Compounds from *C. longicauda*

Two grams of ethanol extract was adsorbed on silica gel and then subjected to column chromatography packed with silica gel (70-230 mesh). This was eluted with n-hexane and ethyl acetate to afford ten fractions A–J. Fraction B was decanted and washed with diethyl ether to give triacontanol (15 mg). Fraction F (200 mg) was further fractionated by CC over SephadexLH-20 and eluted with chloroform and methanol (1:1) to afford β-sitosterol (40 mg).

Isolation of Compounds from *V. leopoldi*

The ethanol extract (4 g) was adsorbed on silica gel, subjected to column chromatography and eluted with n-hexane, ethyl acetate and methanol to afford sixteen fractions A–P. Fraction L (60 mg) was further fractionated by CC over SephadexLH-20 and eluted with $CHCl_3$:MeOH (1:1) to afford α-spinasterol (10 mg). Fraction H (250 mg) was further subjected to CC packed with silica gel elution was done using n-hexane and chloroform to afford five fractions (A'-E'). Fraction A' (70 mg) was fractionated using SephadexLH-20 and its first fraction was repeatedly recrystallized from dichloromethane and methanol to give a sesquiterpene lactone (40 mg).

Isolation of Compounds from *E. cymosa*

5 g ethanol extract was dissolved in n-hexane. The n-hexane insoluble part (2 g) was dissolved in chloroform and methanol (1:1). After concentrating the filtrate, it was recrystallized by methanol and chloroform to afford mixture of compounds (750 mg) α-amyrin and bauerenol**.**

2.4 Results and Discussion

Phytochemical investigations on ethanol extract of *C. longicauda, V. leopoldi,* and *E. cymosa* have led to the isolation of: 1-triacontanol, β-sitosterol, a sesquiterpene lactone, α-spinasterol, α-amyrin and bauerenol. The structure elucidations of these compounds were accomplished using physical and spectroscopic methods.

2.4.1 Characterization of Compounds from *C. longicauda*

Ethanol extract of *C. longicauda* leaves has led to the isolation of 1-triacontanol (**40**) and β-sitosterol (**41**).

Compound 40

Compound **40** was isolated as a white powder from ethanol extract of *C. longicauda* leaves. The TLC (Rf 0.60) developed using n-hexane and ethyl acetate (1:1) as a mobile phase gave light pink spot after spraying with vanillin in H_2SO_4. The compound melts at 70-72^oC. The UV-Vis spectrum showed no absorption band in the region between region 220-600 nm confirmed the absence of chromophore group. The IR spectrum exhibited absorption bands at 3395 cm^{-1} for the OH and 2919 cm^{-1} and 2851 cm^{-1} for aliphatic stretching.

The most down field triplet signal at δ 3.66 and the quintet at δ 1.58 in the ^{1}H-NMR spectrum assigned for oxymethylene and aliphatic methylene protons situated between two methylene groups respectively. The oxymethylene protons were supported by the presence an oxygenated carbon signal at δ 63.2 in ^{13}C-NMR and DEPT spectra. The broad singlet at δ 1.27 was due to many overlapping methylene protons (27 CH_2), which was also supported by the presence an intense carbon signal at δ 29.74 and other signals between 25.8 – 32.0 ppm. The most up field triplet signal at δ 0.90 showed the presence of only one terminal methyl group and which was also confirmed by the presence of carbon signal at δ 14.2. The ^{1}H-NMR and ^{13}C-NMR spectra of compound **40** were in agreement with literature value for 1-tiacontanol (Table 15) [72].

*Table 15: 1H- and ^{13}C- NMR values and literature report for 1-triacontanol (**40**)*

Experimental Result		Literature Report	
δ_H, mult	δ_C (**Position**)	δ_H, mult	δ_C (**Position**)
3.66 (t, 2H, H-1)	63.1 (**C-1**)	3.63 (t, 2H, H-1)	63.1 (**C-1**)
1.58 (m, 2H, H-2)	32.8 (**C-2**)		32.9 (**C-2**)
	25.8 (**C-3**)		25.8 (**C-3**)
	29.4 (**C-4**)		29.4 (**C-4**)
1.27 (br s, 52H, H-3 to H-28)	29.5 (**C-5**)	1.26 (br s, 56H, H-2 to H-29)	29.7 (**C-5 to C-27**)
	29.6 (**C-6**)		
	29.7 (**C-7 to C-27**)		
	32.0 (**C-28**)		32.0 (**C-28**)
1.47 (br s, 2H, H-29)	22.7 (**C-29**)		22.7 (**C-29**)
0.90 (t, 3H, H-30)	14.2 (**C-30**)	0.88 (t, 3H, H-30)	14.1 (**C-30**)

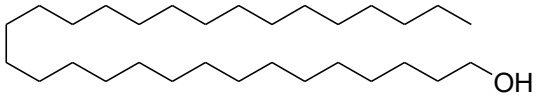

40

Compound 41

Compound **41** was obtained as a white solid recrystallized from methanol and chloroform and melts at 138-140 ^{o}C. The TLC (Rf 0.53) developed using n-hexane and ethyl acetate (1:1) as a mobile phase. The IR spectrum showed absorption bands at 3427 cm^{-1} for O-H stretching; bands at 2957, 2940, 2872 and 2851 for aliphatic C-H stretching; band at 1643 cm^{-1} due to unconjugated C=C bond.

The ^{1}H-NMR spectrum of compound **41** suggested the presence of six methyls at δ 0.70 (3H, s), 0.82-0.88 (9H, m), 0.93 (3H, d, *J* = 6.4 Hz) and 1.02 (3H, s). The signal at δ 3.55 (1H, m) corresponding to a proton attached to an oxygenated carbon. The down field signal at δ 5.37 was due to the presence of an olefinic proton. The above information obtained from ^{1}H-NMR spectrum of compound **41** was evident for the presence of sterol nucleus with one double bond.

The ^{13}C-NMR and DEPT-135 spectra of compound **41** revealed the presence of 28 well resolved signals for 29 carbon atoms. The spectral and physical data suggested that compound **41** was β-sitosterol. The spectroscopic data (^{13}C-NMR) was also in a close agreement with the literature report for β-sitosterol (Table 16) [73].

*Table 16: ^{13}C NMR chemical shift values and literature report for β-sitosterol (**41**)*

Position	Experimental Result	Literature Report
1	37.2	37.5
2	31.9	31.9
3	71.8	72.0
4	42.3	42.5
5	140.8	140.9
6	121.8	121.9
7	31.9	32.1
8	31.9	32.1
9	50.1	50.3
10	36.5	36.7
11	21.1	21.3
12	39.8	39.9
13	42.3	42.6
14	56.8	56.9
15	26.0	26.3
16	28.3	28.5
17	56.0	56.3
18	36.2	36.3
19	19.0	19.2
20	33.9	34.2
21	26.0	26.3
22	45.8	46.1
23	23.0	23.3
24	12.0	12.2
25	29.1	29.4
26	19.8	20.1
27	19.4	19.6
28	18.8	19.0
29	11.9	12.0

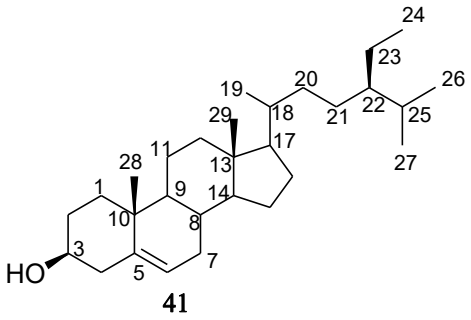

41

2.4.2 Characterization of Compounds from *V. leopoldi*

Chemical investigations on the ethanol extract of *V. leopoldi* leaves have led to the isolation of α-spinasterol (**42**) and sesquiterpene lactone (**49**).

Compound 42

Compound **42** was obtained as a white solid recrystallized from methanol and

dichloromethane and melts at 136-140 ^{O}C. The TLC (Rf 0.48) developed using n-hexane and ethyl acetate (1:1). The IR spectrum showed absorption bands at 3430 cm^{-1} was due to O-H stretching, bands at 2963, 2937, 2851 cm^{-1} for aliphatic C-H stretching and broad band at 1650 cm^{-1} was due to unconjugated olefinic C=C.

The ^{1}H-NMR spectrum of compound **42** showed the presence of six methyls at *δ* 0.57 (3H, *s*), *δ* 0.84 (9H, br. *s*), *δ* 0.87 (3H, d, *J* = 6.4 Hz) and *δ* 1.04 (3H, d, *J* = 6.4 Hz). The signal at *δ* 3.64 (1H, *m*) was due to oxygenated protons positioned at C-3. The signals at *δ* 5.04 (1H, dd, *J* = 8.4 and 14.8 Hz, H-7) and 5.17 (2H, *m,* H-22 and H-23) was due to three olefinic protons in the sterol structure.

The ^{13}C-NMR spectrum analyzed with DEPT-135 spectrum displayed the presence of 29 well resolved carbon signals which are six methyls, nine methylenes, eleven methines and three quaternaries. The signals at δ 139.6, 43.3 and 34.2 assigned for the three quaternary carbons. The signal at δ 71.1 was due to the oxygenated C-3. The presence of two double bonds was evident from the appearance of four signals in olefinic region at δ 139.6 (C-8), 138.2 (C-7), 129.4 (C-22) and 117.5 (C-23). The above spectral data suggested that compound **42** was α-spinasterol. The spectroscopic data (^{13}C-NMR) is in a close agreement with the literature report for α-spinasterol (Table 17) [74].

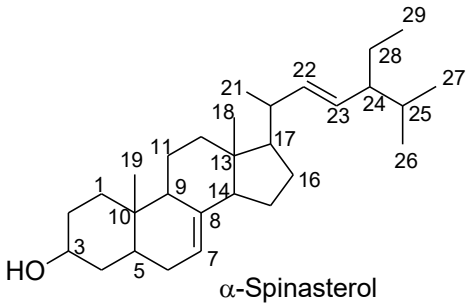

α-Spinasterol

*Table 17: ^{13}C NMR chemical shift values and literature report for α-spinasterol (**42**)*

Position	Experimental Result	Literature Report
1	37.1	37.2
2	31.5	31.5
3	71.1	71.1
4	38.0	38.0
5	40.2	40.3
6	29.7	29.7
7	117.5	117.5
8	139.6	139.6
9	49.4	49.5
10	34.2	34.2

11	21.6	21.6
12	39.5	39.6
13	43.3	43.3
14	55.1	55.1
15	23.0	23.0
16	28.5	28.5
17	55.9	55.9
18	12.1	12.0
19	13.1	13.0
20	40.9	40.8
21	21.4	21.4
22	138.2	138.1
23	129.4	129.5
24	51.2	51.2
25	31.9	31.9
26	21.1	21.1
27	19.0	19.0
28	25.4	25.4
29	12.3	12.2

Sesquiterpene lactone (49)

Compound **49** was obtained as light yellow gel from leaves of *V. leopoldi*. The UV-Vis spectrum of this compound showed absorption maxima at 325 and 265 nm suggesting the presence of conjugation in the compound. The IR spectrum displayed absorption peaks at 1780 and 1714 cm^{-1} confirming the presence of γ-lactone and conjugated δ-lactone. In addition, the spectrum showed peaks at 3442, 2923 and 1624 cm^{-1} due to O-H, -C-H and C=C stretching respectively.

The ^{1}H-NMR spectrum demonstrated signals at δ 5.69 (1H, dd, *J* = 17 and 11 Hz, H-1), 2.84 (1H, d, *J* = 11.2 Hz, H-5), 3.99 (1H, t, *J* = 11.2 Hz, H-6), 1.79 (1H, q, *J* = 11.5 Hz, H-7), 3.92 (1H, td, *J* = 10.6 and 4.4 Hz, H-8) and 2.67 (1H, m, H-11) due to methine protons. It was also showed methylene proton signals at δ 5.25 (2H, m, H-2), 1.91 (1H, dd, *J* = 14.0 and 4.5 Hz H-9), 1.58 (1H, m, H-9), 4.44 (1H, d, *J* = 12.0, H-14), 4.21 (1H, d, *J* = 12.0, H-14), 6.66 (1H, s, H-15) and 5.90 (1H, s, H-15). The proton signal at δ 1.36 (3H, d, *J* = 6.88, H-13) was due to methyl protons.

^{13}C-NMR spectrum investigated with DEPT-135 spectrum showed signals for four quaternaries, four methylenes, six methines and one methyl carbons. The signals at δ 40.8 and 130.6 were due to the quaternary carbons of C-10 and C-4, respectively. The other two quaternary carbons appeared at δ 163.9 and 178.4 assignable for carbonyl of

δ-lactone and γ-lactone, respectively. The signals at δ 116.4 (C-2) and 135.6 (C-15) were due to olefinic methylenes. Among the methine carbons C-6 (δ 78.3) and C-8 (δ 67.7) appeared in the oxygenated region; C-7 (δ 56.7), C-5 (δ 46.3) and C-11 (δ 41.3) were in aliphatic region; C-1 (δ 140.3) in olefinic region. The methylene signals at δ 42.9 and 71.0 were due to C-9 and C-14, respectively. The methyl signal was appeared at δ 14.3 (C-13).

The structure of compound **49** was further deduced using 2D NMR experiments. The COSY experiment showed that correlation of proton signal at δ 2.67 (H-11) with a methyl protons signal at δ 1.36 (H-13) and 1.79 (H-7). In turn, a proton signal at δ 1.79 (H-7) showed correlation with proton signals at δ 3.99 (H-6) and 3.92 (H-8). HMBC spectrum showed correlations of a proton signal at δ 2.67 (H-11) with carbon signals at δ 14.3 (C-13), 56.7 (C-7) and 178.4 (C-12). And a proton signal at δ 1.79 (H-7) correlated with carbon signals at δ 14.3 (C-13), 78.3 (C-6), 41.3 (C-11) and 67.7 (C-8). These COSY and HMBC correlations confirmed that C-6, C-7, C-11 and C-12 are constituents of γ-lactone ring.

The attachment of methyl group on this lactone ring at C-11 suggested from COSY correlation (**43**) of a methyl proton signal and a proton signal at H-11 and from the HMBC correlations (**44**) these protons with carbon at δ 41.3 (C-11), 56.7 (C-7) and 178.4 (C-12).

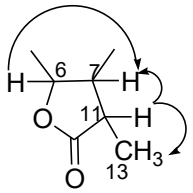

43

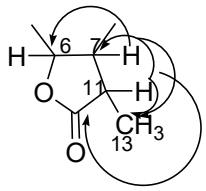

44

The presence δ-lactone ring with exocyclic double bond suggested from HMBC correlations of the methine proton signal at δ 2.84 (H-5) with carbon signals of C-4 (δ 130.6), C-3 (δ 163.9) and C-10 (δ 40.8) (**45**) and the methylene proton signals at δ 4.44 (H-14) and 4.21 (H-14) with carbon signals of C-10 (δ 40.8), C-5 (δ 46.3), C-4 (δ 130.6) and C-3 (δ 163.9) (**45**). The attachment of exocyclic double bond at C-4 was confirmed from correlations of the methylene protons at δ 6.66 (H-15) and 5.90 (H-15) with carbon at δ 46.3 (C-5), 130.6 (C-4) and163.9 (C-3) (**46**)**.**

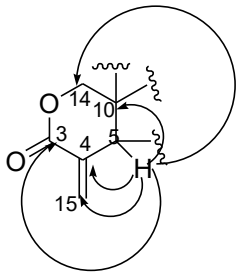

45

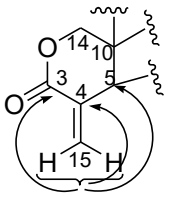

46

The connectivity of the two lactone rings through six membered ring was confirmed from HMBC correlations of H-8 (δ 3.92) with C-10 (40.8), C-11 (41.3), C-9 (42.9), C-7 (56.7), and C-6 (78.3) and H-9 (δ 1.91 and 1.58) with C-10 (δ 40.8), C-5 (δ 46.3), C-7 (δ 56.7), C-8 (δ 67.7) and C-14 (δ 71.0) (**47**).

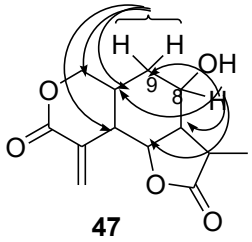

47

The position of vinyl group was determined from strong correlation of H-1 (δ 5.69) and H-2 (δ 5.25) with C-10 (δ 40.8) as showed in **48**. On the basis of the above spectral data the structure of the sesquiterpene lactone was given as in compound **49**.

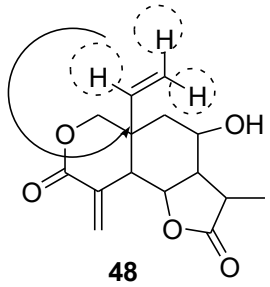

48

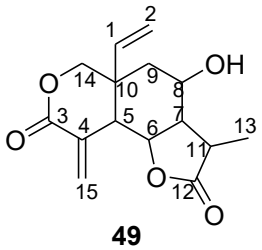

49

2.4.3 Characterization of Compounds from *E. cymosa*

From hexane insoluble portion of ethanol extract mixture of two sterols were obtained in large quantity. The structure elucidation of these two compounds was accomplished by comparing their ^{13}C-NMR data with literature.

Compound 50 and 51

Mixture of compound **50** and **51** were obtained as a white solid after washing of the n-

hexane insoluble portion of ethanol extract of *E. cymosa*. The TLC (Rf 0.60) developed using n-hexane and ethyl acetate (1:1). The IR spectrum displayed absorption band at 3386 cm^{-1} for O-H; band at 3038 cm^{-1} for olefinic =C-H; band at 1616 cm^{-1} for unconjugated olefinic C=C; bands at 2946 cm^{-1} and 2865 cm^{-1} for aliphatic -C-H.

The ^{13}C-NMR spectrum and DEPT-135 showed 46 signals for 60 carbon atoms. The two olefinic signals appeared at δ 116.4 and 145.3 were assignable for C-7 and C-8 of compound **51**, respectively. The other two olefinic signals at δ 124.3 and 139.3 were due to C-12 and C-13 of compound **50,** respectively. The two oxygenated signals at δ 79.0 and 79.3 assigned for C-3 of compound **50** and **51** respectively. The structures were elucidated by comparing the ^{13}C-NMR data with literature (Table 18). The data generated were in close agreement with reported data for α-amyrin (**50**) and bauerenol (**51**) [75, 76].

Table 18: ^{13}C NMR chemical shift values and literature report for α-amyrin and bauerenol

Position	Experimental Result		Literature Report	
	α-amyrin	**bauerenol**	**α-amyrin** [122]	**bauerenol** [121]
1	38.8	36.9	38.7	36.9
2	27.3	27.7	27.2	27.7
3	79.0	79.3	78.3	79.1
4	38.9	38.9	38.7	38.9
5	55.2	50.4	55.2	50.4
6	18. 4	24.2	18.3	24.2
7	32.9	116.4	32.9	116.4
8	40.0	145.3	40.9	145.3
9	47.7	48.2	47.7	48.2
10	37.1	35.3	36.9	35.3
11	23.3	16.8	23.3	16.9
12	124.6	32.4	124.3	32.4
13	139.6	37.7	139.3	37.7
14	42.0	41.2	42.0	41.5
15	28.8	28.9	28.7	28.9
16	26.6	37.7	26.6	37.7
17	33.8	32.0	33.7	32.0
18	59.0	54.9	58.9	54.9
19	39.7	35.2	39.6	35.3
20	39.6	32.0	39.6	32.0
21	31.2	29.2	31.2	29.7
22	41.5	31.5	41.5	31.5
23	28.1	27.6	28.1	27.5
24	15.7	14.7	15.6	14.7
25	15.7	13.0	15.6	13.0
26	16.9	23.7	16.8	23.7
27	23.4	22.7	23.3	22.7
28	28.1	41.2	28.1	40.0
29	17.5	25.7	17.4	25.6
30	21.4	22.6	21.3	22.5

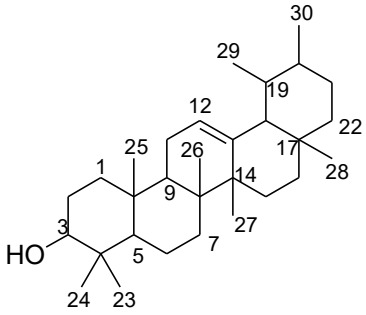

50

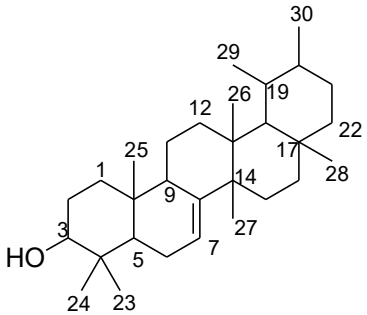

51

Summary

Twenty plant species were collected, on the basis of literature data and information obtained from local botanist, from Yayu coffee forest reserve. Three plants namely *Clematis longicauda, Ehretia cymosa* and *Vernonia leopoldi* were subjected for their chemical constituents and these led to the isolation of four sterols, one sesquiterpene lactone and one long chain aliphatic alcohol.

References

1. Pratihast, A.K., DeVries, B., Avitabile, V., de Bruin, S., Kooistra, L., Tekle, M., and Herold, M. *Combining Satellite Data and Community-Based Observations for Forest Monitoring*. **2014**, Forests, *5*, 2464-2489**.**
2. SCBD: Secretariat of the Convention on Biological Diversity. The Value of Forest Ecosystems. Montreal, SCBD, (CBD Technical Series no. 4): **2001.**
3. EFAP Ethiopian Forestry Action Program (EFAP). Addis Ababa, Ethiopia, **1994.**
4. Burju, T., Hundera, K., and Kelbessa, E. *Floristic Composition and Structural Analysis of Jibat Humid Afromontane Forest, West Shewa Zone, Oromia National Regional State, Ethiopia*. **2013**, Ethiop. J. Educ. & Sc., 8(2), 11-33.
5. Nune, S., Mekonnen, A., and Bluffstone, R. *Policies to increase forest cover in Ethiopia*. **2008**, Proceedings of workshop.
6. Kebede, A. *Delimiting the Interface between Garden Coffee Expansion and Forest Coffee Conservation and its Implication for Protected Area Management: The Case of Kafa Coffee Biosphere Reserve*. **2011**, *MSc Thesis*.
7. Young, J. *Ethiopian Protected Areas a 'Snapshot'. A Reference Guide for Future Strategic Planning and Project Funding*: **2012.**
8. Editorial. Chemical diversity and biological functions of plant volatiles. **2010**, South African Journal of Botany: 76, 607–611.
9. Younes, R.N., Varella, A.D., and Suffredini, I.B. *Discovery of New Antitumoral and Antibacterial Drugs from Brazilian Plant Extracts Using High Throughput Screening*. **2007**, Clinics, 62(6), 763-768.
10. Teketay, D., Anage, A., Mulat, G., and Enyew, M. *Study on Forest Coffee Conservation*: **1998.**
11. Woldemariam, T., Senbeta, F., Tesfaye, K., and Getaneh, F. *Yayu Coffee Forest Biosphere*. **2009**, Reserve Nomination Forum.
12. Chawla, R., Kumar, S., and Sharma, A. *The genus Clematis (Ranunculaceae): chemical and pharmacological perspectives*. **2012**, J Ethnopharmacology: 143(1), 116-150.
13. Ishtiaq, M., Qing, H., Wang, Y., and Cheng, Y.A. *Comparative Study Using Chemometric and Numerical Taxonomic Approaches in the Identification and Classification of Traditional Chinese Medicines of the Genus Clematis*. **2010**, Plant Biosystems, 144(2), 288–297.
14. http://www.memidex.com/leather-flowers+vase-fine
15. Natural Database for Africa (NDA) Version 2.0, August **2011**.
16. Senbeta, F., Tadesse, D.M., Woldemariam, T., and Kellbessa, E. *Diversity of Useful Plants in the Coffee Forests of Ethiopia*. **2013**, Ethnobotany Research & Applications, 1, 1049-1069.
17. Yigezu, Y., Haile, D.B., and Ayen, W.Y. *Ethnoveterinary medicines in four districts of Jimma zone, Ethiopia: cross sectional survey for plant species and mode of use*. **2014**, Veterinary Research, 10(76).
18. Giday, M, Asfaw, Z., and Woldu, Z. *Ethnomedicinal study of plants used by Sheko ethnic group of Ethiopia*. **2010**, Journal of Ethnopharmacology, 132, 75–85.
19. Etana, B. *Ethnobotanical Study of Traditional Medicinal Plants of Goma Wereda, Jima Zone of Oromia Region, Ethiopia*. **2010**, AAU MSc Thesis.
20. Fichtl, R., and Adi, A. *Honeybee Flora of Ethiopia. Addis Ababa, Ethiopia***. 1994**.

21. Okalebo, F.A., Rabah, H.A., Guantai, A.N., Kibwage, I.O., Mwangi, J.W., and Masengo, W. *The antimalarial and antimicrobial activity and brine shrimp toxicity of Clematis brachiata extracts.* **2002**, *East and Central African Journal of Pharmaceutical Sciences*, 5(1), 15-18.
22. http://www.plantzafrica.com/plantcd/clembrach.htm
23. Fu, Q., Zan, K., Zhao, M., Zhou, S., Shi, S., Jiang, Y., and Tu, P. *Triterpene saponins from Clematis chinensis and their potential anti-inflammatory activity*. **2010**, Journal of Natural Product, 73, 1234–1239.
24. Dong, C., Shi, S., Wu, K., and Tu, P. *Chemical Constituents from the Roots and Rhizomes of Clematis hexapetala Pall.* **2007**, Z. Naturforsch, *62b*, 854 – 858.
25. Dong, C.X., Wu, K.S., Shi, S.P., and Tu, P.F. *Flavonoids from Clematis hexapetala*. **2006**, Journal of Chinese Pharmaceutical Sciences, 15(1), 15–20.
26. Gruenwald, J., Brendler, T., and Jaenicke, C. *Physicians' Desk Reference (PDR) for Herbal Medicines, 2nd edition.* **2000**, Medical Economics Company, Montvale, New Jersey, USA, p.769.
27. Li, R.W., Myers, S.P., Leach, D.N., Lin, G.D., and Leach, G. *A cross-cultural study: anti-inflammatory activity of Australian and Chinese plants*. **2003**, Journal of Ethnopharmacology, 85(1), 25-32.
28. Shao, B.Q, Guo, W., Xu, R.S., Wu, H.M., and Ma, K. *Saponins from Clematis chinensis.* **1996**, Phytochemistry, 42(3), 821-825.
29. Zhong, H.M, Chen, C.X., Tian, X., Chui, Y.X., and Chen, Y.Z. *Triterpenoid saponins from Clematis tangutica*. **2001**, Planta Medica, 67(5), 484-488.
30. Thapliyal, R.P, and Bahuguna, R.P. *Clemontanoside-C, a saponin from Clematis montana.* **1993**, Phytochemistry, 33(3), 671-673.
31. Dong, F.Y., Cui, G.H., Zhang, Y.H., Zhu, R.N., Wu, X.J., and Sun, T.T. *Clematom and shurica saponin E, a new triterpenoid saponin from Clematis mandshurica*. **2010**, Journal of Asian Natural Products Research, 12(11-12), 1061-1068.
32. Dong, C.X., Wu, K.S., Shi, S.P., and Tu, P.F. *Flavonoids from Clematis hexapetala*. **2006**, Journal of Chinese Pharmaceutical Sciences, 15(1), 15–20.
33. Zhang, L., Luo, X., and Tian, J. *Chemical constituents from Clematis terniflora.* **2007**, Chemistry of Natural Compounds, 43, 128–131.
34. Li Y., Wang, S.F., Zhao, Y.L., Liu, K.H., Wang, X.M., Yang, Y.P., and Li, X.L. *Chemical constituents from Clematis delavayi var. spinescens*. **2009**, Molecules, 14, 4433–4439.
35. Kizu, H., Shimana, H., and Tomimori, T. *Studies on the constituents of Clematis species. VI. The constituents of Clematis stans Sieb. et Zucc.* **1995**, Chemical & Pharmaceutical Bulletin, 43(12), 2187-2194.
36. Kern, J.R., and Cardellina, J.H. *Native American medicinal plants. Anemonin from the horse stimulant Clematis hirsutissima*. **1983**, Journal of Ethnopharmacology, 8(1), 121-123.
37. Jangwan, J.S., and Bahugun, R.P. *Constituents of Clematis montana*. **1983**, Fitoterapia, 60, 477–479.
38. Ming, H., Jinghua, Z., and Changqi, H. *Studies on the chemical components of Clematis chinensis.* **2001**, Journal of Chinese Pharmaceutical Sciences, 10(4).

39. Sayed, H.M., El-Moghazy, S.A., and Kamel, M.S. *Chemical constituents of stems and leaves of Clematis purpurea hybrida cultivated in Egypt*. **1995**, Indian Journal of Chemistry, 34B, 111–113.
40. Yan, L.H., Xu, L.Z., Lin, J., Yang, S.L., and Feng, Y.L. *Triterpenoid Saponins from the Stems of Clematis parviloba*. **2009**, Journal of Asian Natural Products Research, 11(4), 332-338.
41. Rachel, W.L., Lin, G.D., Leach, D.N., Waterman, P.G., and Myers, S.P*. Inhibition of COXs and 5-LOX and Activation of PPARs by Australian Clematis species (Ranunculaceae)*. **2006**, J. Ethnopharmacol, 104, 138-143.
42. Hawaze, S., Deti, H., and Suleman, S. In vitro *Antimicrobial Activity and Phytochemical Screening of* Clematis Species *Indigenous to Ethiopia*. **2012**, Indian J Pharm Sci., 74(1), 29–35.
43. Buzzini, P., and Pieroni, A. *Antimicrobial Activity of Extracts of Clematis vitalba Toward Pathogenic Yeast and Yeast-like Microorganisms*. **2003**, Fitoterapia, 74, 397-400.
44. Toyang, J., and Verpoorte, R. *A Review of the Medicinal Potentials of Plants of the Genus Vernonia (Asteraceae).* **2013**, Journal of Ethnopharmacology, 146, 681–723.
45. Tadesse, M. *Asteraceae (Compositae).* **2004**, Flora of Ethiopia and Eritrea, 4(2), 75-76.
46. Abegaz, B.M, Keige, A.W., Diaz, J.D., and Herz, W. *Sesquiterpene Lactones and Other Constiruents of Vernonia Species from Ethiopia.* **1994**, Phytochemistry, 37 (1), 191-196.
47. Ijeh, I., and Ejike, C. *Current Perspectives on the Medicinal Potentials of Vernonia amygdalina.* **2011**, Journal of Medicinal Plants Research, 5, 10-51.
48. Mwanauta, R.W., Mtei, K.A., and Ndakidemi, P.A. *Prospective Bioactive Compounds from Vernonia amygdalina, Lippia javanica, Dysphania ambrosioides and Tithonia diversifolia in Controlling Legume Insect Pests.* **2014**, Agricultural Sciences, 5, 1129-1139.
49. Hussain, S.H. *Phytochemistry and Bioactivity of Selected High Altitude Plants Belonging to Ligularia, Senecio and Vernonia Genera*. **2012**, University of Peshawar, Pakistan: Ph.D Dissertation.
50. Nogueira, A.C, de Souza, E.B., and dos Santos, R.O. *A review on Antimicrobial Potential of Species of the Genus Vernonia (Asteraceae).* **2015**, Med. Plants Res., 9(31), 838-850.
51. Kumbi, B. *Chromosome Study of Six Vernonia Species (Asteraceae) From Central Ethiopia*. **2009**, AAU MSc. Thesis.
52. Muthaura, C.N., Rukunga, G.M., Chhabra, S.C., Mungai, G.M., and Njagi, N.M. *Traditional Phytotherapy of Some Remedies used in Treatment of Malaria in Meru District of Kenya.* **2007**, South African Journal of Botany, 73 (3), 402-411.
53. Ojiako, O.A., and Nwanjo, H.U. *Is Vernonia amygdalina Hepatotoxic or Hepatoprotective? Response from Biochemical and Toxicity Studies in Rats.* **2006**, African Journal of Biotechnolgy, 5(18), 1648-1651.
54. Merfort, I. *Perspectives on Sesquiterpene Lactones in Inflammation and Cancer.* **2011**, Current Drug Targets, 12, 1560–1573.

55. N-Krishna, K.G, Masilamani, S., Ganesh, M.R., Aravind, S., and Sridhar, S.R. *Zaluzanin D: A Fungistatic Sesquiterpene from Vernonia arborea.* **2003**, Fitoterapia, 74(5), 479-482.
56. Campos, M., Oropeza, M., Ponce, H., Fernandez, J., Jimenez-Estrada, M., Torres, H., and Reyes-Chilpa, R. *Relaxation of Uterine and Aortic Smooth Muscle by Glaucolides D and E from Vernonia liatroides.* **2003**, Biol Pharm Bull., 26, 112-115.
57. Ong, C.W., Yang, L.M., Huang, J.T., Chen, C.F., and Li, S.Y. *Two Novel Sesquiterpene Lactones, Cytotoxic Vernolide-A and -B, from Vernonia cinerea.* **2003,** Chem Pharm Bull., 51, 425-426.
58. Chea, A., Hout, S., Long, C., Marcourt, L., Faure, R., Azas, N., and Elias, R. *Antimalarial Activity of Sesquiterpene Lactones from Vernonia cinerea.* **2006**, Chem Pharm Bull (Tokyo), 54(10), 1437-1439.
59. Manjunatha, B.K., Vidya, S.M., Rashmi, K.V., Mankani, K.L., Shilpa, H.J., and Singh, J. *Evaluation of Wound-Healing Potency of Vernonia arborea.* **2005**, Indian J Pharmacol, 37 (4), 223-226.
60. Jahan, N., Ahmad, M., Zia-Ul-Haq, M.M., Alam, S.M., and Qureshi, M. *Antimicrobial Screening of Some Medicinal Plants of Pakistan*. **2010**, Pak. J. Bot., 42, 4281-4284.
61. Adetutu, A., Morgan, W.A., and Corcoran, O. *Ethnopharmacological Survey and in vitro Evaluation of Wound-Healing Plants used in Southwestern Nigeria*. **2011**, J. Ethnopharmacol., 137(1), 50-56.
62. Suleiman, M.N., Emua, S.A., and Taiga, A. *Effect of Aqueous Leaf Extracts on a Spot Fungus (Fusarium sp.) Isolated from Compea.* **2008**, J. Sustain. Agric., 2, 261-263.
63. Pagno, T., Blind, L.Z., Biavatti, M.W., and Kreuger, M.R. *Cytotoxic Activity of the Dichloromethane Fraction from Vernonia scorpioides (Lam.) Pers. (Asteraceae) Against Ehrlich's Tumor Cells in Mice.* **2006**, Braz J Med Biol Res., 39, 1483-1491.
64. Sy, G.Y., Cisse, A., Nongonierma, R.B., Sarr, M., Mbodj, N.A., and Faye, B. *Hypoglycaemic and Antidiabetic Activity of Acetonic Extract of* Veronia colorata *Leaves in Normoglycemic and Alloxan Induced Diabetic Rats.* **2005**, Journal of Ethnopharmacolgy, 98, 171–175.
65. Li, L., Yong, P., Xia, Y., Li-jia, X., Ta-na, W., Yong, L., Ren-bing, S., and Pei-gen, X. *Chemical Constituents and Biological Activities of Plants from the genus Ehretia Linn.* **2010**, Chinese Herbal Medicines, 2(2), 106-111.
66. Megersa, M., Asfaw, Z., Kelbessa, E., Beyene, A., and Woldeab, B. *An Ethnobotanical Study of Medicinal Plants in Wayu Tuka District, East Welega Zone of Oromia Regional State, West Ethiopia.* **2013**, Journal of Ethnobiology and Ethnomedicine, 9, 68, 1-18.
67. Pascaline, J., Charles, M., Lukhoba, C., and George, O. *Phytochemical Constituents of Some Medicinal Plants Used by the Nandis of South Nandi district, Kenya.* **2011**, Journal of Animal & Plant Sciences: 9 (3), 1201-1210.
68. Yamamura, S., Simpol, L.R., Ozawa, K., Ohtani, K., Otsuka, H., Kasai, R., and Yamasuki, K. *Antiallergic dimeric prenylbenzoquinones from Ehretia microphylla.* **1995**, Phytochemistry, 39, 105-110.

69. Chien, Y.C., Lin C., Chiang, M.Y., Chang, H.S., and Liao, C.H. *Secondary Metabolites from the Root of Ehretia longiflora and their Biological Activities.* **2012**, Phytochemistry, 80, 50- 57.
70. Selvanayagam, Z.E., Gnanavendhan, S.G., Balakrishna, K., Rao, R.B., Sivaraman ,J., Subramanian, K., Puri, R., and Puri, R.K. *Ehretianone, a Novel Quinonoid Xanthene from Ehretia buxifolia with Antisnake Venom Activity.* **1996**, J. Nat. Prod., 59, 664.
71. Thapliyal, P.C. *et al.*, *J. Inst. Chem. (India)*: **75**, 13- 15, **2003**.
72. Ruangrungsi, N., Aukkanibutra, A., Phadungcharoen, T., Lange, G.L., and Lee, M. *Constituents of Typha elephantine.* **1987**, J. Sci. Thailand., 13, 57-62.
73. Chaturvedula, P., and Prakash, I.P. *Isolation of Stigmasterol and β-Sitosterol from the Dichloromethane Extract of Rubus suavissimus.* **2012**, International Current Pharmaceutical Journal, 1(9), 239-242.
74. Consolacion, Y.R., and Lim, K. *Sterols from Cucurbita maxima.* **2005**, Philippine Journal of Science, 134 (2), 83-87.
75. Trevisan, G., Rossato, M.F., Bandero, C.R., Klafke, J.Z., Rosa, F., Oliveira, S.M., Tonello, R., Guerra, G.P., Boligon, A.A., Zanon, R.B., Athayde, M.L., and Ferreira, J. *Identification of the Plant Steroid α-Spinasterol as a Novel Transient Receptor Potential Vanilloid 1 Antagonist with Antinociceptive Properties.* **2012**, The Journal of Pharmacology and Experimental Therapeutics, 343(2), 258–269.
76. Jeong, G., Li, B., Lee, D., Kim, K.H., Lee, I.K, Lee, K.R., and Kim, Y. *Cytoprotective and anti-inflammatory effects of spinasterol via the induction of hemeoxygenase-1 in murine hippocampal and microglial cell lines.* **2010**, International Immunopharma-cology, 10, 1587–1594.

Appendix 2

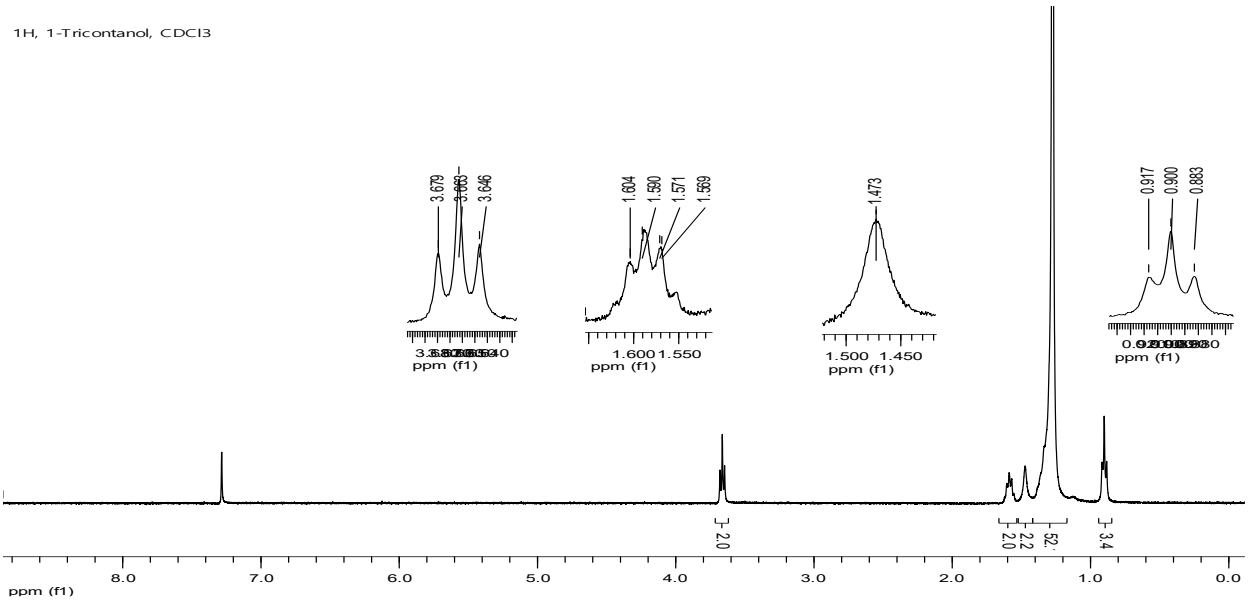
1H, 1-Tricontanol, CDCl3
3.679
3.663
3.646
1.604
1.590
1.571
1.569
1.473
0.917
0.900
0.883
ppm (f1)
2.0
2.2
2.2
6.2
3.4
8.0
7.0
6.0
5.0
4.0
3.0
2.0
1.0
0.0

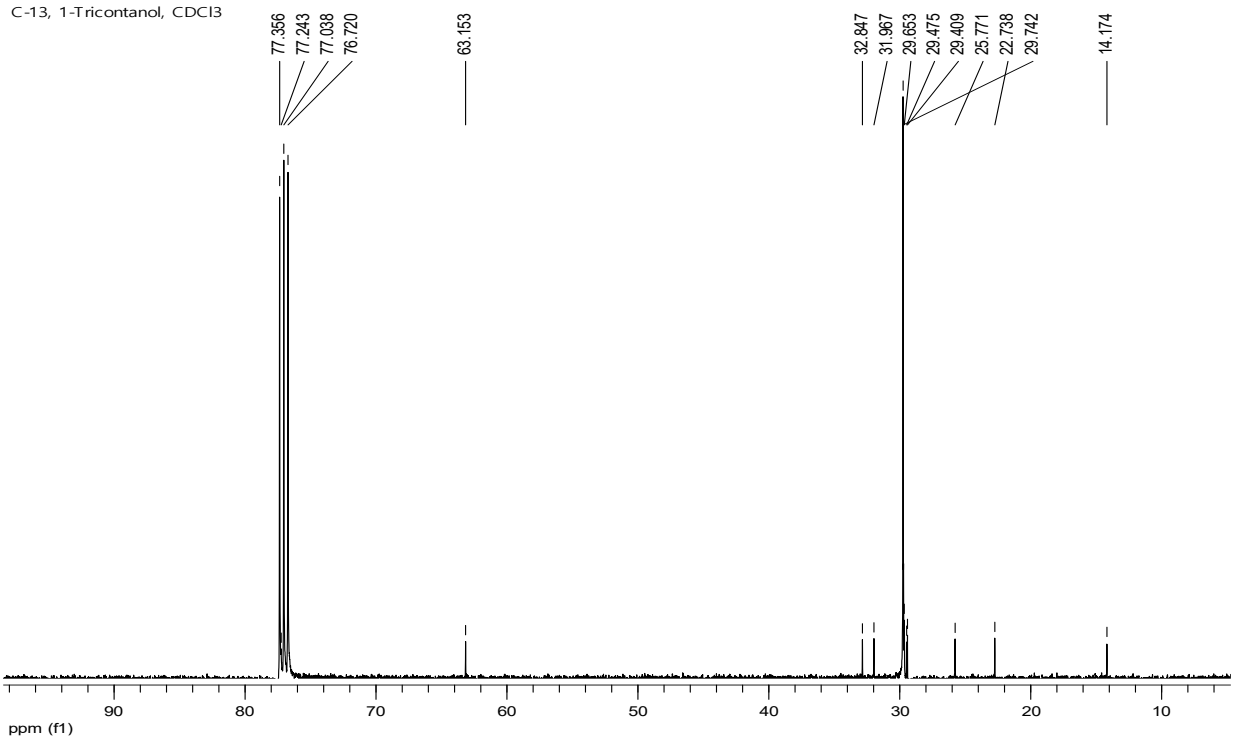
C-13, 1-Tricontanol, CDCl3
77.356
77.243
77.038
76.720
63.153
32.847
31.967
29.653
29.475
29.409
25.771
22.738
29.742
14.174
ppm (f1)
90
80
70
60
50
40
30
20
10

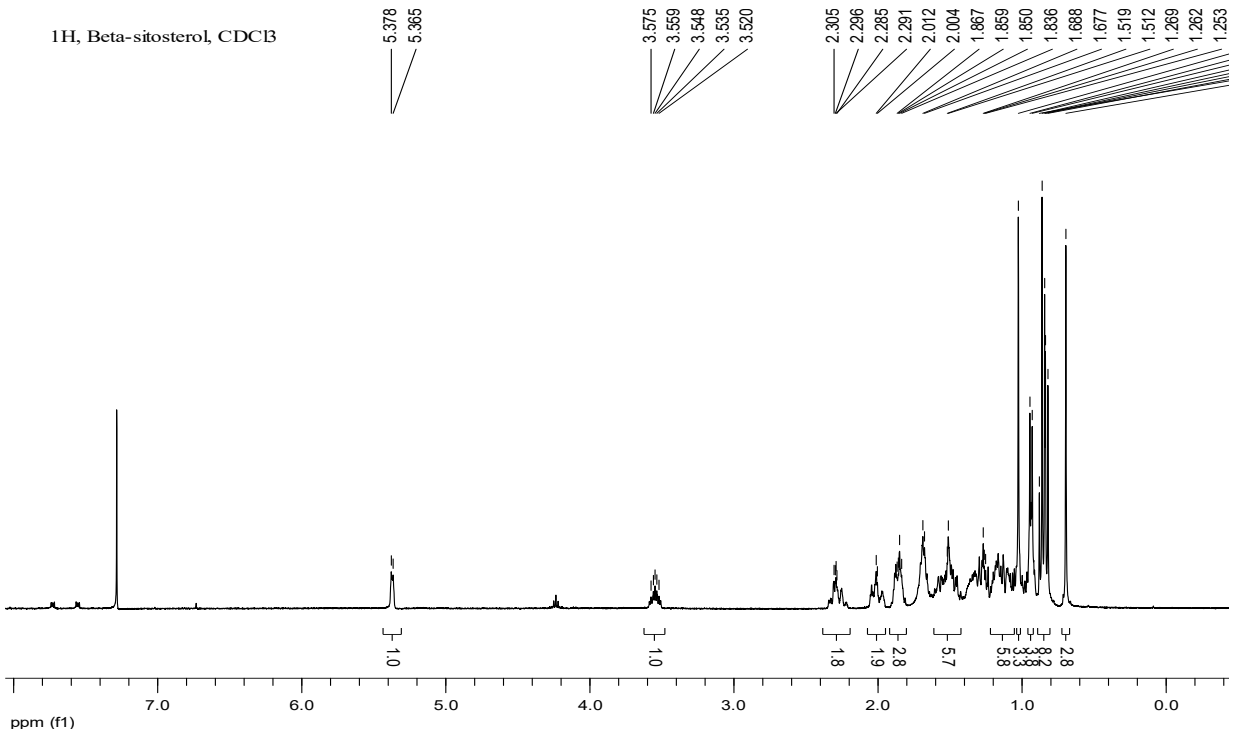
1H, Beta-sitosterol, CDCl3
5.378
5.365
3.575
3.559
3.548
3.535
3.520
2.305
2.296
2.285
2.291
2.012
2.004
1.867
1.859
1.850
1.836
1.688
1.677
1.519
1.512
1.269
1.262
1.253
1.0
1.0
1.8
1.9
2.8
5.7
5.8
2.8
7.0
6.0
5.0
4.0
3.0
2.0
1.0
0.0
ppm (f1)

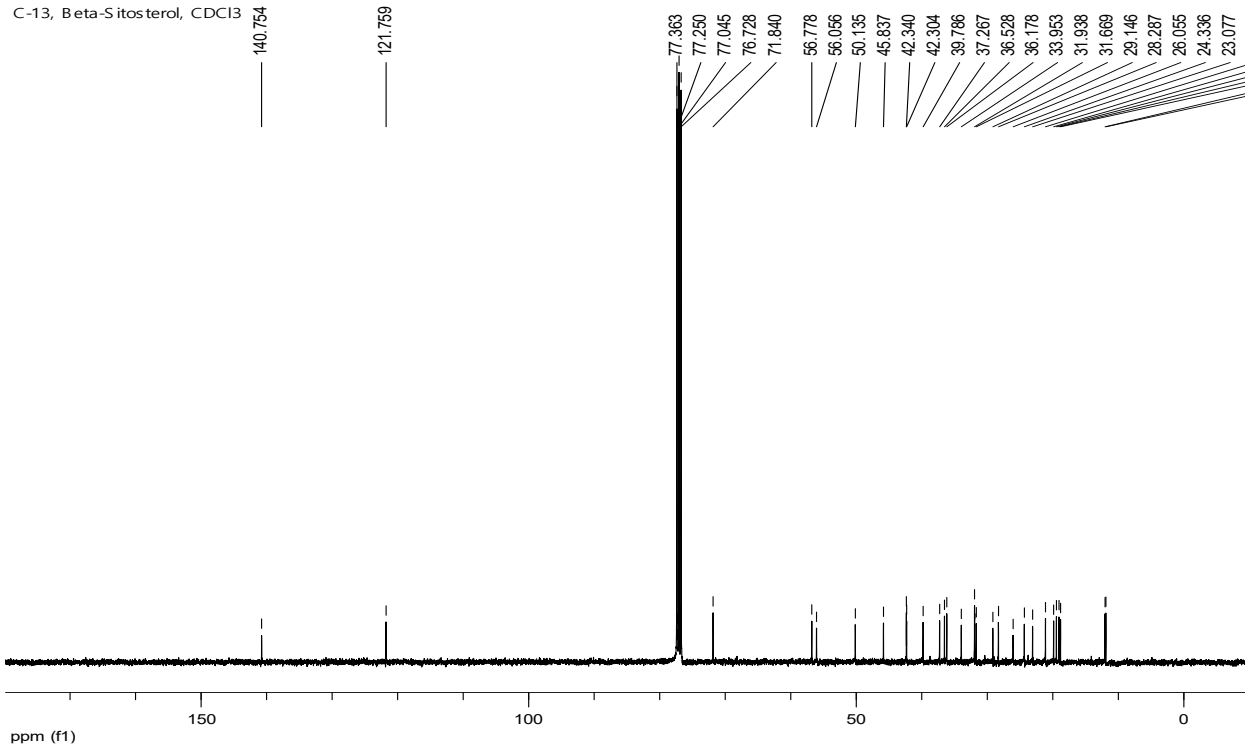
C-13, Beta-Sitosterol, CDCl3
140.754
121.759
77.363
77.250
77.045
76.728
71.840
56.778
56.056
50.135
45.837
42.340
42.304
39.786
37.267
36.528
36.178
33.953
31.938
31.669
29.146
28.287
26.055
24.336
23.077
150
100
50
0
ppm (f1)

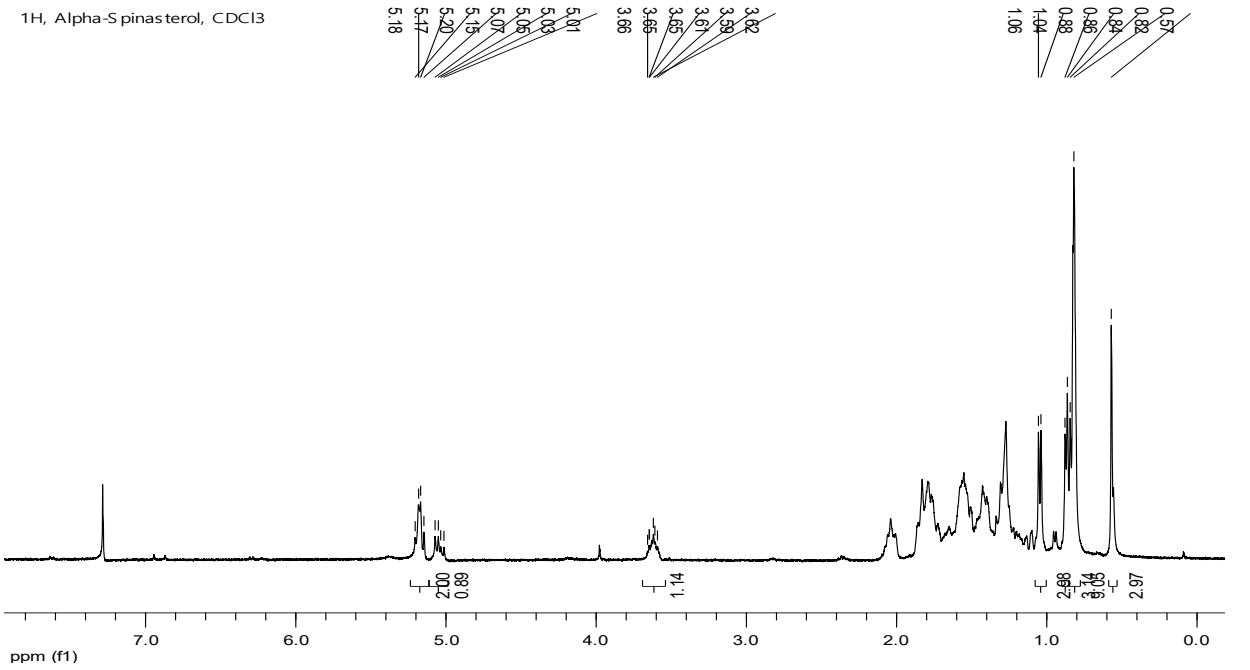
1H, Alpha-Spinasterol, CDCl3
5.18
5.17
5.20
5.15
5.07
5.05
5.03
5.01
3.66
3.65
3.63
3.61
3.59
3.62
1.06
1.04
0.88
0.86
0.84
0.82
0.57
68.0
2.00
1.14
ppm (f1)

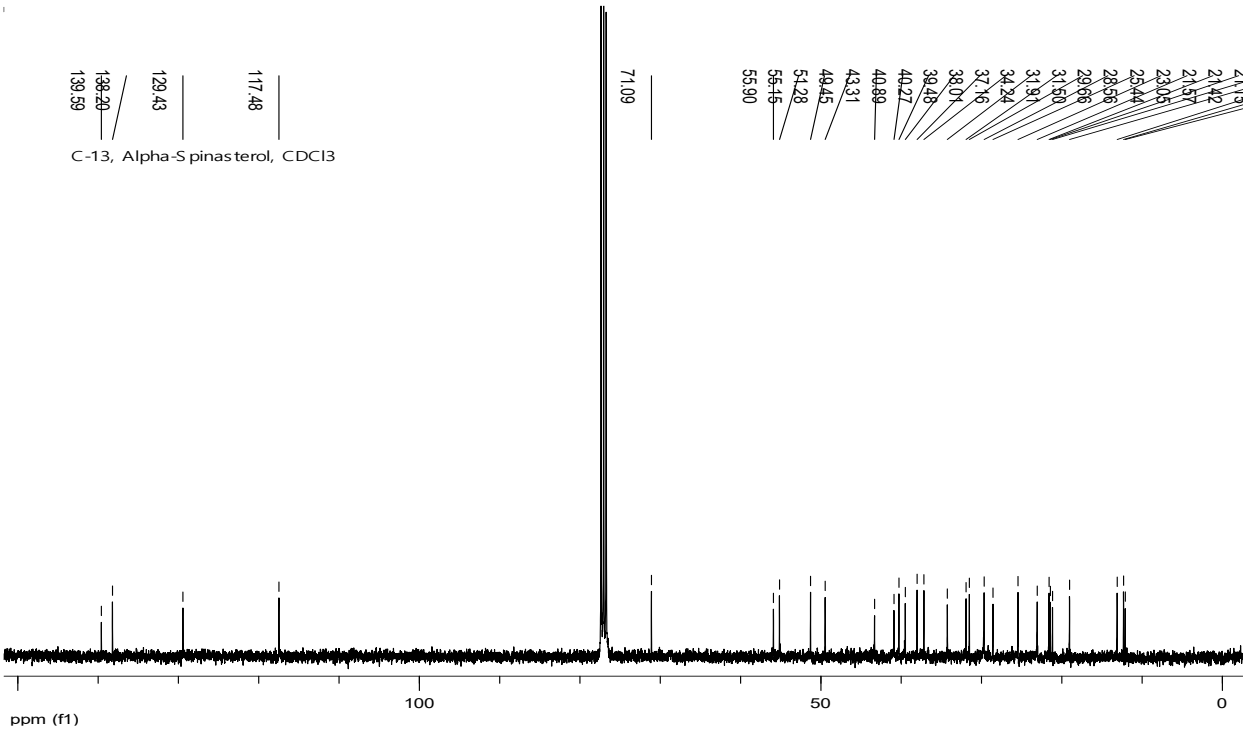
139.59
138.20
129.43
117.48
71.09
55.90
56.15
54.28
49.45
43.31
40.89
40.27
39.48
38.01
37.16
34.24
31.91
31.50
29.66
28.56
25.44
23.05
21.57
21.42
C-13, Alpha-Spinasterol, CDCl3
ppm (f1)

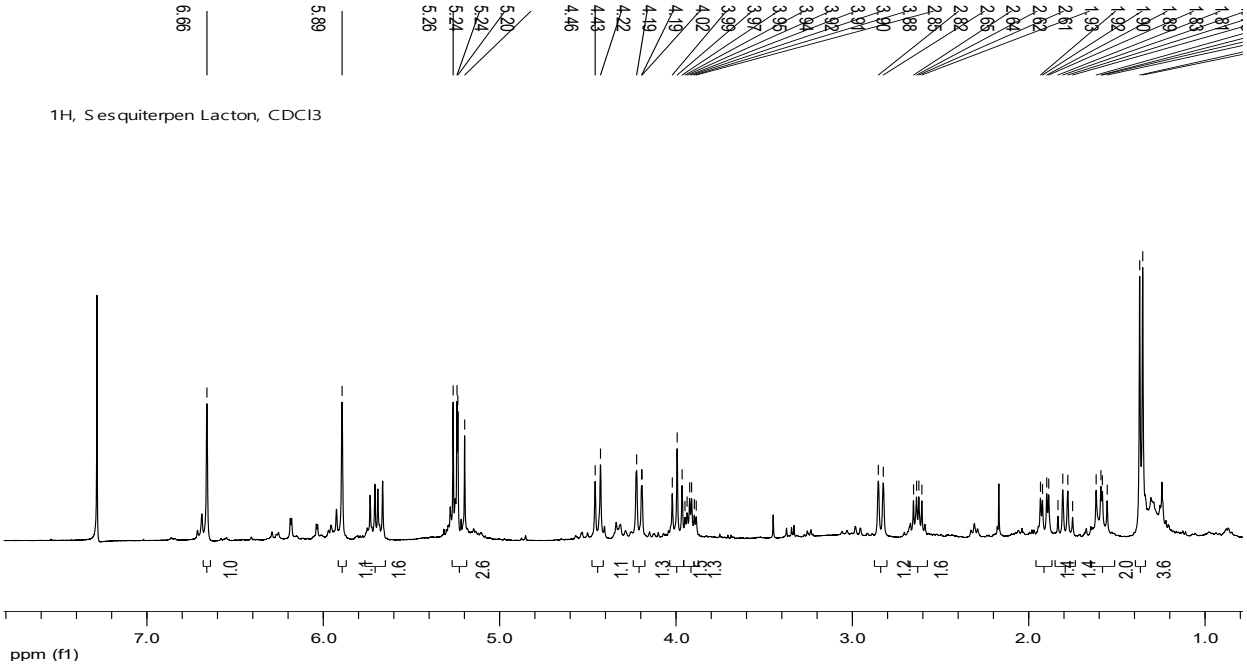
6.66
5.89
5.26
5.24
5.24
5.20
4.46
4.43
4.22
4.19
4.19
4.02
3.99
3.97
3.95
3.94
3.92
3.91
3.90
3.88
2.85
2.82
2.65
2.64
2.62
2.61
1.93
1.92
1.90
1.89
1.83
1.81
1H, Sesquiterpen Lacton, CDCl3
1.0
1.4
1.6
2.6
1.1
1.3
1.2
1.9
2.0
9.3
7.0
6.0
5.0
4.0
3.0
2.0
1.0
ppm (f1)

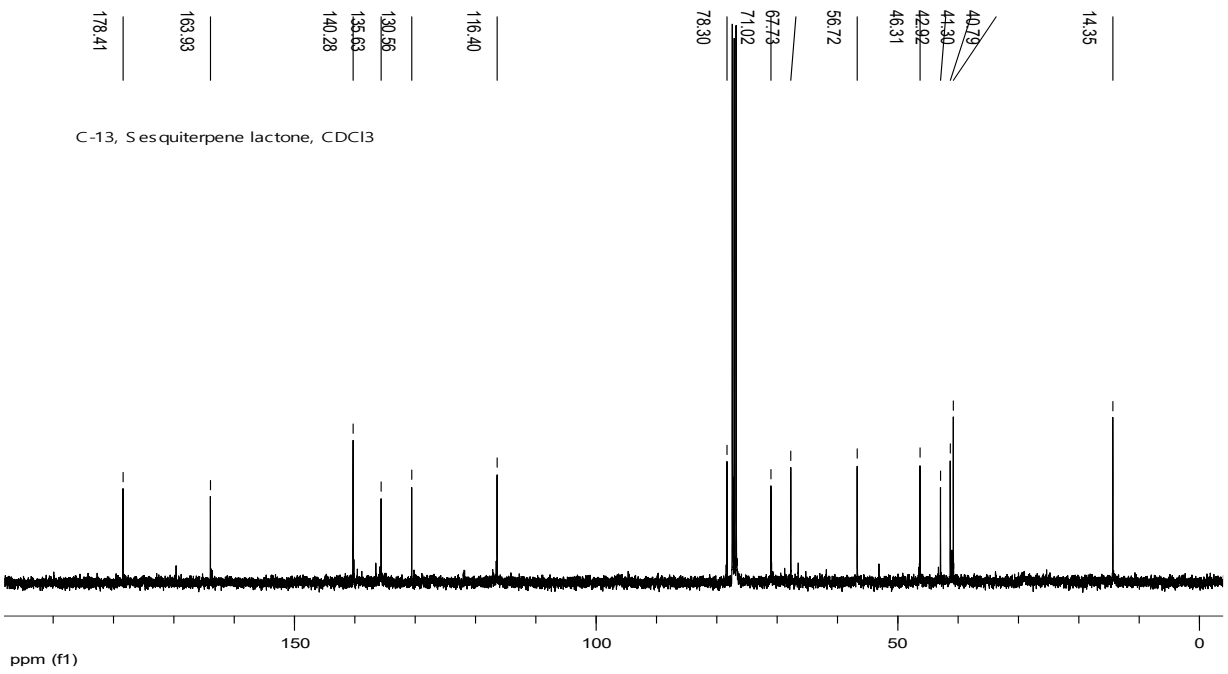
178.41
163.93
140.28
135.63
130.56
116.40
78.30
71.02
67.73
56.72
46.31
42.92
41.30
40.79
14.35
C-13, Sesquiterpene lactone, CDCl3
150
100
50
0
ppm (f1)

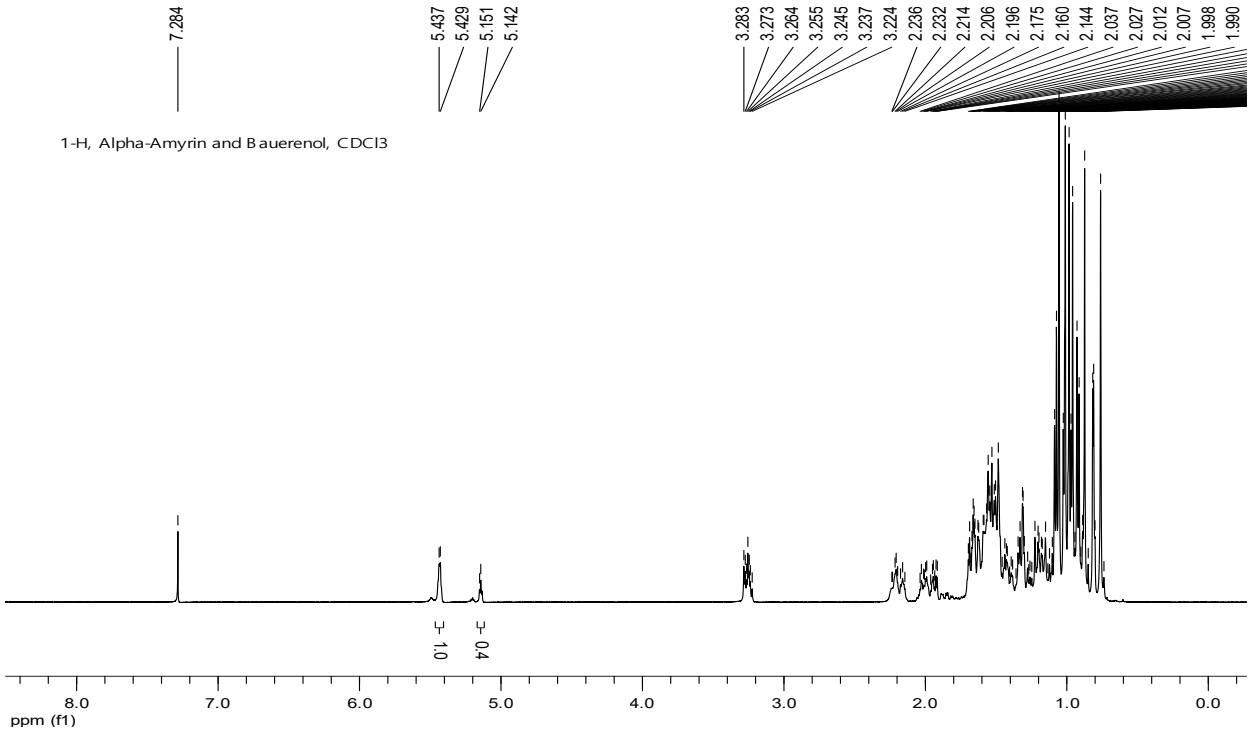
7.284
5.437
5.429
5.151
5.142
3.283
3.273
3.264
3.255
3.245
3.237
3.224
2.236
2.232
2.214
2.206
2.196
2.175
2.160
2.144
2.037
2.027
2.012
2.007
1.998
1.990
1-H, Alpha-Amyrin and Bauerenol, CDCl3
1.10
0.94
8.0
7.0
6.0
5.0
4.0
3.0
2.0
1.0
0.0
ppm (f1)

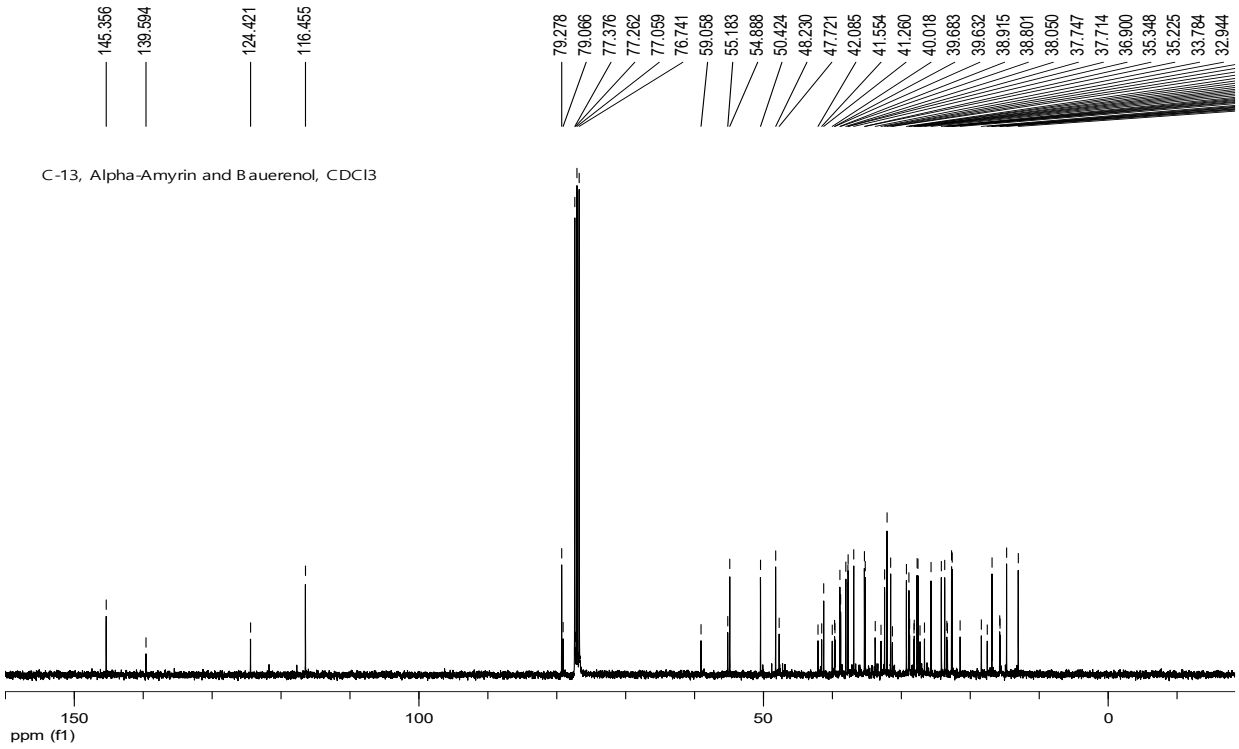
145.356
139.594
124.421
116.455
79.278
79.066
77.376
77.262
77.059
76.741
59.058
55.183
54.888
50.424
48.230
47.721
42.085
41.554
41.260
40.018
39.683
39.632
38.915
38.801
38.050
37.747
37.714
36.900
35.348
35.225
33.784
32.944
C-13, Alpha-Amyrin and Bauerenol, CDCl3
150
100
50
0
ppm (f1)